ESCOLA DE DOUTORAMENTO
INTERNACIONAL DA USC

Victoria
Díaz Tomé

Tese de doutoramento

Development of topical ophthalmic formulations for fungal keratitis treatment

Santiago de Compostela, 2023

Programa de Doutoramento en Investigación e Desenvolvemento de Medicamentos

TESE DE DOUTORAMENTO

DEVELOPMENT OF TOPICAL OPHTHALMIC FORMULATIONS FOR FUNGAL KERATITIS TREATMENT

Victoria Díaz Tomé

ESCOLA DE DOUTORAMENTO INTERNACIONAL DA UNIVERSIDADE DE SANTIAGO DE COMPOSTELA

PROGRAMA DE DOUTORAMENTO EN INVESTIGACIÓN E DESENVOLVEMENTO DE MEDICAMENTOS

SANTIAGO DE COMPOSTELA

2023

DECLARACIÓN DE LA AUTORA DE LA TESIS

Development of topical ophthalmic formulations for fungal keratitis treatment.

D./Dña. Victoria Díaz Tomé

Presento mi tesis, siguiendo el procedimiento adecuado al Reglamento y declaro que:

1) La tesis abarca los resultados de la elaboración de mi trabajo.
2) De ser el caso, en la tesis se hace referencia a las colaboraciones que tuvo este trabajo.
3) Confirmo que la tesis no incurre en ningún tipo de plagio de otros autores ni de trabajos presentados por mí para la obtención de otros títulos.
4) La tesis es la versión definitiva presentada para su defensa y coincide la versión impresa con la presentada en formato electrónico.

Y me comprometo a presentar el Compromiso Documental de Supervisión en el caso que el original no esté depositado en la Escuela.

En Santiago de Compostela, 08 de abril de 2023.

Asdo. Victoria Díaz Tomé

AUTORIZACIÓN DE LOS DIRECTORES

Development of topical ophthalmic formulations for fungal keratitis treatment.

D. Francisco J. Otero Espinar y D. Anxo Fernández Ferreiro

Informan:

Que la presente tesis, se corresponde con el trabajo realizado por Dª Victoria Díaz Tomé, bajo mi dirección/tutorización, y autorizo su presentación, considerando que reúne los requisitos exigidos en el Reglamento de Estudios de Doctorado de la USC, y que como director de esta no incurre en las causas de abstención establecidas en la Ley 40/2015.
De acuerdo con lo indicado en el Reglamento de Estudios de Doctorado, declara también que la presente tesis doctoral es idónea para ser defendida en base a la modalidad de Monográfica con reproducción de publicaciones, en los que la participación del doctorando/a fue decisiva para su elaboración y las publicaciones se ajustan al Plan de Investigación.

En Santiago de Compostela, 8 de febrero de 2023

Asdo. Francisco J. Otero Espinar

Asdo. Anxo Fernández Ferreiro

A mis sobrinos

"Busco un mundo mejor y escarbo en un cajón por si aparece entre mis cosas"
Robe Iniesta

AGRADECIMIENTOS

No podría defender esta tesis doctoral sin agradecer todo el apoyo y confianza puesta en mí a todas aquellas personas que me han acompañado a lo largo de estos años.

En primer lugar, quiero darles las gracias a mis dos directores de tesis. Sin ellos, mi tesis doctoral no hubiese sido posible.
A Francisco J. Otero Espinar por haberme dado la oportunidad de desarrollar mi carrera investigadora a su lado, regalándome su tiempo y su conocimiento y por haberme enseñado a creer en mí. Mi gran mentor y amigo. No sé cómo agradecer tanto.
A Anxo Fernández Ferreiro por apoyar mi desarrollo científico y personal. Gracias por todas las propuestas de investigación, su constancia y su motivación.

Gracias a todas las personas pertenecientes a los diferentes grupos con los que he trabajo, que me han enseñado nuevas técnicas y me han acercado a aspectos científicos a los que no podría haber llegado sin ellos. Gracias al grupo de Imagen Molecular del IDIS, al grupo de Farmacología Clínica del IDIS, al Departamento de Farmacia del CHUS, al Departamento de Microbiología del CHUS y Unidad de Resonancia Magnética Nuclear de la USC. Especial mención a Pablo Aguiar, Miguel Barcia, José Llovo y Manuel Martín.

Quisiera agradecer a todo el equipo de Faes Farma ya que con todos los proyectos realizados he adquirido competencias que no podría haber aprendido de otra forma. Además, gracias a la confianza puesta en nosotros he podido convertir mi pasión en mi trabajo.

A mis compañeros de laboratorio, Carlos, Guille, Xurxo, Vini, Rubén, Iria, Andrea y Víctor. Porque sin ellos esto no hubiera sido una de las mejores etapas de mi vida. Gracias por las risas y los llantos. Gracias por todo lo compartido. Habéis hecho mi vida más grande.

A mis compañeros del Departamento de Farmacia, Farmacología y Tecnología Farmacéutica de la Facultad de Farmacia, doctorandos, TFGs, alumnos de máster, postdoctorales, profesorado y al resto del personal. Es imposible nombrarlos a todos aquí, pero sé que sentirán su nombre entre estas palabras. Gracias a todos ellos por haber compartido todo este tiempo conmigo. Por las conversaciones de pasillo, los consejos, los congresos y los cafés.

A Sole, porque ella fue quien me enseñó a desenvolverme por el laboratorio. Gracias por compartir conmigo su pasión y su sabiduría.

A Mamá, a Papá y a mis hermanos Carlota y Eduardo por su apoyo incondicional, por sus grandes consuelos. Son y serán el soporte más grande de mi vida. Sin ellos no podría a ver llegado donde estoy.

A mi gran amigo Diego, que más que amigo es familia. Por todo lo que me ha sufrido y por toda la ayuda que me ha ofrecido para la realización de esta tesis. Gracias por sus ideas, sus recursos, su tiempo y su comprensión.

A mi amiga del alma, la que siempre está. Mi querida Uxía. Porque el tiempo cuando estoy con ella pasa de otro color. Gracias por el apoyo incondicional.

No podría faltar mi más sincero agradecimiento a mi mejor amigo y compañero, David. No puedo expresar con palabras todo lo que siento cada día. Siempre dispuesto a ayudarme y a apoyarme en cada proyecto, en cada viaje, en cada locura. Él ha sido capaz de hacerme razonar en los momentos más caóticos de mi vida. Por todas las cosas que hemos vivido y por todo lo que nos queda por vivir. Somos fuertes y somos juntos. Sé que lograremos cualquier cosa que nos propongamos. Gracias y mil veces gracias.

**A mi Tula, que me estará mirando desde el cielo de los perros. Por toda la paz que me dio en momentos de tempestad y por haberme hecho mejor humano. La llevaré siempre en el corazón.*

¡Gracias a todos!

SUMMARY

Today, according to the World Health Organization's World Vision Report, at least 2.2 billion people suffer from visual impairment or complete blindness, of which just over half of these cases (1 billion) could have preserved their vision if they had access to effective treatment. Vision impairment or complete blindness can result from a wide and diverse range of conditions ranging from age-related macular degeneration, cataracts, corneal opacity, diabetic retinopathy or glaucoma, among others.
The causes of vision impairment vary from country to country and depend mainly on the availability of adequate and effective ophthalmic care.

The eye is an organ with a complex anatomy and physiology that provides insulation and protection. The cornea represents the main biological barrier of the eye, preventing the entry of microorganisms and foreign substances (including drugs) into the eye. In addition, the high tear fluid turnover rate, high nasolacrimal drainage and blinking effectively remove any substance from the ocular surface. For these reasons, topical-ophthalmic administration has a significantly low bioavailability. However, this route of administration is the most desirable, as formulations for this route are self-administered (improving patient adherence) and cost-effective.
Over the years, research in the development of new formulations has mainly focused on two strategies to improve the bioavailability of drugs through the topical-ophthalmic route: increasing the biopermanence of the drug in the precorneal area and increasing the permeability of the drug through the cornea, sclera and conjunctiva. These goals can be achieved by developing systems based primarily on polymers that increase the viscosity of the formulations and increase their adhesion to the mucin layer, keeping the formulations longer on the ocular surface. Bioavailability can also be improved by increasing transcorneal permeability through the use of penetration promoters such as cyclodextrins.

Fungal keratitis is a disease of infectious origin caused by different types of fungal species. *Arpergillus* spp. *Curvularia* spp., *Penicillium* spp. and *Candida* spp. are the most common species. The severity of the disease lies mainly in the lack of effective drugs available, the difficulty in diagnosis and the delay in starting effective treatment. These factors lead to blindness or even complete loss of the eyeball. It is an uncommon disease in developed countries, although in recent years an increase has been observed due to different factors, such as poor use of contact lenses, long treatments with corticoids or local antibiotics, immunosuppressed patients, etc.
At the same time, there is only one FDA-approved topical-ophthalmic formulation and its efficacy is limited to superficial infections caused by filamentous fungi. For this reason, hospital pharmacy services are forced to reformulate drugs intended for other routes (mainly intravenous (IV)) by means of resuspension or redispersion with ophthalmic buffers. The main problem is that in the vast majority of cases, their toxicity, bioavailability and stability are unknown. In addition, in order to achieve therapeutic concentrations, intense dosages (every hour) are established, which cause systemic side effects and the abandonment of treatment by the patient, generally leading to a worsening of the clinical picture and hospitalization, increasing health care costs.

This doctoral thesis is divided into two sections. The first section consists of the first three chapters. These chapters focus on the design, development and characterization of several topical-ophthalmic formulations for the administration of three different antifungals: econazole, voriconazole and natamycin. These formulations are mainly based on the formation of inclusion complexes with cyclodextrins to increase the aqueous solubility of the drugs and improve their corneal permeability, and their vehicleization in *in-situ* gelling hydrogels and mucoadhesive hydrogels to increase the permanence of the formulations on the ocular surface.
In the second section, we focus on the study of the ocular safety of cyclodextrin solutions, as well as the study of their potential as permanence promoters on the ocular surface. This section is the fourth and final chapter.

In the **introduction** of this thesis, a critical bibliographic review is carried out in which all the possible pharmacological treatments for the treatment of fungal keratitis are compiled, including a large number of active ingredients belonging to different pharmacological groups, such as polyenes, azoles or pyrimidines, among others. It also includes a section detailing the therapeutic regimen used in hospitals when a case of fungal keratitis occurs. In addition, surgical treatments such as keratoplasty, amniotic membrane transplantation or debridement are reviewed.

Chapter 1 describes the design and characterization of ophthalmic hydrogels incorporating econazole. The aim of this chapter was to develop two formulations suitable for topical ophthalmic administration of econazole for the treatment of fungal keratitis. Econazole is an azole antifungal with low water solubility. For this reason, the main objective was to increase its solubility. Based on the results of the solubility study, α-cyclodextrin (αCD) was chosen as the solubilizing agent. The formation of the inclusion complexes was studied by nuclear magnetic resonance (NMR) and molecular modelling studies, suggesting that the imidazole ring of econazole is deeply embedded in the cavity of αCD.
The inclusion complexes formed between econazole and αCD were vehicled into two types of hydrogels using different polymers. An ion-sensitive hydrogel consisting of a mixture of gellan gum (GG) and kappa carrageenan (CK) (4:1) and a second mucoadhesive hydrogel consisting of 0.4 % (w/v) hyaluronic acid were prepared.
Once the hydrogels were prepared, the *in vitro* release of econazole was studied, demonstrating the ability of the hydrogels to control its release. In addition, *ex vivo* transcorneal permeability was studied using bovine corneas, demonstrating that the econazole included in these systems is able to pass through the cornea to reach deeper tissues. Two different types of studies were performed to assess ocular irritation and toxicity, the corneal permeability and opacity test or BCOP and the *in vitro* ocular irritation test HET-CAM. In the BCOP test, a change in transparency was observed, however, corneal permeability was not affected. In the HET-CAM test, using chorioallantoic membrane (CAM) from fertilized eggs, no change in the blood vessels of the membrane was observed, demonstrating that these formulations are non-irritating.
On the other hand, to determine mucoadhesion *in vivo*, the ability of the formulations to remain on the ocular surface was studied. For this purpose, the hydrogels labelled with a

radiopharmaceutical (^{18}F-FDG) were administered to the ocular surface of sprague dawley rats, establishing their clearance over time using experimental molecular imaging techniques based on the use of positron emission tomography (μPET). The study demonstrates that both hydrogels are able to remain on the ocular surface for around 70 minutes, well above the time that the econazole/α-cyclodextrin inclusion complex solution remains without bioadhesive polymers.

The antifungal capacity of several antifungals (econazole, voriconazole, fluconazole, amphotericin B and natamycin) used in the treatment of fungal keratitis was evaluated on different fungal species (*Candida Albicans, Aspergillus Fumigatus* and *Paecilomyces*) using the disc diffusion method. In this study, econazole was found to have large zones of inhibition far superior to those obtained with amphotericin B and natamycin.

Based on all the results obtained, the formulated econazole eye drops have great potential for use in the treatment of fungal keratitis, although due to the modification of corneal transparency they cause, their use should be limited to use in cases where other effective amphotericins with similar activity (such as voriconazole) are not available or where treatment outweighs the risks associated with their use.

Chapter 2, like chapter 1, focuses on the development, optimisation and characterisation of two types of mucoadhesive hydrogels with high ocular permanence for the topical-ophthalmic administration of voriconazole: an ion-sensitive hydrogel composed of a mixture of GG:CK and a hyaluronic acid hydrogel. Despite the great potential of this antifungal for the treatment of fungal infections in different organs and tissues, which makes it increasingly used by ophthalmologists, there is currently no FDA- or EMA-approved ophthalmic formulation of voriconazole. As a result, hospital pharmacy departments are forced to prepare ophthalmic formulations of voriconazole from commercial intravenous formulations by dilution in biocompatible ocular vehicles. This chapter compares the voriconazole mucoadhesive hydrogels we have developed with one of the formulations produced in hospital pharmacy departments from Vfend®, a commercial intravenous injectable of voriconazole. The main problem with this formulation is the limited residence time on the ocular surface, which requires intensive treatment leading to systemic side effects.

Voriconazole is an azole antifungal with very limited water solubility. For the development of the hydrogels, solubility studies of voriconazole with cyclodextrins were carried out. The formation of inclusion complexes between voriconazole and the cyclodextrins 2-hydroxypropyl-β-cyclodextrin (HPβCD), 2-hydroxypropyl-γ-cyclodextrin (HPγCD) was studied by nuclear magnetic resonance (NMR) and molecular modelling. Based on these results, HPβCD (20% w/v) was chosen for the development of the formulations. Previous studies have shown that this cyclodextrin is able to produce a significant improvement in the amount of drug permeated through the cornea and has decreased the ocular toxicity of certain drugs.

The hyaluronic acid gel was formulated at a concentration of 0.4% (w/v) and the ion-sensitive hydrogels were prepared at different ratios of GG and CK (1:1, 2:1, 4:1). The 1:1 mixture was chosen as the best formulation for further development as it was the one that showed the best

performance in terms of admisnistration. *In vitro* release and *ex vivo* transcorneal permeation studies were carried out in bovine corneas to determine the ability of the hydrogels to release voriconazole in a controlled manner and to improve the transcorneal permeation of voriconazole. The osmolality and pH values obtained for all formulations developed except Vfend® were found to be within the appropriate range for ophthalmic administration. The ophthalmic solution prepared using Vfend® shows osmolality values much higher than those recommended for ocular formulations, due to the presence of the cyclodextrin sulfobutileter-β-cyclodextrin (SBEβCD) used to solubilise the voriconazole in the injectable. This is an anionic cyclodextrin that has several sulphobutyl radicals in the form of a sodium salt in its structure and therefore contributes a high concentration of sodium ions to the medium. Ocular irritation and toxicity tests performed by BCOP and HET-CAM showed that all formulations evaluated are safe for ophthalmic use.

To determine the permanence time on the ocular surface, *ex vivo* corneal mucoadhesion studies and *in vivo* corneal surface permanence time studies were performed using PET imaging. These tests confirmed the mucoadhesive properties of the newly prepared voriconazole hydrogels and their superior ocular permanence compared to Vfend® solutions.

Based on all these results, it is possible to conclude that the developed voriconazole hydrogels are excellent candidates for clinical application in cases of fungal keratitis.

The severity of fungal keratitis is aggravated by the emerging resistance of fungal species to current treatments. Combination therapy of several antifungals is often more effective than monotherapy, so **chapter 3** of this doctoral thesis addresses the design and development of several eye drops containing two molecules with antifungal activity: natamycin and voriconazole.

Natamycin is the molecule of first choice in the early treatment of fungal keratitis caused by filamentous fungi. The main problem is that there is only one FDA-approved ophthalmic formulation, Natacyn®, which is based on a conventional natamycin suspension with low transcorneal penetration and is therefore limited to superficial infections. In this chapter, we study improving the water solubility of natamycin through the use of cyclodextrins. As with voriconazole, the cyclodextrin of choice after solubility studies was HPβCD. Due to the type of solubility diagram obtained (AL) (the negative deviation shows the formation of aggregates of the inclusion complexes) the solutions of natamycin, voriconazole and HPβCD were analysed by transmission electron microscopy (TEM). The images demonstrate the presence of nanometre-sized spherical aggregates that may enhance the ability to permeate through the cornea.

The inclusion complex formed between natamycin and HPβCD was studied by NMR. Using this technique, competition studies on complex formation with HPβCD between natamycin and voriconazole were also performed. As could be observed, natamycin competes with voriconazole for the same binding site to HPβCD, which leads to the need to adjust and optimise the concentration of the cyclodextrin. In our case, the use of HPβCD concentrations of 40% (w/v) allowed the preparation of formulations at the desired concentrations (natamycin 7 mg/mL (w/v) and voriconazole 10 mg/mL).

Once the inclusion complexes formed had been studied, two hydrogels were prepared. One hydrogel was made with hyaluronic acid (0.4% (w/v)) and the other with a commercial hydrogel (Liquifilm®) based on polyvinyl alcohol (PVA) (1.4% w/v) frequently used in the preparation of formulations in hospital pharmacy services. The hydrogels were characterized in terms of pH, osmolality, viscosity and transparency. These studies showed that the values obtained are within the accepted range for ophthalmic topical formulations. *In vitro* release studies showed characteristic Fickian-type diffusion process profiles for all new formulations. In addition, *ex vivo* corneal permeability studies demonstrated a significant improvement in the transcorneal permeation of natamycin compared to the commercial formulation Natacyn®. The developed formulations did not show any indication of irritation according to the results of the HET-CAM and BCOP tests and can therefore be considered safe formulations.
The *in vitro* antifungal effectiveness of the eye drops was evaluated by the disc diffusion method, showing that the developed formulations show activity against the tested fungal species (*Candida albicans* ATCC 90231), *Candida albicans* ATCC 90028, *Paelomyces lilacinus* ATCC 90028, *Aspergillus fumigatus*, *Paelomyces lilacinus*, and *Fusarium solanii*).
Ex vivo and *in vivo* mucoadhesion studies demonstrated that the mucoadhesive capacity shown by the new formulations is mainly due to the incorporated cyclodextrin, as no significant differences were observed when HA or PVA were incorporated at the concentrations studied.

During the search for published information on the ophthalmic application of cyclodextrins carried out during the research conducted in the previous 3 chapters, it was found that there is very little information on their toxicity and safety at the ophthalmic level and on their mucoadhesive capacity on the ocular surface. Therefore, in **chapter 4,** the results of safety and ocular permanence studies carried out on cyclodextrin solutions at high concentrations are presented. For this purpose, different varieties of cyclodextrins of interest in the development of ophthalmic drug delivery systems have been included in the study. The effect of αCD, β-cyclodextrin (βCD), γ-cyclodextrin (γCD), 2-hydroxypropyl-α-cyclodextrin (HPαCD), HPβCD, HPγCD, SBEβCD, and partially methylated β-cyclodextrin (RMβCD) solutions on the choriolantoid membrane of fertilized eggs was studied using the HET-CAM assay and on bovine corneas using the BCOP method. According to the results obtained in these tests, all cyclodextrins are safe, with the exception of αCD and RMβCD. The 20% (w/v) solutions of RMβCD caused a significant change in corneal transparency but showed no changes in the chorioallantoic membrane vessels. The changes in transparency are due to the low pH value obtained when dissolving this partially methylated variety (2.447±0.025). At acidic pH, alteration of proteins and other components of the mucosa and epithelium can occur, causing these alterations. The negative effect on corneal transparency was resolved by adjusting the RMβCD solution to pH 7.4. The αCD solutions (in unnaturalized and neutralized solutions at pH 7.4), did not cause hemorrhage, lysis or coagulation on the chorioallantoic membrane vessels of the eggs, but the formation of a thin white precipitate was observed. In addition, a significant change in corneal transparency was also observed during the BCOP test. This phenomenon is probably due to the interaction described for αCD and different phospholipids and lipid components of the membrane, which form insoluble inclusion complexes, which can

precipitate on the membranes. The permeability of fluorescein across corneas studied through BCOP was affected by most of the cyclodextrin solutions studied. Increased fluorescein permeability is normally interpreted as a sign of toxicity; however, it is known that cyclodextrins can interact with cell membrane components to enhance permeability across different epithelia and barriers without showing toxic effects, including transcorneal permeability.

The mucoadhesive capacity of cyclodextrins was studied by *in vitro*, *ex vivo* and *in vivo* assays. These tests demonstrated the ability of the cyclodextrins to interact and bind to the ocular mucosa. The *ex vivo* studies showed that at the concentrations studied there are no significant differences between the different cyclodextrins, and they exhibit similar levels of mucoadhesion to those observed for some biodhesive polymers (such as HA and PVA) and for their blends with cyclodextrins. *In vitro* studies performed on mucin blends and cyclodextrin solutions showed the establishment of interactions between cyclodextrins and mucin in solution, probably through the establishment of weak hydrogen bonding or Van der Waals interactions. *In vivo* studies demonstrated the excellent ability of the cyclodextrin solutions to remain on the ocular surface. All the permanence values (with the exception of the RMβCD solutions) decreased when the solutions were adjusted to pH 7.4. This may be due to an increased difficulty in establishing hydrogen bonds between the cyclodextrins and mucin caused by the ionization of sialic acid. In the case of RMβCD, *in vivo* ocular permanence was increased by neutralizing the dilution. pH values as acidic as those observed for this unneutralized solution exceed the buffering capacity of the eye, producing irritation and damage to the epithelium, which promotes tearing and blinking, increasing clearance at its surface.

αCD was the cyclodextrin that showed the highest MRT value, probably due to the formation of insoluble aggregates formed with the phospholipids of the epithelial cells. HPαCD, HPβCD and HPγCD showed the highest $t_{1/2}$ values, suggesting that it is the hydroxylated cyclodextrins that remain on the ocular surface the longest.

Therefore, taking into account the results obtained on the safety and ocular mucoadhesion of the different cyclodextrins, as well as their capacity to promote the transcorneal penetration of other molecules, make cyclodextrins excellent candidates for the development of ophthalmic formulations of drugs that are poorly soluble in water or with low corneal permeability.

In conclusion, this doctoral thesis has addressed the rational design of different topical-ophthalmic formulations for the treatment of ocular fungal diseases. Using three antifungals with different activity spectra, different formulations for topical-ophthalmic administration have been developed. In addition, a complete preclinical characterization of these formulations has been carried out. These formulations have great potential for the treatment of fungal keratitis caused by different species, which can fill the current therapeutic gap. All the formulations developed have shown adequate levels of safety, *in vitro* activity and excellent mucoadhesive behaviour, with high residence times on the ocular surface.

Finally, safety and bioadhesion studies carried out with cyclodextrin solutions show that even at relatively high concentrations they are suitable excipients for the preparation of ophthalmic

formulations. However, they should be supplemented by further *in vivo* studies to complete the knowledge on the effect of cyclodextrins on the ocular surface.

Actualmente, según o informe mundial sobre a visión da Organización Mundial da Saúde, polo menos 2200 millóns de persoas padecen unha deficiencia visual ou cegueira completa, das cales, algo máis da metade dos casos (1000 millóns) poderían conservar a súa visión se tivesen acceso a un tratamento eficaz. A deficiencia de visión ou cegueira completas poden ser a consecuencia dunha ampla e diversa gama de afeccións que van dende dexeneración macular asociada á idade, cataratas, opacidade corneal, retinopatía diabética ou glaucoma, entre outras. As causas que provocan unha deficiencia na visión varían dun país a outro e dependen principalmente da dispoñibilidade dunha atención oftálmica adecuada e eficaz.

O ollo é un órgano con unha anatomía e fisioloxía complexas, que lle proporcionan illamento e protección. A córnea representa a principal barreira biolóxica do ollo, impedindo a entrada de microorganismos e sustancias extrañas (incluindo fármacos) ó interior do ollo. Ademáis, a alta tasa de renovación do líquido lacrimal, o elevado drenaxe nasolacrimal e o parpadeo, eliminan de maneira eficaz calqueira sustancia da superficie ocular. Por estes motivos, a administración tópico-oftálmica, prensenta unha biodispoñibilidade significativamente baixa. Porén, esta vía de administración é a máis desexable, xa que as formulación destinadas a esta vía son autoadministrables (mellorando a adherencia por parte do doente) e económicamente rentables. Ó longo dos anos, a investigación no desenvolvemento de novas formulacións centrouse principalmente en dúas estratexias para mellorar a biodispoñibilidade dos fármacos a través da ruta tópico-oftálmica: aumentar a biopermanencia do fármaco na áera precorneal e incrementar a permeabilidade do fármaco a través da córnea, esclera e conxuntiva. Estes obxectivos pódense alcanzar mediante o desenvolvemento de sistemas baseados principalmente en polímeros que aumenten a viscosidade das formulacións e incrementen a súa adhesión na capa de mucina, mantendo as formulacións máis tempo sobre a superficie ocular. A biodispoñibilidade tamén se pode mellorar, incrementando a permeabilidade transcorneal mediante o uso de promotores da penetración, como poden ser as ciclodextrinas.

A queratite fúnxica é unha enfermidade de orixen infeccioso causada por diferentes tipos de especies fúnxicas: *Arpergillus* spp. *Curvularia* spp., *Penicillium* spp. y *Candida* spp son as máis habituais. A gravidade da enfermidade radica principalmente na falta de medicamentos efectivos dispoñibles, a dificultade no diagnóstico e no retraso no comezo dun tratamento eficaz. Estos factores dirixen ó paciente a sufrir cegueira ou incluso á perdida completa do globo ocular. É unha enfermidade pouco habitual nos países desenvolvidos, aínda que nos últimos anos observouse un incremento debido a diferentes factores como o mal uso das lentes de contacto, tratamentos prolongados con corticoides ou antibióticos locais, doentes inmunosuprimidos, etc.
Ó memos tempo, só existe unha formulación tópica-oftálmica aprobada pola FDA e ten unha eficacia limitada a infeccións superficiais causadas por fungos filamentosos. Por este motivo, os servizos de farmacia hospitalaria vense na obriga de reformular medicamentos destinados a outras vías, (principalmente a intravenosa (IV)) mediante a súa resuspensión ou redispersión con tampóns oftálmicos. O principal problema é que na gran maioría dos casos descoñécese a súa toxicidade, biodispoñibilidade e estabilidade. Ademais, para alcanzar concentracións

terapéuticas establécense posoloxías intensas (cada hora) que provocan efectos secundarios sistémicos e o abandono do tratamento por parte do doente, provocando xeralmente un empeoramento do cuadro clínico e a súa hospitalización, incrementando o gasto sanitario.
Esta tese de doutoramento divídese en dúas seccións. A primeira sección consta dos tres primeiros capítulos. Estes capítulos céntranse no deseño, desenvolvemento e caracterización de varias formulacións tópico-oftálmicas destinadas á administración de 3 antifúnxicos diferentes: econazol, voriconazol e natamicina. Estas formulacións básanse principalmente na formación de complexos de inclusión con ciclodextrinas para aumentar a solubilidadeacuosa dos fármacos e mellorar a súa permeabilidade corneal , e a súa vehiculización en hidroxeis de xelificación *in situ* e hidroxeis mucoadhesivos que permitan aumentar a permanencia das formulacións sobre a superficie ocular.
Na segunda sección, centrámonos no estudo da seguridade ocular de solucións de ciclodextrinas, así como o estudo do seu potencial como promotores da permanencia sobre a superficie ocular. Esta sección constitúe o cuarto e último capítulo.

Na **introducción** de esta tese abórdase unha revisión bibliográfica crítica onde se recopilan todos os posibles tratamentos farmacolóxicos para o tratamento da queratite fúnxica, incluindo un gran número de principios activos pertencentes a diferentes grupos farmacolóxicos, como os polienos, os azoles ou as pirimidinas, entre outros. Inclúese tamén un apartado onde se detalla o réximen terapéutico utilizado nos hospitais cando aparece un caso de queratite fúnxica. Ademáis, faise un repaso dos tratamentos cirúrxicos empleados, como poden ser a queratoplastia, o transplante de membrana amniótica ou o desbridamento.

O **capítulo 1** describe o deseño e caracterización de hidroxeis oftálmicos que incorporan econazol. O obxetivo deste capítulo foi o de desenvolver dúas formulacións adecuadas á administración tópico-oftálmica do econazol para o tratamento da queratite fúnxica. O econazol é un antifúnxico azólico cunha baixa solubilidade en auga. Por esta razón, o obxetivo principal foi o de aumentar a súa solubilidade. Según os resultados do estudo de solubilidade escolleuse a α-ciclodextrina (αCD) como axente solubilizante. A formación dos complexos de inclusión estudouse mediante estudos de resonancia magnética nuclear (RMN) e modelaxe molecular, suxerindo que o anel imidazólico do econazol encóntrase incluido profundamente na cavidade da αCD.
Os complexos de inclusión formados entre o econazol e a αCD vehiculizáronse en dous tipos de hidroxeis, mediante o uso de diferentes polímeros. Levouse a cabo a elaboración dun hidroxel ión-sensible formado por unha mezcla de goma gellan (GG) e carraxenato kappa (CK) (4:1) e un segundo hidroxel mucoadhesivo formado por un 0,4 % (p/v) de ácido hialurónico.
Unha vez elaborados os hidroxeis, estudouse a liberación *in vitro* do econazol demostrando a capacidade dos hidroxeis para controlar a súa liberación. Ademáis, estudouse a permeabilidade transcorneal *ex vivo* mediante o uso de córneas bovinas, demostrando que o econazol incluido nestes sistemas é capaz de atravesar a córnea para alcanzar ós tecidos máis profundos. Realizáronse dous tipos diferentes de estudos para avaliara irritación e a toxicidade ocular, o test de permeabilidade e opacidade corneal ou BCOP e o test de irritación ocular *in vitro* HET-

CAM. Na proba de BCOP observouse unha modificación da transparencia, con todo, a permeabilidade corneal non se viu afectada. No test de HET-CAM, no que se usa a membrana corioalantoidea (CAM) de ovos fertilizados, non se observaron cambios nos vasos sanguíneos da membrana demostrando que estas formulacións non son irritantes.
Por outra banda, para determinar a mucoadhesión *in vivo* estudouse a capacidade de permanencia das formulacións sobre a superficie ocular. Para acadar isto, os hidroxeis marcados cun radiofármaco (^{18}F-FDG) foron administrados na superficie ocular de ratas sprague dawley, establecendo o seu aclaramento no tempo empregando técnicas de imaxe molecular experimental baseadas na utilización de tomografía por emisión de positróns (μPET). O estudo demostra que ambos hidroxeis son capaces de permanecer sobre a superficie ocular arredor de 70 minutos, moi por enriba do tempo que permanece a solución do complexo de inclusión econazol/ αCD sen polímeros bioadhesivos.
A capacidade antifúnxica de varios antifúnxicos (econazol, voriconazol, fluconazol, anfotericina B e natamicina) utilizados no tratamento da queratite fúnxica evaluóuse sobre diferentes especies fúnxicas (*Candida Albicans*, *Aspergillus Fumigatus* e *Paecilomyces*) mediante o método de difusión en disco. Neste estudo observouse que o econazol presenta grandes zonas/areas de inhibición moi superiores ás obtidas con anfotericina B e natamicina. Segundo os resultados obtidos, os colirios de econazol formulados presentan un gran potencial para o seu emprego no tratamento da queratite fúnxica, ainda que debido á modificación da transparencia corneal que ocasionan, o seu uso debería limitarse ó uso nos casos nos cales non de dispoña de outros antifúnxicos efectivos con actividade similar (como o voriconazol) ou nos que o tratamento supere os riscos asociados a súa utilización.

O **capítulo 2**, ó igual que o capítulo 1, céntrase na elaboración, optimización e caracterización de dous tipos de hidroxeis mucoadhesivos de elevada permanencia ocular para a administración tópico-oftálmica do voriconazol: un hidroxel ión-sensible composto por unha mestura de GG y CK e un hidroxel de ácido hialurónico. A pesar do gran potencial que posúe este antifúnxico para o tratamento de infeccións fúnxicas en diferentes órganos e tecidos, o que fai que cada vez sexa máis utilizado polos oftalmólogos, actualmente non existe ningunha formulación oftálmica de voriconazol aprobada pola FDA ou pola EMA. Debido a isto, os servizos de farmacia hospitalaria vense na obriga de preparar formulacións oftálmicas de voriconazol a partir de formulacións comerciais intravenosas mediante a súa dilución en vehículos oculares biocompatibles. Neste capítulo compáranse os hidroxeis mucoadhesivos de voriconazol que desenvolvimos con unha das formulacións que se elabóran nos servizos de farmacia hospitalaria a partir del Vfend®, un inxectable intravenoso comercial de voriconazol. O principal problema que presenta esta formulación é o tempo limitado de permanencia sobre a superficie ocular, que obriga a un tratamento intensivo provocando efectos secundarios sistémicos.
O voriconazol é un antifúnxico azólico, cunha solubilidade moi limitada en auga. Para levar a cabo a elaboración dos hidroxeis, realizáronse estudos de solubilidade do voriconazol con ciclodextrinas. A formación dos complexos de inclusión formados entre o voriconazol e as ciclodextrinas 2-hidroxipropil-β-ciclodextrina (HPβCD), 2-hidroxipropil-γ-ciclodextrina (HPγCD) estudouse mediante ensaios de resonancia magnética nuclear (RMN) e modelado

molecular. En función destes resultados, escolleuse a HPβCD (20% p/v) para a elaboración das formulacións. Estudos previos realizados demostraron que esta ciclodextrina é capaz de producir unha mellora significativa na cantidade de fármaco permeado a través da córnea e diminuír a toxicidade de certos fármacos.

O hidroxel de ácido hialurónico formulouse a unha concentración de 0,4% (p/v) e os hidroxeis ión-sensibles elaboráronse a diferentes ratios de GG y CK (1:1, 2:1, 4:1). A mestura1:1 foi a que se escolleu como mellor formulación para continuar co seu desenvolvemento xa que foi a que presentou un comportamento mellor de cara a súa administración. Leváronse a cabo estudos de liberación *in vitro* e permeabilidade transcorneal *ex vivo* en córneas bovinas para coñecer a capacidade dos hidroxeis para ceder o voriconazol de forma controlada e para mellorar a permeación transcorneal do voriconazol. A osmolalidade e os valores de pH obtidos para todas as formulacións desenvolvidas, exceptuando a de Vfend®, encontráronse dentro dos intervalos adecuados para a administración oftálmica. A disolución oftálmica preparada empregando Vfend® mostra valores de osmolalidade moi superiores ós recomendados para as formulacións oculares, debido á presenza da ciclodextrina sulfobutileter-β-ciclodextrina (SBEβCD) que empregan para solubilizar o voriconazol no inxectable. Esta trátase dunha ciclodextrina aniónica que presenta varios radicais sulfobutilo en forma de sal sódica na súa estrutura e que polo tanto, aporta unha gran concentración de ións sodio ó medio. Os ensaios de irritación e toxicidade ocular realizados a través de BCOP e HET-CAM demostraron que toda as formulacións avaliadas son seguras para o seu uso oftálmico.

Para determinar o tempo de permanencia sobre a superficie ocular, leváronse a cabo estudos de mucoadhesión corneal *ex vivo* e estudos de permanencia na superficie corneal *in vivo* mediante imaxe PET. Estos ensaios confirmaron as propiedades mucoadhesivas dos novos hidroxeis de voriconazol preparados e a súa superioridade en canto a permanencia ocular en comparación coas solucións de Vfend®.

En base a todos estos resultados, é posible concluír que os hidroxeis de voriconazol desenvolvidos son excelentes candidatos para a súa aplicación clínica en casos de queratite fúnxica.

A severidade da queratite fúnxica vese agravada pola emerxente resistencia das especies fúnxicas ós tratamento actuais. A terapia combinada de varios antifúnxicos adoita ser máis eficaz que a monoterapia, polo que no **capítulo 3** desta tese de doutoramento, abórdase o deseño e desenvolvemento de varios colirios que conteñan dúas moléculas con actividade antifúnxica: a natamicina e o voriconazol.

A natamicina é a molécula de primeira elección no tratamento temperán da queratite fúnxica causada por fungos filamentosos. O problema principal, é que só existe unha formulación oftálmica aprobada pola FDA, o Natacyn®, que se basa nunha suspensión convencional de natamicina cunha baixa penetración transcorneal, polo que se limita a infeccións superficiais. Neste capítulo, estúdase mellorar a solubilidade da natamicina en auga mediante o uso de ciclodextrinas. Ó igual que co voriconazol, a ciclodextrina elexida foi a HPβCD. Debido ó tipo de diagrama de solubilidade obtido (A_N) (a desviación negativa que presenta demostra a formación de agregados dos complexos de inclusión) as solución de natamicina, voriconazol e

HPβCD analizáronse mediante microscopía electrónica de transmisión (TEM). As imaxes demostran a presenza de agregados esféricos de tamaño nanométrico que poden mellorar a capacidade de permeación a través da córnea.
O complexo de inclusión formado entre a natamicina e a HPβCD estudouse mediante RMN. Mediante esta técnica, fixéronse tamén estudos de competición na formación de complexos coa HPβCD entre a natamicina e o voriconazol. Puidose observar que a natamicina compite co voriconazol polo mesmo lugar de unión á HPβCD o que implica á necesidade de axustar e optimizar a concentración da ciclodextrina. No noso caso, o emprego de concentracións de HPβCD ó 40% (p/v) permitiu a preparación das formulacións ás concentracións desexadas (de natamicina 7 mg/mL e voriconazol 10 mg/mL).
Unha vez estudados os complexos de inclusión formados, procedeuse á elaboración dos hidroxeis. Elaborouse un hidroxel con HA (0,4% p/v) e outro con un hidroxel comercial (Liquifilm®) baseado en polivinil alcohol (PVA) (1,4% p/v) a miúdo empregado na elaboración de formulacións nos servizos de farmacia hospitalaria. Os hidroxeis caracterizáronse en canto a pH, osmolalidade, viscosidade e transparencia. Estes estudos demostraron que os valores obtidos están dentro do intervalo aceptado para as formulacións tópicas oftálmicas. Os estudos de liberación *in vitro* mostraron perfís característicos de procesos de difusión de tipo Fickiano para todas as novas formulacións. Ademáis, os estudos de permeabilidade corneal *ex vivo* demostraron unha mellora significativa na permeación transcorneal da natamicina en comparación coa formulación comercial Natacyn®. As formulacións desenvolvidas non mostraron ningún indicio de irritación de acordo cos resultados dos ensayos de HET-CAM e BCOP, polo que se poden considerar formulacións seguras.
A efectividade antifúnxica *in vitro* dos colirios evaluouse mediante o método de difusión de disco, mostrando que as formulacións desenvolvidas presentan actividade contra as especias fúnxicas testadas ((*Candida albicans* ATCC 90231), *Candida albicans* ATCC 90028, *Paelomyces lilacinus* ATCC 90028, *Aspergillus fumigatus*, *Paelomyces lilacinus*, and *Fusarium solanii*).
Os estudos de mucoadhesión *ex vivo* e *in vivo*, demostraron que a capacidade mucoadhesiva que mostran as novas formulacións débese fundamentalmente á ciclodextrina incorporada xa que non se observaron diferencias significativas ó incorporar HA o PVA ás concentracións estudadas.

Durante a búsqueda da información publicada sobre a aplicación oftálmica das ciclodextrinas levada a cabo durante a investigación recollida nos 3 capítulos anteriores, comprobouse que existe moi pouca información sobre a súa toxicidade e seguridade a nivel oftálmico e sobre a súa capacidade mucoadhesiva na superficie ocular. Polo tanto, no **capítulo 4**, móstranse os resultados dos estudos de seguridade e permanencia ocular realizados a partir de disoluciones de ciclodextrinas a altas concentracións. Para isto incluíronse no estudo diferentes variedades de ciclodextrinas que posúen interés na elaboración de sistemas de liberación oftálmica de fármacos. Estudouse o efecto das solucións de αCD, β-ciclodextrina (βCD), γ- ciclodextrina (γCD), 2-hidroxipropil-α-ciclodextrin (HPαCD), HPβCD, HPγCD, SBEβCD, e β-ciclodextrina parcialmente metilada (RMβCD) sobre a membrana corioalantoidea de ovos fertilizados

mediante o ensaio HET-CAM e sobre córneas bovinas, empregando o método BCOP. De acordo cos resultados obtidos nestes ensaios, todas as ciclodextrinas son seguras, con excepción da αCD e a RMβCD. As disolucións de RMβCD ó 20% (p/v) provocaron un cambio significativo na transparencia corneal, pero non mostraron cambios nos vasos da membrana corioalantoidea. Os cambios na transparencia débense ó baixo valor de pH que se obtén ó disolver esta variedade parcialmente metilada (2,447±0,025). A pH ácidos pódese producir a alteración de proteínas e outros compoñentes da mucosa e do epitelio causando estas alteracións. O efecto negativo sobre a transparencia corneal resolveuse ó axustar a disolución de RMβCD a pH 7,4. As disolucións de αCD (en disolucións sen neutralizar e a pH 7,4) non provocaron hemorraxia, lise ou coagulación sobre os vasos da membrana corioalantoidea dos ovos, pero observouse a formación dun fino precipitado branco sobre ela. Además, tamén se observou un cambio significativo na transparencia da córnea durante o ensaio BCOP. Este fenómeno débese probablemente á interacción descrita para a αCD e diferentes fosfolípidos e compoñentes lipídicos da membrana, que forman complexos de inclusión insolubles, que poden precipitar sobre as membranas. A permeabilidade da fluoresceína a través das córneas estudadas a través do BCOP viuse afectada pola maioría das disolucións de ciclodextrina estudadas. Normalmente, o aumento da permeabilidade da fluoresceína interprétase como un signo de toxicidade, non obstante, é coñecido que as ciclodextrinas poden interaccionar cos compoñentes da membrana celular mellorando a permeabilidade a través de diferentes epitelios e barreiras sen mostrar efectos tóxicos, incluindo a permeabilidade transcorneal.

A capacidade mucoadhesiva das ciclodextrinas estudouse mediante ensaios *in vitro* , *ex vivo* e *in vivo.* Estos ensaios demostraron a capacidade das ciclodextrinas para interactuar e unirse á mucosa ocular. Os ensaios *ex vivo* mostraron que nas concentracións estudadas non existen diferencias significativas entre as diferentes ciclodextrinas e presentan niveis similares de mucoadhesión observados para algúns polímeros bioadhesivos (como HA e PVA) e para a súas mesturas con ciclodextrinas. Os estudos *in vitro* realizados a partir de mesturas de mucina e as disolucións de ciclodextrinas puxeron en manifesto o establecemento de interaccións entre as ciclodextrinas e a mucina en disolución, probablemente a partir do establecemento de enlaces débiles tipo pontes de hidróxeno ou interaccións de Van der Waals. Nos estudos *in vivo*, demostrouse a excelente capacidade das disolucións de ciclodextrina para permanecer sobre a superficie ocular. Todos os valores de permanencia (con excepción das disolucións de RMβCD) disminuiron ó axustar as sólucións a pH 7,4. Esto pode ser debido a unha maior dificultade no establecemento de pontes de hidróxeno entre as CD e a mucina causada pola ionización do ácido siálico. No caso da RMβCD, a permanencia ocular *in vivo* aumentou ó neutralizar a disolución. Valores de pH tán ácidos como os observados para esta disolución sen neutralizar, superan a capacidade tamponadora do ollo, producindo irritación e dano no epitelio, o que promove o lagrimeo e o palpabrexo, aumentando o aclaramento na súa superficie.

A αCD foi a ciclodextrina que mostrou o valor de MRT máis alto, probablemente debido á formación de agregados insolubles formados cos fosfolípidos das células epiteliais. HPαCD, HPβCD y HPγCD mostraron os valores máis elevados de $t_{1/2}$, suxerindo que son as ciclodextrinas hidroxiladas as que máis tempo permanecen sobre a superficie ocular.

Polo tanto, tendo en conta os resultados obtidos sobre a seguridade e mucoadhesion ocular das diferentes ciclodextrinas, así como a súa capacidade para promover a penetración transcorneal de outras moléculas, fan das ciclodextrinas uns excelentes candidatos para a elaboración de formulacións oftálmicas de fármacos pouco solubles en auga ou con baixa permeabilidade corneal.

En conclusión, nesta tese de doutoramento abordouse o deseño racional de diferentes formulacións tópico-oftálmicas para o tratamento de enfermidades fúnxicas oculares. Empregando tres antifúnxicos con diferentes espectros de actividade desenvolvéronse diferentes formulacións destinadas a súa administración tópico-oftálmica. Ademáis, realizouse unha completa caracterización preclínica das mesmas. Estas formulacións teñen un gran potencial para o tratamento da queratite fúnxica causada por diferentes especies, que poden cubrir o baleiro terapéutico actual existente. Todas as formulacións desenvolvidas presentaron niveis adecuados de seguridade, actividade *in vitro* e un excelente comportamento mucoadhesivo, con tempos elevados de permanencia na superficie ocular.
Finalmente, os estudos de seguridade e bioadhesión realizados coas disolucións de ciclodextrinas, demostran que incluso a concentracións relativamente elevadas son excipientes adecuados para a elaboración de formulacións oftálmicas. Con todo, deberían completarse con outros estudos *in vivo* para completar o coñecemento sobre o efecto das ciclodextrinas sobre a superficie ocular.

Actualmente, según el informe mundial sobre la visión de la Organización Mundial de la Salud al menos 2200 millones de personas padecen una deficiencia visual o ceguera completa, de las cuales, algo más de la mitad de esos casos (1000 millones) podrían haber conservado su visión si hubieran tenido acceso a un tratamiento eficaz. La deficiencia de visión o ceguera completa puede ser consecuencia de una amplia y diversa gama de afecciones que van desde degeneración macular asociada a la edad, cataratas, opacidad corneal, retinopatía diabética o glaucoma, entre otras.
Las causas que provocan una deficiencia en la visión varían de un país a otro y dependen principalmente de la disponibilidad de una atención oftálmica adecuada y eficaz.

El ojo es un órgano con una anatomía y fisiológica complejas que le proporciona aislamiento y protección. La córnea representa la principal barrera biológica del ojo, impidiendo la entrada de microorganismos y sustancias extrañas (incluyendo fármacos) al interior del ojo. Además, la alta tasa de renovación del líquido lagrimal, el elevado drenaje nasolacrimal y el parpadeo, eliminan de manera eficaz cualquier sustancia de la superficie ocular. Por estos motivos, la administración tópica-oftálmica, presenta una biodisponibilidad significativamente baja. Sin embargo, esta vía de administración es la más deseable, ya que las formulaciones destinadas a esta vía son autoadministrables (mejorando la adherencia por parte del paciente) y económicamente rentables.
A lo largo de los años, la investigación en el desarrollo de nuevas formulaciones se ha centrado principalmente en dos estrategias para mejorar la biodisponibilidad de los fármacos a través de la ruta tópica-oftálmica: aumentar la biopermanencia del fármaco en el área precorneal e incrementar la permeabilidad del fármaco a través de la córnea, esclera y conjuntiva. Estos objetivos se pueden alcanzar mediante el desarrollo de sistemas basados principalmente en polímeros que aumenten la viscosidad de las formulaciones e incrementen su adhesión a la capa de mucina, manteniendo las formulaciones más tiempo sobre la superficie ocular. La biodisponibilidad también se puede mejorar, incrementando la permeabilidad transcorneal mediante el uso de promotores de la penetración, como pueden ser las ciclodextrinas.

La queratitis fúngica en una enfermedad de origen infeccioso causada por diferentes tipos de especies fúngicas. *Arpergillus* spp. *Curvularia* spp., *Penicillium* spp. y *Candida* spp. son las especies más habituales. La gravedad de la enfermedad radica principalmente en la falta de medicamentos efectivos disponibles, la dificultad en el diagnóstico y el retraso en el comienzo de un tratamiento eficaz. Estos factores dirigen al paciente a sufrir ceguera o incluso a la pérdida completa del globo ocular. Es una enfermedad poco habitual en los países desarrollados, aunque en los últimos años se ha observado un incremento debido a diferentes factores, como el mal uso de las lentes de contacto, tratamientos largos con corticoides o antibióticos locales, pacientes inmunosuprimidos, etc.
Al mismo tiempo, sólo existe una formulación tópica-oftálmica aprobada por la FDA y tiene una eficacia limitada a infecciones superficiales causadas por hongos filamentosos. Por este motivo, los servicios de farmacia hospitalaria se ven obligados a la reformulación de medicamentos destinados a otras vías (principalmente la intravenosa (IV)) mediante su

resuspensión o redispersión con tampones oftálmicos. El principal problema es que en la gran mayoría de los casos, se desconoce su toxicidad, biodisponibilidad y estabilidad en la gran mayoría de los casos. Asimismo, para alcanzar concentraciones terapéuticas se establecen posologías intensas (cada hora) que provocan efectos secundarios sistémicos y el abandono del tratamiento por parte del paciente, provocando generalmente un empeoramiento del cuadro clínico y su hospitalización, incrementando el gasto sanitario.

Esta tesis doctoral se divide en dos secciones. La primera sección consta de los tres primeros capítulos. Estos capítulos se centran el diseño, desarrollo y caracterización de varias formulaciones tópico-oftálmicas destinadas a la administración de 3 antifúngicos diferentes: econazol, voriconazol y natamicina. Estas formulaciones se basan principalmente en la formación de complejos de inclusión con ciclodextrinas para aumentar la solubilidad acuosa de los fármacos y mejorar su permeabilidad corneal, y su vehiculización en hidrogeles de gelificación *in-situ* e hidrogeles mucoadhesivos que permitan aumentar la permanencia de las formulaciones sobre la superficie ocular.
En la segunda sección, nos centramos en el estudio de la seguridad ocular de soluciones de ciclodextrinas, así como el estudio de su potencial como promotores de la permanencia sobre la superficie ocular. Esta sección constituye el cuarto y último capítulo.

En la **introducción** de esta tesis se aborda una revisión bibliográfica crítica en donde se recopilan todos los posibles tratamientos farmacológicos para el tratamiento de la queratitis fúngica, incluyendo un gran número de principios activos pertenecientes a diferentes grupos farmacológicos, como los polienos, los azoles o las pirimidinas, entre otros. Se incluye también un apartado donde se detalla el régimen terapéutico utilizado en los hospitales cuando aparece un caso de queratitis fúngica. Además, se hace un repaso de los tratamientos quirúrgicos empleados, como pueden ser la queratoplastia, el trasplante de membrana amniótica o el desbridamiento.

El **capítulo 1** describe el diseño y caracterización de hidrogeles oftálmicos que incorporan econazol. El objetivo de este capítulo fue el de desarrollar dos formulaciones adecuadas a la administración tópico-oftálmica de econazol para el tratamiento de la queratitis fúngica. El econazol es un antifúngico azólico, con una baja solubilidad en agua. Por esta razón el objetivo principal fue el de aumentar su solubilidad. Según los resultados del estudio de solubilidad se escogió la α-ciclodextrina (αCD) como agente solubilizante. La formación de los complejos de inclusión se estudió mediante estudios de resonancia magnética nuclear (RMN) y modelaje molecular, sugiriendo que el anillo imidazólico del econazol se encuentra incluido profundamente en la cavidad de la αCD.
Los complejos de inclusión formados entre el econazol y la αCD se vehiculizaron en dos tipos de hidrogeles mediante el uso de diferentes polímeros. Se llevó a cabo la elaboración de un hidrogel ión-sensible formado por una mezcla de goma gellan (GG) y carragenato kappa (CK) (4:1) y un segundo hidrogel mucoadhesivo formado por un 0,4 % (p/v) de ácido hialurónico.

Una vez elaborados los hidrogeles, se estudió la liberación *in vitro* del econazol demostrando la capacidad de los hidrogeles para controlar su liberación. Además, se estudió la permeabilidad transcorneal *ex vivo* mediante el uso de córneas bovinas, demostrando que el econazol incluido en estos sistemas es capaz de atravesar la córnea para alcanzar a tejidos más profundos. Se realizaron dos tipos diferentes de estudios para evaluar la irritación y la toxicidad ocular, el test de permeabilidad y opacidad corneal o BCOP y el test de irritación ocular *in vitro* HET-CAM. En la prueba de BCOP se observó una modificación de la transparencia, sin embargo, la permeabilidad corneal no se vio afectada. En el test de HET-CAM, en el que se usa la membrana corioalantoidea (CAM) de huevos fertilizados, no se observó ningún cambio en los vasos sanguíneos de la membrana demostrando que estas formulaciones no son irritantes.
Por otra parte, para determinar la mucoadhesión *in vivo* se estudió la capacidad de permanencia de las formulaciones sobre la superficie ocular. Para ello los hidrogeles marcados con un radiofármaco (^{18}F-FDG) fueron administrados en la superficie ocular de ratas Sprague Dawley, estableciendo su aclaramiento en el tiempo empleando técnicas de imagen molecular experimental basadas en la utilización de tomografía por emisión de positrones (μPET). El estudio demuestra que ambos hidrogeles son capaces de permanecer sobre la superficie ocular alrededor de 70 minutos, muy por encima del tiempo que permanece la solución del complejo de inclusión econazol/α-ciclodextrina sin polímeros bioadhesivos.
La capacidad antifúngica de varios antifúngicos (econazol, voriconazol, fluconazol, anfotericina B y natamicina) utilizados en el tratamiento de la queratitis fúngica se evaluó sobre diferentes especies fúngicas (*Candida Albicans*, *Aspergillus Fumigatus* y *Paecilomyces*) mediante el método de difusión en disco. En este estudio se observó que el econazol presenta grandes zonas de inhibición muy superiores a las obtenidas con anfotericina B y natamicina.
Según todos los resultados obtenidos, los colirios de econazol formulados presentan un gran potencial para su empleo en el tratamiento de la queratitis fúngica, aunque debido a la modificación de la transparencia corneal que ocasionan, su uso debería limitarse al uso en casos en que no se disponga de otros antifúngicos efectivos con actividad similar (como el voriconazol) o en el que el tratamiento supere los riesgos asociados a su utilización.

El **capítulo 2,** al igual que el capítulo 1, se centra en la elaboración, optimización y caracterización de dos tipos de hidrogeles mucoadhesivos de elevada permanencia ocular para la administración tópico-oftálmica del voriconazol: un hidrogel ión-sensible compuesto por una mezcla de GG:CK y un hidrogel de ácido hialurónico. Pese al gran potencial que posee este antifúngico para el tratamiento de infecciones fúngicas en diferentes órganos y tejidos, lo que hace que cada vez sea más utilizado por los oftalmólogos, actualmente no existe ninguna formulación oftálmica de voriconazol aprobaba por la FDA o por la EMA. Debido a esto, los servicios de farmacia hospitalaria se ven en la obligación de preparar formulaciones oftálmicas de voriconazol a partir de las formulaciones comerciales intravenosas mediante su dilución en vehículos oculares biocompatibles. En este capítulo se comparan los hidrogeles mucoadhesivos de voriconazol que hemos desarrollado con una de las formulaciones que se elaboran en los servicios de farmacia hospitalaria a partir del Vfend®, un inyectable intravenoso comercial de voriconazol. El principal problema que presenta esta formulación es el tiempo limitado de

permanencia sobre la superficie ocular, que obliga a un tratamiento intensivo provocando efectos secundarios sistémicos.

El voriconazol es un antifúngico azólico, con una solubilidad muy limitada en agua. Para llevar a cabo la elaboración de los hidrogeles, se realizaron estudios de solubilidad del voriconazol con ciclodextrinas. La formación de los complejos de inclusión formados entre el voriconazol, y las ciclodextrinas 2-hidroxipropil-β-ciclodextrina (HPβCD), 2-hidroxipropil-γ-ciclodextrina (HPγCD) se estudió mediante ensayos de resonancia magnética nuclear (RMN) y modelado molecular. En función de estos resultados, se escogió la HPβCD (20% p/v) para la elaboración de las formulaciones. Estudios previos realizados han demostrado que esta ciclodextrina es capaz de producir una mejora significativa en la cantidad de fármaco permeado a través de la córnea y ha disminuido la toxicidad ocular de ciertos fármacos.

El gel de ácido hialurónico se formuló a una concentración de 0,4% (p/v) y los hidrogeles ión-sensibles se elaboraron a diferentes ratios de GG y CK (1:1, 2:1, 4:1). La mezcla 1:1 fue la que se escogió como mejor formulación para continuar con su desarrollo ya que fue la que presentó un comportamiento mejor de cara a su administración. Se llevaron a cabo estudios de liberación *in vitro* y permeabilidad transcorneal *ex vivo* en córneas bovinas para conocer la capacidad de los hidrogeles para ceder el voriconazol de forma controlada y para mejorar la permeación transcorneal del voriconazol. La osmolalidad y los valores de pH obtenidos para todas las formulaciones desarrolladas, excepto la de Vfend® se encontraron dentro de los intervalos adecuados para la administración oftálmica. La disolución oftálmica preparada empleando Vfend® muestra valores de osmolalidad muy superiores a los recomendados para formulaciones oculares, debido a la presencia de la ciclodextrina sulfobutileter-β-ciclodextrina (SBEβCD) que emplean para solubilizar el voriconazol en el inyectable. Esta se trata de una ciclodextrina aniónica que presenta varios radicales sulfobutilo en forma de sal sódica en su estructura y que por lo tanto aporta una gran concentración de iones sodio al medio. Los ensayos de irritación y toxicidad ocular realizados a través de BCOP y HET-CAM, demostraron que todas las formulaciones evaluadas son seguras para su uso oftálmico.

Para determinar el tiempo de permanencia sobre la superficie ocular, se llevaron a cabo estudios de mucoadhesión corneal *ex vivo* y estudios de permanencia en la superficie corneal *in vivo* mediante imagen PET. Estos ensayos confirmaron las propiedades mucoadhesivas de los nuevos hidrogeles de voriconazol preparados y su superioridad en cuanto a permanencia ocular en comparación con las soluciones de Vfend®.

En base a todos estos resultados, es posible concluir, que los hidrogeles de voriconazol desarrollados son excelentes candidatos para su aplicación clínica en casos de queratitis fúngica.

La severidad de la queratitis fúngica se ve agravada por la emergente resistencia de las especies fúngicas a los tratamientos actuales. La terapia combinada de varios antifúngicos suele ser más eficaz que la monoterapia, por lo que en el **capítulo 3** de esta tesis doctoral, se aborda el diseño y desarrollo de varios colirios que contengan dos moléculas con actividad antifúngica: la natamicina y el voriconazol.

La natamicina es la molécula de primera elección en el tratamiento temprano de la queratitis fúngica causada por hongos filamentosos. El problema principal, es que sólo existe una formulación oftálmica aprobada por la FDA, el Natacyn®, que se basa en una suspensión convencional de natamicina con una baja penetración transcorneal, por lo que se limita a infecciones superficiales. En este capítulo, se estudia mejorar la solubilidad de la natamicina en agua mediante el uso de ciclodextrinas. Al igual que con el voriconazol, la ciclodextrina elegida después de realizar los estudios de solubilidad fue la HPβCD. Debido al tipo de diagrama de solubilidad obtenido (A_L) (la desviación negativa que presenta demuestra la formación de agregados de los complejos de inclusión) las soluciones de natamicina, voriconazol y HPβCD se analizaron mediante microscopía electrónica de transmisión (TEM). Las imágenes demuestran la presencia de agregados esféricos de tamaño nanométrico que pueden mejorar la capacidad de permeación a través de la córnea.

El complejo de inclusión formado entre la natamicina y la HPβCD se estudió mediante RMN. Mediante esta técnica, se hicieron también estudios de competición en la formación de complejo con la HPβCD entre la natamicina y el voriconazol. Como se pudo observar, la natamicina compite con el voriconazol por el mismo lugar de unión a la HPβCD lo que conlleva a la necesidad de ajustar y optimizar la concentración de la ciclodextrina. En nuestro caso el empleo de concentraciones de HPβCD al 40% (p/v) permitió. la preparación de las formulaciones a las concentraciones deseadas (de natamicina 7 mg/mL (p/v) y voriconazol 10 mg/mL).

Una vez estudiados los complejos de inclusión formados, se procedió a la elaboración de dos hidrogeles. Se elaboró un hidrogel con ácido hialurónico (0,4% (p/v)) y otro con un hidrogel comercial (Liquifilm®) basado en polivinil alcohol (PVA) (1,4% p/v) frecuentemente utilizado en la elaboración de formulaciones en los servicios de farmacia hospitalaria. Los hidrogeles se caracterizaron en cuanto a pH, osmolalidad, viscosidad y transparencia. Estos estudios demostraron que los valores obtenidos están dentro del intervalo aceptado para formulaciones tópicas oftálmicas. Los estudios de liberación *in vitro* mostraron perfiles característicos de procesos de difusión de tipo Fickiano para todas las nuevas formulaciones. Además, los estudios de permeabilidad corneal *ex vivo* demostraron una mejora significativa en la permeación transcorneal de la natamicina en comparación con la formulación comercial Natacyn®. Las formulaciones desarrolladas no mostraron ningún indicio de irritación de acuerdo con los resultados de los ensayos de HET-CAM y BCOP, por lo que se pueden considerar formulaciones seguras.

La efectividad antifúngica *in vitro* de los colirios se evaluó mediante el método de difusión de disco, mostrando que las formulaciones desarrolladas presentan actividad contra las especies fúngicas testadas (*Candida albicans* ATCC 90231), *Candida albicans* ATCC 90028, *Paelomyces lilacinus* ATCC 90028, *Aspergillus fumigatus*, *Paelomyces lilacinus*, and *Fusarium solanii*).

Los estudios de mucoadhesión *ex vivo* e *in vivo*, demostraron que la capacidad mucoadhesiva que muestran las nuevas formulaciones se debe fundamentalmente a la ciclodextrina incorporada ya que no se han observado diferencias significativas al incorporar HA o PVA a las concentraciones estudiadas.

Durante la búsqueda de la información publicada sobre la aplicación oftálmica de las ciclodextrinas llevada a cabo durante la investigación recogida en los 3 capítulos anteriores, se comprobó que existe muy poca información sobre su toxicidad y seguridad a nivel oftálmico y sobre su capacidad mucoadhesiva en la superficie ocular. Por lo tanto, en el **capítulo 4**, se muestran los resultados de los estudios de seguridad y permanencia ocular realizados a partir de disoluciones de ciclodextrinas a altas concentraciones. Para ello se han incluido en el estudio diferentes variedades de ciclodextrinas que poseen interés en la elaboración de sistemas de liberación oftálmica de fármacos. Se estudió el efecto de las soluciones de αCD, β-ciclodextrina (βCD), γ- ciclodextrina (γCD), 2-hidroxipropil-α-ciclodextrina (HPαCD), HPβCD, HPγCD, SBEβCD, y β-ciclodextrina parcialmente metilada (RMβCD) sobre la membrana coriolantoidea de huevos fertilizados mediante el ensayo HET-CAM y sobre córneas bovinas empleando el método BCOP. De acuerdo con los resultados obtenidos en estos ensayos, todas las ciclodextrinas son seguras, con excepción de la αCD y la RMβCD. Las disoluciones de RMβCD al 20% (p/v) provocaron un cambio significativo en la transparencia corneal, pero no mostraron cambios en los vasos de la membrana corioalantoidea. Los cambios en la transparencia se deben al bajo valor de pH que se obtiene al disolver esta variedad parcialmente metilada (2,447±0,025). A pH ácidos se puede producir la alteración de proteínas y otros componentes de la mucosa y epitelio causando estas alteraciones. El efecto negativo sobre la transparencia corneal se resolvió al ajustar la disolución de RMβCD a pH 7,4. Las disoluciones de αCD (en disoluciones sin neutralizar y neutralizadas a pH 7,4), no provocaron hemorragia, lisis o coagulación sobre los vasos de la membrana corioalantoidea de los huevos, pero se observó la formación de un fino precipitado blanco sobre ella. Además, también se observó un cambio significativo en la transparencia de la córnea durante el ensayo BCOP. Este fenómeno se debe probablemente a la interacción descrita para la αCD y diferentes fosfolípidos y componentes lipídicos de la membrana, que forman complejos de inclusión insolubles, que pueden precipitar sobre las membranas. La permeabilidad de la fluoresceína a través de las córneas estudiada a través del BCOP se vio afectada por la mayoría de las disoluciones de ciclodextrina estudiadas. Normalmente el aumento de la permeabilidad de la fluoresceína se interpreta como un signo de toxicidad, sin embargo, es conocido que las ciclodextrinas pueden interaccionar con componentes de membrana celular mejorando la permeabilidad a través de diferentes epitelios y barreras sin mostrar efectos tóxicos, incluyendo la permeabilidad transcorneal.

La capacidad mucoadhesiva de las ciclodextrinas se estudió mediante ensayos *in vitro, ex vivo* e *in vivo.* Estos ensayos demostraron la capacidad de las ciclodextrinas para interaccionar y unirse a la mucosa ocular. Los estudios *ex vivo* mostraron que a las concentraciones estudiadas no existen diferencias significativas entre las diferentes ciclodextrinas y presentan niveles similares de mucoadhesión a los observados para algunos polímeros biodhesivos (como HA y PVA) y para sus mezclas con ciclodextrinas. Los estudios *in vitro* realizados a partir de mezclas de mucina y las disoluciones de ciclodextrinas pusieron de manifiesto el establecimiento de interacciones entre las ciclodextrinas y la mucina en disolución, probablemente a partir del establecimiento de enlaces débiles tipo puentes de hidrógeno o interacciones de Van der Waals. En los estudios *in vivo*, se demostró la excelente capacidad de las disoluciones de ciclodextrina para permanecer sobre la superficie ocular. Todos los valores de permanencia (con excepción

de las disoluciones de RMβCD) disminuyeron al ajustar las soluciones a pH 7,4. Esto puede ser debido a una mayor dificultad en el establecimiento de puentes de hidrógeno entre las ciclodextrinas y la mucina causada por la ionización del ácido siálico. En el caso de la RMβCD, la permanencia ocular *in vivo* aumentó al neutralizar la disolución. Valores de pH tan ácidos como los observados para esta disolución sin neutralizar, superan la capacidad tamponadora del ojo, produciendo irritación y daño en el epitelio, lo que promueve el lagrimeo y el parpadeo, aumentando el aclaramiento en su superficie.

La αCD fue la ciclodextrina que mostró el valor de MRT más alto, probablemente debido a la formación de agregados insolubles formados con los fosfolípidos de las células epiteliales. HPαCD, HPβCD y HPγCD mostraron los valores más elevados de $t_{1/2}$, sugiriendo que son las ciclodextrinas hidroxiladas las que más tiempo permanecen sobre la superficie ocular.

Por lo tanto, teniendo en cuenta los resultados obtenidos sobre la seguridad y mucoadhesión ocular de las diferentes ciclodextrinas, así como su capacidad para promover la penetración transcorneal de otras moléculas, hacen de las ciclodextrinas unos excelentes candidatos para la elaboración de formulaciones oftálmicas de fármacos poco solubles en agua o con baja permeabilidad corneal.

En conclusión, en esta tesis doctoral se ha abordado el diseño racional de diferentes formulaciones tópico-oftálmicas para el tratamiento de enfermedades fúngicas oculares. Empleando tres antifúngicos con diferentes espectros de actividad se han desarrollado diferentes formulaciones destinadas a su administración tópico-oftálmica. Además, se ha realizado una completa caracterización preclínica de las mismas. Estas formulaciones tienen un gran potencial para el tratamiento de la queratitis fúngica causada por diferentes especies, que pueden cubrir el vacío terapéutico actual existente. Todas las formulaciones desarrolladas han presentado adecuados niveles de seguridad, actividad *in vitro* y un excelente comportamiento mucoadhesivo, con tiempos de permanencia en la superficie ocular elevados.

Finalmente, los estudios de seguridad y bioadhesión realizados con las disoluciones de ciclodextrinas, demuestran que incluso a concentraciones relativamente elevadas son excipientes adecuados para la elaboración de formulaciones oftálmicas. No obstante, deberían completarse con otros estudios *in vivo* para completar el conocimiento sobre el efecto de las ciclodextrinas sobre la superficie ocular.

INDEX

OBJECTIVES AND ORGANIZATION

STATEMENT OF THE PROBLEM

About 1,000,000 new cases of fungal keratitis are reported worldwide each year. Fungal keratitis is the cause of more than 50% of infectious eye ulcers in countries with tropical climates while infection is rare in temperate climates, where the few infections that do occur are usually caused by the genus Candida.

Fungal keratitis is an uncommon disease in developed countries, although we are currently seeing an increase in the number of cases due to different factors such as poor use of contact lenses, long treatments with corticoids or antibiotics, immunocompromised patients, patients with a previous ocular lesion, etc.

In addition, this disease is difficult to diagnose clinically, as the patient is often asymptomatic, with symptoms often taking days or even weeks to appear. It is also common to confuse this infection with other types of infectious keratitis.

Existing topical antifungal preparations are not as effective as existing preparations for bacterial keratitis, so in most cases prolonged topical and systemic antifungal therapy is required.

Currently, there is only one FDA-approved ophthalmic formulation for the treatment of fungal keratitis. This formulation is based on a natamycin suspension, which is limited to use for filamentous fungal infections and superficial infections due to its low transcorneal penetration. Due to this large therapeutic gap, hospital pharmacy departments are obliged to reformulate formulations intended for other routes (mainly intravenous) by dilution in biocompatible ocular vehicles for the preparation of eye drops. The problem with these extemporaneous preparations is that their ocular toxicity, stability and efficacy are unknown. It should be noted that with these formulations an intensive treatment (every hour) is usually applied to maintain the effective concentration on the ocular surface, which allows resolution of the infection. This intensive dosage causes the patient to abandon the treatment, which worsens the clinical picture and often leads to hospitalization of the patient. This intensive dosing is due to the low permanence of these formulations on the ocular surface due to the intense precorneal clearing caused by high tear renewal and blinking.

On the other hand, the need to increase the bioavailability of drugs via the topical-ophthalmic route leads to the objective of increasing the concentration of the active ingredient on the ocular surface. For the administration of drugs that are not very soluble in water, it will be necessary to increase their solubility by means of different strategies. One of these is the use of cyclodextrins, conical or toroidal oligosaccharides with a lipophilic inner cavity and a hydrophilic surface. They are able to internalize hydrophobic molecules, increasing their solubility, stability and even decreasing their toxicity. In addition, they can significantly increase the permeability of different biological membranes. Generally and to a certain extent, as the concentration of cyclodextrin increases, the amount of solubilized drug will increase (this depends on the interaction between drug and cyclodextrin and their natures). Thus, high concentrations of cyclodextrin will often be needed to solubilize the amount of drug intended to be administered in each dose. At present, knowledge of the effects of cyclodextrins at high concentrations on the ocular surface is unknown, which limits their use.

OBJECTIVES

Taking into account the above considerations, the general objective of this thesis was to improve the pharmacological treatment of fungal keratitis through topical-ophthalmic administration.

To achieve this purpose, the following specific objectives were set out:

1. Development of hydrogels containing econazole as a molecule for the treatment of fungal keratitis.

   1.1. Design, optimization, physicochemical characterization of hyaluronic acid mucoadhesive hydrogels and ion-sensitive hydrogels containing econazole.

   1.2. Evaluation of ocular safety and *in vitro* antifungal effectiveness.

   1.3. Evaluation of *in vivo* bioadhesion by determining the residence time on the ocular surface in murine animal models.

2. Development of voriconazole eye drops that improve the extemporaneous formulation used in hospitals, with the aim of improving their posology by increasing their permanence on the ocular surface.

   2.1. Design, optimization and physicochemical characterization of ion-sensitive hydrogels and mucoadhesive hyaluronic acid hydrogels containing voriconazole.

   2.2. Ocular safety assessment.

   2.3. Evaluation of *in vivo* bioadhesion by determining the residence time on the ocular surface in murine animal models.

3. Development of a new eye drop combining natamycin and voriconazole.

   3.1. Design, optimization and physicochemical characterization of the combined formulations of natamycin and voriconazole.

   3.2. Determination of the antifungal effectiveness of the combination of natamycin and voriconazole against different fungal species in comparison with formulations used in hospital pharmacy services.

   3.3. *In vivo* evaluation of the residence time on the ocular surface of the developed eye drops.

4. Evaluation of the mucoadhesive capacity and safety of cyclodextrins at high concentrations on the ocular surface.

ORGANIZATION

Based on the objectives described above, this doctoral thesis is presented as a compendium of four research papers and a literature review.

This doctoral thesis has been organized to comply with the regulations of the International Doctoral School of the University of Santiago de Compostela in terms of structure, language and ethical and intellectual property.

This doctoral thesis is divided into three sections that correspond to:

1. A general and critical review of the state of the art of the problem to be developed.

2. Development and characterization of topical-ophthalmic formulations containing different drugs useful for the treatment of the disease studied.

3. Characterization in terms of ocular irritation and permanence of excipients useful for the development of ophthalmic formulations.

The first section or introduction corresponds to an in-depth review of the pharmacological and non-pharmacological management of fungal keratitis. It also includes a review of the anatomy of the eye, the factors involved in topical-ophthalmic drug delivery to the anterior segment of the eye and the types of formulations useful in increasing the bioavailability of drugs in the precorneal area.

The second section covers the development and characterization of multiple topical-ophthalmic formulations for the treatment of fungal keratitis. This section comprises the first three chapters. In all three chapters, the ocular safety of the developed formulations and their *in vivo* permanence on the ocular surface are evaluated.

Chapter 1 comprises the characterization of two different hydrogels for topical-ophthalmic administration of econazole: an ion-sensitive hydrogel formed by the combination of gellan gum and kappa carrageenan and a mucoadhesive hydrogel formed by hyaluronic acid.

Chapter 2 comprises the characterization of two different hydrogels for the topical-ophthalmic administration of voriconazole: an ion-sensitive hydrogel formed by the combination of gellan gum and kappa carrageenan and a mucoadhesive hydrogel formed by hyaluronic acid.

Chapter 3 comprises the characterization of two different hydrogels for the topical-ophthalmic administration of natamycin and voriconazole: one hydrogel formed by hyaluronic acid and the other by PVA (Liquifilm®).

The third section corresponds to the fourth chapter and is based on the study of the mucoadhesive capacities of different cyclodextrins at high concentrations using different techniques. In addition, their safety on the ocular surface is evaluated.

ANTECEDENTES DEL PROBLEMA

Cada año se registran alrededor de 1.000.000 de nuevos casos de queratitis fúngica en todo el mundo. La queratitis fúngica es la causa de más del 50% de las úlceras oculares infecciosas en países con climas tropicales mientras que la infección es rara en climas templados, donde las pocas infecciones que hay, generalmente están provocadas por el género *Candida.*

La queratitis fúngica es una enfermedad poco habitual en los países desarrollados, aunque actualmente se está viendo un incremento en el número de casos debido a diferentes factores como el mal uso de las lentes de contacto, los tratamientos largos con corticoides o antibióticos, pacientes inmunocomprometidos, pacientes con una lesión ocular previa, etc.

Además, esta enfermedad presenta un diagnóstico clínico complicado ya que es frecuente que el paciente sea asintomático, tardando días o incluso semanas en aparecer los síntomas. Es habitual también confundir esta infección con otros tipos de queratitis infecciosas.

Las preparaciones tópicas antifúngicas existentes a día de hoy no son tan efectivas como las preparaciones existentes para las queratitis bacterianas, por lo que en la mayoría de los casos se requiere una terapia antifúngica tópica y sistémica prolongada.

En la actualidad, sólo existe una formulación oftálmica aprobada por la FDA para el tratamiento de la queratitis fúngica. Esta formulación se basa en una suspensión de natamicina, que se limita a su utilización en caso de infecciones por hongos filamentosos e infecciones superficiales, debido a su baja penetración transcorneal. Debido a este gran vacío terapéutico, los departamentos de farmacia hospitalaria se ven en la obligación de reformular formulaciones destinadas a otras vías (principalmente intravenosas) mediante su dilución en vehículos oculares biocompatibles para la preparación de colirios. El problema de estas preparaciones extemporáneas es que se desconoce su toxicidad ocular, su estabilidad o su eficacia. Cabe destacar, que con estas formulaciones se suele aplicar un tratamiento intensivo (cada hora) para mantener la concentración eficaz sobre la superficie ocular, que permita la resolución de la infección. Esta posología intensiva provoca abandonos del tratamiento por parte del paciente, que empeoran el cuadro clínico provocando en muchas ocasiones la hospitalización del paciente. Esta posología intensiva, se debe a la baja permanencia sobre la superficie ocular que presentan estas formulaciones debido al intenso aclaramiento precorneal, provocado por alta renovación lagrimal y el parpadeo.

Por otra parte, la necesidad de aumentar la biodisponibilidad de los fármacos a través de la vía tópico-oftálmica, nos conduce al objetivo de aumentar la concentración de principio activo sobre la superficie ocular. Para la administración de fármacos poco solubles en agua, será necesario aumentar su solubilidad mediante diferentes estrategias. Una de ellas es el uso de las ciclodextrinas, oligosacáridos con forma cónica o toroidal que presentan una cavidad interior lipofílica y una superficie hidrofílica. Son capaces de internalizar moléculas hidrofóbicas, aumentando su solubilidad, estabilidad e incluso disminuyendo su toxicidad. Además, pueden aumentar de forma considerable la permeabilidad de diferentes membranas biológicas. Generalmente y hasta cierto punto, a medida que se aumenta la concentración de ciclodextrina aumentará la cantidad de fármaco solubilizado (esto es dependiente de la interacción que se genere entre fármaco y ciclodextrina y de sus naturalezas). De esta forma, en muchas ocasiones

se necesitarán altas concentraciones de ciclodextrina para solubilizar la cantidad de fármaco que se pretenda administrar en cada dosis. Hoy en día, el conocimiento sobre los efectos de las ciclodextrinas a altas concentraciones sobre la superficie ocular se desconoce, lo que limita su utilización.

OBJETIVOS

Teniendo en cuenta las consideraciones anteriores, el objetivo general de esta tesis fue el de mejorar el tratamiento farmacológico de la queratitis fúngica a través de la administración tópico-oftálmica.

Para lograr este propósito, se plantearon los siguientes objetivos específicos:

5. Desarrollo de hidrogeles conteniendo econazol como molécula para el tratamiento de la queratitis fúngica.

   5.1. Diseño, optimización, caracterización fisicoquímica de hidrogeles mucoadhesivos de ácido hialurónico y de hidrogeles sensibles a iones conteniendo econazol.

   5.2. Evaluación de la seguridad ocular y de la efectividad antifúngica *in vitro*.

   5.3. Evaluación de la bioadhesión *in vivo* determinando el tiempo de residencia sobre la superficie ocular en modelos animales murinos.

6. Desarrollo de colirios de voriconazol que mejoren la formulación extemporánea utilizada en los hospitales, con el objetivo de mejorar su posología aumentando la permanencia sobre la superficie ocular.

   6.1. Diseño, optimización y caracterización fisicoquímica de hidrogeles ión-sensibles e hidrogeles mucoadhesivos de ácido hialurónico conteniendo voriconazol.

   6.2. Evaluación de la seguridad ocular.

   6.3. Evaluación de la bioadhesión *in vivo* determinando el tiempo de residencia sobre la superficie ocular en modelos animales murinos.

7. Desarrollo de un nuevo colirio que combine natamicina y voriconazol.

   7.1. Diseño, optimización y caracterización fisicoquímica de las formulaciones combinadas de natamicina y voriconazol.

   7.2. Determinación de la efectividad antifúngica de la combinación de natamicina y voriconazol frente a diferentes especies fúngicas en comparación con las formulaciones utilizadas en los servicios de farmacia hospitalaria.

   7.3. Evaluación *in vivo* del tiempo de residencia sobre la superficie ocular de los colirios desarrollados.

8. Evaluación de la capacidad mucoadhesiva y de la seguridad que presentan las ciclodextrinas a altas concentraciones sobre la superficie ocular.

ORGANIZACIÓN

En base a los objetivos descritos, esta tesis doctoral se presenta como un compendio de cuatro trabajos de investigación y un trabajo de revisión bibliográfica.

Esta tesis doctoral se ha organizado para cumplir la normativa de la Escuela Internacional de Doctorado de la Universidad de Santiago de Compostela en cuanto a estructura, idioma y propiedad ética e intelectual.

Esta tesis doctoral se divide en tres apartados que corresponden con:

1. Una revisión general y crítica del estado del arte del problema a desarrollar.
2. Desarrollo y caracterización de formulaciones tópico-oftálmicas que contengan diferentes fármacos útiles para el tratamiento de la enfermedad estudiada.
3. Caracterización en cuanto a irritación y permanencia ocular de excipientes útiles para el desarrollo de formulaciones oftálmicas.

La **primera sección** o introducción corresponde a una revisión profunda del manejo farmacológico y no farmacológico de la queratitis fúngica. Además, se incluye una revisión de la anatomía del ojo, de los factores que intervienen en la administración tópica-oftálmica de fármacos sobre el segmento anterior del ojo y sobre los tipos de formulaciones útiles en el aumento de la biodisponibilidad de los fármacos en el área precorneal.

La **segunda sección** engloba la elaboración y caracterización de múltiples formulaciones tópico-oftálmicas destinadas al tratamiento de la queratitis fúngica. Este apartado comprende los tres primeros capítulos. En los tres capítulos se evalúa la seguridad ocular de las formulaciones desarrolladas y su permanencia *in vivo* sobre la superficie ocular.

El capítulo 1 comprende la caracterización de dos hidrogeles diferentes para la administración tópica-oftálmica del econazol: un hidrogel ión-sensible formado por la combinación de goma gellan y carragenato kappa y otro hidrogel mucoadhesivo formado por ácido hialurónico.

El capítulo 2 comprende la caracterización de dos hidrogeles diferentes para la administración tópica-oftálmica del voriconazol: un hidrogel ión-sensible formado por la combinación de goma gellan y carragenato kappa y otro hidrogel mucoadhesivo formado por ácido hialurónico.

El capítulo 3 comprende la caracterización de dos hidrogeles diferentes para la administración tópica-oftálmica de la natamicina y el voriconazol: un hidrogel formado por ácido hialurónico y otro por PVA (Liquifilm®).

La **tercera sección** corresponde al cuarto capítulo y se basa en el estudio mediante diferentes técnicas de las capacidades mucoadhesivas de diferentes ciclodextrinas a concentraciones altas. Además, se evalúa su seguridad sobre la superficie ocular.

INTRODUCTION

GENERAL INTRODUCTION

1. OCULAR ANATOMY AND PHYSIOLOGY

The eye is the organ responsible for vision. It presents complex anatomy and physiology that provides insulation and protection. The eyeball occupies only one-third of the orbit, the other two-thirds are occupied by muscles, nerves, and blood vessels (1).

The eye can be divided into two segments:

Anterior segment: It comprises the cornea, limbus, conjunctiva, anterior and posterior chambers, trabecular meshwork, Schemm's duct, iris, pupil, lens, zonules, ciliary body, and aqueous humor.

Posterior segment: It comprises the posterior part of the sclera, the uveal tract, the vitreous humor, the retina, the choroid, and the optic nerve.

In addition, the eye is composed of three main layers: the sclerocorneal layer, the uveal layer, and the retinal layer (2).

The sclerocorneal layer is the outermost layer. It is formed by the sclera, which provides structural support, and the cornea, which is the main refractive element towards the retina. The sclera and the cornea are joined through the limbus (2,3).

The middle layer is the uveal layer. It is a highly vascularized layer composed of the choroid, ciliary body, and iris. The iris comprises pigmented epithelial cells and circular muscles that regulate the size of the pupil and thus the entry of light into the eye. The choroid lies between the sclera and the retina. Its main functions are to provide nutrition to the retina, adjust its position and secrete growth factors (4), among others. In the anterior part of the eye, the choroid is attached to the ciliary body, which is attached to the lens through a suspensory ligament (2). The ciliary body secretes aqueous humor, which circulates through the anterior and posterior chambers supplying nutrients and oxygen to the lens and cornea. The aqueous humor drains into Schlemm's canal.

The retinal layer is the innermost layer of the eye. It consists of the photosensitive retina in the posterior segment (ending at the ora serrata) and continues in the anterior segment as a non-photosensitive epithelium covering the posterior part of the iris and the ciliary body. The fovea, located at the back of the retina, is the area of highest visual acuity and is surrounded by the macula, a yellowish region. The optic nerve exits the eye through the laminae cribrosa, the part of the sclera covered by the optic disc, which lacks photoreceptors (2).

2. ANATOMY OF THE CORNEA

The cornea is the front part of the eye. It is a curved and transparent structure (5) and is the main refractive element of the eye (6). It is an avascular connective tissue, highly innervated (7) and organized in 3 overlapping layers (epithelium, stroma, and endothelium) and three interfaces (Bowman's membrane, Dua's layer, and Descemet's membrane) (8,9).

The corneal epithelium is a squamous, stratified, non-keratinized layer consisting of 5 or 6 layers of cells. The superficial layers (2 or 3) are formed by flat polygonal cells that present microvilli and micropliace in their apical part. These structures increase the surface area of interaction between the superficial cells and the mucin layer of the tear film. The suprabasal

layers (2 or 3) are formed by winged cells (wing cells) less flat than the superficial ones and the basal layer is formed by a single layer of columnar cells. All the cells of the different layers of the epithelium present very tight junctions between them (8,10).

Bowman's membrane is an acellular layer formed by type I and type III collagen fibers and proteoglycans (9). It is found between the epithelium and the stroma and its function is not clear (11).

The corneal stroma constitutes 90% of the corneal structure (8). The main cellular components of the stroma are keratocytes, which produce collagen and proteoglycans. Keratocytes are widely dispersed occupying only 2-3% of the total stromal volume, the rest of the stromal volume is mainly occupied by components of the extracellular matrix (collagen and proteoglycans (8)) and collagen fibers (9) arranged in parallel forming lamellae.

Between the stroma and Descemet's membrane, there is Dua's layer (12), recently discovered, although there is controversy regarding its discovery (13). It is an air-impermeable layer formed by 5 - 8 compact sheets of collagen type I and VI and a low density of keratocytes (14).

Descemet's membrane is located between the stroma and the endothelium. It is mainly composed of collagen type IV and VIII, laminin, fibronectin, and proteoglycans (9). Its main functions are to maintain corneal hydration, the differentiation and proliferation of endothelial cells, and the maintenance of corneal curvature, in addition to maintaining the integrity of the corneal structure (15).

The endothelium is the deepest layer of the cornea and is composed of a single layer of hexagonal cells joined together by very tight junctions (8,16). The main function of the endothelium is to control the movement of aqueous humor into the stroma, thus maintaining proper corneal hydration (16).

3. DRUG PASSAGE THROUGH THE CORNEA

The cornea represents the main biological barrier of the eye, preventing the entry of microorganisms and foreign substances (including drugs) into the interior of the eyeball (10). The different anatomical characteristics of its layers greatly complicate the permeability of drug molecules to the interior of the ocular tissues, being conditioned by their lipophilicity, molecular weight, charge, and degree of ionization (17).

The corneal epithelium presents different types of junctions between its cells. Apical cells are joined by desmosomes, adherens junctions, and tight junctions. The winged cells of the suprabasal layer are joined by desmosomes and adherens junctions (18). Basal or columnar cells are joined by desmosomes, GAP junctions, and tight junctions. They are also attached to the basal layer by hemidesmosomes (9). In the corneal stroma, there are no tight junctions, but the stromal cells (keratocytes) are joined together by GAP junctions (9). Endothelial cells present zonula occludens or tight junctions, macula occludens, and macula adherens or desmosomes (9).

The tight junctions present both in the epithelium and in the corneal endothelium are responsible for restricting the passage by diffusion mechanisms of small hydrophilic molecules to the internal ocular tissues (aqueous humor, iris, and uvea) by the paracellular route (9), while the hydrophobic molecules that can cross the epithelium by the transcellular route, will see their

permeability conditioned by the hydrophilic nature of the stroma (7,19). Drugs with a molecular weight greater than 500 Da do not cross the cornea, while those with a molecular weight below 100 Da cross it without any difficulty. Ionization of drug molecules can also interfere with passage through the different layers. Thus, there must be a balance between the ionized and non-ionized forms of the drug so that the molecules can penetrate completely (20). Once the drug has passed through the cornea and reached the aqueous humor, it is distributed by diffusion processes to the surrounding tissues (ciliary body, iris, lens) and to the vitreous humor (21).

In addition, the passage of molecules across the cornea can be affected by the presence of transmembrane efflux and influx pumps expressed on the corneal surface (and in other ocular structures) that also limit the passage of molecules to the inner tissues of the eye (7,22,23). Efflux pumps such as the transmembrane glycoprotein P-gp, multidrug resistance-associated protein (MRP), and breast cancer-resistant protein (BCRP) are members of the ABC (ATP Binding Cassette) family of transporters. These efflux transporters can block drug entry into cells, protecting them from potential damage associated with toxic metabolites and other foreign molecules (22). Efflux pumps belong to the solute carrier (SLC) family of transporters with amino acid and peptide transporters being the most common for ocular delivery, although cation/organic anion (SLC22), monocarboxylate (SLC16), and nucleoside transporters (SLC28 and 29) have also been identified in various ocular tissues. To improve the bioavailability of certain drugs with low permeability, it would be desirable to employ transporter-targeted prodrugs, which would help the evasion of efflux pumps and entry into the cell via an influx transporter (23).

4. OCULAR DRUG DELIVERY: TOPICAL ADMINISTRATION

Ocular administration of drugs can be carried out by three different methods: direct injection (intravitreal, peribulbar, retrobulbar, suprachoroidal...), systemic administration, or topical administration (17).

Topical administration is the most appropriate way to achieve therapeutic levels in the anterior segment, besides representing the least invasive method of ophthalmic application, since it is well tolerated by patients because it is painless, simple, and easy to self-administer (7,23). The main disadvantage is that its bioavailability is significantly low, with less than 5% of the administered drug reaching the intraocular tissues (aqueous humor among others) (24,25) and only 0.001% of the fraction that penetrates reaches the posterior segment of the eye (26). Once the drug is administered on the surface of the eye it is rapidly eliminated from the precorneal area by the protective mechanisms of the eye such as nasolacrimal drainage, blinking (6 to 15 times per minute), tear turnover rate (0.5-2.2 µL/min) and high tear clearance (27,28), as well as unproductive absorption into the systemic circulation through the conjunctiva, choroid, uveal tract, and inner retina.

The topically administered drug is released from the vehicle into the tear film. The tear film has a complete renewal every 2-3 minutes, which accelerates the elimination of the drug from the precorneal area through the nasolacrimal drainage. In addition, enzymes (carbonic anhydrase and esterase enzymes) and proteins present in the tear may influence the metabolization of the active ingredient (26).

The tear drainage rate is conditioned by different factors that can accelerate reflex lacrimation and increase the number of blinks. Among these factors are pH, osmolality, limpidity, and viscosity (among others) of the administered formulations.

4.1. pH

The pH of ophthalmic formulations should be similar to the pH of the tear (7.4) to avoid irritation at the ocular level, since this irritation could produce an increase in lacrimation as a mechanism to restore normal physiological conditions, increasing the elimination of the drug in the precorneal area (29). Although the recommendation is that ophthalmic formulations should have a pH of around 7.4 to avoid irritation of the ocular surface, it is important to consider the pH at which the drug is most stable and at which its absorption is favored. In addition, tears have a certain buffering capacity, between pH 4 and 8 (30) due to the presence of bicarbonate ions, proteins, and mucins (31), so small pH deviations in ophthalmic formulations can be buffered without producing irritation or lacrimation.

4.2. Osmolality

Osmolality is considered a secondary aspect in the development of new ophthalmic formulations, but it should be taken into account that hyperosmolality will produce an osmotic movement of water to the conjunctival sac, producing a dilution of the administered drug, increasing its elimination (32). Thus, the osmolality values of ophthalmic formulations should be as close as possible to the osmolality of the tear fluid (290 mOsm/kg).

4.3. Limpidity

All ophthalmic formulations should be observed for the presence of suspended particles (the size of any particle administered into the eye should be less than 10 µm (29,33)) since at the topical level, these particles can cause epithelial damage leading to infection or corneal scarring (29), as well as the production of tear in excess that increases the rate of drug clearance from the ocular surface. Removal of possible suspended particles can be accomplished by using 0.22 µm membrane filters, which will remove all particles larger than this pore size. In addition, if filtration is performed under sterile conditions, such filters will also serve to sterilize the formulation.

4.4. Viscosity

Normally, the volume of instilled formulation is around 40 - 50 µL, but during blinking, the volume of liquid remaining on the ocular surface is reduced to 10 µL, which when mixed with tear fluid will reduce its concentration to a quarter (34). An increase in the viscosity of the instilled formulation through the use of polymers can prolong the residence time of that volume in the precorneal area if the formulation exceeds a viscosity of 20 cP (29). Increasing the contact time with the precorneal area allows for a decrease in the number of instillations, since increasing the time the drug remains in the eye can increase the bioavailability of the drug by up to 50% (24).

The polymers used to increase viscosity are high molecular weight hydrophilic polymers such as methylcellulose, hydroxyethylcellulose, alginates, poly(vinylpyrrolidone) (PVP),

polyethylene glycol (PEG), polyvinyl alcohol (PVA) or hyaluronic acid (HA), among others (29,35,36).

5. OPHTHALMIC FORMULATIONS INTENDED TO INCREASE DRUG BIOAVAILABILITY IN THE PRECORNEAL AREA.

Generally, to improve the efficacy of topical ophthalmic formulations, there is a tendency to use fortified formulations containing very high drug concentrations. An intensive dosage (repeating the administration every hour, for example) is also often maintained, which can lead to systemic side effects due to unproductive absorption of the drug (through the conjunctiva, choroid, uveal tract, and inner retina) and cellular damage of the ocular surface (37), which leads to early discontinuation of treatment by the patient. This generally leads to a worsening of the clinical picture and hospitalization of the patient, thus increasing healthcare costs.

Over the years, research in the development of new formulations has focused mainly on two strategies to improve the bioavailability of drugs through the ophthalmic topical route: increasing the biopermanence of the drug in the precorneal area and increasing the permeability of the drug through the cornea, sclera, and conjunctiva (38).

These two objectives can be achieved by developing easy-to-administer and easy-to-formulate systems based mainly on polymers that increase the viscosity of the formulations and increase adhesion to the mucin layer of the tear (mucoadhesive systems), or that undergo a change in their conformation on contact with the surface of the eye (*in situ* gelling systems). In addition, there are different tools to improve drug permeability that can be combined with polymeric systems, such as the use of cyclodextrins that can significantly increase the solubility of hydrophobic drugs in aqueous vehicles.

5.1. MUCOADHESIVE SYSTEMS

Mucoadhesive systems are formed by polymer solutions capable of interacting with the acidic remains (sialic remains) of the mucin present in the lacrimal fluid (39) increasing the contact time with the ocular surface.

Several theories have been described to explain the mechanisms by which mucoadhesion takes place, such as the wetting theory that describes the ability to spread through the mucin layer; the electrostatic theory that proposes mucoadhesion as a result of the attractive forces between the charges of the polymer and the mucin; the adsorption theory in which the polymer chains bind to the mucin by Van Der Waals forces, hydrogen bridges, or hydrophobic interactions; the diffusion theory which describes the interpenetration of the polymer chains into the mucin layer forming semi-permanent bonds; and the fraction theory, which analyzes the forces required to separate mucoadhered surfaces (40–42). It is likely that mucoadhesion is a combination of all the described theories.

Numerous polymeric solutions have been used to increase mucoadhesion at the topical ophthalmic level, such as methylcellulose, hydroxyethylcellulose, carboxymethylcellulose, chitosan, sodium alginate, povidone, polyvinyl alcohol or hyaluronic acid (HA) (35,43).

Hyaluronic acid or sodium hyaluronate (HA) is a glycosaminoglycan composed of repeating disaccharide units of D-glucuronic acid and N-acetyl-D-glucosamine. It is a natural polymer

endogenous in the human body, being present in the skin, umbilical cord, synovial fluid, lungs, heart valves, aorta, or vitreous humor, among others (44). HA has anti-inflammatory, immunosuppressive, antiangiogenic, and analgesic properties, which give it numerous applications (45). It also exhibits biophysical characteristics similar to tear mucins, providing long-lasting water retention and hydration (37). Several studies have demonstrated the ability of HA to protect epithelial cells from dehydration and to increase their proliferation (46,47). In addition, it has been shown to be effective in recovery after anterior chamber surgery (48–50) and is widely used in the treatment of dry eye (51–53).

Its negative charge facilitates adhesion to the ocular surface, which gives it mucoadhesive properties, and although its bioadhesive capacity is lower than that of other polymers, it has been shown to improve the bioavailability of several drugs when compared to other polymers. This fact shows that polymers that present properties similar to tear mucin can significantly increase the bioavailability of some drugs (54,55).

5.2. *IN-SITU* GELATION SYSTEMS

In situ gelling systems are liquid polymeric systems that crosslink in the presence of a stimulus or a combination of stimuli, such as ocular surface temperature, pH, or the presence of certain tear ions. They can be classified as thermo-sensitive, pH-sensitive, and ion-sensitive *in situ* gelling systems.

Their main advantages are increased corneal retention, precise dose delivery, and control of drug release (56).

5.3. THERMOSENSITIVE *IN-SITU* GELLING SYSTEMS

Thermo-sensitive *in situ* gelation systems are formed by polymers capable of changing their physical properties through a variation in temperature. These systems are based on the critical solution temperature of polymers such as poloxamer, chitosan, or polyacrylic acid, among others (35). An increase in the temperature of the polymer solution will cause the interactions between the hydrophobic and hydrophilic groups of the polymer chains and the water molecules to change, causing a decrease in the solubility of the polymers in water and thus leading to gel formation (57). Numerous studies have been described proposing various hydrogels for the treatment of ophthalmic pathologies based on thermosensitive polymers (58–61).

5.4. PH-SENSITIVE *IN-SITU* GELLING SYSTEMS

pH-sensitive in situ gelation systems are made up of polymers composed of acidic (anionic) and basic (cationic) groups such as carbomers, macrogol, or methacrylic acid, among others (35). Depending on the pH of the medium in which these systems are applied, the polymers will modify their solubility in water, gelling according to their ionizable groups (62). Several authors have published studies in which they have developed pH-sensitive hydrogels for the treatment of ophthalmic pathologies (63–65).

5.5. ION-SENSITIVE *IN-SITU* GELATION SYSTEMS

Ion-sensitive *in-situ* gelling systems are based on the interaction of anionic polymers with the cations of the tear fluid (Na^+, K^+, Mg^{2+}, Ca^{2+}) (66). The most commonly used natural anionic

polymers for the formulation of these systems are gellan gum (GG), carrageenans, and alginate, among others (30,35,67–70).

In these systems, the transition from solution to gel occurs when the polymer molecules in solution come into contact with the monovalent (Na^+, K^+) and/or divalent (Mg^{2+}, Ca^{2+}) cations of the tear, triggering the union of the polymer chains by ionic bonds between the negatively charged groups of their structures with the positive charges of the cations of the tear.

Gellan gum (GG) is a natural polymer produced by Pseudomonas elodea. It consists of repeating units of glucose, glucuronic acid, and rhamnose with acetate and glycerate groups, although the one used for formulation is deacetylated. The transition from solution to gel occurs when the molecules in solution of GG come into contact with divalent Ca^{2+} cations (it can be triggered with others, but with Ca^{2+} especially) forming aggregation zones between the chains with a double helix structure to form a three-dimensional network (69). This gelation mechanism is simpler in the case of deacetylated GG due to the elimination of acetate and glycerate groups (56,71).

Carrageenans are natural linear polymers from red algae (*Rhodophyceae*). They are composed of repeating units of galactose and anhydrogalactose linked by glycosidic bonds. There are three types of carrageenans and they differ in the degree of substitution of the sulfate group, in the position of the sulfate ester groups, and in the presence or absence of anhydrogalactose units: kappa (κ), iota (ι), and lambda (λ).

Only κ and ι form gels: carrageenan κ (CK) gels in the presence of K+ and carrageenan ι in the presence of Ca^{2+} (69,72). Gelation takes place by aggregation of the helical dimers through intermolecular interactions giving rise to a stable three-dimensional network (73).

Alginate is a linear polymer produced by several types of bacterial strains (*Laminaria hyperborea, Laminaria digitata, Laminaria japonica, Ascophyllum nodosum,* and *Macrocystis pyrifera*) and brown algae (*Phaeophyceae*) (74). It consists of blocks of glucuronic acid and mannuronic acid residues (56). Like gellan gum, the fastest alginate gelation reaction occurs when the polymer solution is brought into contact with Ca^{2+} cations (the gelation reaction can be triggered by other divalent cations) that bind the glucuronic acid blocks together forming the so-called egg-box structure (56). Generally, alginate is used in combination with other polymers (75).

6. CYCLODEXTRINS

Cyclodextrins are cyclic oligosaccharides formed by α-D-glucopyranose units linked by α-D-(1,4) bonds obtained during the enzymatic degradation of starch. Depending on the number of α-D-glucopyranose units forming them, they are classified as alpha-cyclodextrin (αCD) (6 units), beta-cyclodextrin (βCD) (7 units) and gamma-cyclodextrin (ɣCD) (8 units). They have cone- or toroid-shaped structures with a hydrophobic interior cavity (lined by the carbons of the molecular backbone and the oxygens of the glucose residues) and a hydrophilic outer surface (with numerous hydroxyl groups, primary in C6 position and secondary in C2 and C3 position) (76).

There are different types of synthetic cyclodextrins (2-hydroxypropyl-β-cyclodextrin (HPβCD), hydroxypropyl-ɣ-cyclodextrin (HPɣCD), sulfobutylether-β-cyclodextrin (SBECD),

methyl-β-cyclodextrin (MβCD), among others), derived from natural cyclodextrins (αCD, βCD and ɣCD). They are obtained mainly by substitution of the hydroxyl groups present on the external surface. These substitutions improve certain characteristics of natural cyclodextrins, such as the low water solubility exhibited by βCD (77).

Cyclodextrins are able to internalize hydrophobic drug molecules or part of them in their cavity, forming inclusion complexes that can improve the aqueous solubility of the molecule, reduce or decrease toxicity, improve drug stability, etc (78–80). They are widely used as excipients in the formulation of topical ophthalmic drugs and have been shown to increase the bioavailability of poorly soluble drugs, reduce ocular irritation and improve corneal permeability (78,81,82).

SPECIFIC INTRODUCTION

7. FUNGAL KERATITIS

Ocular fungal infections can affect different parts of the eye such as the lacrimal apparatus, conjunctiva, eyelids, and even the bony orbit, although most commonly the affected parts are the cornea (keratitis) or the vitreous humor (endophthalmitis) (83).

Fungal keratitis or mycotic keratitis is an infection of the cornea and can be caused by filamentous fungi, the most common being *Fusarium* spp., *Aspergillus* spp. *Curvularia* spp and *Penicillium* spp, (84) or by yeasts, *Candida albicans* being the most frequent (85), although it can be caused by other genera (Table 1).

The severity of the disease lies mainly in the lack of effective drugs available, the difficulty in diagnosis, and the delay in starting effective treatment. These factors lead to blindness (86) or even omplete loss of the eyeball.

Table 1. Fungal species implicated in fungal keratitis.

Genus	Specie	Reference
	YEAST	
Blastoschizomyces	*B. capitatus*	(87,88)
Candida	spp *(C. albicans, C. guilliermondii, C. parapsilosis, C. tropicalis, C. glabrata)*	(89–94)
Cryptococcus	*C. albidus*	(95,96)
Malassezia	*M. restricta*	(97)
Pichia	spp *(P. ohmeria, P. anomala)*	(98)
Trichosporon	spp *(T. beigelli, T. asahii)*	(93,99)
	SEPTATE FILAMENTOUS FUNGI	
Acremonium	spp	(92,94,100,101)
Alternaria	spp	(92,100,102)
Aspergillus	spp *(A. flavus, A. fumigatus, A. niger, A. nomius, A. pseudonomius, A. sydowii, A. terreus, A. tamrii, A. effusus, A. protuberus, A. minisclerotigenes)*	(90,92–94,103–112)
Beauveria	*B. bassiana*	(113,114)
Bipolaris	spp	(94,100)
Cladosporium	spp	(115)
Colletotrichum	spp *(C. truncatum, C. tropicale, C. fusiforme, C. fructicola, C. gloeosporioides)*	(116–120)
Curvularia	spp	(92,94,100,121,122)
Cylindrocarpon	*C. lichenicola*	(123–125)
Drechslera	spp	(126)
Epicoccum	spp	(100)
Exophiala	spp *(E. Phaeomuriformis)*	(127–129)
Fusarium	spp *(F.epishaesia, F. moniliforme, F. osysporum, F. solanii)*	(90,92,94,107,109,110,130–133)
Histoplasma	*H. capsulatum*	(134)
Lasiodiplodia	spp *(L. threobromae)*	(135–137)
paecilomyces	spp *(P.farinosus, lilacinus)*	(92,94,138)
Penicillium	*(P. expansum, P. marneffei, P. farinosus)*	(92,111,139)
Phialophora	*verrucosa*	(140)
Phoma	spp *(P. gardeniae)*	(94,141)
Scedosporium	spp *(S. apiospermun, S. prolificans)*	(90,94,100,142,143)
Scytalidium	*spp (S. dimidiatum)*	(144,145)
Trichophyton	spp *(S. interdigitale, S. schoenleinii)*	(146–149)
Ulocladium	spp *(U. atrum)*	(100,150)
	NOT SEPTATE FILAMENTOUS FUNGI	
Absidia	*corymbifera*	(151)
Mucor	spp	(92,109)
Rhizopus	spp	(92)
	DIMORPHIC FUNGI	
Blastomyces	spp	(152)
Coccidioides	*immitis*	(153,154)
Paracoccidioides	*brasiliensis*	(153,154)
Sporothirx	*schenckii*	(153,154)

About 1,000,000 new cases of fungal keratitis are reported worldwide each year (84). Fungal keratitis is the cause of more than 50% of infectious ocular ulcers (85,155) in countries with tropical climates, whereas infection is rare in temperate climates, where the few infections that do occur are generally caused by the genus *Candida.*

The most frequent risk factor is trauma with contaminated plant material (135,140,156), and it is most often associated with rural areas, where agriculture is the main resource (144,154).

It is an uncommon disease in more developed countries, although an increase is currently being seen due to different factors such as the misuse of contact lenses (90,113,138,142,145), long treatments with corticosteroids and local or systemic antibiotics, immunocompromised patients (83,116,139,143,157), previous ocular lesions (132), dry eye, or even corneal transplantation (114) since there is no antifungal preventive treatment in the preparation of donated eyeballs (158).

Keratitis presents a complicated clinical diagnosis since it is common for the patient to be asymptomatic after the trauma, and it takes days or even weeks to feel pain, photophobia, or conjunctival injection. Moreover, it is common to confuse it with other types of infectious keratitis since the first symptoms are usually common and non-specific (9) and the clinical features depend on the type of fungus and the progression of the disease. During the latency period, the epithelium may heal completely above the focus of infection. As time passes, inflammatory processes lead to the permanent breakdown of the epithelium, ulceration of the stroma, or even involvement of Descemet's membrane, producing a descemetocele that may lead to perforation of the cornea (83).

The infection usually presents suppurative ulcers (159), recurrent, with irregular borders, dry surface, and occasionally with "satellite" lesions (94,160) peripheral to the infiltration area.

Due to the difficulty of clinical diagnosis, a microbiological diagnosis should be performed in all cases to ensure which species is responsible for the infection. For sampling, corneal scrapings with a spatula or scalpel blade are preferred because the organisms may be in deeper tissue (9). In addition, confocal microscopy allows *in vivo* examination and provides high-resolution images of the corneal layers (110,129,154,161).

8. PHARMACOLOGICAL TREATMENT OF FUNGAL KERATITIS

The mechanism of action in fungal keratitis should aim at early diagnosis, immediate eradication of the infection, effective simultaneous treatment options, minimization of complications, and prevention of recurrence.

The effectiveness of treatment lies primarily in the early initiation of therapy. Antifungal treatment should be initiated as soon as the microbiological diagnosis of fungal keratitis has been made. Formulations developed for this pathology should have good ocular penetration as well as a broad spectrum of action against the fungal pathogens that can cause the disease. The formulations chosen should not cause ocular irritation or toxicity (153), unless there is no other effective treatment with these characteristics against the pathogen causing the lesion. Topical antifungal administration is the most appropriate route to achieve therapeutic levels in the corneal epithelium, where the molecular weight of the active ingredient acts as a key factor due to its influence on corneal permeability. Other routes of administration, such as systemic or

intraocular, are chosen according to the resistance of the pathogen or the affected area of the eyeball (162).

Existing topical antifungal preparations are not as effective as preparations for bacterial keratitis, so in most cases, prolonged topical and systemic antifungal therapy is required. If pharmacologic treatment fails, surgical treatment in the form of penetrating keratoplasty or conjunctival flap may be required. In most cases, fungal keratitis requires the maintenance of topical antifungal medications for a long period of time (greater than 6 weeks) to reduce possible recurrences. In some cases, it may be necessary to extend treatment to 12 weeks, especially in filamentous keratitis or in the presence of deep stromal infiltrates. Local or systemic antifungal drugs have also been shown to be effective after penetrating keratoplasty. Topical medications are generally administered hourly (day and night) for the first 48 hours and thereafter only during the day.

Once the presence of symptoms or signs of corneal fungal infections is detected, effective antifungal treatment based on inhibition of fungal penetration into the corneal stroma and anterior chamber should be established. Early eradication of microorganisms and suppression of inflammation are the main established goals of drug therapy.

Drug selection is dependent on the etiology of the disease, where the diagnosis is made through specific culture media that allow deciding which is the best pharmacological treatment.

Over the years, many drugs (from antiseptics to antibiotics) have been used for the treatment of fungal keratitis, although the most commonly used drugs belong to three different groups: polyenes, azoles, and pyrimidines.

Table 2. Representative drugs in the treatment of fungal keratitis, marketed drugs and formulations used. Table modified from (175).

GROUP	DRUG	MARKETED OPHTHALMIC MEDICINES	PHARMACEUTIAL COMPOUNDING	REF.
Polyenes	Natamycin	Natacyn® (USA)	-	(163–168)
	Amphotericin B	-	0.15 % - 0.2 %	(163,164,169–171)
Imidazoles	Miconazole	-	1 %	(163,164,169)
	Econazole	Aurozole® (India)	0.2 – 1 %	(103,113,121)
	Ketoconazole	-	1 %	(163,168,169)
Triazoles	Itraconazole	Itral® (India) Entozole® (India)	-	(163,165,168)
	Fluconazole	Zocon® (India)	0.2 - 2 %	(153,163,170)
	Voriconazole	Vozole® (India)	1 %	(153,163,170)
Pyrimidines	5-Flucytosine	-	1 % (always in combination with amphotericin B)	(163,173,174)

8.1. POLYENES

Polyenes are characterized by a complex structure, composed by a macrocyclic lactone ring with several carbon-carbon conjugated bonds. Within this group, amphotericin B and natamycin are two of the most used drugs as first-line treatment in fungal keratitis.
In general, resistance to polyenes is rare, but it has been described in some occasions. This resistance occurs due to the ergosterol exhaustion and the 14α-methylphecosterol accumulation in fungal cell membranes as a consequence of a desaturase enzyme inhibition (176).

8.2. AMPHOTERICIN

Amphotericin B was the first broad-spectrum antifungal agent discovered. It was isolated for the first time in 1950 from the *Streptomyces nodosus* actinobacteria (177). It has a broad spectrum of action against yeasts (*Candida* spp.) and filamentous fungi (*Aspergillus* spp., *Penicillum* spp., ...) (178). Anphotericin B represents the treatment of first choice for fungal keratitis.
Its mechanism of action is based on the binding to the fungal membrane ergosterol, an essential component of the fungal cell membrane, leading to an ion-channels formation, which causes to a membrane depolarization, a greater membrane permeability and a leakage of important intracellular components as well as the loss of small intracellular molecules and ions. This leads to cell rupture and, eventually, cell death. It also promotes cellular oxidation by altering its metabolic functions to stimulate host immune cells (163).
The name was given by its amphoteric properties since it is insoluble in water at pH 6-7, but soluble at extreme pH values (pH 2 or pH 11; over 0.1 mg / mL). In addition, it has a high molecular weight (924.0.1 g / mol) which leads to a low corneal penetration, these being improved by eliminating the epithelium layer (179,180).
Generally, amphotericin B topical administration is carried out in concentrations between 0.05-0.3% (153,169,170), although there are references about its use at a 5% concentration (181). n either case, similar pharmacokinetics were described, including penetration into the deep corneal stroma after administration. (182). In addition, it is important to keep in mind that, as concentration increases, so does its toxicity. Eye drops are prepared from commercialized parenteral formulations (Abelcet®, Ambisome®, Amfocan®, Amphotecin B for injection USP X-gen®, Funtex B®) diluted in water for injection (170,183). Significant differences among these formulations are observed, where drug is incorporated into different pharmaceutical forms, including colloidal dispersions, lipid solutions, deoxycholate salts or liposomal complexes (184).
Generally, a 0.15% amphotericin B concentration (550 times higher than the most frequent fungi MIC) is enough for the fungal keratitis treatment and less toxic than higher concentrations, which do not show any therapeutic improvement and can produce an epithelium healing delay, stromal clouding, edema and iritis (169).
In addition to the topical route, intracameral (5-10 μg/0.1 mL) (5-10 μg/0.1 mL) (169,185,186), intracorneal (stroma) (0.5 μg–5 mg/0.1 mL) (153,185), intravitreal (5-10 μg/0.1 mL) (153,187) and intravenous routes (0.25-1 mg/kg/day) (0.25-1 mg/kg/day) (188) were tested, the latter being used for severe cases in which scleral affection or even endophthalmitis were observed,

due to numerous side effects (fever, nausea and vomit, among many others), where high nephrotoxicity is noticed as the most dangerous one. This side effect depends on the pharmaceutical form where the active principle is included, being lower in the liposomal one. (162,189). Besides that, it must be taken into account that subconjunctival administration can produce conjunctival necrosis, being the main disadvantage of this route (182).

Currently, several research lines are based on the new amphotericin B release systems development, these being:

Chitosan-modified nanostructured lipid carriers: the study concludes with an amphotericin B bioavailability improvement due to a permanence time increase in the rabbits corneal epithelium without showing ocular irritation (190).

Lecithin/chitosan nanoparticles: amphotericin B release from this pharmaceutical form was significantly prolonged compared to the commercialized brand (Fungizone®). Ocular bioavailability was improved and nanoparticles showed good mucoadhesive properties. In addition, no eye damage was observed in rabbits compared to the commercial formulation, which caused ocular irritation (191).

Eudragit RS 100 nanoparticles: recent studies showed amphotericin bioavailability from this pharmaceutical form was similar to the reference one, but without no ocular irritation (192).

8.3. NATAMYCIN

Natamycin or Piramicin has been the first antifungal approved by the FDA for topical ophthalmic use (193) in the fungal keratitis treatment. It is an amphoteric macrolide isolated for the first time in 1958 from *Streptomyces natalensis* (169), although it was also later isolated from *Streptomyces chattanoogensis*, *S. gilvosporeus* and *S. lydicus* (194). It has a broad spectrum of action against most filamentous fungi, and it is especially effective against *Fusarium* spp. (166), making it the most successful and first-election drug for early fungal keratitis treatment (195) caused by filamentous fungi. It also has a good activity against yeasts (*Candida* spp.) (194).

Its mechanism of action is based on the inhibition of ergosterol-dependent carriers in the fungal plasma membrane (194).

Due to its amphipathic nature, it is practically water-insoluble (30-50 mg / L) (196) and has a methanol-and-ethanol low solubility, but it is glacial-acetic-acid and dimethylsilfoxide (DMSO) soluble (197). It is a large molecule with a high molecular weight (665.75 g / mol) which prevents its corneal penetration. It is used as monotherapy for the superficial infections treatment (163,182), and combined with an azole antifungal-oral-treatment for severe infections (165). As with amphotericin B, desepithelization improves passage through the cornea.

In an *in vitro* test, natamycin and voriconazole combination proved to have a more effective antifungal activity than the treatment of each of them separately and can be used in the fungal keratitis treatment (198).

Intravenous or subconjunctival injections of antifungals do not achieve therapeutic drug levels in the aqueous humor (195). To overcome this, when an advanced stage infection reaches the

underlying tissues, combined formulations of natamycin and another antifungal are used by an alternative route of administration. (163).

A 5% concentration natamycin suspension is the most used and topically applied pharmaceutical form (153), being a stable formulation and showing a high tolerance that does not cause pain or secondary corneal damage (182).

Natamycin is also a first-line drug for the filamentous fungal keratitis therapy in many countries (182) and unlike amphotericin, there are numerous commercialized formulations worldwide, such as: Elmycin® (India), Natam® (India) Pima Biciron N® (Germany), Natacyn® (Argentina, Colombia, New Zealand, Malaysia, USA), among others.

Currently, new natamycin formulations are being tested, being the most relevant:

PEGylated Nano-lipid carriers: transcorneal permeability and flow showed better results than the commercialized suspension (199).

Complexes with cyclodextrins: several inclusion complexes have shown a natamycin transcorneal-permeability improvement leading to a better antifungal efficacy (197).

9. AZOLES

Azoles are cyclic organic molecules that are divided into two groups according to the number of azole-ring nitrogen atoms, these being: 1) imidazoles, with two azole-ring nitrogen atoms and 2) triazoles, where three azole-ring nitrogen atoms are observed.

Azoles were developed as a less toxic alternative than amphotericin. In 1981, the FDA approved the use of oral ketoconazole as the first compound available for the treatment of systemic fungal infections. During the 90s, first triazoles discovered (fluconazole and itraconazole) showed a greater spectrum of action than imidazoles and a better safety profile than amphotericin B and ketoconazole. From there, new analogues were found (voriconazole, posaconazole, etc.), which showed better efficacy in resistant infections to the previous ones, greater action potency (200) better pharmacokinetic profiles (162).

Its mechanism of action is based on its binding to cytochrome P450 which is responsible for the ergosterol formation. The ergosterol-production blocking produces a methylated-sterols accumulation. That increases the membrane permeability and cell growth inhibition, leading to cell death. The ergosterol-production inhibition also modifies the function of other enzymes associated with the fungal membrane (169).

All of them present similar mechanisms of action; however, differences on the antifungal spectrum variation, tissue penetration, toxicity and pharmacokinetics were observed.

9.1. VORICONAZOLE

Voriconazole is a fluconazole synthetic triazole with a broad spectrum antifungal activity, particularly against *Aspergillus* spp., *Candida* spp., *Fusarium* spp., *Scedosporium* spp. *and Paecilomyces* spp., among others.

(201).

As with other triazole antifungal agents, voriconazole exerts its effect primarily through inhibition of cytochrome P450 CYP-dependent 14α-sterol demethylase, an enzyme responsible for the conversion of lanosterol to 14α-demethyl lanosterol in the ergosterol biosynthetic pathway (202), as well as the cytochrome P-450 CYP3A, P450 2C19 and P450 2C9 inhibition.

This leads not only to an ergosterol depletion and the subsequent disruption of the integrity and function of the fungal cell membrane, but also to the accumulation of toxic sterol precursors including squalene, zymosterol, lanosterol, 4,14-dimethylzymosterol, and 24-methylenedihydrolanostero (202), eventually resulting in fungal cell lysis.

In randomized comparative trials, voriconazole appeared to be as efficacious as fluconazole and conventional or liposomal amphotericin B. Voriconazole may be an alternative therapeutic choice in fungal infections that are refractory to older antifungal agents. Voriconazole has also been tested *in vitro* against yeast, filamentous fungi and dimorphic fungi, appearing to exhibit antifungal activity against a wide variety of clinically important yeasts and molds (203).

Voriconazole, a new azole antifungal agent structurally derived from fluconazole, possesses several advantages over some older azole antifungal agents and other conventional antifungal agents. Unlike some triazole antifungals (e.g. itraconazole and ketoconazole), it is highly orally available (≈ 75%), and its absorption does not appear to be affected by intragastric pH changes. It is rapidly absorbed after oral administration, with a time to maximum plasma concentration (t_{max}) within 2 hours and a 96% oral bioavailability. After single and multiple oral and intravenous doses administration, voriconazole had a 6 hours plasma elimination half-life ($t_{1/2}$) (203).

Voriconazole was approved for use in the United States in 2002 and currently is available as 50 and 200 mg tablets, an oral suspension (40 mg / mL) and several parenteral formulations generically and under the brand name Vfend® (Pfizer, New York). Serious fungal infections are typically treated initially with intravenous voriconazole (4 to 6 mg / kg every 12 h) for 3 to 10 days, followed by more prolonged therapy with oral forms (20 mg / 12 h). It is also available as a 1 mg / mL topical formulation (Vozole®), 50 µg / mL intrasomal injection, 50 µg / mL intracameral injection and 50 µg / mL intravitreal injection (153).

This drug has also been extensively studied as a keratitis and endophthalmitis alternative treatment due to its good concentrations in several ocular tissues, including cornea, vitreous humour and aqueous humour. It is also used as a drug of choice for the deep keratitis, scleritis and endophthalmitis treatment, as well as prophylaxis after penetrating keratoplasty (163).

Common side effects include nausea, photosensitivity, hallucinations, headache, visual disturbances and rash.

In recent years, several new voriconazole release systems for ocular delivery were studied, being an HPβCD-Voriconazole *in situ* gelling system the most promising vehicle for topical ocular administration against *Candida albicans* and *Aspergillus fumigatus*. Its application could reduce the necessity for repeated drug administration due to the sustained release properties, thereby potentially lowering corneal toxicity and increasing patient compliance (204).

9.2. FLUCONAZOLE

Fluconazole is a synthetic triazole antifungal agent introduced in 1990 into the therapeutic arsenal as an alternative treatment for fungal infections. It preferentially inhibits fungal cytochrome P-450 2C9, 2C19 and 3A4 sterol C-14α-demethylation, leading to a fungal 14α-methyl-sterols accumulation and, consequently, disrupting the fungal cell membrane and impairing cell replication.

(205).
Commercialized fluconazole pharmaceutical forms are tablets and IV solutions. Nevertheless, several ocular formulations have been also tested (169). Orally administration is based on a rapid and almost complete GI tract absorption, being the second route reserved for patients who do not tolerate or are unable to take the drug orally. Besides that, oral and IV dosage are identical (206). Fluconazole oral administration presents a good ocular penetration (182). Despite its advantageous pharmacological activity, fluconazole can cause several clinically significant side effects, including headache, hives, itching or skin rash, abdominal pain, and hematemesis (207).
Fluconazole topical administration (0.2-2%) presents a good corneal penetration, while subconjunctival formulations (2-20 mg / 0.5-1 mL, once or twice a day) showed to be effective as a fungal keratitis alternative treatment (153), avoiding surgical procedures (208,209). Besides that, it is also effective by intravenous administration (100-200 mg / day) in natamycin/amphotericin-refractory *Alternaria* spp. infections (210).
It is currently used for both prophylaxis and the treatment of broad-spectrum fungal infections, although the emergence of drug-resistant isolates continues to increase dramatically (211).
(211). In response to this challenge, the use of new drug formulations and delivery systems were studied, including:

Fluconazole-loaded liposomes for topical ophthalmic administration: liposomes showed improved response with *Candida albicans* compared to fluconazole solution (212).

Fluconazole lipid nanoparticles: lipid nanoparticles enhanced *in vitro* antifungal activity against *Candida* spp. (211).

9.3. ECONAZOLE

Econazole is an imidazole derivative mainly used in superficial topical mycosis although it has also been used as an alternative treatment for fungal keratitis since the 1980s (213,214).
Its mechanism of action is the same as the rest of the azoles, although unlike some, it has activity against gram-positive bacteria. (215). It has a broad spectrum of action against most filamentous fungi (*Fusarium* spp. and *Aspergillus* spp.) (216,217) as well as yeasts (*Candida* spp.) (217–219), although some authors suggest that the effectiveness against *Candida* spp. can be variable (159,220).
Its low water solubility (1.48 mM) (219) and its high molecular weight (381,681 g / mol) leads to a low corneal bioavailability, although recent studies have shown that it can be improved using cyclodextrins (221) or others systems, such as nanoparticles, which have been used in an *in vivo* trial with rabbits demonstrating the econazole presence in the aqueous humour and the cornea within 5 min application (222) (Zhang, Tian, Xu, Zhao y Zhang, 2015).
1% or 2% concentration topical econazole eye drops are the most frequent econazole pharmaceutical form used for the fungal keratitis treatment (153). In a study in which 112 cases of filamentous fungal keratitis were studied, comparing a 2% econazole solution against a 5% topical natamycin suspension. Results obtained demonstrated that both drugs showed similar efficacy (172), so econazole could be used as an alternative to topical natamycin in countries where it was not available, or in natamycin refractory infections. It has also been used a 1%

econazole ointment as a prophylactic treatment in cases of ocular traumas with high fungal infection risk, obtaining good results (214). Nevertheless, it must be taken into account that topical administration can be associated with ocular irritation due to the low pH that it presents in aqueous solution (182).

There is an ophthalmic formulation commercialized in India called Aurozole®. Besides that, currently, there are several research and lines focused on new ocular econazole-release-systems development, such as:

Chitosan and sulfobutilether-β-cyclodextrin mucoadhesive nanoparticles: nanoparticles have shown a controlled drug release and a drug-residence-time increase, improving its fungal activity compared with the econazole nitrate solution currently used (223).

Ion-sensitive and mucoadhesive hydrogels: hydrogels are controlled-release devices that improve the econazole permanence in the eye (219).

PLGA (poly-lactic-co-glycolic acid) contact lenses containing econazole: contact lenses have shown a good efficacy against *Candida albicans* (218).

Econazole nitrate nanoparticles: nanoparticles with cyclodextrins and different stabilizers, prepared by using a nanospray-dryer. These nanoparticles have shown a better bioavailability than the drug suspension due to the nanoparticle's solubility in the tear (224).

Econazole ocular nanoemulsifier systems: with hydroxypropylmethylcellulose as a precipitation inhibitor, which can stabilize the supersaturation state created, improving ocular drug bioavailability (225).

9.4. KETOCONAZOLE

Ketoconazole is a phenylpiperazine synthetic derivative with broad antifungal properties and potential antineoplastic activity. It was approved for use in the United States in 1981 and introduced in Europe in 1984 as an alternative treatment into the therapeutic arsenal against superficial and systemic fungal infections. The spectrum of activity includes dermatophytes (e.g. *Microsporum* spp., *Trichophyton* spp., *Epidermophyton* spp.), yeasts (e.g. *Candida* spp., *Cryptococcus neoformans*), dimorphic fungi (e.g. *Coccidioides immitis, Histoplasma capsulatum, Paracoccidioldes brasiliensis*) and various other fungi (226).

As with other imidazole antifungals, ketoconazole has some *in vitro* activity against Gram-positive cocci. Interestingly, it has also showed *in vitro* activity against some parasites, including *Plasmodium falciparum* and *Leishmania tropica* (226).

Likewise, there are reports of cases treated exclusively with 10 to 50 mg / mL topical econazole solution, although other drugs showed to be more effective against fungal keratitis. Currently, ketoconazole is mainly used as an adjuvant treatment of deep fungal keratitis (163).

It is believed to work by several mechanisms of action, including the fungal sterol 14α-dimethylase inhibition (201). Other mechanisms may involve the endogenous respiration inhibition, interaction with membrane phospholipids, yeast transformation inhibition to mycelial forms, purine-uptake inhibition and/or impairment of triglyceride and/or phospholipid biosynthesis. Ketoconazole can also inhibit the thromboxane and sterols synthesis such as aldosterone, cortisol or testosterone (227,228).

Most patients tolerate ketoconazole well, even those who are immunosuppressed for prolonged periods at high doses (211). Common side effects include pruritus, gastrointestinal reactions (nausea), headache, dizziness, fatigue, impotence, menstrual abnormalities and gynaecomastia. Serious adverse events include anaphylaxis, hepatotoxicity (LD50 = 86mg/kg), endocrine dysregulation and QTc interval prolongation. Because of this, it is no longer recommended as a first-line antifungal agent, being replaced by other antifungal agents with fewer side effects and a wider range of activity (228).

Ketoconazole is also available in 200 mg capsules under the brand name Nizoral® and also in various generic forms. An ophthalmic formulation is available in India under the name Ketostar® (229), although the manufacturer recommends its use only when no other treatment is available.

Formulations for topical ophthalmic administration of ketoconazole are being developed in several research lines:

Ketoconazole-loaded solid lipid nanoparticles: nanoparticles showed ocular biocompatibility and safety in *in vitro* (in corneal and retinal cells) and in *in vivo* (in rabbits) (230).

Ketoconazole nanoparticles: nanoparticles vehicleised in a hydrogel in situ showed good permeability in epithelial cell lines (231).

9.5. ITRACONAZOLE

Itraconazole is a synthetic triazole agent with antimycotic properties (232). It was synthesized in 1980 and approved in the United States in 1992 as an alternative treatment for both topical and systemic use, being widely used today as an antifungal agent (233).

This agent can be used for long-term maintenance treatment of chronic fungal infections, such as the ones caused by *Aspergillus* spp. (aspergillosis), *Candida* spp. (candidiasis), *Curvularia* spp. or *Cryptococcus* spp (165,234). Itraconazole has not enough efficacy against *Fusarium* spp. (169).

Itraconazole is orally administrated (100 - 200 mg / day) (153) due to its excellent safety profile and good absorption. Its oral absorption improves if the administration is carried out with food (169,232). It is not the most appropriate route for the fungal keratitis treatment due to its poor ocular penetration (163), and a drug minimum concentration that reaches the aqueous humour (235) although it has been effective in non-severe fungal keratitis cases caused by *Aspergillus* spp. (236). Topically (1%) (153), easily crosses corneal epithelium and endothelium but, due to its lipophilicity, it is not able to cross the corneal stroma, being less effective than 5% topical natamycin formulation (165).

Intravitreal injections have been experimentally used causing retinal necrosis areas when it exceeded a dose greater than 10 μg / 0.1 mL itraconazole injection, but lower doses are interesting for the several fungal infections treatment that unleash on endophthalmitis (237,238).

Itraconazole is available in several pharmaceutical forms, being the commercialized ones: 100 mg capsules (Sporanox®, Canadiol®, Hongoseril®), 200 mg tablets (Onmel®), 10 mg / mL oral solutions (Sporanox®) and eye drops (Itral®, Entozole®). The daily typical dose is 100 to 400

mg based upon the fungal infection type and severity. Common side effects include nausea, vomit, diarrhea, rash and hypokalemia, even that the most important one is still being the hepatotoxicity (239).
Several innovative itraconazole formulations are currently being developed, should be mentioned:

Spanlastic nanosystem vesicles: nanosystem have increased the inhibition zone of *Candida albicans* cultures compared to powdered itraconazole, showing a transcorneal permeability improvement and a better controlled drug-release profile than conventional niosomes (234).

Stearic acid solid-lipid nanoparticles: nanoparticles showed an inhibition zone against *Aspergillus flavus* cultures, as well as a good corneal permeability in an *ex vivo* test (240).

Itraconazole polymeric micelles: micelles included in an *in-situ* ion-sensitive gel showed a better transcorneal permeation than the eye drops commercialized formulation (Itral®) (241).

9.6. MICONAZOLE

Miconazole is an imidazole synthetic derivative, an aromatic heteromonocyclic compound that belongs to the benzylethers group (242). It was synthesized in 1969, being the first azole approved by the FDA for parenteral use (200).
It is active against most yeasts (*Candida* spp.) (243) and filamentous fungi (*Aspergillus* spp. and *Scedosporium* spp.), showing a variable activity against *Fusarium* spp. (200,243,244).
Miconazole selectively affects the fungal cell-membranes integrity which present a higher ergosterol content and different composition from mammalian cell membranes (245). Its mechanism of action is based on the interaction with the 14α- demethylase, a necessary cytochrome P-450 enzyme for the conversion of lanosterol to ergosterol. Even though, miconazole may also inhibit endogenous respiration, interact with membrane phospholipids, inhibit the transformation of yeasts to mycelial forms, inhibit purine uptake and impair triglyceride and/or phospholipid biosynthesis (246).
Several *in vivo* studies using rabbits showed that a 1% (w/v) miconazole topical administration (153) was effective in fungal infections by *Candida albicans*, *Fusarium solani* and *Aspergilus fumigatus* (243,244), obtaining better results once the epithelium was eliminated (163). It has also been used by subconjunctival injection (10 mg / 0.5 mL) and/or intravenous infusion (600-1200 mg / day) (153). The latter, at a 30 mg / kg dose was test in a *in vivo* assay with rabbits, observing antifungal high levels in the aqueous humour from the administration starting time (247). Due to this, it would be suitable to treat severe fungal infections that have reached ocular deeper areas. In addition, good results were obtained by using miconazole oral administration, although it is a disuse route due to the associated cardiovascular-and-hepatic toxicity (163).

Likewise, there are no commercialized miconazole ophthalmic formulations and currently, there are not enough clinical trials that assess their real effectiveness, so it is difficult to draw any conclusions about the miconazole use as a fungal keratitis alternative treatment.

9.7. POSACONAZOLE

Posaconazole is an itraconazole hydroxylated derivative that belongs to the second-generation-triazoles group, due to the chlorine substituents replacement with flourine in the phenyl ring, as well as triazolone side chain hydroxylation. These modifications enhance the potency and activity spectrum of the drug Posaconazole can be fungicidal or fungistatic (248).

Posaconazole shows an *in vitro* action spectrum similar to voriconazole's, being effective against a very large number of fungal agents (249). Good results were achieved against most *Candida* spp. and other yeasts like *Cryptococcus neoformans*, as well as filamentous fungi such as *Fusarium* spp. and *Aspergillus* spp. (250), among others. It was used in medical practice for a relatively short time, being effective against recalcitrant infections unsuccessfully treated with other antifungals such as fluconazole, voriconazole, amphotericin B and/or natamycin (251,252).

Posaconazole strongly inhibits 14α-demethylase, a cytochrome P450-dependent enzyme. Even though, compared to other azole antifungals, posaconazole is a significantly more potent inhibitor of sterol 14α-demethylase (253).

It is currently commercially available as injectable, oral suspension tablets and delayed-release tablets (Noxafil®). Its use in the fungal keratitis treatment is quite limited, but an oral (200 mg every 6 hours or 400 mg every 12 hours) and topical combined treatment has given good results (163,251,254). Posaconazole levels were detected in the posterior segment of the eye after topical and oral administration, although their corneal penetration is unknown (252).

Generally, it is a well-tolerated drug, although different side effects, including those related to the gastrointestinal system (nausea, gastric juices, diarrhea), were observed. Besides that, transient elevations in serum aminotransferase levels occur in 2% to 12% of patients on posaconazole. These elevations are usually mild, asymptomatic and self-limited, rarely requiring a medication discontinuation (255).

10. PYRIMIDINES: FLUCYTOSINE (5-FLUOROCYTOSINE)

In 1957, flucytosine was synthesized as an antitumor drug, not showing enough effectiveness, being its antifungal power discovered later. It only shows antifungal activity when it is introduced into the cell. Its mechanism of action is based on its deamination by the cytosine-deaminase action once the drug crosses the fungal membrane, leading to the 5-fluoroacil production. As a result, a pyrimidine antimetabolite is incorporated into the fungal DNA, avoiding cellular replication (256).

It has a great activity against yeasts such as *Candida* spp., *Cryptococcus* spp. and a variable susceptibility against *Aspergillus* spp. (163). Nevertheless, it shows resistance to many other etiological agents that cause fungal keratitis such as *Fusarium* spp., where it is topically applied (10-15 mg / mL) in combination with amphotericin due to their synergistic effects (153,169).

In an *in vivo* assay using rabbits, significant flucytosine levels were detected in the aqueous humour after the drug was subconjunctival and orally administered. This later pathway also showed flucytosine therapeutic levels in the vitreous humour (247,257).

Currently, new flucytosine release systems are being studied, where gold-nanoparticles liposomal systems were the most effective ones comparing them with the control flucytosine solution in an experimental treatment by using *Candida albicans* infected rabbits (258).

11. ECHINOCANDINS: CASPOFUNGIN

Caspofungin is the acetate salt of an antimycotic echinocandin lipopeptide, semisynthetically derived from a fermentation product of the fungus *Glarea lozoyensis*. It was discovered by James Balkovec, Regina Black and Frances A. Bouffard and currently belongs to Merck & Co., Inc, being commercialized under the name Cancidas®. Cancidas® is a sterile and lyophilized product for intravenous infusion (259).

β-(1,3)-D-glucan decreased synthesis, an essential component of the fungal cell wall, weakening it and, eventually, leading to a fungal cell wall rupture (163,260).

Currently, it is available under two different pharmaceutical forms, these been: 0.5% Caspofungin suspension (261) and 100 µg / 0.1 mL intravitreal injection. The latter proved to be effective in an *in vivo* assay by using infected rabbits with *Candida* spp. (237).

12. OTHER ANTIFUNGALS

12.1. POVIDONE-IODINE

Povidone-Iodine preparations have a broad antimicrobial spectrum. Povidone-Iodine shows a very low antigenicity and this, taken with the clinical effectiveness, makes this preparation very suitable for clinical use. However, its mechanism of action on fungal mycelium or how rapidly it works is barely known (262).

Las preparaciones de povidona yodada tienen un amplio espectro antimicrobiano incluyendo bacterias, virus y hongos (263).

In several cases, 2.3% povidone-iodine solution was successfully used on the fungal keratitis treatment caused by *Candida albicans* and *Acremonium strictum* (264), although its mechanism of action on fungal mycelium and the speed with which it works is not known (262). Nevertheless, a comparative study by using 0.5% povidone-iodine solution showed no benefit compared to 5% natamycin suspension in the *Fusarium solani* keratitis treatment (163).

12.2. CHLORHEXIDINE DIGLUCONATE

Chlorhexidine digluconate is a cationic microbicidal antiseptic with a broad spectrum of action against bacteria, fungi and amoebae (265,266) and has been used in combination with antifungal drugs for the treatment of fungal keratitis (267,268).

In a study comparing the *in vitro* activity of chlorhexidine with seven antifungals (amphotericin B, voriconazole, posaconazole, miconazole, natamycin, flucytosine and caspofungin) in cultures of various Fusarium species, chlorhexidine showed superior antifungal activity to flucytosine, posaconazole, miconazole and caspofungin against F. oxysporum and F. solanii (269).

12.3. POLYHEXAMETHYLENE BIGUANIDE (PHMB)

Polyhexamethylene biguanide (PHMB), also known as polyhexanide, polyaminopropyl biguanide, polymeric biguanide hydrochloride or polyhexanide biguanide, is an antiseptic with antiviral and antibacterial properties used as an alternative for fungal keratitis treatment. It also shows a broad viricide and antifungal spectrum and has amoebicidal activity. Certainly, its antimicrobial efficacy has been demonstrated on *Acanthamoeba polyphaga*, *A. castellanii*, and *A. hatchetti* (270) by using 0.02% to 0.053% solutions without causing side effects.

Focusing on the fungal keratitis treatment, Fiscella et al. demonstrated that 0.02% PHMB solution is effective in the fungal infections treatment by *Fusarium solani* in rabbits. In addition, no growth was obtained in 58% of PHMB-treated eyes, compared to 17% of placebo-treated eyes (271). Even that, more studies must be done to corroborate these preliminary results.

13. POSSIBLE ANTIFUNGALS THERAPEUTIC COMBINATIONS

Currently-available antifungal therapies exhibit limited effectiveness and a complete response mainly depends on correction of the underlying disease. Nevertheless, concurrent or sequential antifungal treatment for invasive mycosis has been considered as an option to improve monotherapy results. Several alternatives were studied:

Voriconazole plus natamycin: the combination of these two antifungals has shown synergistic antifungal efficacy against Candida spp., Curvularia spp., Fusarium spp. and Aspergillus spp. in an *in vitro* assay and no antagonism was shown (198).

Azole agents plus flucytosine: combinations of flucytosine and both older and newer azole agents (e.g., voriconazole or posaconazole) have exhibited synergy against several fungi species such as *C. neoformans* (174,272–274), leading to an increased used as a fungal alternative treatment.

Azole agents plus terbinafine: azoles (fluconazole, itraconazole, voriconazole or posaconazole) and terbinafine combinations have shown synergy in *in vitro* studies against *Candida* spp., *Aspergillus* spp. and *Mucorales* spp. (275–277).

Amphotericin B plus echinocandins: the combination of amphotericin B and caspofungin has shown a synergistic effect for some strains of *Criptococcus neoformas* and no antagonism was found. (278).

Combinations of antifungal and antibacterial agents: synergy was found for amphotericin B plus rifampicin combination against *Candida* spp., *Aspergillus* spp., *Fusarium* spp. and *C. neoformans* and antagonism was not observed (276,279–282).

Antifungal agents and non-antimicrobial agents: Calcineurin inhibitors (e.g. cyclosporin or tacrolimus) enhanced fluconazole and caspofungin *in vitro* activity against *Candida* spp., *Aspergillus* spp. and *C. neoformans* (283–286). Combinations of antifungal agents with proton pump inhibitors, antiarrhythmic agents and immunomodulators have also been explored (276,287,288).

14. USE OF TOPICAL STEROIDS

Steroids role in the fungal keratitis treatment remains controversial (289). Some authors describe that topical steroids early use for infectious keratitis helps reduce neovascularization, scarring and pain. Activated immune cells release cytokines, collagenases and growth factors, leading to keratocytes apoptosis and collagen destruction. Viable corneal keratocytes are transformed into activated fibroblasts, which restore the tissue defects by irregularly depositing collagen and the extracellular matrix. This causes opacification or haze during the scarring process.

Actualmente no hay revisiones multicéntricas o de literatura sobre el uso de corticoides en la queratitis fúngica. Sin embargo, los estudios sobre úlceras bacterianas han demostrado que el tratamiento antibiótico apropiado mejora los resultados visuales.

There are currently no multicentric or literature reviews concerning the steroids use in fungal keratitis. However, studies on bacterial ulcers have shown that appropriate antibiotic treatment improves visual outcomes. Fungal keratitis differs from bacterial ulcers, as it is often more severe, usually affects deeper corneal layers and causes more inflammation (hypopyon). Although steroids have been a key factor in the inflammatory processes treatment in modern medicine, their use reduces defense mechanisms and creates a fungal-proliferation favourable environment. Several studies have revealed that fungal keratitis management should aim not only for early diagnosis, but also for effective treatment schemes which eradicate the infection, reduce complications and prevent recurrence (261,290). Topical steroids use for fungal keratitis may stimulate microorganism penetration to deeper layers, even invading Descemet's membrane, and reduce some antifungal agents effectiveness, such as natamycin, flucytosine and miconazole. Therefore, it is recommended to avoid their use, especially during the first 2 or 3 weeks of specific treatment or until the infection is under control. Once this is achieved, steroids may be beneficial for reducing inflammation and corneal scarring, but they must be used in combination with antifungal drugs.

Steroids are occasionally used in patients before diagnosis is confirmed and adequate targeted treatment is prescribed. Its abrupt withdrawal can lead to a clinical profile worsening due to the inflammatory response activation and a symptoms' exacerbation.

Although topical steroids can also be beneficial in patients who have undergone keratoplasty, as they help prevent graft rejection, they should only be used once the fungal infection has been eradicated. Topical 0.05% cyclosporin A may also be considered due to its immunosuppressant and antifungal properties.

Finally, scientific evidence for the treatment success is still limited and clinical trials should be carried out to determine the most favourable type of steroid, dosage and duration of treatment.

15. FINAL PHARMACOTHERAPY MANAGEMENT RECOMMENDATIONS

15.1. KERATITIS CAUSED BY FILAMENTOUS FUNGI

Natamycin (0.5%, eye drops) (Natacyn®) is the drug of choice when filamentous keratitis is suspected. Epithelial debridement should be performed prior to administration in order to help drug penetrance (83,291).

Natamycin is the only drug available for treating fungal keratitis in USA and India, and it has been approved by the FDA. Alternatively, 1% voriconazole solution or 0.2% chlorhexidine solution can be used (83,267). In severe cases affecting the anterior chamber and/or the sclera, it is important to combine two or more antifungal drugs (e.g. voriconazole and chlorhexidine), starting a systemic (oral or intravenous) antifungal treatment (292–295).
In patients with filamentous keratitis with poor response to treatment, it may be useful to add 1% voriconazole solution, which has been found to be superior to natamycin monotherapy (296)- Esto se demostró en un estudio
A recent *in vitro* study showed that the combination of natamycin and voriconazole provided superior antifungal activity than monotherapy for treating *Fusarium* spp., *Aspergillus* spp., *Candida* spp. and *Curvularia* spp. (198) A natamycin and 0.2% chlorhexidine solution combination may also be effective.
In deep stromal infections, intrastromal/intracamerular voriconazole administration (50 - 100 mg / 0.1 mL) may also be useful.
In severe cases requiring treatment with voriconazole, a 400 mg induction dose should be administered on the first day, followed by 200 mg maintenance dose every 12 hours for 2 weeks. Administered voriconazole orally yields plasma levels of 53% and intravitreal levels of 88% (292,293).

15.2. KERATITIS CAUSED BY YEAST-FUNGI

The initial drug of choice for fungal keratitis caused by yeasts is 0.15 - 0.25% amphotericin B eye drops or 0.05% amphotericin B liposomal form following epithelial debridement.
Amphotericin B presents a good stroma penetrance and can be administered in topical, intracameral, intravitreal or intravenous solutions. If amphotericin is not available, 1% voriconazole eye drops may be used.
In severe keratitis which does not respond to treatment with amphotericin, fluconazole (topical, subconjunctival or oral) may be added. This combination provides better outcomes than amphotericin monotherapy (297).
Keratitis caused by yeasts involving the sclera or the anterior chamber should be treated with an oral/intravenous-antifungal-agents combination (amphotericin, voriconazole or fluconazole).

16. SURGICAL APPROACH

Surgical treatment is necessary when fungal keratitis does not respond to pharmacological treatment or if corneal thinning is present. Surgery can eradicate the infection, preserve the eyeball integrity and improve visual acuity in many patients. However, further surgical interventions may be deemed necessary to manage complications which may arise after the first surgery.

16.1. EPITHELIAL DEBRIDEMENT

Epithelial debridement is important for improving drug penetration and reducing the infective load. This procedure may be repeated within 24 - 48 hours in some cases.

Periodic debridement is an excellent procedure for removing necrotic tissue from the cornea, stimulating blood circulation and increasing the drug topical efficacy, thus reducing the infective load and providing a symptoms faster resolution.

16.2. CORNEAL ADHESIVES

Thin corneas or small perforations may be treated with tissue adhesives such as cyanoacrylate and therapeutic contact lenses or fibrin adhesives.

16.3. AMNIOTIC MEMBRANE TRANSPLANT

Several clinical effects of amniotic membrane transplant have been described in the fungal keratitis treatment. This procedure acts as a drug release system, reduces pain, inflammation and neovascularization, as well as stimulates re-epithelialization and minimizes scarring. In patients with fungal keratitis, it may be used from day 3 to 5 following treatment and once the microbiological analysis is complete (298,299).

16.4. KERATOPLASTY

Sometimes, it is difficult to determine when keratoplasty should be performed in patients with fungal keratitis. Despite medical treatment, infection progression should be considered as an indication for keratoplasty, as spreading to the limbus or sclera may lead to scleritis and endophthalmitis, worsening the prognosis (300).

These therapeutic keratoplasties represent a risk for intraocular dissemination of the infection but, in some cases, they are necessary to preserve the eyeball integrity.

The type of surgical intervention depends on the microorganism, location and affected area by the keratitis. When the infection is limited to the corneal surface, lamellar keratoplasty may be performed to eliminate lesions. Deep anterior lamellar keratoplasty (DALK) eliminates all the corneal stroma to Descemet's membrane and does not penetrate the anterior chamber, minimizing the risk of endothelial rejection (301).

In cases of perforation or deep keratitis, penetrating keratoplasty is the first-line surgical treatment to prevent pathogens from entering the anterior chamber and causing fungal endophthalmitis.

Surgical technique correct choice is important. Complete elimination of hypopyon and fibrin from the anterior chamber, as well as corneal lesion eradication, may reduce the fungal infection recurrence. Trepanation at 1 - 1.5 mm from the affected area must be attempted when possible. In patients with cataract it is not recommended to extract the lens during the same intervention in order to prevent microorganisms from reaching the vitreous cavity.

The graft diameter should be determined in accordance with the size of the affected area. The risk of rejection is higher when grafts larger than 8 mm are needed or when these are eccentric. Tissues should be analyzed by both a pathologist and a microbiologist to confirm elimination of all the infected area and to identify the type of fungus.

Interrupted sutures should be used. On finalizing the intervention, an intraocular or intrastromal antifungal drug should be injected to eliminate any remaining microorganisms.

Topical antifungal treatment should be maintained during the post-operative period to prevent recurrence. Systemic treatment is also recommended. Steroids use in these patients is controversial, although they are deemed to reduce postsurgical inflammation, which is an important risk factor for graft failure.

Some authors suggest that topical steroids routine use following transplant is beneficial for inflammation control, even in fungal keratitis. However, as these drugs may facilitate invasion by residual fungi, they should not be used until two weeks after surgery. Intravenous steroids may be administered in patients with severe postoperative inflammation. Cyclosporin A may also be useful for controlling and preventing graft rejection (289).

These transplants success is inferior to that of those performed in eyes without inflammation or with bacterial keratitis although, in some cases, keratoplasty outcomes in fungal keratitis may be relatively good. Postoperative complications are frequent and, in many cases, a second corneal transplant is necessary.

16.5. CONJUNTIVAL FLAP

Conjunctival flap involves conjunctiva's release near the lesion in order to cover the ulcer afterwards. This procedure may be used in peripheral ulcers which do not respond to pharmacological treatment or in severe keratitis with a corneal-perforation high risk when corneal transplant is not available.

17. OTHER TREATMENTS

17.1. CROSS-LINKING

Corneal cross-linking (CXL) has been proposed as an adjutant treatment for infectious keratitis with poor response and has been named as *Photo Activated Chromophore for keratitis: 'PACK-CXL'* (180,302).

The CXL procedure creates junctions linking polymer chains by using type ultraviolet-A light and a photoreactive agent such as riboflavin (vitamin B_2). This technique is used for tissue fixation and prosthetic cardiac valves hardening. Foote et al. first introduced the concept of photo-oxidation in 1968 (303).

In 2003, Wollensak et al. applied CXL in patients with keratoconus to artificially fortify the cornea biomechanics and also reduce the disease progression (304). A combination of ultraviolet-A light (365 nm, intensity 3 mW / cm^2), irradiated over the cornea for 30 minutes and riboflavin application, creates free radicals which interact with corneal collagen and proteoglycans. New covalent bonds between collagen monomers are created, strengthening the corneal structure.

Based on this fortification principle, CXL has been proposed as a treatment for other corneal ectasias (305), bullous keratopathy (306), progressive corneal lysis associated or not with infectious ulcers (307,308) or as a therapeutic alternative in infectious keratitis with poor response to conventional pharmacological treatment (309–312). This procedure aims to reduce the infective load by destroying microorganisms DNA and RNA through photo-oxidation and reducing/removing enzymatic digestion (proteases and collagenases), actions that promote corneal reconstruction.

Application protocols in infectious keratitis differ among studies. The following are the most common: a) UV-A irradiation at 365 nm and 3 mW/cm^2 for 30 minutes (Dresden protocol), b) UV-A irradiation at 365 nm and 9 mW/cm^2 for 10 minutes. The superiority of one technique over another cannot been determined (313,314).

Infectious keratitis is linked to corneal injury risk entailing vision loss, especially if there is a diagnosis and treatment delay. Moreover, an increased incidence of drug resistance has been detected, hampering recovery. Although the pharmaceutical industry has launched new molecules, these are expensive and have stimulated the development of alternative treatments such as CXL.

Most studies with CXL in infectious keratitis concern bacterial infections as the most frequent ones. Alio et al. (315) carried out a meta-analysis about published cases of infectious keratitis treated with CXL between 2000 and 2013. Only 5 out of 12 studies included fungal infections. The meta-analysis showed that the average time to resolution of corneal lysis by fungal keratitis was 53.2 days and the need for corneal transplant was superior in this group.

In other studies, the response to CXL in fungal keratitis was variable (316–318). One of the most important contraindications for this treatment is the infiltrate's depth. Nevertheless, it must be taken into account that a 50% of the radiation is absorbed in the first 100 µm and a larger endothelial lesion can be produced if the infiltrate overcomes a 250 µm depth. Fungal keratitis tends to penetrate the deep stroma, so this treatment is not usually very effective, increasing the corneal perforation risk (319). However, it may be considered as an adjutant treatment in infection early stages.

In a recent review on CXL and microbial keratitis by Garg et al. (320) reported that the evidence is poor to date and is based on isolated cases or case series, and prospective randomised comparative studies are considered necessary. In addition, "severe keratitis" is not a standardised term, as research on infections caused by fungi, viruses and parasites is scarce. Furthermore, they consider that the criteria for poor response to conventional treatment are not uniform and that protocols for CXL are variable, and the safety of this procedure cannot be proven in cases of severe stromal cell loss or stromal irregularity (in keratoconus a minimum of 400 µm is established). Although CXL can be considered as part of an alternative treatment in bacterial ulcers with superficial infiltrates, it may be unsafe in keratitis caused by fungi or *Acanthamoeba* spp.

BIBLIOGRAPHY

1. Malhotra A, Minja FJ, Crum A, Burrowes D. Ocular Anatomy and Cross-Sectional Imaging of the Eye. Semin Ultrasound CT MRI. 2011 Feb;32(1):2–13.
2. Young B, Woodford P, O'Dowd G. Wheater's Functional Histology E-Book: A Text and Colour Atlas. Elsevier Health Sciences; 2013. 468 p.
3. Peynshaert K, Devoldere J, De Smedt SC, Remaut K. *In vitro* and *ex vivo* models to study drug delivery barriers in the posterior segment of the eye. Adv Drug Deliv Rev. 2017 Sep 19;
4. Nickla DL, Wallman J. THE MULTIFUNCTIONAL CHOROID. Prog Retin Eye Res. 2010 Mar;29(2):144–68.
5. Corneal-PAMPA: A novel, non-cell-based assay for prediction of corneal drug permeability. - PubMed - NCBI [Internet]. [cited 2020 Mar 17]. Available from: https://www.ncbi.nlm.nih.gov/pubmed/30553815
6. Proteins of the corneal stroma: importance in visual function. - PubMed - NCBI [Internet]. [cited 2020 Mar 18]. Available from: https://www.ncbi.nlm.nih.gov/pubmed/26905288
7. Cholkar K, Patel SP, Vadlapudi AD, Mitra AK. Novel Strategies for Anterior Segment Ocular Drug Delivery. J Ocul Pharmacol Ther. 2013 Mar;29(2):106–23.
8. La córnea. Parte I.: Estructura, función y anatomía microscópica. - Dialnet [Internet]. [cited 2020 Mar 17]. Available from: https://dialnet.unirioja.es/servlet/articulo?codigo=3368053
9. Mannis MJ, Holland EJ. Cornea E-Book. Elsevier Health Sciences; 2016. 2014 p.
10. Anatomy and physiology of the cornea. - PubMed - NCBI [Internet]. [cited 2020 Mar 17]. Available from: https://www.ncbi.nlm.nih.gov/pubmed/21333881
11. Bowman's layer transplantation: evidence to date [Internet]. [cited 2020 Mar 17]. Available from: https://www.ncbi.nlm.nih.gov/pmc/articles/PMC5842778/
12. Dua HS, Faraj LA, Said DG, Gray T, Lowe J. Human corneal anatomy redefined: a novel pre-Descemet's layer (Dua's layer). Ophthalmology. 2013 Sep;120(9):1778–85.
13. McKee HD, Irion LCD, Carley FM, Brahma AK, Jafarinasab MR, Rahmati-Kamel M, et al. Re: Dua et al.: Human corneal anatomy redefined: a novel pre-Descemet layer (Dua's layer) (Ophthalmology 2013;120:1778-85). Ophthalmology. 2014 May;121(5):e24-25.
14. Dua HS, Said DG. Clinical evidence of the pre-Descemets layer (Dua's layer) in corneal pathology. Eye. 2016 Aug;30(8):1144–5.
15. Singhal D, Sahay P, Goel S, Asif MI, Maharana PK, Sharma N. Descemet membrane detachment. Surv Ophthalmol. 2020 Jan 8;
16. Hatou S, Shimmura S. Review: corneal endothelial cell derivation methods from ES/iPS cells. Inflamm Regen. 2019;39:19.
17. Varela-Fernández R, Díaz-Tomé V, Luaces-Rodríguez A, Conde-Penedo A, García-Otero X, Luzardo-Álvarez A, et al. Drug Delivery to the Posterior Segment of the Eye: Biopharmaceutic and Pharmacokinetic Considerations. Pharmaceutics. 2020 Mar 16;12(3).

18. Mantelli F, Mauris J, Argüeso P. The ocular surface epithelial barrier and other mechanisms of mucosal protection: from allergy to infectious diseases. Curr Opin Allergy Clin Immunol. 2013 Oct;13(5):563–8.
19. Awwad S, Mohamed Ahmed AHA, Sharma G, Heng JS, Khaw PT, Brocchini S, et al. Principles of pharmacology in the eye. Br J Pharmacol. 2017 Dec;174(23):4205–23.
20. Garg A, Sheppard JD, Donnenfeld ED, Friedlaender M. Clinical Applications of Antibiotics and Anti-inflammatory Drugs in Ophthalmology. Lippincott Williams & Wilkins; 2007. 598 p.
21. Kompella UB, Edelhauser HF, American Association of Pharmaceutical Scientists, editors. Drug product development for the back of the eye. New York : [Arlington]: Springer ; AAPS Press; 2011. 590 p. (AAPS advances in the pharmaceutical sciences series).
22. (12) Utility of transporter/receptor(s) in drug delivery to the eye [Internet]. ResearchGate. [cited 2018 Apr 6]. Available from: https://www.researchgate.net/publication/236974311_Utility_of_transporterreceptors_in_drug_delivery_to_the_eye
23. Gaudana R, Ananthula HK, Parenky A, Mitra AK. Ocular drug delivery. AAPS J. 2010 Sep;12(3):348–60.
24. Morgan SR, Pilia N, Hewitt M, Moses RL, Moseley R, Lewis PN, et al. Controlled *in vitro* delivery of voriconazole and diclofenac to the cornea using contact lenses for the treatment of Acanthamoeba keratitis. Int J Pharm. 2020 Apr 15;579:119102.
25. Janga KY, Tatke A, Balguri SP, Lamichanne SP, Ibrahim MM, Maria DN, et al. Ion-sensitive in situ hydrogels of natamycin bilosomes for enhanced and prolonged ocular pharmacotherapy: *in vitro* permeability, cytotoxicity and *in vivo* evaluation. Artif Cells Nanomedicine Biotechnol. 2018;46(sup1):1039–50.
26. Kaur IP, Kakkar S. Nanotherapy for posterior eye diseases. J Control Release Off J Control Release Soc. 2014 Nov 10;193:100–12.
27. Boddu SHS, Gunda S, Earla R, Mitra AK. Ocular microdialysis: a continuous sampling technique to study pharmacokinetics and pharmacodynamics in the eye. Bioanalysis. 2010 Mar;2(3):487–507.
28. Bravo-Osuna I, Andrés-Guerrero V, Pastoriza Abal P, Molina-Martínez IT, Herrero-Vanrell R. Pharmaceutical microscale and nanoscale approaches for efficient treatment of ocular diseases. Drug Deliv Transl Res. 2016;6(6):686–707.
29. (12) Ophthalmic preparations [Internet]. ResearchGate. [cited 2020 Apr 2]. Available from: https://www.researchgate.net/publication/288293117_Ophthalmic_preparations
30. Rupenthal ID, Green CR, Alany RG. Comparison of ion-activated in situ gelling systems for ocular drug delivery. Part 1: Physicochemical characterisation and *in vitro* release. Int J Pharm. 2011 Jun 15;411(1–2):69–77.
31. Jitendra, Sharma B, Dixit S. A new trend: ocular drug delivery system. Pharma Sci Monit [Internet]. 2011 Jul [cited 2020 Feb 20];2(3). Available from: https://www.semanticscholar.org/paper/A-NEW-TREND-%3A-OCULAR-DRUG-DELIVERY-SYSTEM-Jitendra-Banik/b1fb13f814726a805e7ed2fcd2b8b15cd129832c

32. Majumdar D, Mishra S, Mohanty B. Effect of formulation factors on *in vitro* transcorneal permeation of voriconazole from aqueous drops. J Adv Pharm Technol Res. 2013;4(4):210.
33. Ali Y, Lehmussaari K. Industrial perspective in ocular drug delivery. Adv Drug Deliv Rev. 2006 Nov 15;58(11):1258–68.
34. Baeyens V, Gurny R. Chemical and physical parameters of tears relevant for the design of ocular drug delivery formulations. Pharm Acta Helv. 1997 Sep;72(4):191–202.
35. Dubald M, Bourgeois S, Andrieu V, Fessi H. Ophthalmic Drug Delivery Systems for Antibiotherapy-A Review. Pharmaceutics. 2018 Jan 13;10(1).
36. Graça A, Gonçalves LM, Raposo S, Ribeiro HM, Marto J. Useful *In Vitro* Techniques to Evaluate the Mucoadhesive Properties of Hyaluronic Acid-Based Ocular Delivery Systems. Pharmaceutics [Internet]. 2018 Aug 1 [cited 2019 Mar 10];10(3). Available from: https://www.ncbi.nlm.nih.gov/pmc/articles/PMC6161121/
37. Ludwig A. The use of mucoadhesive polymers in ocular drug delivery. Adv Drug Deliv Rev. 2005 Nov 3;57(11):1595–639.
38. Jumelle C, Gholizadeh S, Annabi N, Dana R. Advances and limitations of drug delivery systems formulated as eye drops. J Controlled Release. 2020 May 10;321:1–22.
39. Alvarez-Trabado J, Diebold Y, Sanchez A. Designing lipid nanoparticles for topical ocular drug delivery. Int J Pharm. 2017 Oct 30;532(1):204–17.
40. Kumar A, Naik PK, Pradhan D, Ghosh G, Rath G. Mucoadhesive Formulations: Innovations, Merits, Drawbacks and Future Outlook. Pharm Dev Technol. 2020 Apr 8;1–43.
41. Shaikh R, Raj Singh TR, Garland MJ, Woolfson AD, Donnelly RF. Mucoadhesive drug delivery systems. J Pharm Bioallied Sci. 2011;3(1):89–100.
42. Mucoadhesive polymers in the treatment of dry X syndrome. Drug Discov Today. 2016 Jul 1;21(7):1051–62.
43. Baranowski P, Karolewicz B, Gajda M, Pluta J. Ophthalmic Drug Dosage Forms: Characterisation and Research Methods. Sci World J [Internet]. 2014 Mar 18 [cited 2016 Sep 23];2014. Available from: http://www.ncbi.nlm.nih.gov/pmc/articles/PMC3977496/
44. Papakonstantinou E, Roth M, Karakiulakis G. Hyaluronic acid: A key molecule in skin aging. Dermatoendocrinol. 2012 Jul 1;4(3):253–8.
45. Suárez-Barrio C, Etxebarria J, Hernáez-Moya R, del Val-Alonso M, Rodriguez-Astigarraga M, Urkaregi A, et al. Hyaluronic Acid Combined with Serum Rich in Growth Factors in Corneal Epithelial Defects. Int J Mol Sci [Internet]. 2019 Apr 3 [cited 2020 Apr 11];20(7). Available from: https://www.ncbi.nlm.nih.gov/pmc/articles/PMC6480555/
46. Salzillo R, Schiraldi C, Corsuto L, D'Agostino A, Filosa R, De Rosa M, et al. Optimization of hyaluronan-based eye drop formulations. Carbohydr Polym. 2016 Nov 20;153:275–83.
47. M I, C K. The effect of hyaluronic acid on corneal epithelial cell proliferation. Invest Ophthalmol Vis Sci. 1993 1993;34(7):2313–5.
48. Salwowska NM, Bebenek KA, Żądło DA, Wcisło-Dziadecka DL. Physiochemical properties and application of hyaluronic acid: a systematic review. J Cosmet Dermatol. 2016 Dec;15(4):520–6.

49. Ntonti P, Panagiotopoulou EK, Karastatiras G, Breyannis N, Tsironi S, Labiris G. Impact of 0.1% sodium hyaluronate and 0.2% sodium hyaluronate artificial tears on postoperative discomfort following cataract extraction surgery: a comparative study. Eye Vis Lond Engl. 2019;6:6.
50. Yoon DY, Kim JH, Jeon HS, Jeon HE, Han SB, Hyon JY. Evaluation of the Protective Effect of an Ophthalmic Viscosurgical Device on the Ocular Surface in Dry Eye Patients during Cataract Surgery. Korean J Ophthalmol KJO. 2019 Oct;33(5):467–74.
51. Huynh A, Priefer R. Hyaluronic acid applications in ophthalmology, rheumatology, and dermatology. Carbohydr Res. 2020 Mar 1;489:107950.
52. Fezza JP. Cross-linked hyaluronic acid gel occlusive device for the treatment of dry eye syndrome. Clin Ophthalmol Auckl NZ. 2018 Nov 8;12:2277–83.
53. Beck R, Stachs O, Koschmieder A, Mueller-Lierheim WGK, Peschel S, van Setten GB. Hyaluronic Acid as an Alternative to Autologous Human Serum Eye Drops: Initial Clinical Results with High-Molecular-Weight Hyaluronic Acid Eye Drops. Case Rep Ophthalmol. 2019 Aug;10(2):244–55.
54. Herrero-Vanrell R, Fernandez-Carballido A, Frutos G, Cadórniga R. Enhancement of the mydriatic response to tropicamide by bioadhesive polymers. J Ocul Pharmacol Ther Off J Assoc Ocul Pharmacol Ther. 2000 Oct;16(5):419–28.
55. Chen Q, Yin C, Ma J, Tu J, Shen Y. Preparation and Evaluation of Topically Applied Azithromycin Based on Sodium Hyaluronate in Treatment of Conjunctivitis. Pharmaceutics. 2019 Apr 15;11(4).
56. Chowhan A, Giri TK. Polysaccharide as renewable responsive biopolymer for in situ gel in the delivery of drug through ocular route. Int J Biol Macromol. 2020 May 1;150:559–72.
57. Matanović MR, Kristl J, Grabnar PA. Thermoresponsive polymers: Insights into decisive hydrogel characteristics, mechanisms of gelation, and promising biomedical applications. Int J Pharm. 2014 Sep 10;472(1):262–75.
58. Üstündağ Okur N, Yozgatlı V, Okur ME, Yoltaş A, Siafaka PI. Improving therapeutic efficacy of voriconazole against fungal keratitis: Thermo-sensitive in situ gels as ophthalmic drug carriers. J Drug Deliv Sci Technol. 2019 Feb 1;49:323–33.
59. Chan PS, Xian JW, Li Q, Chan CW, Leung SSY, To KKW. Biodegradable Thermosensitive PLGA-PEG-PLGA Polymer for Non-irritating and Sustained Ophthalmic Drug Delivery. AAPS J. 2019 24;21(4):59.
60. Shi H, Wang Y, Bao Z, Lin D, Liu H, Yu A, et al. Thermosensitive glycol chitosan-based hydrogel as a topical ocular drug delivery system for enhanced ocular bioavailability. Int J Pharm. 2019 Oct 30;570:118688.
61. Mohammed S, Chouhan G, Anuforom O, Cooke M, Walsh A, Morgan-Warren P, et al. Thermosensitive hydrogel as an in situ gelling antimicrobial ocular dressing. Mater Sci Eng C. 2017 Sep 1;78:203–9.
62. Huh KM, Kang HC, Lee YJ, Bae YH. pH-sensitive polymers for drug delivery. Macromol Res. 2012 Mar 1;20(3):224–33.

63. Pathak MK, Chhabra G, Pathak K. Design and development of a novel pH triggered nanoemulsified in-situ ophthalmic gel of fluconazole: ex-vivo transcorneal permeation, corneal toxicity and irritation testing. Drug Dev Ind Pharm. 2013 May;39(5):780–90.
64. Srividya B, Cardoza RM, Amin PD. Sustained ophthalmic delivery of ofloxacin from a pH triggered in situ gelling system. J Control Release Off J Control Release Soc. 2001 Jun 15;73(2–3):205–11.
65. Wu H, Liu Z, Peng J, Li L, Li N, Li J, et al. Design and evaluation of baicalin-containing in situ pH-triggered gelling system for sustained ophthalmic drug delivery. Int J Pharm. 2011 May 30;410(1–2):31–40.
66. Willcox MDP, Argüeso P, Georgiev GA, Holopainen JM, Laurie GW, Millar TJ, et al. TFOS DEWS II Tear Film Report. Ocul Surf. 2017 Jul 1;15(3):366–403.
67. Sun J, Zhou Z. A novel ocular delivery of brinzolamide based on gellan gum: *in vitro* and *in vivo* evaluation. Drug Des Devel Ther. 2018 Feb 23;12:383–9.
68. Liu Y, Liu J, Zhang X, Zhang R, Huang Y, Wu C. In Situ Gelling Gelrite/Alginate Formulations as Vehicles for Ophthalmic Drug Delivery. AAPS PharmSciTech. 2010 Mar 31;11(2):610–20.
H. B. Nirmal, S. R. Bakliwal, S. P. Pawar. In-situ gel: New trends in Controlled and Sustained Drug Delivery System. Int. J. Pharm. Tech. Res., 2 (2010), pp. 1398-1408
70. Li P, Wang S, Chen H, Zhang S, Yu S, Li Y, et al. A novel ion-activated in situ gelling ophthalmic delivery system based on κ-carrageenan for acyclovir. Drug Dev Ind Pharm. 2018 May;44(5):829–36.
71. Cui SW, Wu Y, Ding H. 5 - The range of dietary fibre ingredients and a comparison of their technical functionality. In: Delcour JA, Poutanen K, editors. Fibre-Rich and Wholegrain Foods [Internet]. Woodhead Publishing; 2013 [cited 2020 Apr 8]. p. 96–119. (Woodhead Publishing Series in Food Science, Technology and Nutrition). Available from: http://www.sciencedirect.com/science/article/pii/B978085709038650005X
72. Kariduraganavar MY, Kittur AA, Kamble RR. Chapter 1 - Polymer Synthesis and Processing. In: Kumbar SG, Laurencin CT, Deng M, editors. Natural and Synthetic Biomedical Polymers [Internet]. Oxford: Elsevier; 2014 [cited 2020 Apr 9]. p. 1–31. Available from: http://www.sciencedirect.com/science/article/pii/B9780123969835000016
73. Rhein-Knudsen N, Ale MT, Meyer AS. Seaweed Hydrocolloid Production: An Update on Enzyme Assisted Extraction and Modification Technologies. Mar Drugs. 2015 May 27;13(6):3340–59.
74. Lee KY, Mooney DJ. Alginate: properties and biomedical applications. Prog Polym Sci. 2012 Jan;37(1):106–26.
75. Almeida H, Amaral MH, Lobão P, Lobo JMS. In situ gelling systems: a strategy to improve the bioavailability of ophthalmic pharmaceutical formulations. Drug Discov Today. 2014 Apr;19(4):400–12.
76. Loftsson T, Jarho P, Másson M, Järvinen T. Cyclodextrins in drug delivery. Expert Opin Drug Deliv. 2005 Mar;2(2):335–51.
77. Brewster ME, Loftsson T. Cyclodextrins as pharmaceutical solubilizers. Adv Drug Deliv Rev. 2007 Jul 30;59(7):645–66.

78. European Medicines Agency (EMA). Background review for cyclodextrins used as excipients. 2014 Nov;17.
79. Santana ACSGV, Nadvorny D, da Rocha Passos TD, de La Roca Soares MF, Soares-Sobrinho JL. Influence of cyclodextrin on posaconazole stability, release and activity: Improve the utility of the drug. J Drug Deliv Sci Technol. 2019 Oct 1;53:101153.
80. Loftsson T, Brewster ME. Pharmaceutical applications of cyclodextrins. 1. Drug solubilization and stabilization. J Pharm Sci. 1996 Oct;85(10):1017–25.
81. Abdelkader H, Fathalla Z, Moharram H, Ali TFS, Pierscionek B. Cyclodextrin Enhances Corneal Tolerability and Reduces Ocular Toxicity Caused by Diclofenac. Oxid Med Cell Longev. 2018;2018:5260976.
82. Loftsson T, Stefánsson E. Cyclodextrins and topical drug delivery to the anterior and posterior segments of the eye. Int J Pharm. 2017 Oct 15;531(2):413–23.
83. FlorCruz NV, Evans JR. Medical interventions for fungal keratitis. Cochrane Database Syst Rev. 2015 Apr 9;(4):CD004241.
84. Niu L, Liu X, Ma Z, Yin Y, Sun L, Yang L, et al. Fungal keratitis: Pathogenesis, diagnosis and prevention. Microb Pathog. 2020 Jan 1;138:103802.
85. Mellado F, Rojas T, Cumsille C. Fungal keratitis: review of diagnosis and treament. Arq Bras Oftalmol. 2013 Feb;76(1):52–6.
86. Thomas PA. Current perspectives on ophthalmic mycoses. Clin Microbiol Rev. 2003 Oct;16(4):730–97.
87. Sahu SK, Dora J, Hota G. Keratomycosis caused by Blastoschizomyces capitatus. Indian J Pathol Microbiol. 2016 Mar;59(1):117–8.
88. Levy J, Benharroch D, Peled N, Lifshitz T. Blastoschizomyces capitatus keratitis and melting in a corneal graft. Can J Ophthalmol J Can Ophtalmol. 2006 Dec;41(6):772–4.
89. Kitazawa K, Fukuoka H, Inatomi T, Aziza Y, Kinoshita S, Sotozono C. Safety of retrocorneal plaque aspiration for managing fungal keratitis. Jpn J Ophthalmol. 2020 Mar;64(2):228–33.
90. Roth M, Daas L, Renner-Wilde A, Cvetkova-Fischer N, Saeger M, Herwig-Carl M, et al. [The German keratomycosis registry : Initial results of a multicenter survey]. Ophthalmol Z Dtsch Ophthalmol Ges. 2019 Oct;116(10):957–66.
91. Patel NA, Miller D, Relhan N, Alfonso EC, Flynn HW. Novel Use of Fluorescence In Situ Hybridization for the Rapid Identification of Microorganisms in Endophthalmitis and Keratitis. Ophthalmic Surg Lasers Imaging Retina. 2019 01;50(5):S9–12.
92. Satpathy G, Ahmed NH, Nayak N, Tandon R, Sharma N, Agarwal T, et al. Spectrum of mycotic keratitis in north India: Sixteen years study from a tertiary care ophthalmic centre. J Infect Public Health. 2019 Jun;12(3):367–71.
93. Rosa RH, Miller D, Alfonso EC. The changing spectrum of fungal keratitis in south Florida. Ophthalmology. 1994 Jun;101(6):1005–13.
94. Watson SL, Cabrera-Aguas M, Keay L, Khoo P, McCall D, Lahra MM. The clinical and microbiological features and outcomes of fungal keratitis over 9 years in Sydney, Australia. Mycoses. 2020 Jan;63(1):43–51.

95. Huang YH, Lin IH, Chang TC, Tseng SH. Early diagnosis and successful treatment of Cryptococcus albidus keratitis: a case report and literature review. Medicine (Baltimore). 2015 May;94(19):e885.
96. de Castro LEF, Sarraf OA, Lally JM, Sandoval HP, Solomon KD, Vroman DT. Cryptococcus albidus keratitis after corneal transplantation. Cornea. 2005 Oct;24(7):882–3.
97. Suzuki T, Hori N, Miyake T, Hori Y, Mochizuki K. Keratitis caused by a rare fungus, Malassezia restricta. Jpn J Ophthalmol. 2007 Aug;51(4):292–4.
98. Park KA, Ahn K, Chung ES, Chung TY. Pichia anomala fungal keratitis. Cornea. 2008 Jun;27(5):619–20.
99. Keating A, Pineda R. Trichosporon asahii keratitis in a patient with a type I Boston keratoprosthesis and contact lens. Eye Contact Lens. 2012 Mar;38(2):130–2.
100. Kumar A, Khurana A, Sharma M, Chauhan L. Causative fungi and treatment outcome of dematiaceous fungal keratitis in North India. Indian J Ophthalmol. 2019;67(7):1048–53.
101. Zbiba W, Kharrat M, Sayadi J, Baba A, Bouayed E, Abdessalem NB. Fungal keratitis caused by acremonium: A case report and literature review. J Fr Ophtalmol. 2018 Jun;41(6):e261–3.
102. McGirr S, Andersen D, Halgren J. Alternaria keratitis after corneal crosslinking. Am J Ophthalmol Case Rep. 2020 Mar;17:100616.
103. Alshehri B, Palanisamy M. Evaluation of molecular identification of Aspergillus species causing fungal keratitis. Saudi J Biol Sci. 2020 Feb 1;27(2):751–6.
104. Balakrishnan Sangeetha A, Abdel-Hadi A, Hassan AS, Shobana CS, Suresh S, Abirami B, et al. Evaluation of *in vitro* activities of extracellular enzymes from Aspergillus species isolated from corneal ulcer/keratitis. Saudi J Biol Sci. 2020 Feb;27(2):701–5.
105. Barakat GII, Kamal YN, Sultan AM. Could aflatoxin B1 production by Aspergillus flavus affect the severity of keratitis: an experience in two tertiary health care centers, Egypt. Eur J Clin Microbiol Infect Dis Off Publ Eur Soc Clin Microbiol. 2019 Nov;38(11):2021–7.
106. Jagadeesh N, Belur S, Hegde P, Kamalanathan AS, Swamy BM, Inamdar SR. An L-fucose specific lectin from Aspergillus niger isolated from mycotic keratitis patient and its interaction with human pancreatic adenocarcinoma PANC-1 cells. Int J Biol Macromol. 2019 Aug 1;134:487–97.
107. Zhang Y, Wang ZQ, Deng SJ, Tian L, Liang QF. [Diagnostic value of fungal fluorescence staining on corneal scrapings for fungal keratitis]. Zhonghua Yan Ke Za Zhi Chin J Ophthalmol. 2019 Aug 11;55(8):601–8.
108. Al-Hatmi AMS, Castro MA, de Hoog GS, Badali H, Alvarado VF, Verweij PE, et al. Epidemiology of Aspergillus species causing keratitis in Mexico. Mycoses. 2019 Feb;62(2):144–51.
109. Konar P, Joshi S, Mandhare SJ, Thakur R, Deshpande M, Dayal A. Intrastromal voriconazole: An adjuvant approach for recalcitrant mycotic keratitis. Indian J Ophthalmol. 2020;68(1):35–8.
110. Tabatabaei SA, Soleimani M, Tabatabaei SM, Beheshtnejad AH, Valipour N, Mahmoudi S. The use of *in vivo* confocal microscopy to track treatment success in fungal

keratitis and to differentiate between Fusarium and Aspergillus keratitis. Int Ophthalmol. 2020 Feb;40(2):483–91.
111. Hodkin MJ, Gustus RC. Fungal Keratitis Associated With Airborne Organic Debris and Soft Contacts Lenses: Case Reports and Review of the Literature. Eye Contact Lens. 2018 Sep;44 Suppl 1:S16–21.
112. Karimizadeh Esfahani M, Eslampoor A, Dolatabadi S, Najafzadeh MJ, Houbraken J. First case of fungal keratitis due to Aspergillus minisclerotigenes in Iran. Curr Med Mycol. 2019 Jun;5(2):45–8.
113. Lara Oya A, Medialdea Hurtado ME, Rojo Martín MD, Aguilera Pérez A, Alastruey-Izquierdo A, Miranda Casas C, et al. Fungal Keratitis Due to Beauveria bassiana in a Contact Lenses Wearer and Review of Published Reports. Mycopathologia. 2016 Oct;181(9–10):745–52.
114. Ogawa A, Matsumoto Y, Yaguchi T, Shimmura S, Tsubota K. Successful treatment of Beauveria bassiana fungal keratitis with topical voriconazole. J Infect Chemother. 2016 Apr;22(4):257–60.
115. Cheng SCH, Lin YY, Kuo CN, Lai LJ. Cladosporium keratitis - a case report and literature review. BMC Ophthalmol. 2015 Aug 19;15:106.
116. Hung N, Hsiao CH, Yang CS, Lin HC, Yeh LK, Fan YC, et al. Colletotrichum keratitis: A rare yet important fungal infection of human eyes. Mycoses. 2020 Apr;63(4):407–15.
117. Breval IZY, Sanabria AM, González AG, Abreu AT. Queratitis fúngica por Colletotrichum gloeosporioides: A propósito de un caso. Rev Esp Quimioter. 2019 Apr;32(2):198–9.
118. Wang L, Yu H, Jiang L, Wu J, Yi M. Fungal keratitis caused by a rare pathogen, Colletotrichum gloeosporioides, in an east coast city of China. J Mycol Medicale. 2020 Jan 7;100922.
119. Pote ST, Chakraborty A, Lahiri KK, Patole MS, Deshmukh RA, Shah SR. Keratitis by a rare pathogen Colletotrichum gloeosporioides: A case report. J Mycol Medicale. 2017 Sep;27(3):407–11.
120. Buchta V, Nekolová J, Jirásková N, Bolehovská R, Wipler J, Hubka V. Fungal Keratitis Caused by Colletotrichum dematium: Case Study and Review. Mycopathologia. 2019 Jun;184(3):441–53.
121. Kiss N, Homa M, Manikandan P, Mythili A, Krizsán K, Revathi R, et al. New Species of the Genus Curvularia: C. tamilnaduensis and C. coimbatorensis from Fungal Keratitis Cases in South India. Pathog Basel Switz. 2019 Dec 20;9(1).
122. Miqueleiz Zapatero A, Hernando C, Barba J, Buendía B. [First report of a case of fungal keratitis due to Curvularia hominis in Spain]. Rev Iberoam Micol. 2018 Sep;35(3):155–8.
123. Gaujoux T, Borsali E, Gavrilov JC, Touzeau O, Goldschmidt P, Despiau MC, et al. [Fungal keratitis caused by Cylindrocarpon lichenicola]. J Fr Ophtalmol. 2012 May;35(5):356.e1-5.
124. Mitra A, Savant V, Aralikatti A, Dean S, Shah S. The use of voriconazole in the treatment of cylindrocarpon keratomycosis. Cornea. 2009 Feb;28(2):217–8.

125. Kaliamurthy J, Jesudasan C a. N, Prasanth DA, Thomas PA. Keratitis due to Cylindrocarpon lichenicola. J Postgrad Med. 2006 Jun;52(2):155–7.
126. Echavez MI, Agahan ALD, Carino NS. Fungal Keratitis Caused by Drechslera spp. Treated with Voriconazole: A Case Report. Case Rep Ophthalmol Med. 2013;2013:626704.
127. Machen L, Chau FY, de la Cruz J, Sugar J, Cortina MS. Recognition of Fungal Keratitis in Boston Type I Keratoprosthesis: Importance of Awareness and Novel Identification of Exophiala phaeomuriformis. Cornea. 2018 May;37(5):655–7.
128. Vicente A, Pedrosa Domellöf F, Byström B. Exophiala phaeomuriformis keratitis in a subarctic climate region: a case report. Acta Ophthalmol (Copenh). 2018 Jun;96(4):425–8.
129. Aggarwal S, Yamaguchi T, Dana R, Hamrah P. Exophiala phaeomuriformis Fungal Keratitis: Case Report and *In Vivo* Confocal Microscopy Findings. Eye Contact Lens. 2017 Mar;43(2):e4–6.
130. Li Y, Zhang P, Huang C, Wang W. Dual effect of blue light on Fusariumsolani clinical corneal isolates *in vitro*. Lasers Med Sci. 2020 Feb 29;
131. Lopez-Vazquez A, Mora-Cantallops A, Mingo-Botín D. Fungi and paper-based archives. A case report of fungal keratitis in a documentalist. Arch Soc Espanola Oftalmol. 2020 Mar 14;
132. Rosa PD, Sheid K, Locatelli C, Marinho D, Goldani L. Fusarium solani keratitis: role of antifungal susceptibility testing and identification to the species level for proper management. Braz J Infect Dis Off Publ Braz Soc Infect Dis. 2019 Jun;23(3):197–9.
133. Ortega-Rosales A, Quizhpe-Ocampo Y, Montalvo-Flores M, Burneo-Rosales C, Romero-Ulloa G. A case of fungal keratitis due to Fusarium solani after an indigenous healing practice. IDCases. 2019;18:e00618.
134. Arcieri ES, Rocha A, Mendonça CN, Andreo EGV, Finotti IGA, Furlanetto RL, et al. Infectious keratitis secondary to Histoplasma capsulatum: the first case reports in humans. Braz J Infect Dis Off Publ Braz Soc Infect Dis. 2007 Dec;11(6):595–7.
135. Samudio M, Laspina F, Fariña N, Franco A, Mino de Kaspar H, Giusiano G. [Keratitis by Lasiodiplodia theobromae: a case report and literature review]. Rev Chil Infectologia Organo Of Soc Chil Infectologia. 2014 Dec;31(6):750–4.
136. Li STL, Yiu EPF, Wong AHY, Yeung JCT, Yu LWH. Successful Treatment of Lasiodiplodia theobromae Keratitis - Assessing the Role of Voriconazole. Case Rep Ophthalmol. 2016 Dec;7(3):179–85.
137. Lekhanont K, Nonpassopon M, Nimvorapun N, Santanirand P. Treatment with intrastromal and intracameral voriconazole in 2 eyes with Lasiodiplodia theobromae keratitis: case reports. Medicine (Baltimore). 2015 Feb;94(6):e541.
138. Hübner L, Tourtas T, Weller J. [Contact lens-associated superficial stromal keratitis caused by Paecilomyces lilacinus]. Ophthalmol Z Dtsch Ophthalmol Ges. 2020 Mar 24;
139. Vyawahare CR, Misra RN, Gandham NR, Angadi KM, Paul R. Pencillium keratitis in an Immunocompetent Patient from Pune, Maharashtra, India. J Clin Diagn Res JCDR. 2014 Jul;8(7):DD01-02.

140. Taechajongjintana M, Kasetsuwan N, Reinprayoon U, Sawanwattanakul S, Pisuchpen P. Effectiveness of voriconazole and corneal cross-linking on Phialophora verrucosa keratitis: a case report. J Med Case Reports. 2018 Aug 19;12(1):225.
141. Miyakubo T, Todokoro D, Makimura K, Akiyama H. Fungal keratitis caused by Didymella gardeniae (formerly Phoma gardeniae) successfully treated with topical voriconazole and miconazole. Med Mycol Case Rep. 2019 Jun;24:90–2.
142. Lenk J, Raiskup F, Pillunat LE, Rößler S. [Scedosporium apiospermum-a rare pathogen of keratomycosis]. Ophthalmol Z Dtsch Ophthalmol Ges. 2020 Mar 3;
143. Galvis V, Berrospi R, Tello A, Ramírez D, Villarreal D. Mycotic keratitis caused by Scedosporium apiospermum in an immunocompetent patient. Arch Soc Espanola Oftalmol. 2018 Dec;93(12):613–6.
144. Kindo AJ, Anita S, Kalpana S. Nattrassia mangiferae causing fungal keratitis. Indian J Med Microbiol. 2010 Jun;28(2):178–81.
145. Farjo QA, Farjo RS, Farjo AA. Scytalidium keratitis: case report in a human eye. Cornea. 2006 Dec;25(10):1231–3.
146. Zhang M, Jiang L, Li F, Xu Y, Lv S, Wang B. Simultaneous dermatophytosis and keratomycosis caused by Trichophyton interdigitale infection: a case report and literature review. BMC Infect Dis. 2019 Nov 21;19(1):983.
147. Jin KW, Jeon HS, Hyon JY, Wee WR, Suh W, Shin YJ. A case of fungal keratitis and onychomycosis simultaneously infected by Trichophyton species. BMC Ophthalmol. 2014 Jul 11;14:90.
148. Mravicić I, Dekaris I, Gabrić N, Romac I, Glavota V, Sviben M. Trichophyton Spp. fungal keratitis in 22 years old female contact lenses wearer. Coll Antropol. 2010 Apr;34 Suppl 2:271–4.
149. Mohammad A, Al-Rajhi A, Wagoner MD. Trichophyton fungal keratitis. Cornea. 2006 Jan;25(1):118–22.
150. Badenoch PR, Halliday CL, Ellis DH, Billing KJ, Mills R a. D. Ulocladium atrum keratitis. J Clin Microbiol. 2006 Mar;44(3):1190–3.
151. Mesa Varona D, Celis Sánchez J, Alfaya Muñoz L, Avendaño Cantos EM, Romero Moraleda L. Keratitis caused by Absidia corymbifera in an immunocompetent male with no corneal injuries. Arch Soc Espanola Oftalmol. 2015 Mar;90(3):139–41.
152. Rodrigues M, Laibson P. Exogenous mycotic keratitis caused by blastomyces dermatitidis. Am J Ophthalmol. 1973 May;75(5):782–9.
153. Thomas PA, Kaliamurthy J. Mycotic keratitis: epidemiology, diagnosis and management. Clin Microbiol Infect Off Publ Eur Soc Clin Microbiol Infect Dis. 2013 Mar;19(3):210–20.
154. Rai M, Occhiutto ML. Mycotic Keratitis. CRC Press; 2019. 367 p.
155. Austin A, Lietman T, Rose-Nussbaumer J. Update on the Management of Infectious Keratitis. Ophthalmology. 2017;124(11):1678–89.
156. Thamke DC, Mendiratta DK, Dhabarde A, Shukla AK. Mycotic keratitis due to Engyodontium album: first case report from India. Indian J Med Microbiol. 2015 Jun;33(2):303–4.

157. Anutarapongpan O, Thanathanee O, Suwan-Apichon O. Penicillium keratitis in a HIV-infected patient. BMJ Case Rep. 2016 Aug 17;2016.
158. original14_anexo_a.pdf [Internet]. [cited 2019 Dec 30]. Available from: http://scielo.isciii.es/img/revistas/asisna/v29s2/original14_anexo_a.pdf
159. Thomas PA. Fungal infections of the cornea. Eye. 2003;17(8):852–62.
160. García B, Juana PD, Hidalgo F, Bermejo T. 1 BASES FISIOLÓGICAS. :37.
161. Kanavi MR, Javadi M, Yazdani S, Mirdehghanm S. Sensitivity and specificity of confocal scan in the diagnosis of infectious keratitis. Cornea. 2007 Aug;26(7):782–6.
162. Manzouri B, Vafidis GC, Wyse RKH. Pharmacotherapy of fungal eye infections. Expert Opin Pharmacother. 2001;2(11):1849–57.
163. Müller GG, Kara-José N, Castro RS de. Antifungals in eye infections: drugs and routes of administration. Rev Bras Oftalmol. 2013 Apr;72(2):132–41.
164. GP Handbook | Moorfields Eye Hospital NHS Foundation Trust [Internet]. [cited 2020 Apr 4]. Available from: https://www.moorfields.nhs.uk/content/gp-handbook
165. Kalavathy CM, Parmar P, Kaliamurthy J, Philip VR, Ramalingam MDK, Jesudasan CAN, et al. Comparison of topical itraconazole 1% with topical natamycin 5% for the treatment of filamentous fungal keratitis. Cornea. 2005 May;24(4):449–52.
166. Lalitha P, Vijaykumar R, Prajna NV, Fothergill AW. *In Vitro* Natamycin Susceptibility of Ocular Isolates of Fusarium and Aspergillus Species: Comparison of Commercially Formulated Natamycin Eye Drops to Pharmaceutical-Grade Powder. J Clin Microbiol. 2008 Jan 10;46(10):3477–8.
167. Qiu S, Zhao GQ, Lin J, Wang X, Hu LT, Du ZD, et al. Natamycin in the treatment of fungal keratitis: a systematic review and Meta-analysis. Int J Ophthalmol. 2015;8(3):597–602.
168. Homa M, Manikandan P, Szekeres A, Kiss N, Kocsubé S, Kredics L, et al. Characterization of Aspergillus tamarii Strains From Human Keratomycoses: Molecular Identification, Antifungal Susceptibility Patterns and Cyclopiazonic Acid Producing Abilities. Front Microbiol. 2019;10:2249.
169. Ganegoda N, Rao SK. Antifungal therapy for keratomycoses. Expert Opin Pharmacother. 2004 Apr;5(4):865–74.
170. McElhiney LF. Compounding guide for ophthalmic preparations. Washington, D.C: American Pharmacists Association; 2013. 259 p.
171. Ji Y, Ji Y, Zhang F. Efficacy and Safety of Amphotericin B with Autologous Serum for Fungal Corneal Ulcer. J Coll Physicians Surg--Pak JCPSP. 2019 Feb;29(2):133–6.
172. Prajna NV, John RK, Nirmalan PK, Lalitha P, Srinivasan M. A randomised clinical trial comparing 2% econazole and 5% natamycin for the treatment of fungal keratitis. Br J Ophthalmol. 2003 Oct;87(10):1235–7.
173. Bennett JE, Dismukes WE, Duma RJ, Medoff G, Sande MA, Gallis H, et al. A comparison of amphotericin B alone and combined with flucytosine in the treatment of cryptoccal meningitis. N Engl J Med. 1979 Jul 19;301(3):126–31.
174. Nguyen MH, Barchiesi F, McGough DA, Yu VL, Rinaldi MG. *In vitro* evaluation of combination of fluconazole and flucytosine against Cryptococcus neoformans var. neoformans. Antimicrob Agents Chemother. 1995 Aug;39(8):1691–5.

175. SEFH: Sociedad Española de Farmacia Hospitalaria [Internet]. [cited 2017 Nov 22]. Available from: https://www.sefh.es/sefhpublicaciones/fichalibrolibre.php?id=24
176. Cowen LE, Sanglard D, Howard SJ, Rogers PD, Perlin DS. Mechanisms of Antifungal Drug Resistance. Cold Spring Harb Perspect Med [Internet]. 2015 Jul;5(7). Available from: https://www.ncbi.nlm.nih.gov/pmc/articles/PMC4484955/
177. Caffrey P, Lynch S, Flood E, Finnan S, Oliynyk M. Amphotericin biosynthesis in Streptomyces nodosus: deductions from analysis of polyketide synthase and late genes. Chem Biol. 2001 Jul 1;8(7):713–23.
178. Ellis D. Amphotericin B: spectrum and resistance. J Antimicrob Chemother. 2002 Feb;49 Suppl 1:7–10.
179. Pleyer U, Grammer J, Pleyer JH, Kosmidis P, Friess D, Schmidt KH, et al. [Amphotericin B--bioavailability in the cornea. Studies with local administration of liposome incorporated amphotericin B]. Ophthalmol Z Dtsch Ophthalmol Ges. 1995 Aug;92(4):469–75.
180. Qu L, Li L, Xie H. Corneal and aqueous humor concentrations of amphotericin B using three different routes of administration in a rabbit model. Ophthalmic Res. 2010;43(3):153–8.
181. Peyron F, Elias R, Ibrahim E, Amarit-Combralier V, Bues-Charbit M, Balansard G. Stability of amphotericin B in 5% dextrose ophthalmic solution. Int J Pharm Compd. 1999 Aug;3(4):316–20.
182. Thomas PA. Fungal infections of the cornea. Eye Lond Engl. 2003 Nov;17(8):852–62.
183. Jose María Alonse Herreros. Preparación de medicamentos y formulación magistral para oftalmología. 2013;
184. Bes D, Sberna N, Rosanova M. Ventajas y desventajas de los distintos tipos de anfotericina en pediatría: revisión de la bibliografía. Arch Argent Pediatría. 2012 Feb 1;110:46–51.
185. Hu J, Zhang J, Li Y, Han X, Zheng W, Yang J, et al. A Combination of Intrastromal and Intracameral Injections of Amphotericin B in the Treatment of Severe Fungal Keratitis. J Ophthalmol [Internet]. 2016;2016. Available from: https://www.ncbi.nlm.nih.gov/pmc/articles/PMC5046035/
186. Shao Y, Yu Y, Pei CG, Tan YH, Zhou Q, Yi JL, et al. Therapeutic efficacy of intracameral amphotericin B injection for 60 patients with keratomycosis. Int J Ophthalmol. 2010 Sep 18;3(3):257–60.
187. Bae JH, Lee SC. Intravitreal liposomal amphotericin B for treatment of endogenous candida endophthalmitis. Jpn J Ophthalmol. 2015 Sep;59(5):346–52.
188. Queratitis infecciosas: fundamentos, técnicas diagnósticas y tratamiento. Ergon; 2006. 278 p.
189. Falci DR, da Rosa FB, Pasqualotto AC. Comparison of nephrotoxicity associated to different lipid formulations of amphotericin B: a real-life study. Mycoses. 2015 Feb;58(2):104–12.
190. Fu T, Yi J, Lv S, Zhang B. Ocular amphotericin B delivery by chitosan-modified nanostructured lipid carriers for fungal keratitis-targeted therapy. J Liposome Res. 2017 Sep;27(3):228–33.

191. Chhonker YS, Prasad YD, Chandasana H, Vishvkarma A, Mitra K, Shukla PK, et al. Amphotericin-B entrapped lecithin/chitosan nanoparticles for prolonged ocular application. Int J Biol Macromol. 2015 Jan;72:1451–8.
192. Das S, Suresh PK. Nanosuspension: a new vehicle for the improvement of the delivery of drugs to the ocular surface. Application to amphotericin B. Nanomedicine Nanotechnol Biol Med. 2011 Apr;7(2):242–7.
193. O'Brien TP. THERAPY OF OCULAR FUNGAL INFECTIONS. Ophthalmol Clin. 1999 Mar 1;12(1):33–50.
194. Aparicio JF, Barreales EG, Payero TD, Vicente CM, de Pedro A, Santos-Aberturas J. Biotechnological production and application of the antibiotic pimaricin: biosynthesis and its regulation. Appl Microbiol Biotechnol. 2016;100:61–78.
195. Pradhan L, Sharma S, Nalamada S, Sahu SK, Das S, Garg P. Natamycin in the treatment of keratomycosis: Correlation of treatment outcome and *in vitro* susceptibility of fungal isolates. Indian J Ophthalmol. 2011;59(6):512–4.
196. Koontz JL, Marcy JE. Formation of Natamycin:Cyclodextrin Inclusion Complexes and Their Characterization. J Agric Food Chem. 2003 Nov 1;51(24):7106–10.
197. Badhani A, Dabral P, Rana V, Upadhyaya K. Evaluation of cyclodextrins for enhancing corneal penetration of natamycin eye drops. J Pharm Bioallied Sci. 2012 Mar;4(Suppl 1):S29–30.
198. Sradhanjali S, Yein B, Sharma S, Das S. *In vitro* synergy of natamycin and voriconazole against clinical isolates of Fusarium, Candida, Aspergillus and Curvularia spp. Br J Ophthalmol. 2018;102(1):142–5.
199. Patil A, Lakhani P, Taskar P, Wu KW, Sweeney C, Avula B, et al. Formulation Development, Optimization, and *In vitro* - *In vivo* Characterization of Natamycin Loaded PEGylated Nano-lipid Carriers for Ocular Applications. J Pharm Sci. 2018 Apr 23;
200. Maertens JA. History of the development of azole derivatives. Clin Microbiol Infect Off Publ Eur Soc Clin Microbiol Infect Dis. 2004 Mar;10 Suppl 1:1–10.
201. NCI Thesaurus-ketoconazole [Internet]. [cited 2018 Jul 4]. Available from: https://ncit.nci.nih.gov/ncitbrowser/ConceptReport.jsp?dictionary=NCI_Thesaurus&ns=NCI_Thesaurus&code=C1707
202. M Ghannoum HS, P Belanger. A new triazole, voriconazole (UK-109,496), blocks sterol biosynthesis in Candida albicans and Candida krusei. [Internet]. [cited 2018 Jul 4]. Available from: http://aac.asm.org/content/41/11/2492.short
203. Jeu L, Piacenti FJ, Lyakhovetskiy AG, Fung HB. Voriconazole. Clin Ther. 2003 May 1;25(5):1321–81.
204. Pawar P, Kashyap H, Malhotra S, Sindhu R, Pawar P, Kashyap H, et al. Hp--CD-Voriconazole In Situ Gelling System for Ocular Drug Delivery: *In Vitro*, Stability, and Antifungal Activities Assessment, Hp--CD-Voriconazole In Situ Gelling System for Ocular Drug Delivery: *In Vitro*, Stability, and Antifungal Activities Assessment. BioMed Res Int BioMed Res Int. 2013 May 9;2013, 2013:e341218.
205. Fluconazole - MeSH - NCBI [Internet]. [cited 2018 Jul 4]. Available from: https://www.ncbi.nlm.nih.gov/mesh/68015725

206. Fluconazole Monograph for Professionals - Drugs.com [Internet]. 2016. Available from: https://web.archive.org/web/20161220231218/https:/www.drugs.com/monograph/fluconazole.html
207. Jain BD. FORMULATION DEVELOPMENT AND EVALUATION OF FLUCONAZOLE GEL IN VARIOUS POLYMER BASESFORMULATION DEVELOPMENT AND EVALUATION OF FLUCONAZOLE GEL IN VARIOUS POLYMER BASES. Asian J Pharm AJP Free Full Text Artic Asian J Pharm [Internet]. 2016 Sep 9 [cited 2018 Jul 4];1(1). Available from: https://www.asiapharmaceutics.info/index.php/ajp/article/view/742
208. Isipradit S. Efficacy of fluconazole subconjunctival injection as adjunctive therapy for severe recalcitrant fungal corneal ulcer. J Med Assoc Thail Chotmaihet Thangphaet. 2008 Mar;91(3):309–15.
209. Yilmaz S, Maden A. Severe fungal keratitis treated with subconjunctival fluconazole. Am J Ophthalmol. 2005 Sep;140(3):454–8.
210. Tsai SH, Lin YC, Hsu HC, Chen YM. Subconjunctival Injection of Fluconazole in the Treatment of Fungal Alternaria Keratitis. Ocul Immunol Inflamm. 2016;24(1):103–6.
211. Kelidari HR, Moazeni M, Babaei R, Saeedi M, Akbari J, Parkoohi PI, et al. Improved yeast delivery of fluconazole with a nanostructured lipid carrier system. Biomed Pharmacother Biomedecine Pharmacother. 2017 May;89:83–8.
212. Habib FS, Fouad EA, Abdel-Rhaman MS, Fathalla D. Liposomes as an ocular delivery system of fluconazole: in-vitro studies. Acta Ophthalmol (Copenh). 2010 Dec;88(8):901–4.
213. Arora I, Kulshrestha OP, Upadhaya S. Treatment of fungal corneal ulcers with econazole. Indian J Ophthalmol. 1983 Jan 12;31(7):1019.
214. Mahashabde S, Nahata MC, Shrivastava U. A comparative study of anti-fungal drugs in mycotic corneal ulcer. Indian J Ophthalmol. 1987;35(5–6):149–52.
215. NCI Thesaurus - Econazole [Internet]. [cited 2018 Jul 3]. Available from: https://ncit.nci.nih.gov/ncitbrowser/ConceptReport.jsp?dictionary=NCI_Thesaurus&ns=NCI_Thesaurus&code=C47506
216. Jones BR, Clayton YM, Oji EO. Recognition and chemotherapy of oculomycosis. Postgrad Med J. 1979 Sep;55(647):625–8.
217. Martin MJ, Rahman MR, Johnson GJ, Srinivasan M, Clayton YM. Mycotic keratitis: susceptibility to antiseptic agents. Int Ophthalmol. 1995 1996;19(5):299–302.
218. Ciolino JB, Hudson SP, Mobbs AN, Hoare TR, Iwata NG, Fink GR, et al. A Prototype Antifungal Contact Lens. Invest Ophthalmol Vis Sci. 2011 Aug;52(9):6286–91.
219. Díaz-Tomé V, Luaces-Rodríguez A, Silva-Rodríguez J, Blanco-Dorado S, García-Quintanilla L, Llovo-Taboada J, et al. Ophthalmic Econazole Hydrogels for the Treatment of Fungal Keratitis. J Pharm Sci. 2018 May;107(5):1342–51.
220. Krachmer JH, Mannis MJ, Holland EJ. Cornea. Mosby/Elsevier; 2011. 1967 p.
221. El-Gawad AEGHA, Soliman OA, El-Dahan MS, Al-Zuhairy SAS. Improvement of the Ocular Bioavailability of Econazole Nitrate upon Complexation with Cyclodextrins. AAPS PharmSciTech. 2016 Nov 9;1–15.

222. Zhang B, Tian X, Xu Y, Zhao W, Zhang L. Efficacy Analysis of Econazole Nitrate Nanoparticle Formulation [Internet]. 2015 [cited 2018 Jul 3]. Available from: https://www.ingentaconnect.com/content/asp/jctn/2015/00000012/00000008/art00070
223. Mahmoud AA, El-Feky GS, Kamel R, Awad GEA. Chitosan/sulfobutylether-β-cyclodextrin nanoparticles as a potential approach for ocular drug delivery. Int J Pharm. 2011 Jul 15;413(1–2):229–36.
224. Maged A, Mahmoud AA, Ghorab MM. Nano Spray Drying Technique as a Novel Approach To Formulate Stable Econazole Nitrate Nanosuspension Formulations for Ocular Use. Mol Pharm. 2016 06;13(9):2951–65.
225. Elkasabgy NA. Ocular supersaturated self-nanoemulsifying drug delivery systems (S-SNEDDS) to enhance econazole nitrate bioavailability. Int J Pharm. 2014 Jan 2;460(1–2):33–44.
226. Heel RC, Brogden RN, Carmine A, Morley PA, Speight TM, Avery GS. Ketoconazole: a review of its therapeutic efficacy in superficial and systemic fungal infections. Drugs. 1982 Feb;23(1–2):1–36.
227. Ketoconazole [Internet]. [cited 2018 Jul 4]. Available from: https://www.drugbank.ca/drugs/DB01026
228. Ketoconazole [Internet]. [cited 2018 Jul 4]. Available from: https://livertox.nlm.nih.gov/Ketoconazole.htm
229. Ketostar 0.50% Eye Drop - Uses, Side Effects, Substitutes, Composition And More [Internet]. Lybrate. [cited 2020 Apr 15]. Available from: https://www.lybrate.com/medicine/ketostar-0-50-eye-drop
230. Kakkar S, Karuppayil SM, Raut JS, Giansanti F, Papucci L, Schiavone N, et al. Lipid-polyethylene glycol based nano-ocular formulation of ketoconazole. Int J Pharm. 2015 Nov 10;495(1):276–89.
231. Ahmed TA, Aljaeid BM. A potential in situ gel formulation loaded with novel fabricated poly(lactide-co-glycolide) nanoparticles for enhancing and sustaining the ophthalmic delivery of ketoconazole. Int J Nanomedicine. 2017;12:1863–75.
232. Van Cauteren H, Heykants J, De Coster R, Cauwenbergh G. Itraconazole: pharmacologic studies in animals and humans. Rev Infect Dis. 1987 Feb;9 Suppl 1:S43-46.
233. Itraconazole [Internet]. [cited 2018 Jul 4]. Available from: https://livertox.nlm.nih.gov/Itraconazole.htm
234. ElMeshad AN, Mohsen AM. Enhanced corneal permeation and antimycotic activity of itraconazole against Candida albicans via a novel nanosystem vesicle. Drug Deliv. 2016 Sep;23(7):2115–23.
235. Mochizuki K, Niwa Y, Ishida K, Kawakami H. Intraocular penetration of itraconazole in patient with fungal endophthalmitis. Int Ophthalmol. 2013 Oct;33(5):579–81.
236. Thomas PA, Abraham DJ, Kalavathy CM, Rajasekaran J. Oral itraconazole therapy for mycotic keratitis. Mycoses. 1988 May;31(5):271–9.
237. Kusbeci T, Avci B, Cetinkaya Z, Ozturk F, Yavas G, Ermis SS, et al. The effects of caspofungin and voriconazole in experimental Candida endophthalmitis. Curr Eye Res. 2007 Jan;32(1):57–64.

238. Schulman JA, Peyman GA, Dietlein J, Fiscella R. Ocular toxicity of experimental intravitreal itraconazole. Int Ophthalmol. 1991 Jan;15(1):21–4.
239. Pubchem. Itraconazole [Internet]. [cited 2018 Jul 4]. Available from: https://pubchem.ncbi.nlm.nih.gov/compound/55283
240. Mohanty B, Majumdar DK, Mishra SK, Panda AK, Patnaik S. Development and characterization of itraconazole-loaded solid lipid nanoparticles for ocular delivery. Pharm Dev Technol. 2015 Jun;20(4):458–64.
241. Jaiswal M, Kumar M, Pathak K. Zero order delivery of itraconazole via polymeric micelles incorporated in situ ocular gel for the management of fungal keratitis. Colloids Surf B Biointerfaces. 2015 Jun 1;130:23–30.
242. Pubchem. Miconazole [Internet]. [cited 2018 Jun 20]. Available from: https://pubchem.ncbi.nlm.nih.gov/compound/4189
243. Gyanfosu L, Koffuor GA, Kyei S, Ababio-Danso B, Peprah-Donkor K, Nyansah WB, et al. Efficacy and safety of extemporaneously prepared miconazole eye drops in Candida albicans-induced keratomycosis. Int Ophthalmol. 2017 Sep 12;
244. K Gupta S. Efficacy of miconazole in experimental keratomycosis. Aust N Z J Ophthalmol. 1986 Dec 1;14:373–6.
245. NCI Thesaurus-miconazole [Internet]. [cited 2018 Jun 20]. Available from: https://ncit.nci.nih.gov/ncitbrowser/pages/concept_details.jsf?dictionary=NCI_Thesaurus&version=18.05d&code=C62048&ns=NCI_Thesaurus&type=properties&key=null&b=1&n=0&vse=null)
246. Preissner S, Kroll K, Dunkel M, Senger C, Goldsobel G, Kuzman D, et al. SuperCYP: a comprehensive database on Cytochrome P450 enzymes including a tool for analysis of CYP-drug interactions. Nucleic Acids Res. 2010 Jan;38(suppl_1):D237–43.
247. Foster CS, Stefanyszyn M. Intraocular penetration of miconazole in rabbits. Arch Ophthalmol Chic Ill 1960. 1979 Sep;97(9):1703–6.
248. Posaconazole [Internet]. [cited 2018 Jun 20]. Available from: https://www.drugbank.ca/drugs/DB01263
249. Cuenca-Estrella M, Gomez-Lopez A, Mellado E, Buitrago MJ, Monzon A, Rodriguez-Tudela JL. Head-to-Head Comparison of the Activities of Currently Available Antifungal Agents against 3,378 Spanish Clinical Isolates of Yeasts and Filamentous Fungi. Antimicrob Agents Chemother. 2006 Mar;50(3):917–21.
250. Nagappan V, Deresinski S. Posaconazole: A Broad-Spectrum Triazole Antifungal Agent. Clin Infect Dis. 2007 Dec 15;45(12):1610–7.
251. Altun A, Kurna SA, Sengor T, Altun G, Olcaysu OO, Aki SF, et al. Effectiveness of Posaconazole in Recalcitrant Fungal Keratitis Resistant to Conventional Antifungal Drugs. Case Rep Ophthalmol Med [Internet]. 2014;2014. Available from: https://www.ncbi.nlm.nih.gov/pmc/articles/PMC4144149/
252. Tu EY, McCartney DL, Beatty RF, Springer KL, Levy J, Edward D. Successful Treatment of Resistant Ocular Fusariosis With Posaconazole (SCH-56592). Am J Ophthalmol. 2007 Feb 1;143(2):222-227.e1.

253. Schiller DS, Fung HB. Posaconazole: an extended-spectrum triazole antifungal agent. Clin Ther. 2007 Sep;29(9):1862–86.
254. Sponsel WE, Graybill JR, Nevarez HL, Dang D. Ocular and systemic posaconazole(SCH-56592) treatment of invasive Fusarium solani keratitis and endophthalmitis. Br J Ophthalmol. 2002 Jul;86(7):829–30.
255. Zimmerman HJ. Hepatotoxicity: The Adverse Effects of Drugs and Other Chemicals on the Liver. Lippincott Williams & Wilkins; 1999. 816 p.
256. Vermes A, Guchelaar HJ, Dankert J. Flucytosine: a review of its pharmacology, clinical indications, pharmacokinetics, toxicity and drug interactions. J Antimicrob Chemother. 2000 Aug;46(2):171–9.
257. O'Day DM, Head WS, Robinson RD, Stern WH, Freeman JM. Intraocular penetration of systemically administered antifungal agents. Curr Eye Res. 1985 Feb;4(2):131–4.
258. Salem HF, Ahmed SM, Omar MM. Liposomal flucytosine capped with gold nanoparticle formulations for improved ocular delivery. Drug Des Devel Ther. 2016 Jan 13;10:277–95.
259. Cancidas (Caspofungin) - Description and Clinical Pharmacology [Internet]. [cited 2018 Jul 4]. Available from: http://www.druglib.com/druginfo/cancidas/description_pharmacology
260. NCI Thesaurus-Caspofungine [Internet]. [cited 2018 Jul 4]. Available from: https://ncit.nci.nih.gov/ncitbrowser/ConceptReport.jsp?dictionary=NCI_Thesaurus&ns=NCI_Thesaurus&code=C28910
261. Thomas PA, Kaliamurthy J. Mycotic keratitis: epidemiology, diagnosis and management. Clin Microbiol Infect. 2013 Mar;19(3):210–20.
262. Manna VK, Pearse AD, Marks R. The effect of povidone-iodine paint on fungal infection. J Int Med Res. 1984;12(2):121–3.
263. Isenberg SJ, Apt L, Campeas D. Ocular applications of povidone-iodine. Dermatol Basel Switz. 2002;204 Suppl 1:92–5.
264. Ndoye Roth PA, Ba EA, Wane AM, De Meideros M, Dieng M, Ka A, et al. Fungal keratitis in an intertropical area: diagnosis and treatment problems. Advantage of local use of polyvidone iodine. J Fr Ophtalmol. 2006 Oct;29(8):e19.
265. mechanism of action of chlorhexidine | FEMS Microbiology Letters | Oxford Academic [Internet]. [cited 2020 Apr 17]. Available from: https://academic.oup.com/femsle/article/100/1-3/211/564040
266. Fernández-Ferreiro A, Santiago-Varela M, Gil-Martínez M, González-Barcia M, Luaces-Rodríguez A, Díaz-Tome V, et al. *In Vitro* Evaluation of the Ophthalmic Toxicity Profile of Chlorhexidine and Propamidine Isethionate Eye Drops. J Ocul Pharmacol Ther Off J Assoc Ocul Pharmacol Ther. 2017;33(3):202–9.
267. Rahman MR, Johnson GJ, Husain R, Howlader SA, Minassian DC. Randomised trial of 0.2% chlorhexidine gluconate and 2.5% natamycin for fungal keratitis in Bangladesh. Br J Ophthalmol. 1998 Aug;82(8):919–25.
268. Boral H, van Diepeningen A, Erdem E, Yağmur M, de Hoog GS, Ilkit M, et al. Mycotic Keratitis Caused by Fusarium solani sensu stricto (FSSC5): A Case Series. Mycopathologia. 2018 Oct 1;183(5):835–40.

269. Santos CO dos, Kolwijck E, Lee HA van der, Tehupeiory-Kooreman MC, Al-Hatmi AMS, Matayan E, et al. *In Vitro* Activity of Chlorhexidine Compared with Seven Antifungal Agents against 98 Fusarium Isolates Recovered from Fungal Keratitis Patients. Antimicrob Agents Chemother [Internet]. 2019 Aug 1 [cited 2020 Apr 17];63(8). Available from: https://aac.asm.org/content/63/8/e02669-18
270. Asiedu-Gyekye IJ, Mahmood AS, Awortwe C, Nyarko AK. Toxicological assessment of polyhexamethylene biguanide for water treatment. Interdiscip Toxicol. 2015 Dec;8(4):193–202.
271. Fiscella RG, Moshifar M, Messick CR, Pendland SL, Chandler JW, Viana M. Polyhexamethylene biguanide (PHMB) in the treatment of experimental Fusarium keratomycosis. Cornea. 1997 Jul;16(4):447–9.
272. Barchiesi F, Gallo D, Caselli F, Di Francesco LF, Arzeni D, Giacometti A, et al. In-vitro interactions of itraconazole with flucytosine against clinical isolates of Cryptococcus neoformans. J Antimicrob Chemother. 1999 Jul;44(1):65–70.
273. Ghannoum MA, Fu Y, Ibrahim AS, Mortara LA, Shafiq MC, Edwards JE, et al. *In vitro* determination of optimal antifungal combinations against Cryptococcus neoformans and Candida albicans. Antimicrob Agents Chemother. 1995 Nov;39(11):2459–65.
274. Schwarz P, Dromer F, Lortholary O, Dannaoui E. *In vitro* interaction of flucytosine with conventional and new antifungals against Cryptococcus neoformans clinical isolates. Antimicrob Agents Chemother. 2003 Oct;47(10):3361–4.
275. 1812.full.pdf [Internet]. [cited 2018 Jul 4]. Available from: http://aac.asm.org/content/41/8/1812.full.pdf
276. Dannaoui E, Afeltra J, Meis JFGM, Verweij PE, Network TE. *In Vitro* Susceptibilities of Zygomycetes to Combinations of Antimicrobial Agents. Antimicrob Agents Chemother. 2002 Jan 8;46(8):2708–11.
277. Gómez-López A, Cuenca-Estrella M, Mellado E, Rodríguez-Tudela JL. *In vitro* evaluation of combination of terbinafine with itraconazole or amphotericin B against Zygomycota. Diagn Microbiol Infect Dis. 2003 Mar;45(3):199–202.
278. Franzot SP, Casadevall A. Pneumocandin L-743,872 enhances the activities of amphotericin B and fluconazole against Cryptococcus neoformans *in vitro*. Antimicrob Agents Chemother. 1997 Feb;41(2):331–6.
279. Clancy CJ, Yu YC, Lewin A, Nguyen MH. Inhibition of RNA synthesis as a therapeutic strategy against Aspergillus and Fusarium: demonstration of *in vitro* synergy between rifabutin and amphotericin B. Antimicrob Agents Chemother. 1998 Mar;42(3):509–13.
280. Guarro J, Pujol I, Mayayo E. *In vitro* and *in vivo* experimental activities of antifungal agents against Fusarium solani. Antimicrob Agents Chemother. 1999 May;43(5):1256–7.
281. Hughes CE, Harris C, Moody JA, Peterson LR, Gerding DN. *In vitro* activities of amphotericin B in combination with four antifungal agents and rifampin against Aspergillus spp. Antimicrob Agents Chemother. 1984 May;25(5):560–2.
282. Rodero L, Córdoba S, Cahn P, Hochenfellner F, Davel G, Canteros C, et al. *In vitro* susceptibility studies of Cryptococcus neoformans isolated from patients with no clinical response to amphotericin B therapy. J Antimicrob Chemother. 2000 Feb 1;45(2):239–42.

283. Del Poeta M, Cruz MC, Cardenas ME, Perfect JR, Heitman J. Synergistic antifungal activities of bafilomycin A(1), fluconazole, and the pneumocandin MK-0991/caspofungin acetate (L-743,873) with calcineurin inhibitors FK506 and L-685,818 against Cryptococcus neoformans. Antimicrob Agents Chemother. 2000 Mar;44(3):739–46.
284. Kontoyiannis DP, Lewis RE, Osherov N, Albert ND, May GS. Combination of caspofungin with inhibitors of the calcineurin pathway attenuates growth *in vitro* in Aspergillus species. J Antimicrob Chemother. 2003 Feb;51(2):313–6.
285. Marchetti O, Moreillon P, Glauser MP, Bille J, Sanglard D. Potent synergism of the combination of fluconazole and cyclosporine in Candida albicans. Antimicrob Agents Chemother. 2000 Sep;44(9):2373–81.
286. Onyewu C, Blankenship JR, Del Poeta M, Heitman J. Ergosterol biosynthesis inhibitors become fungicidal when combined with calcineurin inhibitors against Candida albicans, Candida glabrata, and Candida krusei. Antimicrob Agents Chemother. 2003 Mar;47(3):956–64.
287. Afeltra J, Verweij PE. Antifungal activity of nonantifungal drugs. Eur J Clin Microbiol Infect Dis Off Publ Eur Soc Clin Microbiol. 2003 Jul;22(7):397–407.
288. Lupetti A, Paulusma-Annema A, Welling MM, Dogterom-Ballering H, Brouwer CPJM, Senesi S, et al. Synergistic activity of the N-terminal peptide of human lactoferrin and fluconazole against Candida species. Antimicrob Agents Chemother. 2003 Jan;47(1):262–7.
289. Wang T, Li S, Gao H, Shi W. Therapeutic dilemma in fungal keratitis: administration of steroids for immune rejection early after keratoplasty. Graefes Arch Clin Exp Ophthalmol Albrecht Von Graefes Arch Klin Exp Ophthalmol. 2016 Aug;254(8):1585–9.
290. Acharya Y, Acharya B, Karki P. Fungal keratitis: study of increasing trend and common determinants. Nepal J Epidemiol. 2017 Jun;7(2):685–93.
291. Perez Santonja JJ HHJ, Celis Sánchez J. Actualización en infecciones de la córnea. Métodos de diagnóstico y tratamiento. [Internet]. Madrid; 2018 [cited 2018 Jul 5]. Available from: https://www.agapea.com/libros/ACTUALIZACIoN-EN-INFECCIONES-DE-LA-CoRNEA-MeTODOS-DE-DIAGNoSTICO-Y-TRATAMIENTO-9788493989835-i.htm
292. Prajna NV, Krishnan T, Rajaraman R, Patel S, Shah R, Srinivasan M, et al. Adjunctive Oral Voriconazole Treatment of Fusarium Keratitis: A Secondary Analysis From the Mycotic Ulcer Treatment Trial II. JAMA Ophthalmol. 2017 Jun 1;135(6):520–5.
293. Prajna NV, Krishnan T, Rajaraman R, Patel S, Srinivasan M, Das M, et al. Effect of Oral Voriconazole on Fungal Keratitis in the Mycotic Ulcer Treatment Trial II (MUTT II): A Randomized Clinical Trial. JAMA Ophthalmol. 2016 01;134(12):1365–72.
294. Ramakrishnan T, Constantinou M, Jhanji V, Vajpayee RB. Factors affecting treatment outcomes with voriconazole in cases with fungal keratitis. Cornea. 2013 Apr;32(4):445–9.
295. Sharma N, Singhal D, Maharana PK, Sinha R, Agarwal T, Upadhyay AD, et al. Comparison of Oral Voriconazole Versus Oral Ketoconazole as an Adjunct to Topical Natamycin in Severe Fungal Keratitis: A Randomized Controlled Trial. Cornea. 2017 Dec;36(12):1521–7.

296. Sharma N, Chacko J, Velpandian T, Titiyal JS, Sinha R, Satpathy G, et al. Comparative evaluation of topical versus intrastromal voriconazole as an adjunct to natamycin in recalcitrant fungal keratitis. Ophthalmology. 2013 Apr;120(4):677–81.
297. Nada WM, Al Aswad MA, El-Haig WM. Combined intrastromal injection of amphotericin B and topical fluconazole in the treatment of resistant cases of keratomycosis: a retrospective study. Clin Ophthalmol Auckl NZ. 2017;11:871–4.
298. Lockington D, Agarwal P, Young D, Caslake M, Ramaesh K. Antioxidant properties of amniotic membrane: novel observations from a pilot study. Can J Ophthalmol J Can Ophtalmol. 2014 Oct;49(5):426–30.
299. Park WC, Tseng SC. Modulation of acute inflammation and keratocyte death by suturing, blood, and amniotic membrane in PRK. Invest Ophthalmol Vis Sci. 2000 Sep;41(10):2906–14.
300. Prajna NV, Krishnan T, Rajaraman R, Patel S, Shah R, Srinivasan M, et al. Predictors of Corneal Perforation or Need for Therapeutic Keratoplasty in Severe Fungal Keratitis: A Secondary Analysis of the Mycotic Ulcer Treatment Trial II. JAMA Ophthalmol. 2017 Sep 1;135(9):987–91.
301. Sabatino F, Sarnicola E, Sarnicola C, Tosi GM, Perri P, Sarnicola V, et al. Early deep anterior lamellar keratoplasty for fungal keratitis poorly responsive to medical treatment. Eye Lond Engl. 2017 Dec;31(12):1639–46.
302. Zeng B, Wang P, Xu LJ, Li XY, Zhang H, Li GG. Amniotic membrane covering promotes healing of cornea epithelium and improves visual acuity after debridement for fungal keratitis. Int J Ophthalmol. 2014;7(5):785–9.
303. Foote CS. Mechanisms of photosensitized oxidation. There are several different types of photosensitized oxidation which may be important in biological systems. Science. 1968 Nov 29;162(3857):963–70.
304. Wollensak G, Spoerl E, Seiler T. Riboflavin/ultraviolet-a-induced collagen crosslinking for the treatment of keratoconus. Am J Ophthalmol. 2003 May;135(5):620–7.
305. Richoz O, Mavrakanas N, Pajic B, Hafezi F. Corneal collagen cross-linking for ectasia after LASIK and photorefractive keratectomy: long-term results. Ophthalmology. 2013 Jul;120(7):1354–9.
306. Arora R, Manudhane A, Saran RK, Goyal J, Goyal G, Gupta D. Role of corneal collagen cross-linking in pseudophakic bullous keratopathy: a clinicopathological study. Ophthalmology. 2013 Dec;120(12):2413–8.
307. Said DG, Elalfy MS, Gatzioufas Z, El-Zakzouk ES, Hassan MA, Saif MY, et al. Collagen cross-linking with photoactivated riboflavin (PACK-CXL) for the treatment of advanced infectious keratitis with corneal melting. Ophthalmology. 2014 Jul;121(7):1377–82.
308. Tóth G, Bucher F, Siebelmann S, Bachmann B, Hermann M, Szentmáry N, et al. In Situ Corneal Cross-Linking for Recurrent Corneal Melting After Boston Type 1 Keratoprosthesis. Cornea. 2016 Jun;35(6):884–7.
309. Iseli HP, Thiel MA, Hafezi F, Kampmeier J, Seiler T. Ultraviolet A/riboflavin corneal cross-linking for infectious keratitis associated with corneal melts. Cornea. 2008 Jun;27(5):590–4.

310. Makdoumi K, Mortensen J, Sorkhabi O, Malmvall BE, Crafoord S. UVA-riboflavin photochemical therapy of bacterial keratitis: a pilot study. Graefes Arch Clin Exp Ophthalmol Albrecht Von Graefes Arch Klin Exp Ophthalmol. 2012 Jan;250(1):95–102.
311. Müller L, Thiel MA, Kipfer-Kauer AI, Kaufmann C. Corneal cross-linking as supplementary treatment option in melting keratitis: a case series. Klin Monatsbl Augenheilkd. 2012 Apr;229(4):411–5.
312. Price MO, Tenkman LR, Schrier A, Fairchild KM, Trokel SL, Price FW. Photoactivated riboflavin treatment of infectious keratitis using collagen cross-linking technology. J Refract Surg Thorofare NJ 1995. 2012 Oct;28(10):706–13.
313. Papaioannou L, Miligkos M, Papathanassiou M. Corneal Collagen Cross-Linking for Infectious Keratitis: A Systematic Review and Meta-Analysis. Cornea. 2016 Jan;35(1):62–71.
314. Price MO, Price FW. Corneal cross-linking in the treatment of corneal ulcers. Curr Opin Ophthalmol. 2016 May;27(3):250–5.
315. Alio JL, Abbouda A, Valle DD, Del Castillo JMB, Fernandez JAG. Corneal cross linking and infectious keratitis: a systematic review with a meta-analysis of reported cases. J Ophthalmic Inflamm Infect. 2013 May 29;3(1):47.
316. Li Z, Jhanji V, Tao X, Yu H, Chen W, Mu G. Riboflavin/ultravoilet light-mediated crosslinking for fungal keratitis. Br J Ophthalmol. 2013 May;97(5):669–71.
317. Shetty R, Nagaraja H, Jayadev C, Shivanna Y, Kugar T. Collagen crosslinking in the management of advanced non-resolving microbial keratitis. Br J Ophthalmol. 2014 Aug;98(8):1033–5.
318. Uddaraju M, Mascarenhas J, Das MR, Radhakrishnan N, Keenan JD, Prajna L, et al. Corneal Cross-linking as an Adjuvant Therapy in the Management of Recalcitrant Deep Stromal Fungal Keratitis: A Randomized Trial. Am J Ophthalmol. 2015 Jul;160(1):131-134.e5.
319. Vajpayee RB, Shafi SN, Maharana PK, Sharma N, Jhanji V. Evaluation of corneal collagen cross-linking as an additional therapy in mycotic keratitis. Clin Experiment Ophthalmol. 2015 Mar;43(2):103–7.
320. Garg P, Das S, Roy A. Collagen Cross-linking for Microbial Keratitis. Middle East Afr J Ophthalmol. 2017;24(1):18–23.

Chapter 1

OPHTHALMIC ECONAZOLE HYDROGELS FOR THE TREATMENT OF FUNGAL KERATITIS

1. INTRODUCTION

Fungal keratitis (FK) is a severe and difficult to treat disease which can be caused by different fungal species. Filamentous fungi, such as *Aspergillus spp* or *Fusarium spp*, are the main etiological agents in tropical and subtropical regions, where contaminated vegetables (by penetrating trauma) act as the most frequent transmission vehicles, causing the disease later in 40–60% of patients (1). In colder regions, *Candida albicans* is the most common causing-FK species, and the disease incidence is related to corneal surface surgeries, abrasions caused by contaminated contact lenses, neurotrophic ulcers or chronic use of topical corticosteroids (2).

Pain, vision loss, photosensitivity or tearing are the most frequent symptoms in FK, leading this to a subsequent complete blindness if not treated correctly (3). The ophthalmic FK treatment complexity requires the use of topical ophthalmic antifungal drugs for a prolonged time period, with frequent instillations and occasional corneal debridement to ensure the antifungals penetration (4,5). The current treatment mainly consists of polyene drugs such as natamycin for the filamentous fungi and amphotericin B for yeasts (6). Other treatments include azole drugs such as econazole, fluconazole or voriconazole (7,8), the latter being the most commonly used. Nevertheless, recent studies have shown econazole is a potential therapeutic alternative in the treatment of filamentous fungal keratitis caused by *Aspergillus* spp and *Fusarium* spp, showing therapeutic effects similar to natamycin (9,10).

However, nowadays there is a significant lack of commercial ophthalmic antifungal formulations due to their high cost and low stability. Therefore, a significant number of patients are in distress and ophthalmologists are forced to seek alternative options such as antifungal eye drops prepared at hospital pharmacy departments (11). A common practice consists of using commercial drugs for parenteral administration for the ophthalmic formulations' preparation by simply dissolving or diluting them in physiological buffers. However, the poor aqueous solubility of econazole nitrate requires complementary preparation methods to reach an optimum solubilization into the formulation, such as the complexation with the oligosaccharides derivatives cyclodextrins (12–14).

Additionally, one of the main challenges in ocular therapeutic design is the formulation of ophthalmic solutions that increase drug residence time in the ocular surface as well as allowing controlled drug release in order to increase bioavailability and effect duration (15). Hence, some ocular polymeric formulations, such as hydrogels, are developed to improve the viscosity and mucoadhesion of eye drops. To overcome these limitations *in situ* gelling systems based on smart polymers were studied in previous works due to their capability to recognize changes in the environmental conditions, modifying their conformation as a result of the stimulation (16–19).

In this work, econazole nitrate was solubilized with cyclodextrins and incorporated into ophthalmic hydrogels, being a better alternative to current pharmaceutical formulations prepared at hospital pharmacy departments. *In vitro* (drug release, antifungal effectiveness*)* and *ex vivo* (transcorneal permeation and Hen's Egg Test Chorionallantoic Membrane) studies were developed for validating this approach. In addition, novel *in vivo* studies using Positron Emission Tomography (PET) were performed in order to determine the ocular biopermanence of the econazole ophthalmic hydrogels prepared. Two different polysaccharide hydrogels were

selected to formulate econazole: an *in situ* ion sensitive hydrogel (20) and a mucoadhesive hydrogel based on hyaluronic acid (21), both previously developed by our group.

2. MATERIALS

Econazole nitrate and hyaluronic acid were obtained from Acofarma®, Spain; 2-hydroxypropyl-β-cyclodextrin (HPβCD, Kleptose HPβCD® with a 0.65 molar substitution ratio and MW 1399 Da) was purchased from Roquette Laisa S.A. (Valencia, Spain); 2-hydroxypropyl-Y-cyclodextrin (HPγCD, 0.6 molar substitution ratio, MW 1580) was acquired from Sigma Aldrich® (Darmstadt, Germany); α-cyclodextrin (αCD, Cavamax® W6, MW 972.84) was procured from Wacker Chemie AG (München Germany); gellam gum (GG, Kelcogel® CG-LA molecular weight 1.5–2.5 · 106 Da) and κ-carrageenan (CK, Genugel® carrageenan GC-130 molecular weight 3.5–8.0 · 105 Da) were provided by CP Kelco® (Atlanta, Georgia).

3. METHODS

3.1. PHASE SOLUBILITY DIAGRAMS

Phase solubility diagrams were employed to estimate the econazole nitrate stability constants with HPβCD, HPγCD and αCD. Solubility measurements were carried out according to Higuchi and Connors (22) methodology following the protocols previously described by Anguiano-Igea et al (23). An excess amount of econazole nitrate was added to a series of aqueous solutions of increasing cyclodextrin concentrations. Econazole nitrate solubility in distilled water and in PBS (Phosphate buffer saline pH 7.4) was also studied. Solutions were shaken in an orbital shaking bath (VWR) at 25 °C and 100 rpm for 7 days to reach equilibrium. Afterwards, an aliquot was centrifuged for 20 min at 16625G (SIGMA 2-16P) and 1 mL of the supernatant was diluted 100 times. Econazole nitrate concentration was determined for each sample using a diode-array spectrophotometer (Hewlett Packard 8452A, λ = 220 nm). Econazole nitrate solubility final values were shown as mean of three replicate measurements. Phase solubility diagrams were obtained by plotting mean solubility against cyclodextrin concentration. Apparent stability constant, assuming cyclodextrin inclusion complex formation with a 1:1 stoichiometry ($K_{1:1}$), was calculated from the slope, and drug solubility (S_0) or the intercept (S_0 extrap) from linear regions was obtained by least squares regression using the following equation:

$$K_{1:1} = \frac{Slope}{So\ (1-Slope)} \qquad \text{eq. 1}$$

Complexation efficiency (CE) parameter was produced by:

$$CE = So\ .K_{1:1} = \frac{\left[\frac{D}{CD}\right]}{[CD]} = \frac{Slope}{1-Slope} \qquad \text{eq. 2}$$

In addition, D:CD relation was calculated by using the CE obtained according to:

$$D{:}\,CD_{relation} = 1{:}\,(1 + \frac{1}{CE}) \qquad \text{eq. 3}$$

3.2. ^{1}H-NMR AND MOLECULAR MODELLING STUDIES

The inclusion complex showing best econazole nitrate solubilization characteristics was studied by carrying out ^{1}H-NMR and molecular modelling studies. Mono and bidimensional ^{1}H-NMR spectra of econazole, αCD, and the inclusion complex formed were obtained in a Bruker DRX 500 (Karlsruhe, Germany) spectrometer at 500.13 MHz. Rotating-frame Overhauser Effect Spectroscopy (ROESY) spectra were obtained in the same spectrometer. All the samples were prepared in D_2O solutions. Molecular modelling was performed by using Avogadro 20.8.0 software. Econazole molecular geometry was generated by an energy-minimization subroutine (maximum no. interactions 500; minimizer cut off 0.01). αCD molecular geometry was obtained by imputing X-ray diffraction monocrystal data. Complex molecular geometry was based on the previous ^{1}H-NMR results and generated using manual docking and, subsequently, by the same energy-minimization subroutine.

3.3. STUDY OF THE ECONAZOL-CD COMPLEX INCORPORATED INTO OPHTHALMIC HYDROGELS

First, a 2 mg/mL econazole nitrate solution with 15% (w/v) αCD (ECN) was prepared in warm distilled water (40ºC) under magnetic stirring for an hour. Subsequently, hydrogels were prepared by dispersing polysaccharides in warm distilled water (55°C), stirring for 24h and filtering for sterilization in a horizontal laminar flow hood. The Ion Sensitive Hydrogel (ISH) was prepared by using a 0.82% (w/v) GG (deacylated Gellan Gum) and CK (κ-carrageenan) mixture in a 4:1 ratio. 0.4% (w/v) hyaluronic acid was added in order to obtain a mucoadhesive hyaluronic acid hydrogel (HAH). Polymer concentrations and ratios were selected based on previous works (20,24).

3.4. *IN VITRO* RELEASE OF ECONAZOLE FROM OPHTHALMIC HYDROGELS

Econazole–αCD *in vitro* release from the hydrogel systems (ISH and HAH) and the econazole control solution (ECN) in contact with simulated lacrimal fluid (SLF) was estimated by using Franz diffusion cells and GVS 0.22 μm cellulose acetate membranes (membrane surface area of 0.784 cm^2). 500μl of each formulation containing 1 mg of econazole were placed in the upper compartment, adding 175 μL of SLF prepared as detailed by Ceulemans et al. (25). Sink conditions were maintained in the receptor compartment, which was filled with 6 mL of SLF. During the experiment, cell compartments were continuously homogenized by magnetic stirring at 200 rpm in a thermostated bath at 36ºC. Serial sampling was performed at different times. The Hewlett Packard 8452A diode-array spectrophotometer (λ = 220nm) was used for econazole content determination. Each experiment was repeated three times. Release data were fitted to Higuchi diffusion kinetics (26) and Peppas-Korsmeyer (27) equation using GraphPad Prism 6.0 software (GraphPad Software Inc.). Drug release was compared among formulations by using a one-way ANOVA with GraphPad Prism 6.0 software at different times.

3.5. *EX VIVO* CORNEAL PERMEABILITY STUDIES

For this purpose, bovine eyes were removed within the first hour after animal death and transported following the BCOP test protocol (28). Once received, corneas were isolated with 2-4 mm of surrounding sclera, washed with an isotonic saline solution and mounted on Franz diffusion cells. The cornea was placed on the receptor chamber and the donor one was attached. The receptor chamber was filled with 6 mL of SLF and the donor one with 500µl of each formulation containing 1 mg of econazole (area available for permeation: 0.785 cm^2) and 175µl of SLF. During the experiment, both compartments were continuously homogenized as previously reported (magnetic stirring at 200 rpm in a thermostated bath at 36ºC) and serial sampling was performed at different times. Each experiment was repeated three times.

Econazole nitrate determination was performed by a HPLC system (Merck® Hitachi, Germany), consisted of UV–VIS photodiode array detector model L-4500 (Merck® Hitachi, Germany), a solvent delivery pump system model L6200 A (Merck® Hitachi, Germany) and an auto injector fitted with 100µL loop model AS4000 A (Merck® Hitachi, Germany). D-7000 HMS 4.0 software (Merck® Hitachi, Germany) was used for data processing. Analyses were performed by an isocratic method. The column used was a C18 (3.9x150mm, 5µm of particle size Symmetry® Waters) keeping its temperature at 25ºC by using a thermostat model L-5025 (Merck® Hitachi, Germany). The mobile phase was methanol-water (85:15 v/v), using a flow rate of 1 mL min^{-1}. The sample injected volume was 50µl and the retention time was 4.5 minutes. A 320 nm wavelength was employed for the econazole quantification.

Apparent corneal permeability (Papp) was calculated according to the equation:

$$P_{app} = \frac{\delta Q/\delta t}{A \cdot C_0} \qquad \text{eq. 4}$$

Where $\delta Q/\delta t$ represents the econazole flux across corneal tissues in the linear portion of the representation, A the corneal surface (in this study 0.785 cm^2) and C_0 the initial drug concentration at the epithelial side. T_{lag} was calculated extrapolating the linear portion of the graph to the X-axis.

Nonparametric Kruskal Wallis test was used to compare the econazole corneal permeability from formulations using GraphPad Prism 6.0 software.

3.6. IRRITATION OCULAR TEST

HEN'S EGG TEST CHORIONALLANTOIC MEMBRANE (HET-CAM)

The HET-CAM assay was performed in order to evaluate possible acute ocular irritation caused by the econazole solubilized with αCD, as described in a previous work (29). 0.3 mL of econazole-αCD formulations (ECN, ISH, and HAH) were deposited onto the egg chorioallantoic membrane (three eggs per compound). Blood vessels were observed for 300 seconds with a stereomicroscope (Olympus SZ-STN), aiming at detecting episodes of bleeding, coagulation and partial lysis. The compounds' irritation score (IS) was determined as described in the INVITTOX 96 Protocol (30).

BOVINE CORNEAL OPACITY AND PERMEABILITY TEST (BCOP)

Corneal Opacity

BCOP assay was a variation of the method described in Protocol Invittox nº 437 (31), used to identify potential ocular corrosives and severe irritants. This method was carried out using fresh bovine corneas, where changes in corneal transparency, opacity and permeability were assessed.

Corneas were obtained, prepared, and placed in Franz diffusion cells as previously described (see "*Ex vivo* Corneal Permeability studies" section). Opacity (transmitted light, (TL)) was measured by using a luxmeter (Gossen Mavolux 5032C USB). Corneas were placed between two cylindrical supporting black holders (fabricated with polylactic acid filaments using a 3D printer, Wilbox® BQ) and illuminated with a pipe light (Olympus® Highlight 200) with fixed brightness values (32). The difference between light intensity measurements with and without cornea in the luxmeter was also calculated (% TL initial).

Corneal transparency was measured in transmittance values by UV-Vis spectrophotometry (Agilent® Cari 60 UV) from 800 to 200 nm, and a transmittance against wavelength spectrum was obtained for each cornea. After opacity and transparency initial readings of untreated corneal tissue, corneas were placed in Franz diffusion cells. Epithelial part of the cornea was placed towards the donor compartment and the receptor compartment was filled with PBS and homogenized by magnetic stirring in a thermostatic bath at 36°C during assay.

The test consisted of two parts. First, corneas placed in Franz diffusion cells were incubated for 60 min with 1 mL PBS in the donor chamber. Then, the PBS was removed, and opacity and transparency values were measured again. In the second part of the assay, 1 mL formulation, positive control (ethanol) or negative control (PBS) was placed in the donor compartment of each cell and kept in contact with the epithelial part of the cornea for 10 minutes, after which the solutions were removed with a Pasteur pipette. Donor compartment was subsequently cleaned and refilled with 1 mL PBS. After 120 min of incubation, corneal opacity and transparency were measured for the last time.

Corneal permeability

The same corneas used in the previous assay (see "Corneal Opacity" section) were placed back into the Franz cells with 6 mL PBS in the receptor compartment. Then, 1 mL of a 0.4% (w/v) fluorescein aqueous solution was placed in the donor compartment. Samples were collected at 90 min, and fluorescein amount was measured by Uv-Vis spectrophotometry at a 490 nm wavelength (Agilent® Cary 60 UV). Results are shown in µg of fluorescein per cm^2 of corneal surface.

3.7. ANTIFUNGAL EFFECTIVENESS

Candida Albicans ATCC 90028 (CA), *Aspergillus Fumigatus* KM8001 (AF) and *Paecilomyces* (PA), isolated from culture collection of the University Clinical Hospital of Santiago de Compostela microbiology department, were inoculated onto Mueller Hinton agar and RPMI culture medium (33). Kirby-Bauer disk diffusion susceptibility method was used to evaluate antifungal effectiveness. Filter paper disks, impregnated with 20 µL of econazole, natamycin,

amphotericin b, voriconazole and fluconazole, were placed into the Petri dish (previously seeded) and incubated at 37 °C for 24 h with CA and for 48 h with AF and PA. Digital pictures of the discs were taken using a Leica CLS-150 stereomicroscope connected to a Nikon digital camera and the econazole inhibition zone was measured and compared to other antifungals.

3.8. *IN VIVO* ASSAYS: QUANTITATIVE OCULAR PERMANENCE STUDY BY PET

PET studies were carried out on male Sprague-Dawley rats (500 g of average weight), supplied by the animal facility at the University of Santiago Compostela. Animals were kept in individual cages with free access to food and water under controlled temperature (22±1ºC) and humidity (60±5%), with day-night cycles regulated by artificial light (12/12 hours) for, at least, one week before experiments. Animals were treated according to the laboratory animals' guidelines (34). Experiments were approved by the Galician Network Committee for Ethics Research following the Spanish and European Union (EU) rules (86/609/CEE, 2003/65/CE, 2010/63/EU, RD 1201/2005 and RD 53/2013)".

Hydrogel ocular pharmacokinetic studies were performed as described in previous works (35). Briefly, Positron Emission Tomography (PET) and Computed Tomography (CT) images were acquired using the Albira PET/CT Preclinical Imaging System (Bruker Biospin, Woodbridge, Connecticut, United States). Anesthetized animals were placed in the small animal bed, and 7.5 µL of ECN or 7.5 µL econazole hydrogels labelled with ^{18}F-fluorodeoxyglucose (^{18}F-FDG) were instilled into the conjunctival sac eye by using a pipette. The administered radioactivity was 0.35 MBq per eye. Single frames of 10 minutes at 0.5, 1, 2 and 3 hours after instillation were acquired. Three animals (6 eyes) were tested for each formulation. Different Regions of Interest (ROIs) were manually drawn containing the signal on each eye. ROIs were replicated on different frames over time and results were corrected for radioactive decay. Afterwards, graphical representations of radioactivity versus time were obtained. Fitting of the remaining formulation vs time to a monoexponential decay equation using a single compartmental model was made with pKSolver software (36). Non-compartmental analysis was also performed, calculating the mean residence time (MRT) and the total area under the curve of the remaining concentration vs time.

4. RESULTS

4.1. ECONAZOLE NITRATE SOLUBILIZATION WITH CYCLODEXTRINS, ^{1}H-NMR AND MOLECULAR MODELLING STUDIES

Evidence of the inclusion-complex formation was obtained from the solubility curves for the three cyclodextrin hosts. In addition, the most favourable interaction between cyclodextrin and econazole nitrate was determined as well as the most stable inclusion complex formed. Diagrams obtained in water solutions with all cyclodextrins were A_L type (22) (Figure 1A). These diagrams suggest the formation of high solubility complexes characterized by a linear increase in solubility with the cyclodextrins concentration, also showing a constant stoichiometry of the complexes. Apparent stability constants ($K_{1:1}$), complexation efficiency (CE) and econazole-cyclodextrin relations with different cyclodextrins are shown in Table 1.

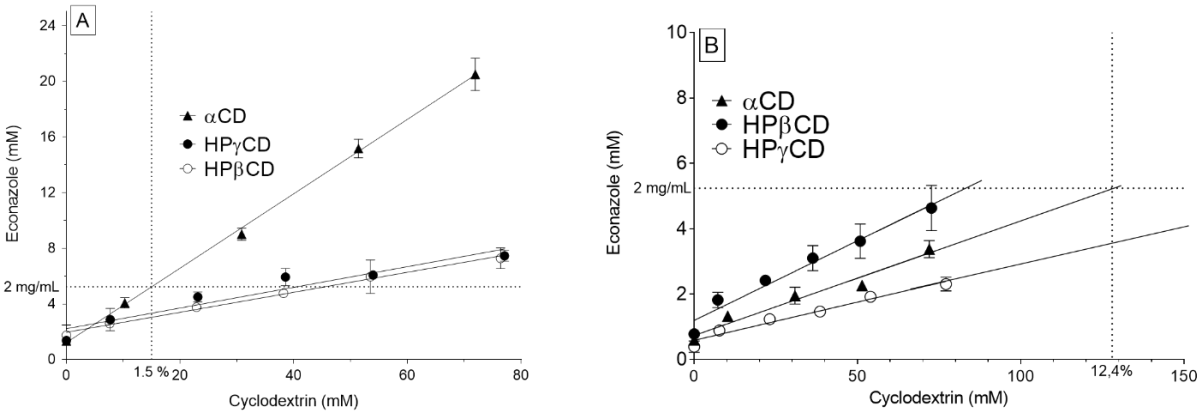

Figure 1. Phase solubility diagrams for econazole obtained with three cyclodextrin derivatives at 25 °C A) in water and B) in PBS (mean ± SD, *n* = 6). The dotted lines indicate the minimum CD concentration required to solubilize the required dose of the drug in hydrogels.

Table 1. Values for $K_{1:1}$, CE and the D:CD relation obtained from the econazole-cyclodextrin complex in A) water and B) PBS at 25 °C.

(A) Water	**S_0 (mM)**	**S_0 extrap (mM)**	**$K_{1:1}$* (mM^{-1})**	**$K_{1:1}$ extrap** (mM^{-1})**	**CE**	**D:CD (mol:mol)**	**R^2**
HPβCD	1.48	1.96	52.21	39.51	0.077	1:13.91	0.9187
HPγCD	1.48	2.22	54.11	36.18	0.080	1:13.46	0.8877
αCD	1.48	0.79	505.54	948.32	0.750	1:2.33	0.9936
(B) PBS	**S_0 (mM)**	**S_0 extrap (mM)**	**$K_{1:1}$* (mM^{-1})**	**$K_{1:1}$ extrap** (mM^{-1})**	**CE**	**D:CD (mol:mol)**	**R^2**
HPβCD	0.59	1.2	86.34	42.86	0.051	1: 20.5	0.7981
HPγCD	0.59	0.59	40.35	40.75	0.0245	1:42.8	0.8807
αCD	0.59	0.74	61.28	49.44	0.036	1:28.5	0.8942

*$K_{1:1}$ calculated using S_0 (solubility of free drug)

**$K_{1:1}$ calculated using S_0 extrap (free drug solubility calculated from the phase solubility diagram).

The $K_{1:1}$ highest value ($K_{1:1}$=505.54) was found for αCD, indicating econazole interacts more strongly with this cyclodextrin. αCD also showed the best solubilization properties for the econazole and forms the most stable complex presenting relatively high CE (0.75) and small D:CD (1:2.33) relation.

Despite eye drops were elaborated in water, the econazole-cyclodextrins phase solubility diagram was also made in PBS in order to evaluate the effect of pH and salt concentration in the econazole solubility once the eye drops are administered. The PBS graph showed a considerable decrease in the econazole affinity for αCD when it was dissolved in PBS (Figure 1B). HPβCD and HPγCD were less affected by the pH.

^{1}H-NMR was carried out to characterize the econazole-αCD complex. 1D-RMN econazole and αCD spectra (with the correspondent proton assignation for each signal) are shown in Figure 2. Chemical displacement changes were observed in the inclusion complex spectra (Figure 3), for both drug and cyclodextrin signals due to interactions between these molecules in solution. 2D-RMN assays were executed to elucidate the type of interactions. Specifically, a 2D-ROESY assay was developed, which allows obtaining the bidimensional spectra shown in Figure 3. There, it can be seen the interactions' formation between protons of the econazole imidazolic group and αCD's H5 and H3 protons (which were the ones that face the inside of the cavity). Moreover, interactions between econazole's H2 and cyclodextrine's H2 and H4 protons located in the narrow edge of cavity are observed. These results suggest the imidazole group remains inside the cavity and the econazole´s H2 proton is located in the αCD cavity edge. Figure 4 contains the built molecular model, showing how econazole is included into the αCD cavity. Chlorine, nitrogen, oxygen, carbon and hydrogen atoms are represented in green, blue, red, grey and pale grey, respectively. Nitrogen atoms, which are part of the econazole imidazolic ring, are located into cyclodextrin's cavity, while Cl atoms, which are fixed to phenyl groups, remain in the external area.

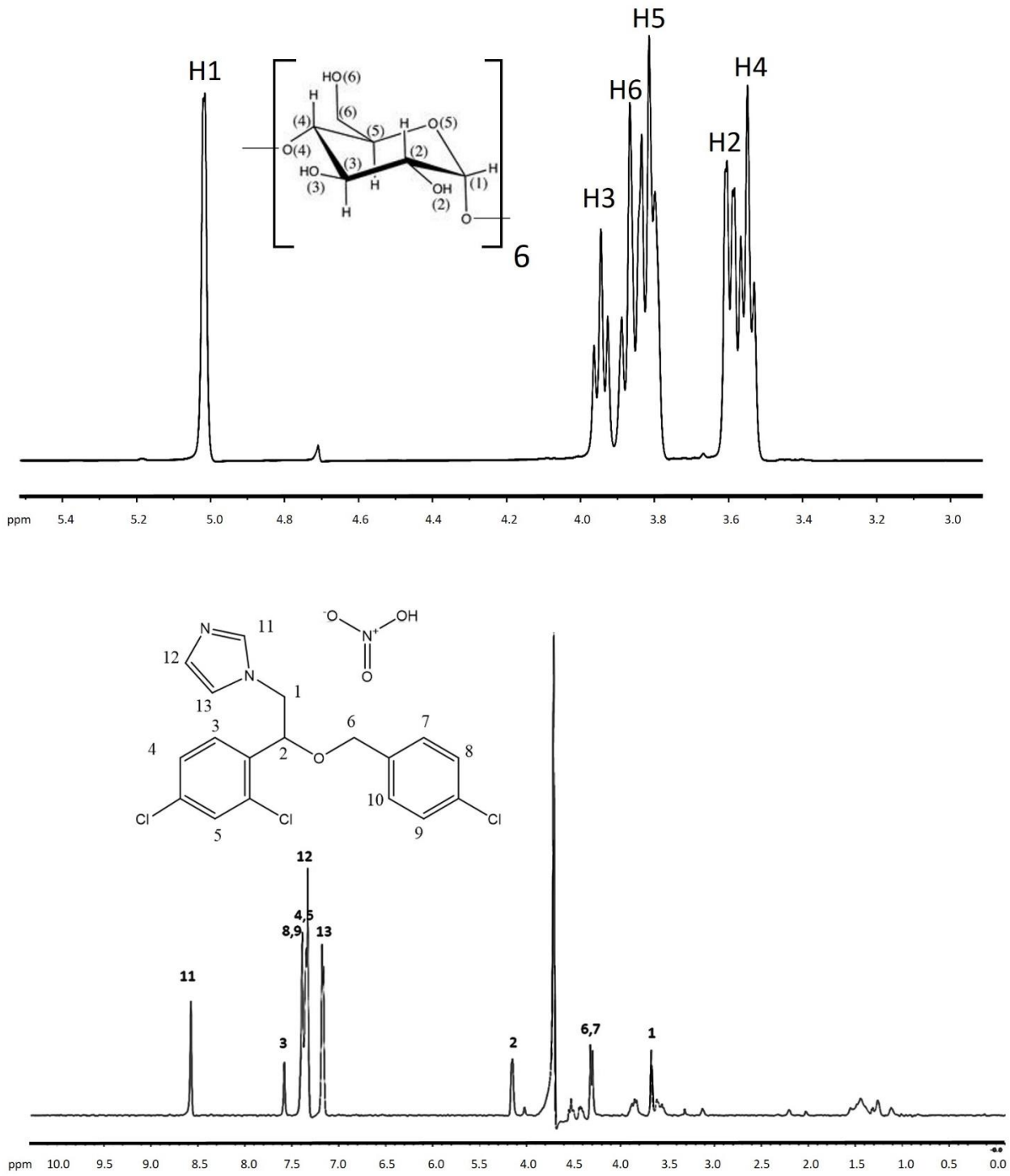

Figure 2. [1]H-NMR spectrum of α-cyclodextrin (top) and econazole (bottom) indicating the assignment of protons to the different signals [1]H-NMR.

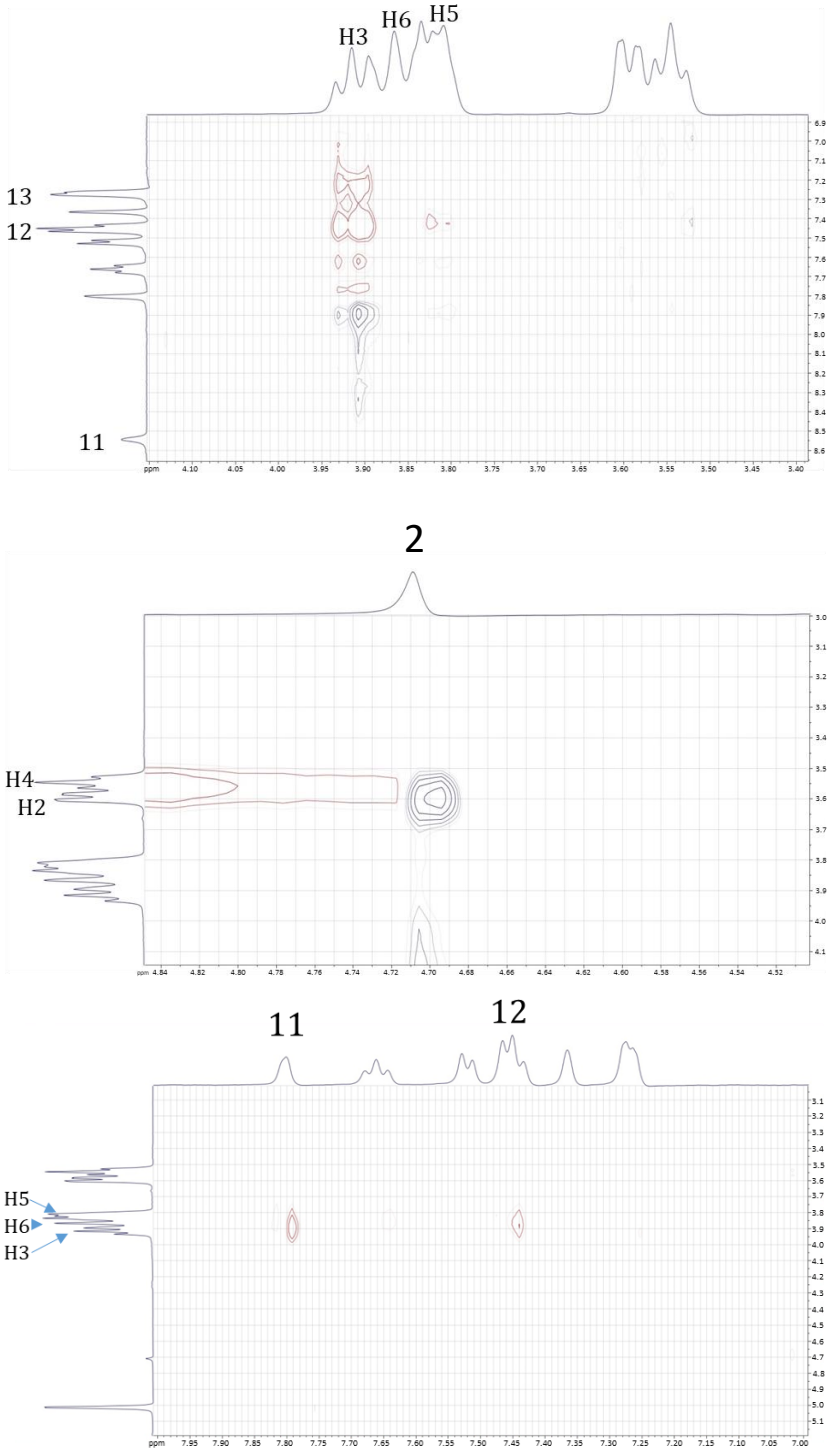

Figure 3. 2D-ROESY spectrum (details of the more significant area) of the complex econazole-α-cyclodextrin.

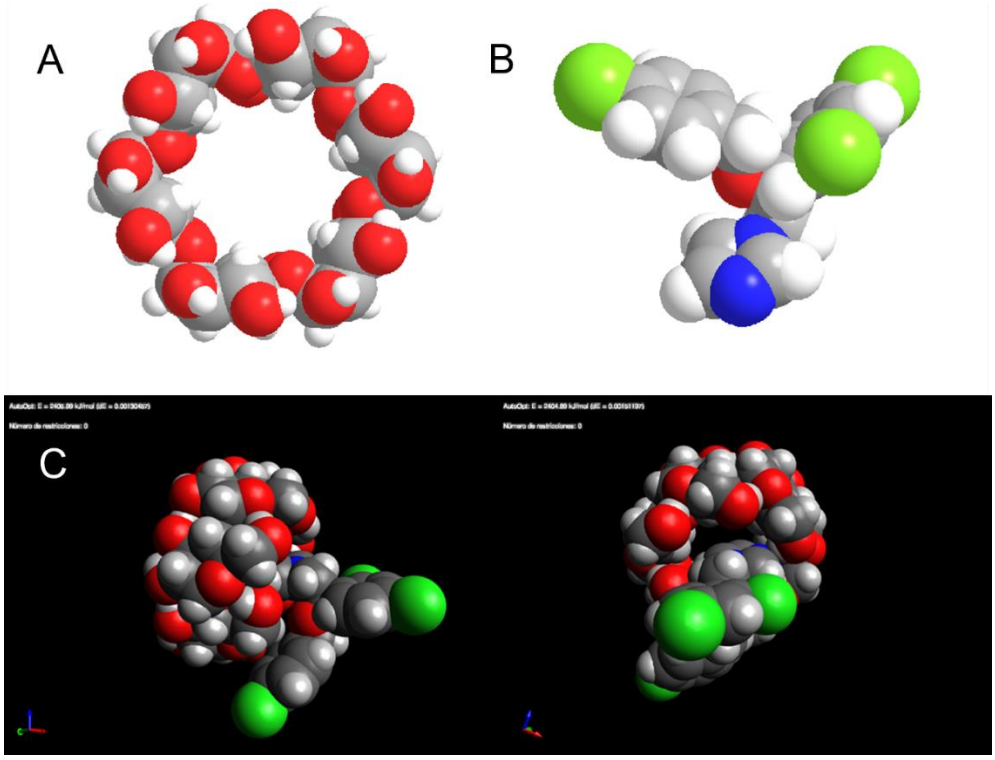

Figure 4. Molecular model of A) α-cyclodextrin, B) econazole and C) econazole-αCD inclusion complex obtained from NMR results.

4.2. STUDY OF THE ECONAZOL-ACD COMPLEX INCORPORATED INTO OPHTHALMIC HYDROGELS

Considering the results presented above, αCD was selected as the best econazole nitrate solubilising agent and the inclusion complex was added to the ISH and HAH hydrogels. Although αCD minimum concentrations necessary to solubilise 2 mg/mL econazole nitrate in accordance with solubility diagrams results were 1.2% (w/v) in water and 10.5% (w/v) in PBS, the cyclodextrin concentration selected was 15% (w/v) in order to avoid possible drug precipitation problems in environments with high ion concentration such in tears. The pH values for ISH, HAH and ECN were 4.86, 5.16 and 4.52, respectively.

4.3. ECONAZOLE RELEASE STUDY

Figure 5 shows both hydrogels have great capacity to control the econazole release during the 24 hours study. Peppas and Korsmeyer kinetics fitting with n~0.5 and Higuchi kinetics best fitting of HAH suggest the drug release is produced by a diffusion-controlled mechanism through the polymeric network. In the ISH case, the n value of Peppas and Korsmeyer equation (n=1.053) suggests the release kinetics are close to a pseudo-zero order process (Table 2). This value indicates the ISH gelation in contact with the SLF may have an important role in the drug release. The two-way variance analysis, including correlations for time point and formulation, shows a significant influence of both factors for $\alpha<0.01$. The analysis shows differences between the control solution and the hydrogels after ten minutes, and between both hydrogels after one hour.

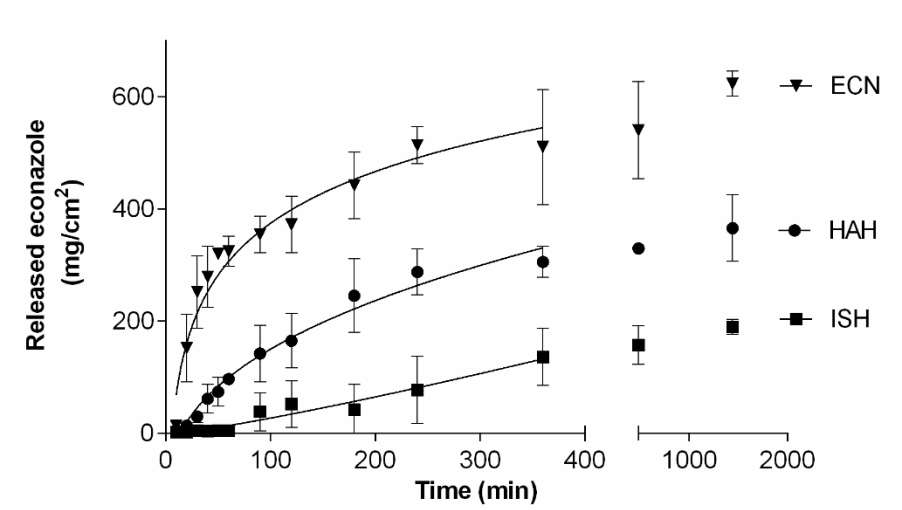

Figure 5. Release profiles of econazole in SLF from the ion sensitive hydrogel (ISH), hyaluronic acid hydrogel (HAH) and econazole control solution (ECN) (mean ± SEM, n=3).

Table 2. Fitting of the release data from the hydrogels in the *in vitro* release of econazole to the diffusion kinetics of Higuchi and Peppas and Korsmeyer.

	Higuchi		Peppas and Korsmeyer		
Formulation	**K ($mg \cdot cm^{-2} \cdot min^{-0.5}$)**	**R^2**	**k**	**n**	**R^2**
ISH	9.45	0.8624	4.58	1.05	0.9685
HAH	19.71	0.9477	29.71	0.63	0.9615
ECN	29.20	0.8624	77.71	0.35	0.8983

4.4. *EX VIVO* TRANSCORNEAL PERMEABILITY

The results from the corneal permeability study for the drug solution and the bioadhesive hydrogels are shown in Table 3. Econazole nitrate shows a good permeability across the bovine cornea and the formulations do not affect the drug corneal flux nor the apparent permeability parameter (Nonparametric Kruskal Wallis α n.s.). However, there are differences (α<0.05) in terms of lag time comparing ISH results with the ones obtained from ECN and the HAH.

Table 3. Parameters obtained in the *ex vivo* transcorneal permeation assay.

Formulation	**T_{lag} min**	**Flux (µg/min) (mean±SE)**	**P_{app} x 10^{-6} (cm/s)**	**% Permeation at 5 h**
HAH	65	0.084±0.0093	2.52±0.27	0.79
ISH	100	0.083±0.0044	2.50±0.13	0.35
ECN	60	0.089±0.0060	2.67±0.18	0.63

4.5. IRRITATION OCULAR TEST

HET CAM

Het-Cam results show no damage on blood vessels after the addition of econazole hydrogels and econazole solution after 5 minutes of contact (IS = 0). Therefore, it seems these compounds are non-irritating for the ocular surface.

BCOP

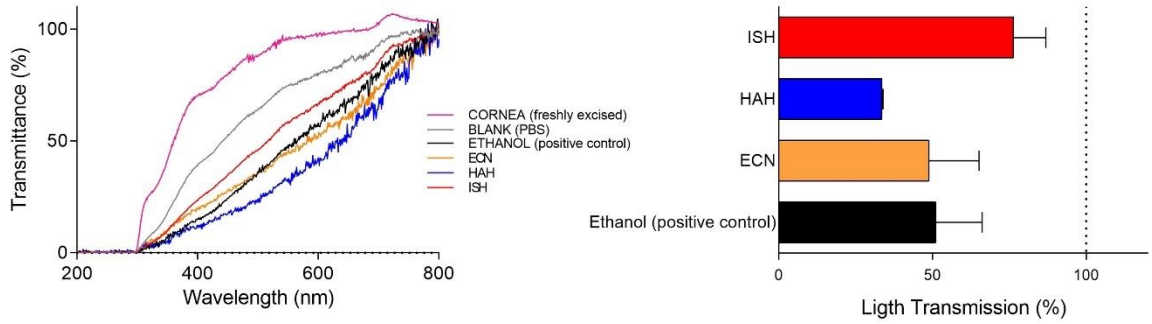

Figure 6. Left: Ultraviolet-visible (UV-Vis) scan (from 200 to 800 nm) of corneal transmittance (%) after 10 min drug treatment and 120 min PBS treatment. Right: Opacity (TL %) values of bovine corneas treated with ISH, HAH, ECN and Ethanol after 10 min drug treatment and 120 min PBS treatment. 100% corresponds to the total light transmitted through bovine corneas incubated in PBS.

The results obtained in the BCOP test (Figure 6) show that all formulations caused significant changes in corneal transparency and opacity. A one-way ANOVA was performed and no significant differences (α=n.s) were found between the positive control and the formulations, no modification of fluorescein permeability was observed.

4.6. ANTIFUNGAL EFFECTIVENESS

Results obtained from the diameters (mm) of fungal growth inhibition (Figure 7) zones by each antifungal are shown in Table 4. Both econazole and voriconazole produce the largest inhibition zones, being much bigger of those created by fluconazole, amphotericin and natamycin.

Table 4. Zone diameters (mm) of fungal growth inhibition by antifungals.

	Candida albicans		***Aspergillus fumigatus***		***Paecilomyces***	
Antifungal	**RPMI**	**Mueller Hinton**	**RPMI**	**Mueller Hinton**	**RPMI**	**Mueller Hinton**
Econazole-αCD	36	40	>50	40	>50	>50
Fluconazole	34	39	-	-	-	-
Amphotericine B	15	15	-	-	-	-
Voriconazole	55	65	>50	>50	>50	>50
Natamycin	15	13	25	15	-	-

Figure 7. Inhibition zone images of Econazole and VFEND against *Aspergillus fumigatus, Candida albicans* ATCC 90231, *Candida albicans* ATCC 90028, *Fusarium solani and Paelomyces lilacinus.*

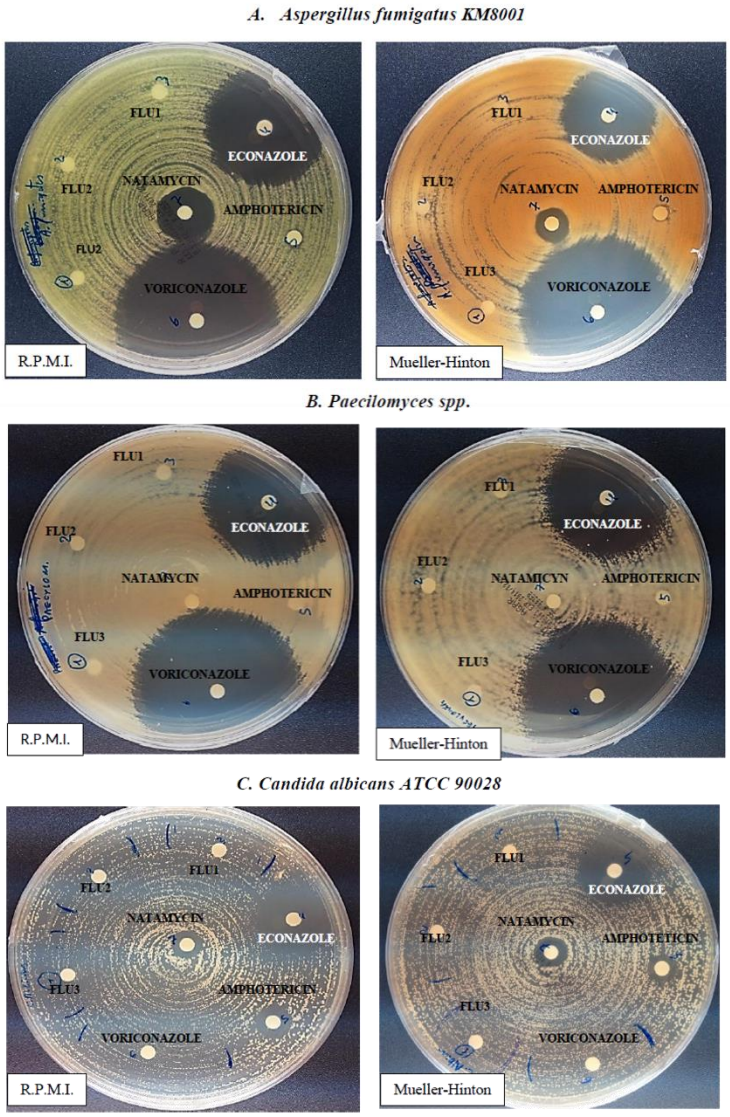

4.7. BIOPERMANENCE PET STUDY

The biopermanence of radiolabelled econazole hydrogels was measured in rats by using a small-animal PET system and compared to a radiolabelled solution. A strong signal at early times after instillation was observed for both formulations. It was shown after 2 hours of contact, 21.71±10.23 % of the ISH, 20.17±10.11% of HAH and only 10.15±6.34% of ECN remained in the ocular surface. Data were fitted to a mono exponential model with time, as it is shown in Figure 8. The pharmacokinetic parameters obtained by fitting to the mono compartmental model are shown in Table 5. The average half-life time ($t_{1/2}$) and mean residence time (MRT) were 49.3±28.88 and 71.08±41.66 minutes respectively for the HAH, 50.16±18.64 and 72.37±26.90 minutes for the ISH and 20.73±8.01 and 29.9±11.56 minutes for the ECN.

The hydrogels labelling was considered as optimum since the remaining ^{18}F-FDG in both hydrogels was above 95% at 180 minutes post-preparation.
Figure 9 contains axial and sagittal views of co-registered PET/CT animal head images right after the HAH hydrogel administration and 1 hour post-instillation. CT images show the head structure, while PET images show the labelled hydrogel distribution. Initially, all the hydrogel is located on the ocular surface. After 1 hour, the amount of hydrogel on the eye is still significant, indicating a high retention time on the ocular surface. In addition, the radiotracer is also detected in the nasolacrimal duct and in the nasal cavity due to the hydrogel partial clearance from the lacrimal sac into the nasal cavity.

Table 5. Parameters obtained by the fitting of the % formulation remaining on the ocular surface obtained by PET imaging to a mono-compartmental model.

Formulation	$t_{1/2}$ (min)	AUC_0^{∞} (mg/L·min)	MRT (min)
HAH	49.3±28.88	6689.02±6689.52	71.08±41.66
ISH	50.16±18.64	6812.83±2426.91	72.37±26.90
ECN	20.73±8.01	2920.13±1078.09	29.9±11.56

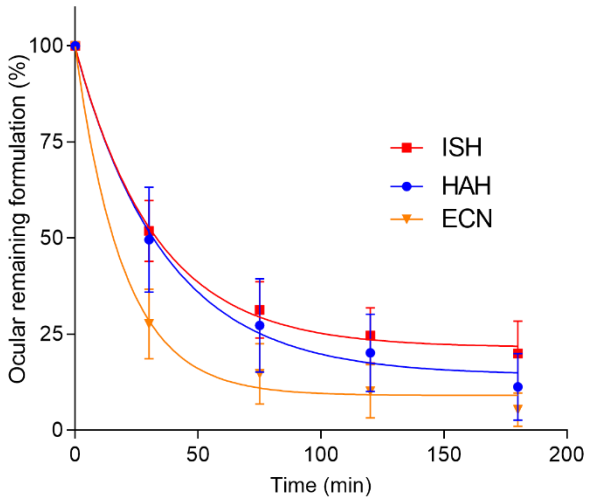

Figure 8. Clearance ratio of the formulations from the ocular surface determined by PET.

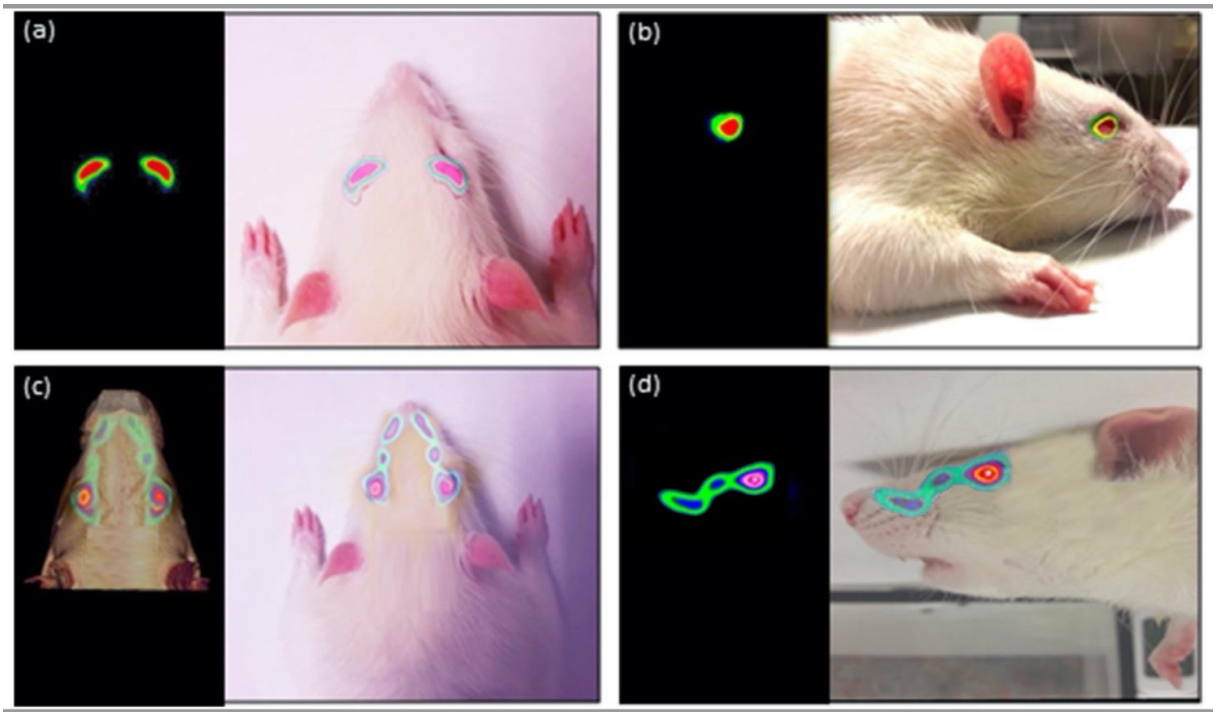

Figure 9. Fusion PET-CT-Real images of the eat´s head in wich the formulation (HAH) remains on the ocular surface after instillation [(a) and (b)] subsequently observed as it is eliminated by the nasolacrimal ducts [(c) and (d)]. Sagittal (a) and axial (b) PET image and fusion PET-Real images of the rat post-administration. Sagittal (c) funsion PET-CT image and axial (d) fusion PET-Real images of the rat 60 min post-administration.

5. DISCUSSION

Topical antifungal ophthalmic formulations are not available in several countries. Therefore, alternatives are elaborated at hospital pharmacy departments, using isotonic solutions compatible with the ocular surface as the main vehicle for their elaboration. These manufactured solutions present many limitations, mainly related to their low retention time on the ocular surface (37). In addition, the low water solubility of these drugs prevents their formulation, limiting the therapeutic arsenal in pathologies with reduced pharmacological alternatives as fungal keratitis. For this reason, achieving the solubilization of antifungal drugs is an essential task in order to increase the odds for a successful treatment (38). Many authors have performed solubility studies using cyclodextrins and co-solvents due to econazole low water solubility (1.48mM) (39-42).

The diagrams obtained with HPɣCD, HPβCD and αCD in water were of the A_L type (22). These diagrams show the formation of high solubility complexes characterised by a linear increase in solubility with the cyclodextrins concentration. Additionally, complexes presented a constant composition. This behaviour agrees with the results reported by Mura et al (43), while El-Gawad et al. obtained B_s type diagrams (44). B_s type diagrams are typical of natural β-cyclodextrins, the least soluble cyclodextrins used, showing inclusion complexes with limited solubility. Nevertheless, HPβCD inclusion complexes usually present A_L or A_p type diagrams. HPβCD is an amorphous cyclodextrin composed by a mixture of cyclodextrin molecules with different mode and substitution degree. This structure prevents the inter and intra-molecular

hydrogen bounds formation among inclusion complexes and cyclodextrins. The inter and intra-molecular hydrogen bounds are an important factor involved in the aggregates formation which is responsible of the natural β-cyclodextrin limited water-solubility. The highest values of $K_{1:1}$ ($K_{1:1}$ = 505.54 M^{-1}) and CE (0.75) as well as the smallest ratio of D:CD (1:2.33) relation were found for αCD, indicating econazole interacts more strongly with this cyclodextrin. These results are in good agreement with Mura et al (43), where authors also reported the best results for αCD and econazole base. In this work, a stability constant ($K_{1:1}$) value of 2630 M^{-1} was obtained. This higher stability constant is related to the econazole base low water solubility (0.013 mM) compared to econazole nitrate (1.48 mM). Nevertheless, using econazole nitrate in combination with αCD allows achieving higher drug concentration than using the base. Similar results were obtained by Mura et al. (43) using different organic acids in combination with cyclodextrins.

In order to determine the cause of the stronger interaction with the αCD, 1H-NMR structural studies were performed. 1D and 2D NMR results suggest the econazole imidazole ring is more deeply included into the cyclodextrin cavity and interactions between them are stronger. The PBS graph shows a considerable decrease in the econazole affinity for αCD. This may be due to the amino group ionisation of its imidazole ring at pH 7.4, which decreases the drug affinity for the cyclodextrin cavity. In the case of HPβCD and HPɣCD, due to their bigger cavity size, they would probably include the clorophenylmethoxil or the diclorophenylethyl group in the cavity, which are less influenced by the econazole ionisation; and therefore, they are less affected by pH.

The importance of increasing the therapeutic arsenal in ophthalmology is a key factor for the optimisation of the fungal keratitis therapeutics. In this work, the econazole-αCD inclusion complex effectiveness against the main fungi which caused fungal keratitis was studied. Compared to the antifungal tested, only econazole-αCD and voriconazole solubilised with sulphobutylether-β-cyclodextrin (Vfend®) showed activity against all the studied fungi. Therefore, the econazole-αCD complex is a very attractive therapeutic alternative for the treatment of these infectious diseases due to its advantages described above. Moreover, the fact that the compound is not irritating for the ocular surface it is also important. The econazole-αCD inclusion complex does not show any type of damage in the vessels. However, in the BCOP test, a significant change in corneal transparency was observed, showing values similar to those obtained with the positive control. For this reason, further testing would be necessary.

In vitro release studies using vertical Franz cells show both ISH and HAH can successfully control the econazole nitrate release over time. ECN release the drug for 250 min, where the high molecular volume of the inclusion complex could decrease the drug diffusion rate through the membrane filter. The econazole nitrate proportion released from ISH is significantly lower than the one obtained from HAH. This is due to the hydrogel ion sensitive characteristics, and it gels in contact with the lacrimal fluid (45-46). This causes the econazole-cyclodextrin complex to be trapped into the hydrogel and so the release to be slower than the hyaluronic acid hydrogel network.

It is important to point out that the biopermanence study of ophthalmic formulations is an essential requirement to be able to determine their appropriate dosages (47). In this work, a

novel *in vivo* image methodology based on PET/CT for evaluating the hydrogels ocular surface residence time was used (35). PET/CT images confirm the hydrogels high retention time compared to the econazole solution used as control. Furthermore, PET studies allow obtaining the quantitative analysis of the ophthalmic formulations pharmacokinetic profile, by calculating the elimination constant, the half-live and the zero and first order pharmacokinetic parameters AUC_0^∞ and MRT. Hydrogels show a mean residence time of 71-72 minutes in the ocular surface, much more than the ECN. Results from the ocular biopermanence assay show both hydrogels are mucoadhesive compounds and have an adequate consistence to remain on the ocular surface for a long time.

The combination of the good results from the release study and the high retention time of the hydrogels in the ocular surface confirms the interest on these formulations for the controlled econazole release in the eye. These two properties of econazole hydrogels might lead to an increase in the effect duration, decreasing the administration frequency. In most of the occasions, the fungal infection reaches the aqueous humour and eye internal structures; therefore, the drug needs to be able to cross the cornea. Hence, in order to verify hydrogels were able to allow the econazole nitrate penetration into the cornea, an *ex vivo* transcorneal study was performed. Results show econazole have equivalent apparent corneal permeability from both inclusion complex solution and hydrogels. Despite the release study shows differences among formulations, transcorneal study results suggest the drug permeation rate limiting step in the eye is their own diffusion across the corneal structure and it is independent of the hydrogels drug release properties.

The development of the proposed formulations at hospital pharmacy departments is feasible when commercial alternatives are not available or ineffective. Results obtained through this work demonstrate both HAH and ISH hydrogels are promising as vehicles for econazole nitrate-αCD ocular administration. Both hydrogels demonstrated a prolonged retention time on the ocular surface, an adequate econazole nitrate controlled release and safety. Considering hyaluronic acid is an auxiliary substance habitually used and authorised for eye drops elaboration, HAH can be considered a more suitable vehicle for increasing the econazole nitrate effectivity.

BIBLIOGRAPHY

1. Thomas PA, Kaliamurthy J. Mycotic keratitis: epidemiology, diagnosis and management. Clin Microbiol Infect. marzo de 2013;19(3):210-20.
2. Durand ML. Bacterial and Fungal Endophthalmitis. Clin Microbiol Rev. julio de 2017;30(3):597-613.
3. Wu J, Zhang WS, Zhao J, Zhou HY. Review of clinical and basic approaches of fungal keratitis. Int J Ophthalmol. 2016;9(11):1676-83.
4. Kalavathy CM, Parmar P, Kaliamurthy J, Philip VR, Ramalingam MDK, Jesudasan CAN, et al. Comparison of topical itraconazole 1% with topical natamycin 5% for the treatment of filamentous fungal keratitis. Cornea. mayo de 2005;24(4):449-52.
5. Rautaraya B, Sharma S, Kar S, Das S, Sahu SK. Diagnosis and treatment outcome of mycotic keratitis at a tertiary eye care center in eastern India. BMC Ophthalmol. 22 de diciembre de 2011;11:39.
6. Thomas PA. Fungal infections of the cornea. Eye. 2003;17(8):852-62.
7. Ansari Z, Miller D, Galor A. Current Thoughts in Fungal Keratitis: Diagnosis and Treatment. Curr Fungal Infect Rep. 1 de septiembre de 2013;7(3):209-18.
8. Hariprasad SM, Mieler WF, Lin TK, Sponsel WE, Graybill JR. Voriconazole in the treatment of fungal eye infections: a review of current literature. Br J Ophthalmol. julio de 2008;92(7):871-8.
9. Prajna NV, John RK, Nirmalan PK, Lalitha P, Srinivasan M. A randomised clinical trial comparing 2% econazole and 5% natamycin for the treatment of fungal keratitis. Br J Ophthalmol. octubre de 2003;87(10):1235-7.
10. Jones BR, Clayton YM, Oji EO. Recognition and chemotherapy of oculomycosis. Postgrad Med J. septiembre de 1979;55(647):625-8.
11. Fernandez-Ferreiro A, González-Barcia M, Gil Martinez M, Blanco Mendez J, Lamas M, Otero Espinar F. Current use of Antifungal Eye Drops and How to Improve Therapeutic Aspects in Keratomycosis. Fungal Genomics Biol. 2016;6(1).
12. Mahmoud AA, El-Feky GS, Kamel R, Awad GEA. Chitosan/sulfobutylether-β-cyclodextrin nanoparticles as a potential approach for ocular drug delivery. Int J Pharm. 15 de julio de 2011;413(1–2):229-36.
13. Gaudana R, Jwala J, Boddu SHS, Mitra AK. Recent Perspectives in Ocular Drug Delivery. Pharm Res. 1 de mayo de 2009;26(5):1197.
14. Loftsson T, Brewster ME. Cyclodextrins as functional excipients: methods to enhance complexation efficiency. J Pharm Sci. septiembre de 2012;101(9):3019-32.
15. Almeida H, Amaral MH, Lobão P, Lobo JMS. In situ gelling systems: a strategy to improve the bioavailability of ophthalmic pharmaceutical formulations. Drug Discov Today. abril de 2014;19(4):400-12.
16. Carmen Alvarez-Lorenzo BBF. Crosslinked ionic polysaccharides for stimuli-sensitive drug delivery. Adv Drug Deliv Rev. 2013;
17. Pawar P, Kashyap H, Malhotra S, Sindhu R. Hp-β-CD-Voriconazole In Situ Gelling System for Ocular Drug Delivery: *In Vitro*, Stability, and Antifungal Activities Assessment. BioMed Res Int [Internet]. 2013 [citado 20 de enero de 2014];(DOI: 10.1155/2013/341218). Disponible en: http://www.ncbi.nlm.nih.gov/pmc/articles/PMC3665163/
18. Gupta H, Velpandian T, Jain S. Ion- and pH-activated novel in-situ gel system for sustained ocular drug delivery. J Drug Target. agosto de 2010;18(7):499-505.

19. Reed K, Li A, Wilson B, Assamoi T. Enhancement of Ocular In Situ Gelling Properties of Low Acyl Gellan Gum by Use of Ion Exchange. J Ocul Pharmacol Ther Off J Assoc Ocul Pharmacol Ther. noviembre de 2016;32(9):574-82.
20. Fernández-Ferreiro A, González Barcia M, Gil-Martínez M, Vieites-Prado A, Lema I, Argibay B, et al. *In vitro* and *in vivo* ocular safety and eye surface permanence determination by direct and Magnetic Resonance Imaging of ion-sensitive hydrogels based on gellan gum and kappa-carrageenan. Eur J Pharm Biopharm. 14 de junio de 2015;
21. Luaces-Rodríguez A, Díaz-Tomé V, González-Barcia M, Silva-Rodríguez J, Herranz M, Gil-Martínez M, et al. Cysteamine polysaccharide hydrogels: Study of extended ocular delivery and biopermanence time by PET imaging. Int J Pharm. 7 de agosto de 2017;528(1-2):714-22.
22. Higuchi T, Connors KA. Phase-Solubility Techniques. En: Advances in Analitycal Chemistry and Instrumentation. New York: Interscience; 1965. p. 117-212.
23. Anguiano-Igea S, Otero-Espinar FJ, Vila-Jato JL, Blanco-Méndez J. Interaction of clofibrate with cyclodextrin in solution: phase solubility, 1H NMR and molecular modelling studies. Eur J Pharm Sci. 1 de julio de 1997;5(4):215-21.
24. Luaces-Rodríguez A, Díaz-Tomé V, González-Barcia M, Silva-Rodríguez J, Herranz M, Gil-Martínez M, et al. Cysteamine polysaccharide hydrogels: study of extended ocular delivery and biopermanence time by PET imaging. Int J Pharm [Internet]. Disponible en: http://www.sciencedirect.com/science/article/pii/S0378517317305689
25. Ceulemans J, Ludwig A. Optimisation of carbomer viscous eye drops: an *in vitro* experimental design approach using rheological techniques. Eur J Pharm Biopharm Off J Arbeitsgemeinschaft Für Pharm Verfahrenstechnik EV. julio de 2002;54(1):41-50.
26. Siepmann J, Peppas NA. Higuchi equation: Derivation, applications, use and misuse. Int J Pharm. 10 de octubre de 2011;418(1):6-12.
27. Peppas NA. Analysis of Fickian and non-Fickian drug release from polymers. Pharm Acta Helv. 1985;60(4):110-1.
28. OECD. Test No. 437: Bovine Corneal Opacity and Permeability Test Method for Identifying Ocular Corrosives and Severe Irritants [Internet]. Paris: Organisation for Economic Co-operation and Development; 2009 [citado 28 de enero de 2014]. Disponible en: http://www.oecd-ilibrary.org/content/book/9789264076303-en
29. Fernández-Ferreiro A, González Barcia M, Gil Martínez M, Blanco Mendez J, Lamas Díaz MJ, Otero Espinar FJ. Analysis of ocular toxicity of fluconazole and voriconazole eyedrops using HET-CAM. Farm Hosp. agosto de 2014;38(4):300-4.
30. Hen's Egg Test on the Chorioallantoic Membrane (HET-CAM) INVITTOX n° 96 [Internet]. [citado 27 de enero de 2014]. Disponible en: http://www.vitrotox.com/uploadfile/UploadFile/2008121382926916.pdf
31. Test No. 437: Bovine Corneal Opacity and Permeability Test Method for Identifying i) Chemicals Inducing Serious Eye Damage and ii) Chemicals Not Requiring Classification for Eye Irritation or Serious Eye Damage [Internet]. [citado 13 de febrero de 2020]. Disponible en: https://www.oecd-ilibrary.org/environment/test-no-437-bovine-corneal-opacity-and-permeability-test-method-for-identifying-i-chemicals-inducing-serious-eye-damage-and-ii-chemicals-not-requiring-classification-for-eye-irritation-or-serious-eye-damage_9789264203846-en
32. Fernández-Ferreiro A, Santiago-Varela M, Gil-Martínez M, González-Barcia M, Luaces-Rodríguez A, Díaz-Tome V, et al. *In Vitro* Evaluation of the Ophthalmic Toxicity Profile of Chlorhexidine and Propamidine Isethionate Eye Drops. J Ocul Pharmacol Ther Off J Assoc Ocul Pharmacol Ther. 2017;33(3):202-9.

33. Jones RN, Ballow CH, Biedenbach DJ. Multi-laboratory assessment of the linezolid spectrum of activity using the Kirby-Bauer disk diffusion method: Report of the Zyvox® Antimicrobial Potency Study (ZAPS) in the United States. Diagn Microbiol Infect Dis. abril de 2001;40(1–2):59-66.
34. The Association for Research in Vision and Ophthalmology. Statement for the Use of Animals in Ophthalmic and Visual Research [Internet]. 2014. Disponible en: http://www.arvo.org/About_ARVO/Policies/Statement_for_the_Use_of_Animals_in_Ophthalmic_and_Visual_Research/
35. Fernández-Ferreiro A, Silva-Rodríguez J, Otero-Espinar FJ, González-Barcia M, Lamas MJ, Ruibal A, et al. Positron Emission Tomography for the Development and Characterization of Corneal Permanence of Ophthalmic Pharmaceutical Formulations. Invest Ophthalmol Vis Sci. 1 de febrero de 2017;58(2):772-80.
36. Zhang Y, Huo M, Zhou J, Xie S. PKSolver: An add-in program for pharmacokinetic and pharmacodynamic data analysis in Microsoft Excel. Comput Methods Programs Biomed. septiembre de 2010;99(3):306-14.
37. Fernández-Ferreiro A, González-Barcia M, Otero Espinar FJ, Blanco Méndez J, Lamas MJ. Ophthalmic formulations new goals. Farm Hosp Órgano Of Expr Científica Soc Esp Farm Hosp. febrero de 2016;40(1):1-2.
38. Loftsson T, Stefánsson E. Cyclodextrins and topical drug delivery to the anterior and posterior segments of the eye. Int J Pharm. 6 de abril de 2017;
39. Jansook P, Kurkov SV, Loftsson T. Cyclodextrins as solubilizers: Formation of complex aggregates. J Pharm Sci. 1 de febrero de 2010;99(2):719-29.
40. Fernández-Ferreiro A, Bargiela NF, Varela MS, Martínez MG, Pardo M, Ces AP, et al. Cyclodextrin–polysaccharide-based, in situ-gelled system for ocular antifungal delivery. Beilstein J Org Chem. 8 de diciembre de 2014;10(1):2903-11.
41. Firooz A, Nafisi S, Maibach HI. Novel drug delivery strategies for improving econazole antifungal action. Int J Pharm. 10 de noviembre de 2015;495(1):599-607.
42. Shah RM, Eldridge DS, Palombo EA, Harding IH. Microwave-assisted microemulsion technique for production of Miconazole nitrate- and Econazole nitrate-loaded solid lipid nanoparticles. Eur J Pharm Biopharm Off J Arbeitsgemeinschaft Pharm Verfahrenstechnik EV. 11 de abril de 2017;
43. Mura P, Faucci MT, Manderioli A, Bramanti G. Multicomponent Systems of Econazole with Hydroxyacids and Cyclodextrins. J Incl Phenom Macrocycl Chem. 1 de febrero de 2001;39(1-2):131-8.
44. El-Gawad AEGHA, Soliman OA, El-Dahan MS, Al-Zuhairy SAS. Improvement of the Ocular Bioavailability of Econazole Nitrate upon Complexation with Cyclodextrins. AAPS PharmSciTech. 9 de noviembre de 2016;1-15.
45. Thrimawithana TR, Young SA, Bunt CR, Green CR, Alany RG. In-vitro and in-vivo evaluation of carrageenan/methylcellulose polymeric systems for transscleral delivery of macromolecules. Eur J Pharm Sci Off J Eur Fed Pharm Sci. 9 de octubre de 2011;44(3):399-409.
46. Kushwaha SK, Saxena P, Rai A. Stimuli sensitive hydrogels for ophthalmic drug delivery: A review. Int J Pharm Investig. 2012;2(2):54-60.
47. Eter N. Molecular Imaging of the Eye. Br J Ophthalmol. agosto de 2009;bjo.2009.158105v1.

Chapter 2

IN SITU FORMING AND MUCOADHESIVE OPHTHALMIC VORICONAZOLE/HPβCD HYDROGELS FOR THE TREATMENT OF FUNGAL KERATITIS

1. INTRODUCTION

Fungal keratitis (FK) is a serious infectious corneal disease mostly caused by filamentous fungi such as *Aspergillus* spp., *Fusarium* spp. or yeasts like *Candida albicans* (1), although it may be also associated to many others species (2,3). The infection is usually produced by corneal epithelium damage. This pathology is typical from tropical regions or developing countries, being generally associated to corneal trauma by a contaminated vegetable (stick, thorn or plant) (Rai and Occhiutto, 2019; Taechajongjintana et al., 2018), although its incidence is increasing in developed countries due to new etiological factors, such as: (I) misuse of contact lens (3,8), (II) prolonged use of topical corticosteroids (9), (III) immunocompetent patients (Anutarapongpan et al., 2016;; Hung et al., 2020) or (IV) corneal transplant (14), among others. FK presents a complicated clinical diagnosis since it is common for the patient to be asymptomatic after the corneal trauma, taking days or even weeks for symptoms to appear (e.g., pain, photophobia or episphagm, among others). Besides that, it is often confused with other types of infectious keratitis since initial symptoms are usually common and non-specific (15), and the clinical characteristics depend on the type of etiological agent and the disease's progression. It also must be taken into account that, during the latency period, the epithelium can be completely healed, even above the infection focus. As time goes, inflammatory processes may cause a permanent rupture of the epithelium, stromal ulceration or even severe damages on the Descemet's membrane, leading to the development of a descemetocele or corneal perforation (10).

Clinical diagnosis of FK is extremely complicated and the treatment election depends on the disease`s ethology; thus, a microbiological diagnosis is always required in order to ensure the etiological agent identification.

Polyenes are the first-line FK treatment, where natamycin is mainly used against filamentous fungi, while amphotericin B is the first-line drug against yeast (16). However, since 70s, azoles began to be used due to their greater action spectra and fewer side effects compared to amphotericin B (17). Nowadays, voriconazole, a fluconazole derived synthetic triazole, is one of the most used drugs due to its broad action spectrum (particularly against *Aspergillus* spp., *Candida* spp., *Fusarium* spp., *Scedosporium* spp. and *Paecilomyces* spp., among others (18)) that can reach therapeutic concentrations in different ocular tissues (cornea, vitreous humor, aqueous humor) and it has shown to be effective against resistant infections to polyenes and other first-line azoles (17).

Currently, no voriconazole's topical ophthalmic formulations are approved by the Food and Drug Administration (FDA) or the European Medicines Agency (EMA). This lack of therapeutic alternatives leads to the reformulation of intravenous administrated commercialized formulations by the hospital pharmacy departments in order to prepare the appropriate ophthalmic formulations. VFEND® is an intravenous voriconazole commercial presentation that is usually used in the reformulation processes, by dilution in biocompatible ocular vehicles for the eye drops preparation. In order to point out, intensive treatment (every hour) is commonly applied with these formulations, due to their low permanence on the corneal surface, which may lead to local and systemic side effects (19).

Topical ophthalmic drug administration presents numerous challenges in terms of drug penetration through the cornea. The passage of molecules through this tissue depends on several key factors, including lipophilicity, molecular weight, charge and ionization degree, among others (20,21). This administration route represents the least invasive method of ophthalmic application, being well tolerated by patients since it embodies a painless, simple and easily self-administered method. Nevertheless, the main disadvantage is associated with the rapid formulation removal by the ocular protection mechanisms, such as nasolacrimal drainage, blinking (6-15 times/min, tear renewal rate (0.5-2.2 μL/min)) and high lacrimal clearance (22,23), as well as the unproductive absorption to systemic circulation through the conjunctiva, choroid, uveal tract and inner retina.

The use of polymers is a crucial factor to improve the adhesive properties of the topical ophthalmic formulations, achieving a greater permanence in the ocular surface and, subsequently, a drug bioavailability increase (24). Stimulus sensitive hydrogels (involving various polymers) may seem to be suitable for this purpose, as the one previously developed by our group, consisting of a *in situ* gelling system (formulated with gellan gum and κ-carrageenan), which gelifies in contact with the tear, increasing its viscosity and improving the drug's permanence in the eye (25). The use of mucoadhesive polymers, such as hyaluronic acid, is also considered an appropriate option to increase the drug's permanence and bioavailability, due to the chemical interactions with the anionic groups of the mucin layer in the corneal and conjunctival epithelium. In addition, an increase in the formulation's ocular permanence will considerably reduce the number of necessary instillations (up to 1 application per hour (26,27)), improving patient's adherence-to-treatment and compliance.

The aim of this work was based on the design and development of new voriconazole ophthalmic formulations as improved pharmacological alternatives compared to the existent voriconazole eye drops prepared at hospital pharmacy departments (28). Voriconazole was incorporated into two different types of novel hydrogels: (I) a gelling *in situ* hydrogel and (II) a mucoadhesive hydrogel. Physicochemical characterization was performed by solubility studies, solution NMR, squeezing force, pH, and osmolality measurements. *In vitro* release studies were subsequently made in order to determine the pharmacokinetic profile. Ocular irritation assays (HET-CAM and BCOP) were carried out to ensure their safety. Permanence and bioavailability properties were studied by corneal permeability, corneal mucoadhesiveness and *in vivo* ocular permanence assays.

2. MATERIALS

Voriconazole was purchased from Normon® (Madrid, Spain); VFEND® was acquired from Pfizer® (New York, USA); hyaluronic acid (HA) was obtained from Acofarma® (Barcelona, Spain); 2-hydroxypropyl-β-cyclodextrin (HPβCD) (Kleptose®, 0.65 molar substitution ratio, M_W 1399 Da) was purchased from Roquette® Laisa S.A. (Valencia, Spain); 2-hydroxypropyl-γ-cyclodextrin (HPγCD) (0.6 molar substitution ratio, M_W 1580 Da) was acquired from Sigma Aldrich® (Darmstadt, Germany); α-cyclodextrin (αCD) (Cavamax® W6, M_W 972.84 Da) was procured by Wacker Chemie AG® (München, Germany); gellam gum (GG) (Kelcogel® CG-

LA M_w1.5–2.5 · 10^6 Da) and κ-carrageenan (CK) (Genugel® carrageenan GC-130 M_w 3.5–8.0 · 10^5 Da) were provided by CP Kelco® (Atlanta, Georgia).

3. METHODS

3.1. PHASE SOLUBILITY DIAGRAMS

The stability constants of voriconazole/cyclodextrin (HPβCD, HPγCD and αCD) inclusion complexes were estimated by phase solubility diagrams according to the Higuchi and Connors methodology (29). Voriconazole solubility was determined by adding an excess of drug to a series of aqueous solutions with increasing concentrations of aforementioned cyclodextrins. These solutions were incubated for 7 days in an orbital shaker (VWR®) (25 ± 0.5°C, 200 rpm). Afterwards, 1 mL of each formulation was centrifuged (Eppendorf® Centrifuge 5804R) at 11500 rpm for 20 minutes and 25°C. An aliquot of each sample was diluted in distilled water and concentration was determined by a diode-array spectrophotometer (Hewlett Packard® 8452A, λ = 260 nm). Each measurement was made in triplicate.

Solubility diagrams were subsequently obtained by representing voriconazole concentration (mM) against cyclodextrin concentration (mM).

The apparent stability constant ($K_{1:1}$ or Kd) was calculated considering the slope, the voriconazole water solubility (S_0) and the voriconazole solubility in the intercept ($S_{0\ extrap.}$), assuming the formation of 1:1 ratio inclusion complex between voriconazole and cyclodextrin. The complexation efficiency (CE) was calculated using the slope of the solubility profile or the concentration ratio between the complexed cyclodextrin and the non-complexed cyclodextrin. Drug:cyclodextrin molar ratio (D:CD) was then estimated using CE values. The formulas used were previously described by Loftsson et al. (30).

3.2. NUCLEAR MAGNETIC RESONANCE (NMR) STUDIES

Liquid-state NMR experiments were conducted at 25˚C on a Bruker NEO 17.6 T spectrometer (proton resonance 750 MHz), equipped with a $^1H/^{13}C/^{15}N$ triple resonance PA-TXI probe and PFG shielded z-gradient that uses 5 mm standard OD tubes. The spectrometer control software was TopSpin® 4.0. The chemical shifts are referenced to the lock deuterium solvent. Spectra were processed and analyzed with Mestrenova® software v14.0 (Mestrelab® Inc.).

NMR sample preparation: three different NMR samples were prepared for the study. A sample of the pure drug voriconazole was prepared at a concentration of 20 mM in 0.6 mL of deuterated methanol (MeOD). Two samples consisting of a voriconazole/HPβCD mixture and voriconazole/HPɣCD mixture were respectively prepared. Each sample was prepared in 0.6 mL of D_2O with a molar ratio voriconazole:cyclodextrin 1:1 and a concentration of 20 mM for each substance.

The following NMR experiments were acquired for the three samples:

A *one-dimensional ^1H spectrum* (pulse sequence "*zg*" of the Bruker library) with 32 scans, a relaxation delay (d_1) of 2 s and a *fid (free induction decay)* acquisition time (aq) of 2.75 s was measured.

A *one-dimensional ^{19}F spectrum* without ^{1}H decoupling (pulse sequence "*zg30*" of the Bruker library) with 32 scans, a d_1 of 4 s and an aq of 1.83 s was measured. The spectral window covered the region where the ^{19}F-NMR voriconazole signals are expected, with the center of the spectrum placed at -120 ppm and a spectral width of 100 ppm.

A *two-dimensional Heteronuclear Single Quantum Correlation multiplicity edited ^{1}H-^{13}C spectrum (2D HSQC)* was measured (pulse sequence "*inviedgpph*" of the Bruker library). The spectra were acquired with 1024 and 160 complex points in the t_2 and t_1 dimensions (t_1: indirectly detected time dimension for heteronucleus, which in this case is ^{13}C, t_2: directly detected time dimension for ^{1}H), respectively. The INEPTs (insensitive nuclei enhanced by polarization transfer) transfers of HSQC were optimized for a nominal value of $^{1}J_{CH}$ (coupling constant) of 145 Hz. The d_1 and the *fid* aq were1.6 s and 0.112 s, respectively. The spectra were acquired with 16 scans per t_1 increment and the total measurement time was ~2 h.

A *two-dimensional Heteronuclear Multiple Bond Correlation ^{1}H-^{15}N (2D HMBC) spectrum* was measured (pulse sequence "*hmbcgplpndqf*" of the Bruker library). The spectra were acquired in the magnitude mode in t_1 with 1024 and 300 points in the t_2 and t_1 dimensions, respectively. The low-pass filter for the suppression of the one-bond ^{1}H-^{15}N couplings was set to 95 Hz. The delay for the evolution of the long range ^{1}H-^{15}N couplings was set to 50 ms, corresponding to a nominal ^{1}H-^{15}N coupling of 10 Hz. The d_1 and the *fid* aq were 1.5 and 0.212 s, respectively. The spectral window in the ^{15}N dimension was set with the center at 160 ppm and a spectral width of 400 ppm. The spectra were acquired with 16 scans per t_1 increment and the total measurement time was ~2 h and 20 min.

The following NMR experiments were acquired only for the two samples prepared containing a mixture 1:1 voriconazole:cyclodextrin to study their intermolecular binding interactions:

One *dimensional Saturation Transferred Difference ^{1}H spectra (STD)* (31) were measured. The experiment consists of a selective saturation pulse train, a WET selective solvent suppression module and finally a 90-degrees hard-pulse followed by the acquisition of the *fid*. The selective saturation consisted of a train of soft gaussian shaped pulses of 50 ms duration with a 1 ms interpulse delay. The selective saturation was applied during 2 s at a specific frequency of the ^{1}H spectrum and covers a region of the spectrum of ±125 Hz around the chosen frequency (i.e. ±0.17 ppm in a 750 spectrometer). The STD^{off} saturation was applied at 20 ppm. The STD^{on} saturation was applied at the frequency of one specific aromatic proton signal of voriconazole and does not affect any of the signals of the cyclodextrin receptor. The STD^{on} and STD^{off} scans were measured in alternate scans and subtracted by the phase cycling providing the subtracted $STD^{off\text{-}on}$ spectrum. Three STD spectra were obtained by STD^{on} saturation of the voriconazole signal at 6.96, 6.86 and 4.52 ppm, respectively. Each spectrum was acquired in 15 min with 128 scans and a 6.75 s total scan duration consisting of a 2 s pre-scan d_1, a 2 s STD saturation-time and a 2.75 s *fid* aq.

A *two-dimensional Nuclear Overhauser Spectroscopy (NOESY) ^{1}H-^{1}H spectrum with zero-quantum artefacts filtration* (pulse sequence "*noesygpphzspr"* of the Bruker library) was measured with presaturation of the residual deuterated water (D_2O) peak at ca. 4.7 ppm. The NOESY mixing was 500 ms. The spectrum was acquired with 2048 and 256 complex points in the t_2 and t_1 dimensions, respectively. The d_1 and the *fid* aq were 2.0 and 0.27 s, respectively.

The spectrum was acquired with 16 scans per t_1 increment and the total measurement time was ~2 h.

A *two-dimensional Diffusion-Ordered Spectroscopy (DOSY) spectrum* (pulse sequence "*ledbpgp2s*" of the Bruker library) was measured. The gradient pulses that encode diffusion were linearly varied between 1 and 50 G cm^{-1} along 32 points in the diffusion dimension. The duration of each pair of bipolar gradients δ was 3 ms (1.5 and 1.5 ms) and the diffusion time variation was 200 ms. The spectrum was acquired with a d_1 of 2 s, an acquisition time of 2.75 s and 16 scans per each point in the diffusion dimension. After Fourier transformation in the ^1H dimension with zero-filling to 8 k points, the points along the diffusion dimension were processed with the exponential peak-fitting algorithm implemented in MestreNova® software in order to generate the DOSY representation of the spectrum with one dimension of chemical shifts (d, ppm), and the other with self-diffusion coefficients (D, m^2 s^{-1}).

3.3. MOLECULAR MODELLING

Molecular modelling of the voriconazole/HPβCD complex was carried out using the Chem3D® (PerkinElmer) and the HyperChem® 8.0 (Hypercube Inc) software. The initial geometry of the inclusion complex was built based on the intermolecular proton-proton proximities found by NMR, by performing a manual docking of voriconazole into the HPβCD cavity. The conformational energy of the initial geometry was extensively minimized using the MM+ force field. The final energy optimized model was represented and analyzed with the Pymol® v 0.99 (Delano Scientific LLD) software.

3.4. PREPARATION OF FORMULATIONS

VFEND® solution (VFEND®) (VFEND® powder was reconstituted in 19 mL of balanced salt solution (BSS) to obtain a 1% (w/v) voriconazole final concentration) and a 1% (w/v) voriconazole - 20% (w/v) HPβCD solution (VZS) were used to prepared all formulations.

Preparation of the ion-sensitive hydrogels

An attempt to formulate the VFEND®-loaded ion-sensitive hydrogel (developed in previous studies (25,32)) was made. κ-carrageenan (CK) immediately gelled after adding it to the VFEND® solution due to the presence of monovalent sodium ions in the cyclodextrin structure (sulfobutyl-ether-β-cyclodextrin (SBECD) used in the VFEND® composition. Therefore, ion-sensitive hydrogel was only formulated with the voriconazole solution and 20% (w/v) HPβCD. Several ion-sensitive hydrogels were prepared with a deacylated gellam gum (GG) and CK in different proportions (1:1, 2:1, 4:1) (w/w) (see Table 1), adding the polysaccharides into the VZS at 70°C under magnetic stirring until its complete solubilization. VZISH 0.65 (w/v), VZISH 0.75 (w/v) and VZISH 0.82 (w/v) were the final formulations for the GG:CK mixtures previously described.

Table 1. Ion-sensitive hydrogel composition (32).

Ion-sensitive hydrogel	% polymers in 100 mL of hydrogel (w/v)	GG:CK Ratio
VZISH 0.65	0.65	1:1
VZISH 0.75	0.75	2:1
VZISH 0.82	0.82	4:1

Preparation of the mucoadhesive hyaluronic acid hydrogel

A predetermined volume of a 0.4% (w/v) hyaluronic acid (HA) solution (the concentration was selected based on previous studies (33)) was added to the VFEND® solution or VZS under magnetic stirring, until its complete solubilization.

3.5. SQUEEZING FORCE MEASUREMENTS

This method was carried out to choose the optimum VZISH polymer's mixture. All the results were compared with the VZHAH (control), which showed an easy administration. The aim of this trial was to determine the necessary force to dispense a single drop from the polypropylene eyedropper bottles used in the Clinical University Hospital of Santiago de Compostela.

Squeeze measurement system was developed based on the method established by Charles H. Cox, with minor modifications (34), as presented in Figure 1. A Shimadzu® texturometer equipped with a load cell (1000 N maximum force) was used. The eyedropper bottle was placed in a specifically designed wedge. A 0.5 mm/s speed was used to move the upper probe. The necessary force to dispense was tested in quintuplicate (i.e., 25 measurements per formulation). The squeezing force procedure was recorded for each formulation and photographs were subsequently taken in order to determine the differences in terms of drop formation, according to the formulations tested. A statistical analysis was performed using the one-way ANOVA test to assess the presence or absence of significant differences in the necessary strength of administration on the different formulations. Furthermore, Tukey multiple comparisons test was subsequently carried out.

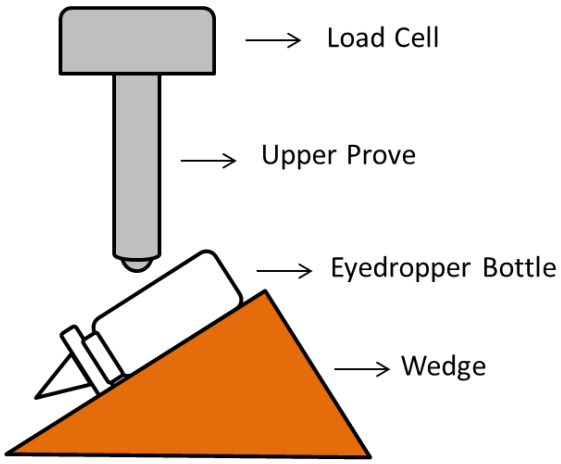

Figure 1. Simplified representation of squeezing force method.

3.6. pH AND OSMOLALITY MEASUREMENTS

The pH measurements were performed with a pHmeter (HI5221 HANNA®) at 25 ± 0.5°C, while the osmolality was measured using a MicroOsmometer (Fiske® Model 210). Each determination was carried out in triplicate.

3.7. *IN VITRO* RELEASE STUDIES

In vitro release profiles were obtained using Franz diffusion cells and Visking® dialysis membranes (Medicel® membranes Ltd) with a 12-14 KDa cut-off (0.784 cm^2 available surface area). Donor compartment was filled with 0.5 mL formulation (containing 5 mg voriconazole). 175 µL simulated lacrimal fluid (SLF) were also added to the donor chamber to imitate the amount of tear in the eye. Receptor compartment was filled with SLF. Receptor chamber was then homogenized by magnetic stirring in a thermostatic bath at 36°C during the assay. Voriconazole concentration in each sample was determined by using a Cary 60 UV-VIS spectrophotometer (Agilent® technologies) (λ = 260 nm). Each experiment was repeated three times.

Available permeation area of the Franz diffusion cells (0.784 cm^2) was taken into account to calculate apparent permeability (P_{app}) as follows:

$$P_{app} = \frac{\delta Q/\delta t}{A \cdot C_0 \cdot 60} \quad \text{(Eq. 1)}$$

Where δQ/δt represents the voriconazole flux across membrane in the graph linear portion, A is the membrane area (0.785 cm^2), C_0 is the initial drug concentration at the donor compartment and 60 is the minute-to-second conversion factor.

The formulation's flux across the membrane was established as the slope of the regression line obtained from the linear part of the curve between the amount of permeated voriconazole versus time.

3.8. *EX VIVO* CORNEAL PERMEABILITY STUDIES

Fresh bovine eyes were obtained from a local nearby slaughterhouse and transported in phosphate buffered saline (PBS) at 4°C to the laboratory in order to carry out the corneal permeability studies. Corneas were excised with 2-4 mm of surrounding sclera by using a scalpel and subsequently mounted on Franz diffusion cells. Epithelial surface of the cornea was placed towards the donor compartment. Receptor compartment was filled with PBS (6 mL) and the donor compartment was loaded with 0.5 mL formulation (containing 5 mg voriconazole) and 175 µL SLF. Receptor compartment was homogenized by magnetic stirring in a thermostatic bath at 36°C during the assay. Voriconazole concentration was determined by High Performance Liquid Chromatography (HPLC) (Merck® Hitachi, Darmstadt, Germany). The column used was a Waters Symmetry C18 (3.9 x 150 mm, 5 µm) thermostatized at 35°C. The mobile phase was acetonitrile:methanol:water (45:10:45 v/v/v) using a 1 $mL \cdot min^{-1}$ flow rate. A 260 nm wavelength was employed for voriconazole quantification. 50 µL of sample were injected and the retention time of 3.25 min was observed. Available permeation area of the Franz diffusion cells (0.784 cm^2) was taken into account to calculate the apparent permeability (P_{app}) as it was described in Eq. 1 (see 3.6. *In vitro* release studies section).

The formulation's flux across the cornea was established as the slope of the regression line obtained from the linear part of the curve between the voriconazole permeated amount (μg/cm^2) versus time (min).

3.9. OCULAR IRRITATION TEST

Alternative ocular toxicity methods were chosen to comply with the animal replacement criteria in experimentation procedures based on the 3Rs principles (replacement, reduction and refinement) described on the Directive 2010/63/EU of the European Parliament and of the Council of September 22nd 2010 on the protection of animals used for scientific purposes (35). Bovine Corneal Opacity and Permeability Assay (BCOP) and Hen´s Egg Test Chorioallantoic Membrane (HET-CAM) were selected as alternatives to the Draïze Test (36), where albino rabbits are used to classify substances according to the irritation produced on the ocular surface of the rabbits.

3.10. BOVINE CORNEAL OPACITY AND PERMEABILITY ASSAY (BCOP)

Corneal Opacity

BCOP assay was a variation of the method described in Protocol Invittox nº 437 (37), used to identify potential ocular corrosives and severe irritants. This method was carried out using fresh bovine corneas, where changes in corneal transparency, opacity and permeability were assessed.

Corneas were obtained, prepared, and placed in Franz diffusion cells as previously described (see "*Ex vivo* Corneal Permeability studies" section). Opacity (transmitted light, (TL)) was measured by using a luxmeter (Gossen Mavolux 5032C USB). Corneas were placed between two cylindrical supporting black holders (fabricated with polylactic acid filaments using a 3D printer, Wilbox® BQ) and illuminated with a pipe light (Olympus® Highlight 200) with fixed brightness values (38). The difference between light intensity measurements with and without cornea in the luxmeter was also calculated (% TL initial).

Corneal transparency was measured in transmittance values by UV-Vis spectrophotometry (Agilent® Cari 60 UV) from 800 to 200 nm, and a transmittance against wavelength spectrum was obtained for each cornea. After opacity and transparency initial readings of untreated corneal tissue, corneas were placed in Franz diffusion cells. Epithelial part of the cornea was placed towards the donor compartment and the receptor compartment was filled with PBS and homogenized by magnetic stirring in a thermostatic bath at 36°C during assay.

The test consisted of two parts. First, corneas placed in Franz diffusion cells were incubated for 60 min with 1 mL PBS in the donor chamber. Then, the PBS was removed, and opacity and transparency values were measured again. In the second part of the assay, 1 mL formulation, positive control (ethanol) or negative control (PBS) was placed in the donor compartment of each cell and kept in contact with the epithelial part of the cornea for 10 minutes, after which the solutions were removed with a Pasteur pipette. Donor compartment was subsequently cleaned and refilled with 1 mL PBS. After 120 min of incubation, corneal opacity and transparency were measured for the last time.

Corneal permeability

The same corneas used in the previous assay (see "Corneal Opacity" section) were placed back into the Franz cells with 6 mL PBS in the receptor compartment. Then, 1 mL of a 0.4% (w/v) fluorescein aqueous solution was placed in the donor compartment. Samples were collected at 90 min, and fluorescein amount was measured by Uv-Vis spectrophotometry at a 490 nm wavelength (Agilent® Cary 60 UV). Results are shown in μg of fluorescein per cm^2 of corneal surface.

3.11. HEN´S EGG TEST - CHORIOALLANTOIC MEMBRANE (HET-CAM)

The HET-CAM was carried out by using the method previously described in ICCVAM (39), by using fertile Broiler chicken eggs. Eggs were placed in an automatic rotation incubator for 8 days at 38 ± 0.5°C and 65% relative humidity (RH). The rotation process was stopped during the last 24 h, so that air chamber remained in the widest part of the egg. The assay was made the 9^{th} incubation day. A tiny drill (Dremel®) was used to open the eggs. The inner membrane was moistened with 0.9% (w/v) NaCl aqueous solution and subsequently removed with adequate forceps. 0.3 mL formulation, negative control (0.9% (w/v) NaCl solution) or positive control (0.1% (w/v) NaOH solution) were directly applied onto the chorioallantoic membrane (CAM) surface. The CAM was observed over a period of 300 s and three reactions were assessed (if applicable): (I) hemorrhage (bleeding from the vessels), (II) vascular lysis (blood vessel disintegration), and (III) coagulation (intra- and/or extra- vascular protein denaturation).

3.12. CORNEAL MUCOADHESIVENESS

Corneal mucoadhesiveness, also known as corneal bioadhesion, is defined as the work required for detaching the formulation from the bovine cornea. It is used as a characterization method based on the quantitative determination of the interaction between the formulation and corneal surface.

This method was designed and developed by our group using fresh bovine corneas and a Shimadzu® Texturometer. Corneas were fixed to plaster supports, which were attached to the upper probe of the texturometer, while formulations were deposited in weighing bottles (diameter: 40 mm, height 20 mm) and placed in the lower part of the analyzer. The method is shown in Figure 2. Each experiment was carried out in triplicate.

Procedure's key parameters were previously studied and subsequently established. Corneas were 2 mm lowered into the formulation at a 1 mm/s speed until contact was observed to obtain force data (N). Corneas were kept in touch with the formulation for 30 s and then returned to the initial position at a 1 mm/s speed, measuring the work (J). Force-displacement curve was registered, and the maximum work was calculated from the area under the curve (AUC).

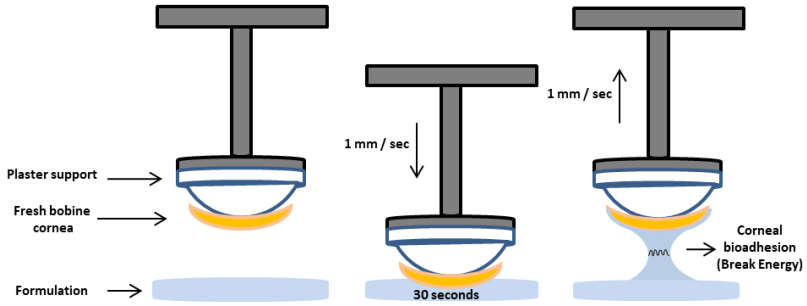

Figure 2. Simplified representation of corneal mucoadhesiveness method.

3.13. PET *IN VIVO* ASSAY: QUANTITATIVE OCULAR PERMANENCE STUDY

The ocular permanence of voriconazole and VFEND® formulations was carried out by Positron Emission Tomography and Computed Tomography Preclinical Imaging (PET/CT Albira® microPET/CT Bruker Biospin, Woodbridge, Connecticut, United States). This method was already described in previous studies (25,33,40) on Sprague-Dawley rats with a 250 g average weight. One week before assays, rats were kept in cages (2 animals/cage) with free access to water and food. The room temperature and humidity conditions were controlled (22 ± 1°C/60 ± 5% RH) and the day-night cycles were regulated by artificial light (12/12 h). Experiments were approved by the Galician Network Committee for Ethics Research following by Spanish and EU rules (86/609/CEE, 2003/65/CE, 2010/63/EU, RD 1201/2005 and RD 53/2013). 100 µl of each formulation were labelled with ^{18}F-fluorodeoxyglucose (^{18}F-FDG). Animals were anesthetized in a gas chamber containing 2.5-3% (v/v) isoflurane in oxygen and placed into the microPET/CT bed provided with an anesthesia system to maintain animal's unconsciousness. 7.5 µL formulation (0.25 MBq radioactivity) were instilled into each eye using a micropipette. At once, static PET frame was acquired (10 min duration). The imaging acquisition was repeated at predetermined times (0, 30, 75, 120, 240 and 300 min). Animals were only anesthetized during the PET acquisition. An Elizabethan collar was placed in each animal between PET studies to prevent the rat from scratching their eyes and remove the eye drops. Two animals (four eyes) were used for each formulation. Likewise, a unique CT frame was acquired by using a control animal in order to accomplish the 3Rs frameworks. Results were obtained by Regions of Interest (ROIs), manually delineated and corrected for radioactive decay. Data was processed using the *pKsolver* software. Resulting data was represented in $C_t/C_{initial}$ ratio of remaining formulations vs acquisition time diagrams. In addition, the total area under the curve (AUC), elimination constant (K), half-life time ($t_{1/2}$) and mean residence time (MRT) were also calculated.

4. RESULTS AND DISCUSSION

The need for a topical ophthalmic treatment of fungal eye infections leads hospital pharmacy departments to use reconditioned injectable drugs for ophthalmic use. These drugs have several limitations in terms of retention time on the eye surface and ocular safety, which remains unknown. At present, despite the proven efficacy of voriconazole in numerous corneal infections by different fungal genre and species, there are no available commercial ophthalmic formulations in Europe.

4.1. SOLUBILIZATION STUDIES

It is essential to seek methods to improve voriconazole's water solubility (0.46 mg/mL). For this purpose, phase solubility diagrams were obtained using different cyclodextrins, which were previously studied for the eye drops formulation (40–42). In addition, previous studies have shown that cyclodextrins can increase the bioavailability of poorly soluble drugs, reduce eye irritation and improve corneal permeability (43,44).

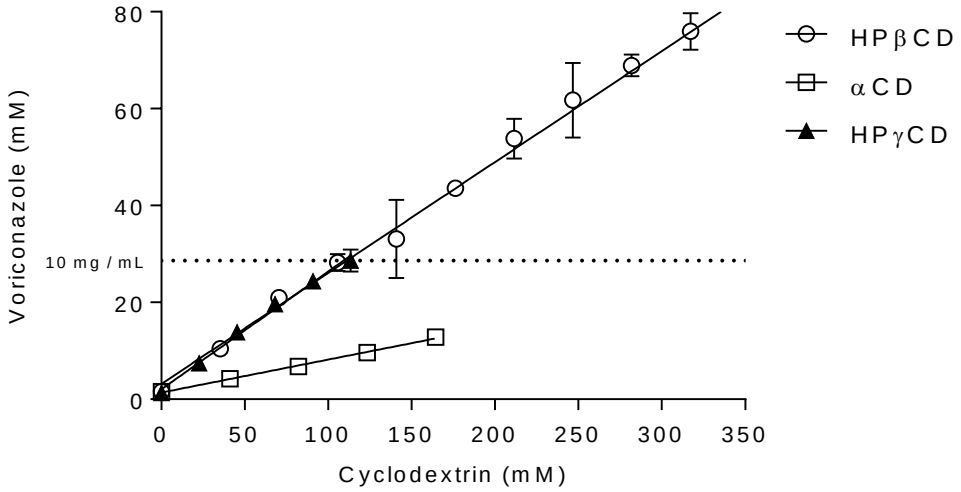

Figure 3. Phase Solubility diagrams for voriconazole, obtained with 3 different types of cyclodextrin at 25°C in water (mean ± SD, n=6). Dotted line represents the minimum CD concentration value that enables the solubilization of a 10 mg/mL voriconazole concentration.

Table 2. Values for $K_{1:1}$, CE, and the D:CD ratio, obtained from the voriconazole/cyclodextrin complex in water at 25°C.

Voriconazole-CD complex	S_0 (mM)	S_O extrap (mM)	$K_{1:1*}$ (M^{-1})	$K_{1:1}$ extrap** (M^{-1})	CE (M)	D:CD (mol:mol)	R^2
HPβCD	1.32	2.35	224.27	126.55	0.29	1:4.367	0.98
αCD	1.32	1.23	55.14	59.17	0.07	1:14.70	0.98
HPγCD	1.32	1.77	242.65	181.34	0.32	1:4.11	0.98

*$K_{1:1}$ calculated using S_0 (free drug solubility)

**$K_{1:1}$ calculated using S_0 extrap (free drug solubility calculated from the phase solubility diagram).

Phase solubility diagrams for voriconazole/cyclodextrin inclusion complexes (Figure 3) were A_L type (water solution, 25°C) (45). These diagrams confirmed the formation of high solubility complexes between the substrate (voriconazole) and the ligand (each cyclodextrin). These complexes are characterized by a linear increase in drug solubility with the cyclodextrin concentration, showing that the complexes are of constant stoichiometry. Table 2 lists the maximum solubility voriconazole values for each cyclodextrin (S_0), as well as apparent stability constants ($K_{1:1}$), complexation efficiency (CE), voriconazole:cyclodextrin complex molar ratio (D:CD) and coefficient of determination (R^2).

HPβCD and HPɣCD showed similar $K_{1:1}$ values, higher than αCD, suggesting that the voriconazole/HPβCD and voriconazole/HPɣCD interactions are stronger than voriconazole/αCD's. Furthermore, HPβCD and HPɣCD obtained the best solubilization properties for the voriconazole and showed high CE values (0.30M and 0.32M, respectively) and small D:CD ratio (1:4.37 and 1:4.11). Drug bioavailability often increases if drug:cyclodextrin complex molar ratio (D:CD) is relatively low, obtaining good results with a small amount of cyclodextrin (30); thus, HPβCD and HPɣCD have shown the best voriconazole complexation properties.

Phase solubility diagrams for voriconazole/HPβCD A_L types were also obtained in previous studies (46,47). However, they were described A_N diagrams from 160 mM cyclodextrin concentration. The present work results are in disagree with the aforementioned described studies, since voriconazole concentration was linear up to the maximum concentration of cyclodextrin used (352.42 mM).

4.2. NMR CHARACTERIZATION OF THE VORICONAZOLE/HPβCD AND VORICONAZOLE/HPɣCD COMPLEXES IN SOLUTION

The higher solubility of the mixtures of voriconazole with HPβCD or HPɣCD in water respect to the pure voriconazole suggest the formation of a complex between this drug acting as guest and one of the host cyclodextrins (HPβCD or HPɣCD). The formation of inclusion complexes of stoichiometry 1:1 is suggested by our previous results (Table 2). The driving force for the formation of these complexes is presumably the formation of a number of favorable guest:host intermolecular interactions as well as the high hydrophobicity of voriconazole in water.

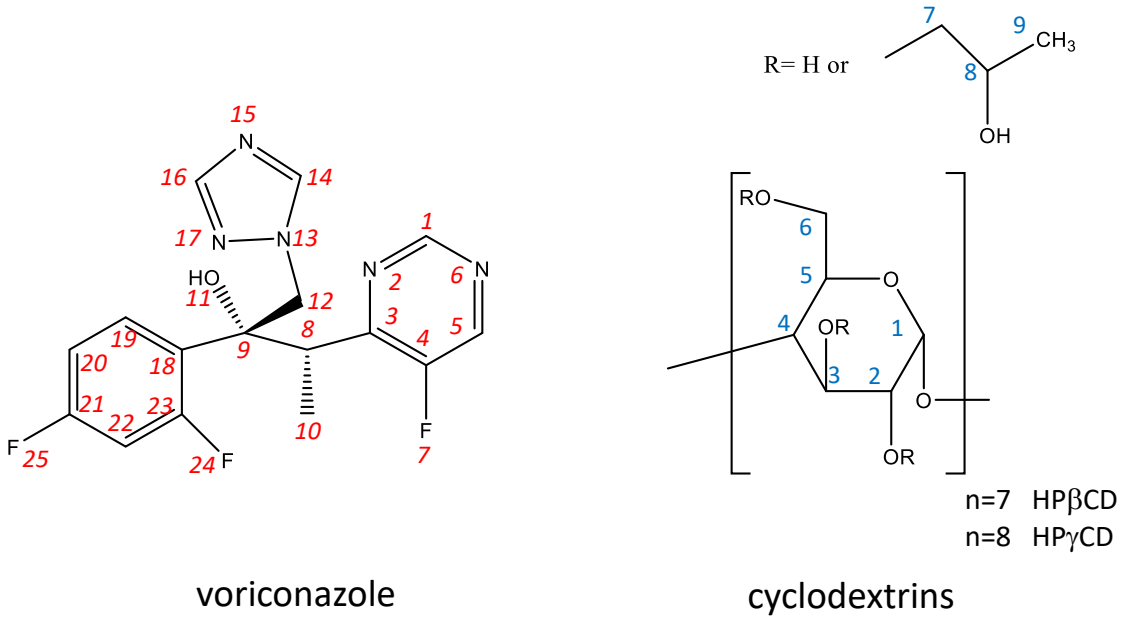

Figure 4. Voriconazole, HPβCD and HPɣCD structures. Numbering scheme referred in the NMR study.

Several NMR methods have been applied in this section to demonstrate the guest:host interactions and to achieve insight in the structure of the inclusion complex in solution.

Due to the low solubility of voriconazole in water, the pure drug was dissolved in MeOD to measure a series of 1D and 2D NMR spectra in order to perform the assignment of the ^{1}H,^{13}C,^{15}N and ^{19}F resonances. The assignment of the ^{1}H and ^{13}C signals of the cyclodextrins (HPβCD or HPγCD) in the mixture is based on previous results (48). The initial NMR signal assignment of ^{1}H, ^{13}C, ^{15}N and ^{19}F resonances of voriconazole (MeOD) was taken from the literature (49). The assignment was then modified and adapted to our samples by using our 1D and 2D correlation spectra (^{1}H, ^{19}F, HSQC ^{1}H-^{13}C, and HMBC ^{1}H-^{15}N). The signal assignment of the three NMR samples is provided in Table 3.

Table 3. NMR chemical shifts (d) in ppm and chemical shift perturbations (CSP) in ppm measured for selected voriconazole signals in samples: voriconazole in MeOD, and the 1:1 aqueous mixtures voriconazole/HPβCD (D_2O) and voriconazole/HPγCD (D_2O). The CSPs are calculated for the mixtures by subtracting the chemical shift of each aqueous mixtures with the chemical shift of voriconazole in MeOD.

Atom	Voriconazole (MeOD) d (ppm)	Voriconazole/ HPβCD d (ppm)	Voriconazole/ HPγCD d (ppm)	Voriconazole/ HPβCD CSP (ppm)	Voriconazole/ HPγCD CSP (ppm)
H-1	8.65	8.54	8.61	-0.11	-0.04
H-5	8.90	8.66	8.84	-0.24	-0.06
H-8	4.07	4.06	3.98	-0.01	-0.09
H-10	1.05	1.03	1.00	-0.02	-0.05
H-12	4.74	4.55	4.69	-0.19	-0.05
H-12'	4.27	4.52	4.21	0.25	-0.06
H-14	8.17	7.53	7.57	-0.64	-0.60
H-16	7.49	7.53	7.57	0.04	0.08
H-19	7.38	7.55	7.25	0.17	-0.13
H-20	6.76	6.86	6.80	0.10	0.04
H-22	6.88	6.96	6.91	0.08	0.03
F7	-137.32	-133.81	-134.25	3.51	3.07
F24	-109.48	-107.47	-108.34	2.01	1.14
F25	-112.93	-109.93	-110.06	3.00	2.87
N-2	294.07	285.63	287.22	-8.44	-6.85
N-6	293.77	noise	noise	-	-
N-13	213.14	211.25	211.89	-1.89	-1.25
N-15	242.50	244.05	244.05	1.55	1.55
N-17	296.41	211.39	211.39	-85.02	-85.02
C-8	37.91	37.91	37.91	0.00	0.00
C-10	14.25	17.74	19.65	3.49	5.40
C-12	56.78	57.41	56.78	0.63	0.00
C-19	129.56	129.56	129.56	0.00	0.00
C-20	110.56	111.51	111.92	0.95	1.36
C-22	103.18	104.14	104.57	0.96	1.39

In a given NMR spectrum, the comparison between the chemical shifts of voriconazole in the pure sample and in their mixtures with HPβCD or HPγCD provides the so-called Chemical Shift Perturbations (CSPs). They are frequently used in the context of ligand binding to a macromolecular receptor to probe binding and discern intermolecular interactions (50). The ^{1}H-

CSPs obtained in the mixtures of voriconazole with HPβCD and HPγCD in the aqueous solutions in comparison to the voriconazole MeOD solution are evident in Figure 5.

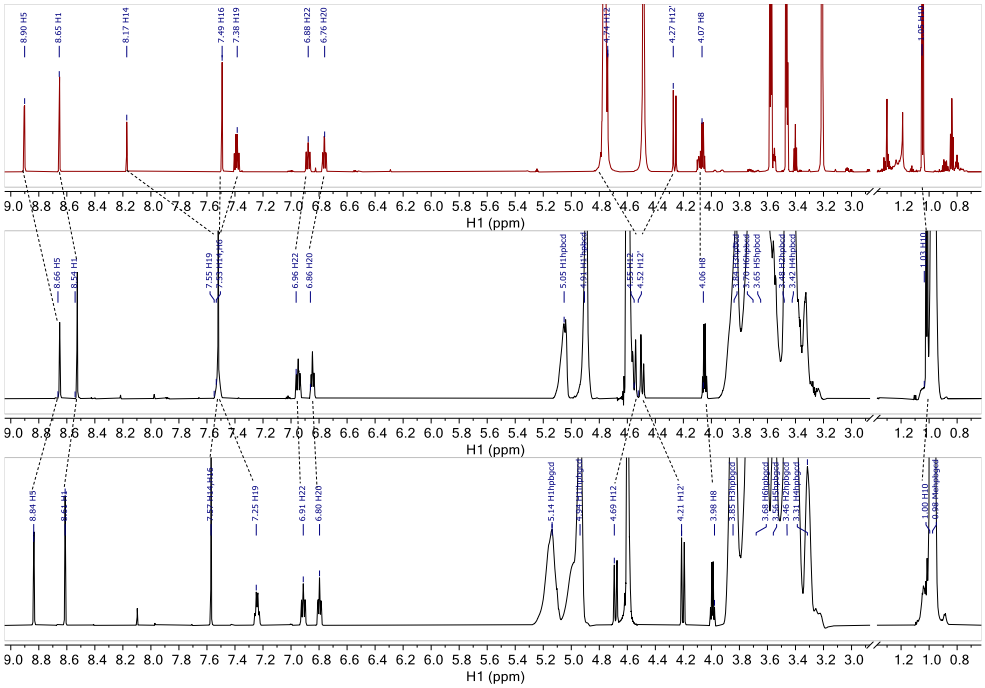

Figure 5. Top: ^{1}H-NMR spectra of the pure voriconazole MeOD solution. **Middle**: voriconazole/HPβCD mixture in D_2O. **Bottom**: voriconazole/HPγCD mixture in D_2O.
The stripped lines guide the eye to connect signals of voriconazole with the same assignment in the three spectra. Some signals of voriconazole and the cyclodextrin are identified in the three spectra using the atom numbering of Figure 4.

In addition, CSPs are observed for cyclodextrin protons but some of them could not be assigned due to the signal overlapping in this region of the spectrum. It must be taken under consideration the change of solvent used to prepare the NMR sample of the drug (MeOD) and the drug/cyclodextrin mixture (D_2O) in order to interpretate the CSPs. It is expected to introduce new contributions to the CSPs due to the differences in the magnetic susceptibility of these solvents. However, these contributions should be constant for all the signals of a solute that do not bind with another molecule and do not suffer a change of conformation.
Interestingly, the differences in the CSPs observed in Figure 5 are very variable in the magnitude and even in the sign depending on the considered signal. Therefore, the variations in these CSPs cannot be completely explained by the differences in the solvent, and also reflect the shielding and de-shielding effects in the proton resonances due to the formation of an inclusion complex between voriconazole and the HPβCD or HPγCD cyclodextrins. Analogously, CSPs were also observed for the ^{13}C signals by comparison of 2D HSQC ^{1}H,^{13}C spectra of these samples (Figure 6) and for the ^{15}N signals by comparison of 2D HMBC ^{1}H,^{15}N spectra (Figure 7).
In the case of the 2D HSQC ^{1}H,^{13}C spectra (Figure 6), relevant CSPs occur for the ^{1}H and ^{13}C resonances of the di-fluorophenyl ring signals and also for the protons and carbons labelled as

12 and 12'. These CSPs suggest the inclusion of the mentioned aromatic ring in the HPβCD cavity.

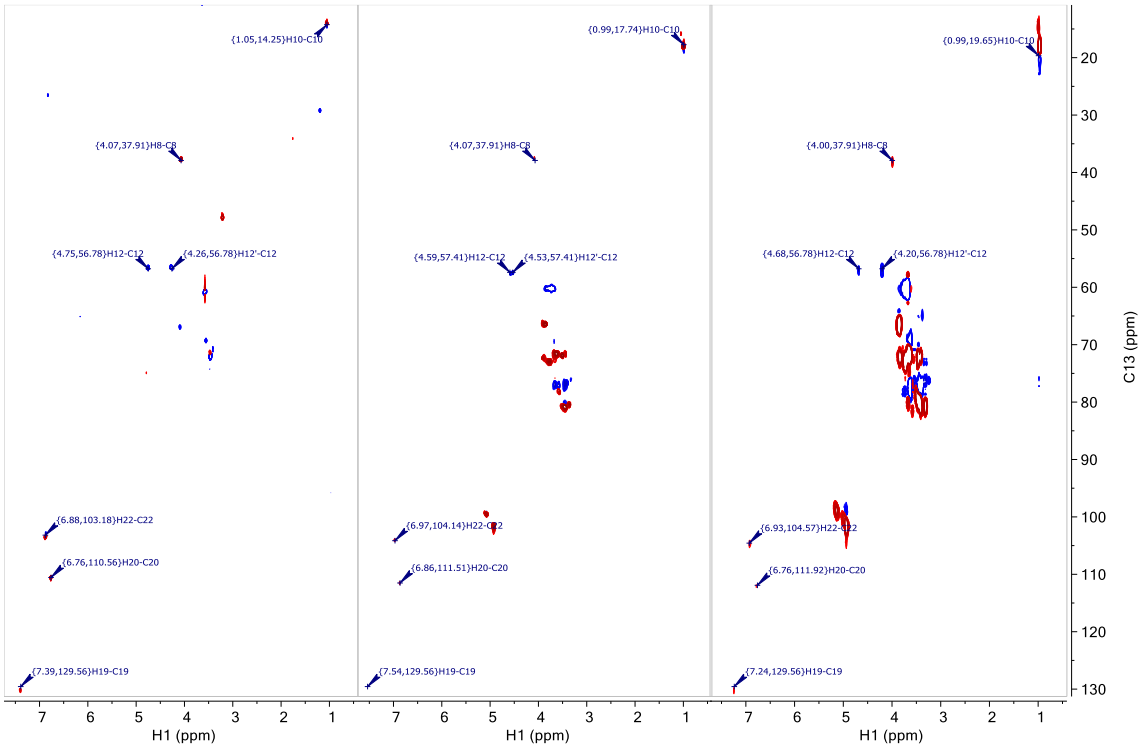

Figure 6. Left: 2D HSQC $^{1}H,^{13}C$ spectrum of pure voriconazole in MeOD. **Middle:** 2D HSQC $^{1}H,^{13}C$ spectrum of voriconazole/HPβCD in D_2O. **Right:** 2D HSQC $^{1}H,^{13}C$ spectrum of voriconazole/HPγCD in D_2O. Some ^{1}H-^{13}C signals of voriconazole are identified in the three spectra using the atom numbering of Figure 4.

In the case of the 2D HMBC-$^{1}H^{15}N$ spectra (Figure 7), the peaks highlighted in green belong to the triazole ring of voriconazole and show considerably small ^{15}N CSPs. On the other hand, the peaks highlighted in yellow belong to the pyrimidine ring of voriconazole and have considerably larger ^{15}N CSPs. The referred ^{15}N CSPs are very similar for the two cyclodextrin derivatives.

A summary of the CSPs occurring for the ^{1}H, ^{13}C, ^{15}N, ^{19}F signals of voriconazole in the three samples (voriconazole (MeOD), voriconazole/HPβCD mixture (D_2O) and voriconazole/HPγCD mixture (D_2O)) is given in Table 3.

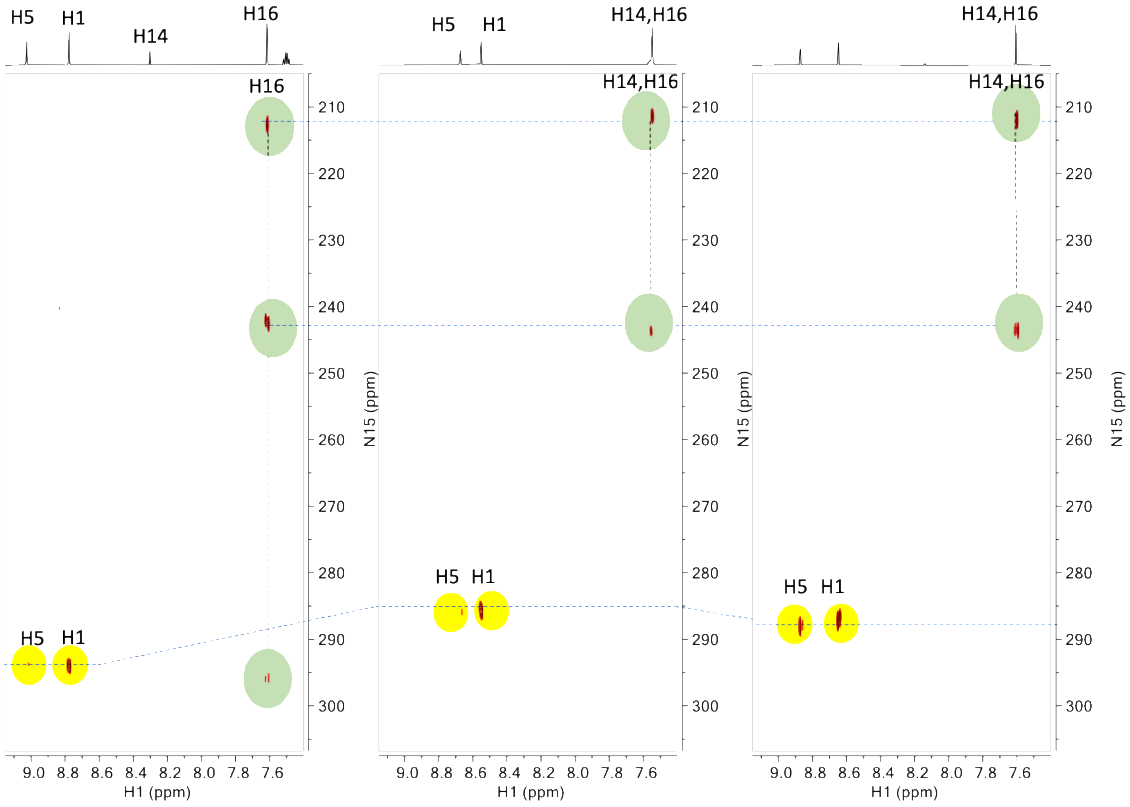

Figure 7. HMBC-^{1}H,^{15}N spectra of voriconazole in MeOD and of their 1:1 voriconazole/HPβCD and voriconazole/HPγCD mixtures in D_2O. The ^{1}H-^{15}N signals of voriconazole are identified in the three spectra using the atom numbering of Figure 4. The stripped lines guide the eye to connect voriconazole signals with the same ^{15}N assignment in the three spectra.

NMR experiments relying on the Nuclear Overhauser Effect (NOE) are aimed to detect spatial proximities between a pair of nuclei, such as protons. Among these experiments STD (31) and NOESY were used to detect intermolecular NOEs between pairs of protons belonging to voriconazole and cyclodextrins (HPβCD or HPγCD). The observation of one or more of these intermolecular NOEs demonstrates the molecular association between both compounds. Moreover, a quantitative or qualitative interpretation of the intermolecular NOEs intensity is useful to build plausible models of the voriconazole/cyclodextrin complex.

Three STD$^{off\text{-}on}$ spectra were measured for the voriconazole/HPβCD mixture. In each spectrum, the selective STD^{on} irradiation was placed in one aromatic signal of voriconazole. The signals irradiated were those at 6.96 (signal H-22), 6.86 (signal H-20) and 4.52 ppm (signals H-12' and H-12) respectively, and the correspondingly spectra are given in Figure 8. It can be seen that the three STD$^{off\text{-}on}$ spectra show the presence of NOE signals, usually referred as STD responses, in the 3.4-4.2 ppm region that can only be attributed to the HPβCD. They reflect intermolecular NOEs occurring between the selected proton of voriconazole and different protons of the cyclodextrin that could not be specifically assigned due to the overlapping signal in that area; however, their appearance clearly implies the formation of either a transient or a fairly stable complex between voriconazole and HPβCD.

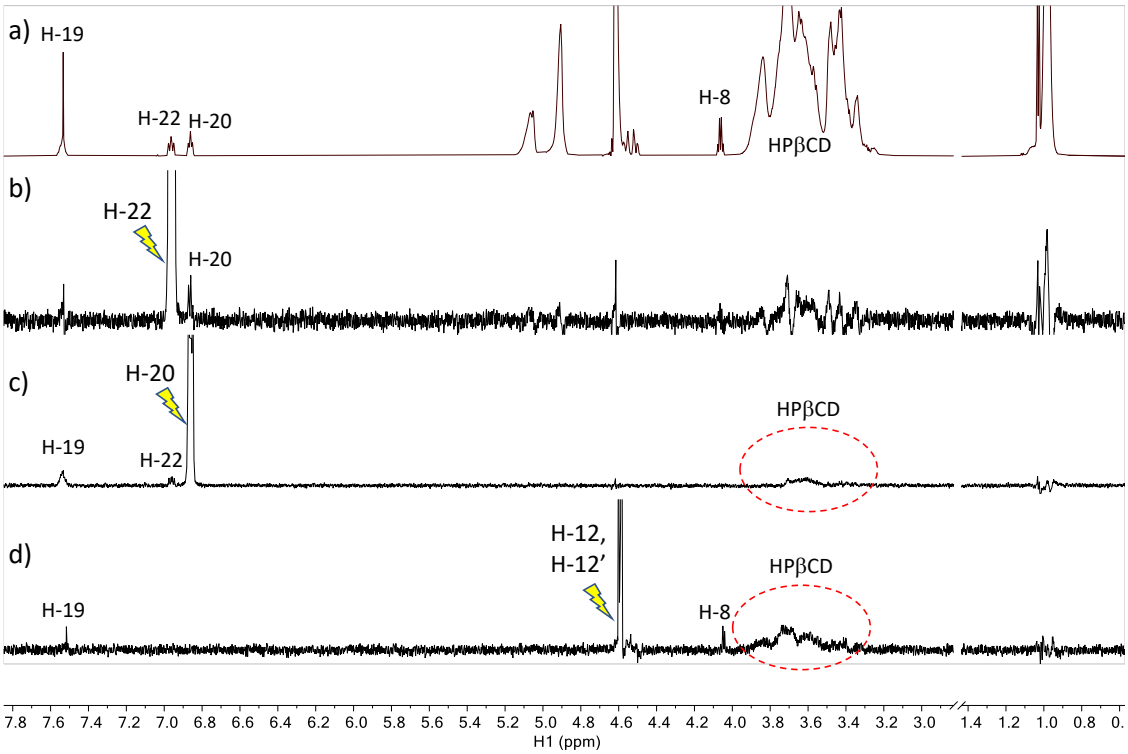

Figure 8. Spectra of voriconazole/HPβCD 1:1 in D_2O. a) ^1H spectrum. b) $STD^{off\text{-}on}$ spectrum with on-saturation at 6.96 ppm (H-22 signal). c) $STD^{off\text{-}on}$ spectrum with on-saturation at 6.86 ppm (H-20 signal). d) $STD^{off\text{-}on}$ spectrum with on-saturation at 4.52 ppm (H-12'and H-12 signals). The atom numbering used to identify the signals of voriconazole follows Figure 4.

A NOESY spectrum of the voriconazole/HPβCD and voriconazole/HPγCD aqueous mixtures provided more information about the complexes structure (Figure 9). In the voriconazole/HPβCD sample, six intermolecular NOEs were identified (Figure 9); three are NOEs between H-5, H-1 and H-19 of voriconazole with the H-9 methyl group of HPβCD, and the other three NOEs are between protons H-19 (overlapped with H-14, H-16), H-20, and H-22 and one or several unidentified proton/s of the pyranose sugar ring of HPβCD. In the voriconazole/HPγCD sample, five intermolecular NOEs were identified (Figure 9) between protons H-5, H-1, H-14 (overlapped with H-16), H-19, and H-22 of voriconazole and one or several unidentified proton/s of the pyranose sugar ring of HPγCD.

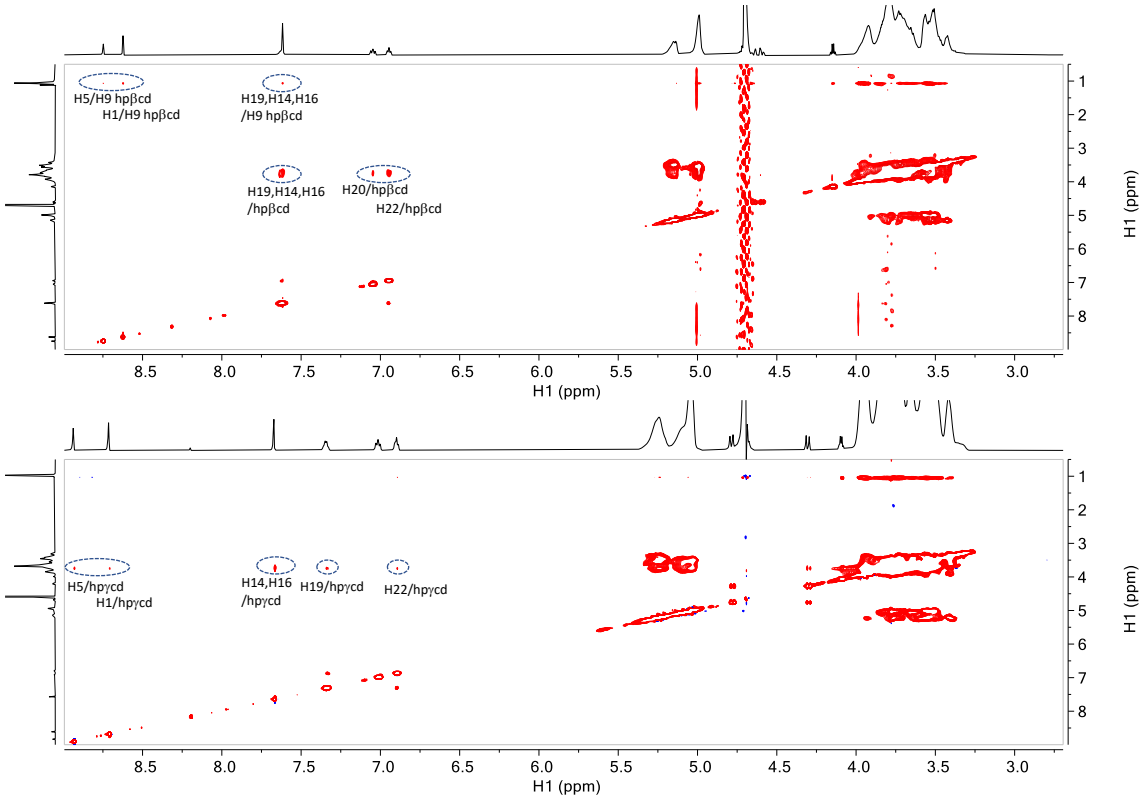

Figure 9. Top: 2D NOESY ^{1}H-^{1}H NMR spectrum with a 500 ms of the voriconazole/HPβCD sample in D_2O. **Bottom**: 2D NOESY ^{1}H-^{1}H NMR spectrum with a 500 ms mixing time of the voriconazole/HPγCD sample in D_2O. Intermolecular NOEs between aromatic protons of voriconazole and the sugar ring protons of the cyclodextrin are indicated. The numbering system used to refer to the protons of voriconazole corresponds are given in Figure 4 (left).

Intermolecular NOEs were observed between the protons of the difluorophenyl ring and the protons of the HPβCD cavity, confirming the inclusion of this voriconazole aromatic ring. In the case of the HPγCD intermolecular, NOEs occur between the HPγCD cavity protons and the difluorophenyl as well as with 5-fluoro-4-pyrimidinyl ring protons. These intermolecular NOEs suggest the complete inclusion of the voriconazole molecule into the cyclodextrin cavity.

Once the complexes formation in the aqueous mixtures of voriconazole with HPβCD or HPγCD was well established by the CSPs, STD and NOESY spectra, the determination of the self-diffusion coefficients in these mixtures was carried out by measuring the DOSY spectra (Figure 10 B). In the case of the voriconazole/HPβCD mixture, the experimentally-measured voriconazole self-diffusion (D^{obs}=3.27x10^{-10} m^{2}s^{-1}) and of the HPβCD (D^{bound} =2.32x10^{-10} m^{2}s^{-1}) were different, indicating that voriconazole is not permanently attached to the cyclodextrin in the complex, but forming a dynamic or transient complex promoted by weak intermolecular interactions. A transient complex implies a balance between free voriconazole and inclusion complexes with the cyclodextrins (Figure 10 A).

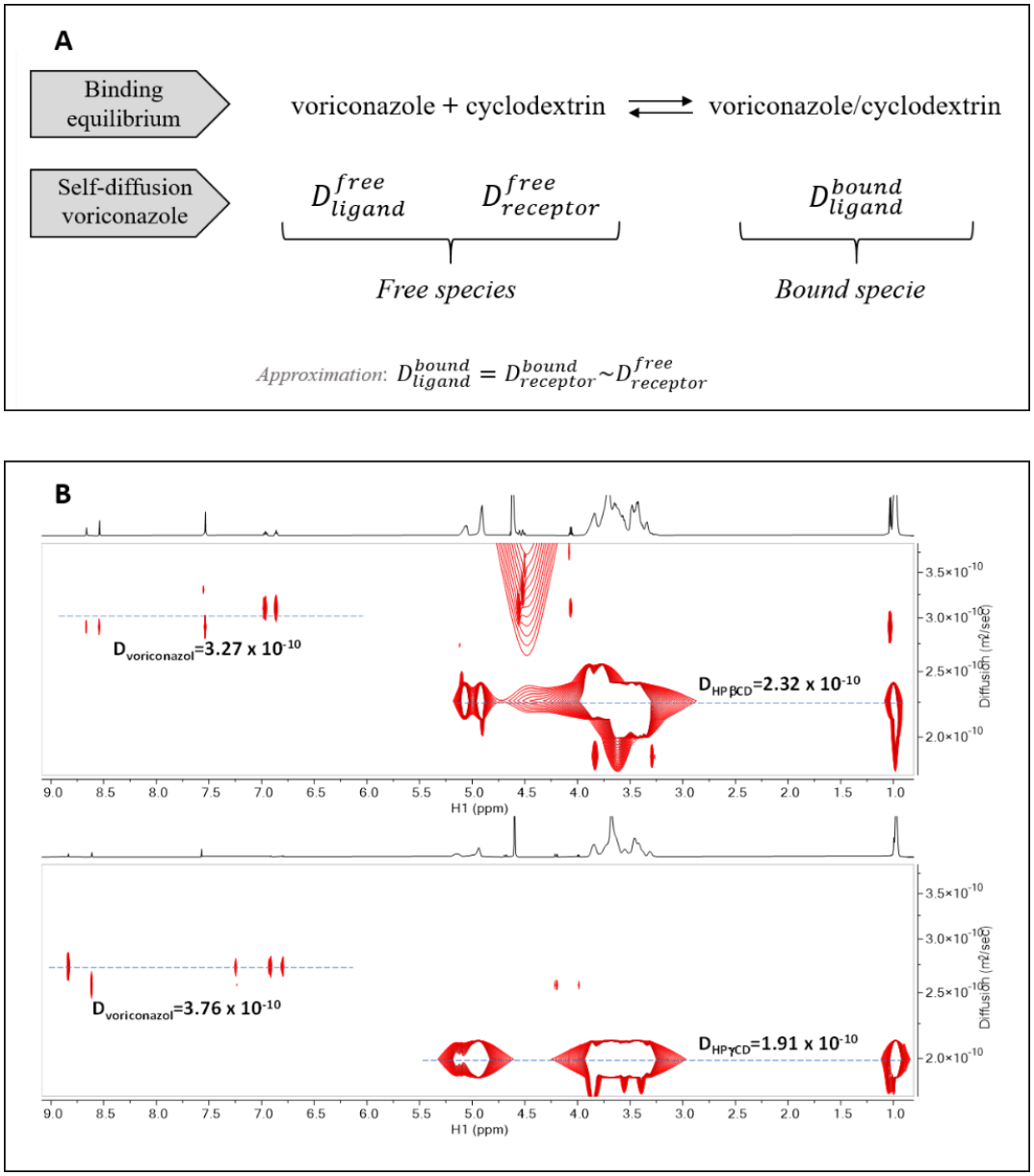

Figure 10. **A:** Binding equilibrium voriconazole and cyclodextrin and the self-diffusion coefficient of several species participating in the equilibrium. B: Top: DOSY diffusion spectrum of voriconazole/HPβCD in D2O. **B:** DOSY diffusion spectrum voriconazole/HPγCD in D2O. The stripped line indicates the average diffusion coefficients measured for the signals of voriconazole and HPβCD or HPγCD.

Under fast exchange balance conditions, the association equilibrium of Figure 10 A is described by eq. 2 (51). In this procedure, it is assumed that the diffusion coefficient of the inclusion complex (voriconazole/HPβCD and voriconazole/HPγCD) follows the same pattern as that of the free drug (voriconazole):

$$D^{obs} = X^{free} \cdot D^{free} + (1 - X^{free}) \cdot D^{bound} \qquad \text{(Eq. 2)}$$

Table 4. Free and bounded voriconazole diffusion coefficients for the inclusion complexes with HPβCD and HPγCD.

Sample	D^{obs} (m^2s^{-1})	D^{bound} (m^2s^{-1})	D^{free} (m^2s^{-1})	X^{free}
Voriconazole/HPβCD	$3.27x10^{-10}$	$2.32x10^{-10}$	$4.2x10^{-10}$	0.51
Voriconazole/HPγCD	$2.76\ x10^{-10}$	$1.91\ x10^{-10}$	$4.2x10^{-10}$	0.37

Two of the four parameters of Eq. 2 are measured in the DOSY spectrum. $D^{obs}$is related to the experimental diffusion determined for voriconazole in the mixture (D^{obs}=$3.27x10^{-10}$ m^2s^{-1}). The parameter D^{bound} corresponds to the experimental diffusion for the bound voriconazole, which is the same diffusion as the HPβCD in the mixture (D^{bound}=$2.32x10^{-10}$ m^2s^{-1}). The parameter D^{free} refers to the self-diffusion coefficient of the voriconazole ligand in the free state and under the same experimental conditions of solvent and temperature. Given the low solubility of voriconazole in D_2O, D^{free}cannot be experimentally obtained in a sample without the receptor; nevertheless, it can be theoretically predicted using the Stokes-Einstein-Gierer-Wirtz Estimation model (SEGWE model) (D^{free}= $4.2\ x10^{-10}$ m^2s^{-1}) (52). The X^{free} =0.51 result was obtained by applying Eq. 2, which corresponds to a K_d = 250 mM under the preparation conditions of this mixture.

In the case of the voriconazole/HPγCD sample, the self-diffusion for voriconazole (D^{obs}=$2.76\ x10^{-10}$ m^2s^{-1}) and HPγCD (D^{bound}=$1.91\ x10^{-10}$ m^2s^{-1}) were also different. This result is also an indication of the formation of a dynamic complex. Using the same type of interpretation of the diffusion coefficients described above based in the Eq. 2 and the SEGWE model, the result of the molar fraction X^{free}=0.37 which under the conditions of the preparation of this mixture corresponds to a K_d= 230 mM.

Despite the approximations used, the K_d values obtained by the analysis of the diffusion coefficients agree with the K_a values obtained in the phase solubility diagram studies (Figure 3) (note that K_a is equal to $1/K_d$ for the inclusion complex balance of Figure 10 A). K_a values are in the same affinity range that those obtained for isoflavones/βCD or clonidine/HPβCD inclusion complexes with the same technique. Zhao et al. (51) reported values of self-diffusion coefficient between D=$4.0x10^{-10}$ m^2s^{-1} and D=$4.3x10^{-10}$ m^2s^{-1} for the diadzein, daidzin and puerarin isoflavones and βCD, and Braga et al. (53) reported values of D=$2.47x10^{-10}$ m^2s^{-1} for HPβCD and D=$5.68x10^{-10}$ m^2s^{-1} for clonidine in the complex with Ka of 20 M^{-1}.

In order to better visualize the results obtained by the NMR experiments, the carried-out molecular modeling of the complexes qualitatively agree with the intermolecular STD and NOEs results (i.e. interproton distances <3.5 Å) (Figure 11). Molecular models show that voriconazole is completely hosted into the HPβCD and HPγCD cavities. The size and the molecular structure of the voriconazole allows to penetrate in both cavities without causing any high-energy conformational distortion in any of the two cyclodextrins. Thus, the structure of the voriconazole inclusion complex for HPβCD and HPγCD after the docking calculations are in good agreement with the NMR data.

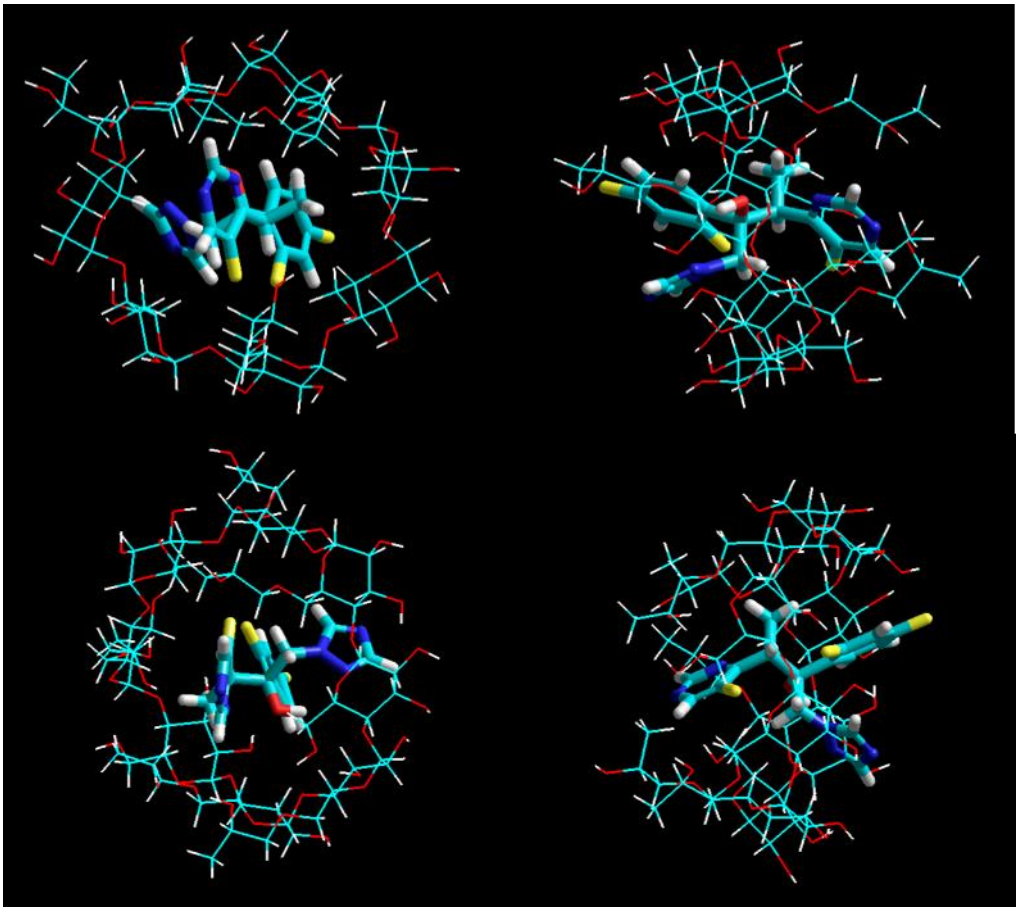

Figure 11. Top: Molecular structure of voriconazole/HPβCD. **Bottom**: voriconazole/HPγCD. Both images were obtained by molecular modelling.

The formation of these complexes in which the voriconazole is deeply inserted into the cavity of HPβCD or HPγCD provides an explanation to the enhanced solubility of voriconazole in these mixtures compared to the pure sample of voriconazole in aqueous solution. Moreover, the binding affinity of voriconazole to form the complex with HPβCD or HPγCD is similar according to the obtained K_d values.

HPβCD is one of the cyclodextrin derivatives that are currently used in the preparation of formulations for parenteral administration in humans, also proving to be safe for ophthalmic instillation (54). Furthermore, HPβCD has shown an improvement in the amount of drugs that permeated the eye surface, increasing their concentration in aqueous humor (55,56), leading to a decrease in the drug ocular toxicity (43). Consequently, HPβCD was selected as the cyclodextrin of choice for the preparation of the VZN, VZHAH and VZISH formulations.

4.3. SQUEEZING FORCE MEASUREMENT

According to Conner et al. (57), at least 50% of the patients, who were prescribed an ophthalmic topical treatment, reported difficulty for self-administration due to the needed force to be applied to the boat for the formulation to come out, among other causes.

Squeeze force test was carried out after a formulation macroscopic analysis based on the high viscosity of different VZISH (VZISH 0.65, VZISH 0.75 and VZISH 0.82) after their

elaboration. The homogeneity in terms of volume and structure of the formulation drops is also an important property that ensures a precise drug dosage, avoiding therapeutic variability. High dosages can lead the patient to suffer side effects, while an underdosage may compromise or prolong the pharmacological treatment. Squeeze force can be influenced by different factors, such as formulation viscosity, surface tension or design of the eye dropper tip (58). For this reason, the same type of packaging was used to perform the test.

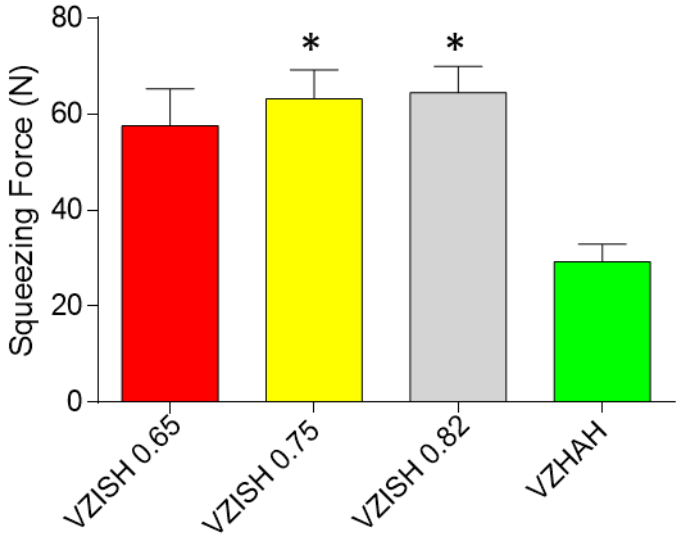

Figure 12. Comparison of Squeeze Force values among different hydrogels. ANOVA results show significant differences among formulations ($\alpha < 0.05$); * indicates no significant differences between both hydrogels.

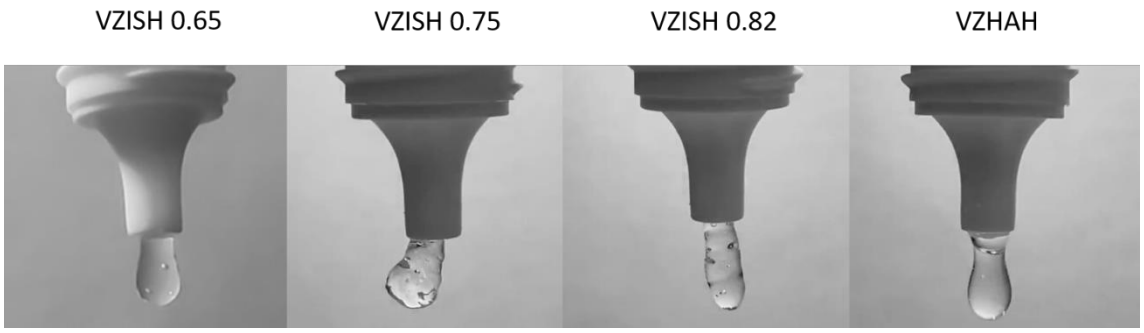

Figure 13. Formulation drops images.

The one-way ANOVA analysis allows concluding that the required force to dispense a drop of VZISH 0.65 (Figure 12) is significantly lower than VZISH 0.75 and VZISH 0.82 ($p < 0.0001$). Based on these results, VZISH 0.65 was selected as the optimum formulation for the following-assays' execution.

In addition, the drop image analysis also shows more homogeneous drops (structure and volume) for VZISH 0.65 than for VZISH 0.75 and VZISH 0.82 (Figure 13).

4.4. *IN VITRO* RELEASE STUDIES

The release study of voriconazole from all formulations (VFEND®, VFEND®HAH, VZN, VZHAH and VZISH 0.65) was fitted to a zero-order kinetics model. The cumulative release of voriconazole is shown in Figure 14. Papp (cm/s), flux (µg/min) and R^2 are shown in Table 6. Release mechanism from all formulations was examined by data fitting to various mathematical models such as the zero-order, Higuchi and Korsmeyer-Peppas (Table 5). Zero order model showed a R^2=0.99 value for all formulations except for VFEND® and VZN (0.96 and 0.97 respectively), although it can be considered a good fit to a zero-order kinetic model.

A linear increase in the voriconazole released amount from all formulations (VFEND®, VFEND®HAH, VZN, VZHAH and VZISH 0.65) was observed. There were not significant differences in the *in vitro* release of voriconazole in any of the formulations for the 0-120 min interval, but statistically significantly differences were found between VFEND® and VZHAH, as well as between VFEND® HAH and VZISH at the 240 min measurement.

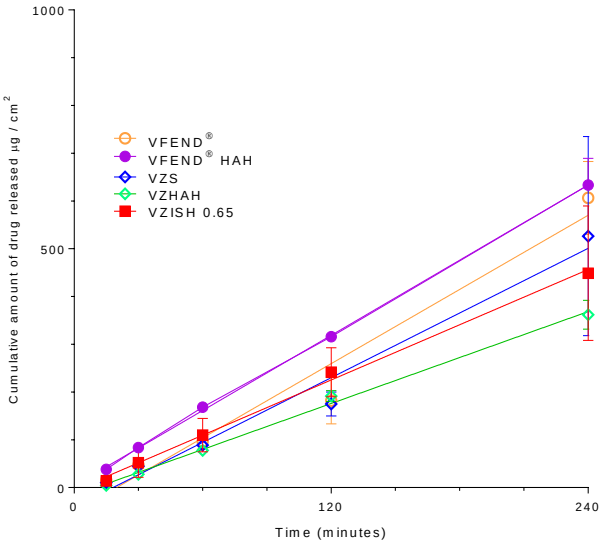

Figure 14. Release profiles of voriconazole formulations. Data were fitted to a zero-order kinetics.

Table 5. Kinetic profiles of *in vitro* drug release from VFEND®, VFEND®HAH, VZS, VZHAH and VZISH 0.65 through Visking® dialysis membranes (Medicel® membranes Ltd) with a 12-14 KDa cut-off (0.784 cm^2 available surface area).

	R^2		
Formulations	**Zero Order**	**Higuchi**	**Korsmeyer-Peppas**
VFEND®	0.96	0.87	0.97
VFEND®HAH	0.99	0.88	0.96
VZS	0.97	0.79	0.95
VZHAH	0.99	0.78	0.99
VZISH 0.65	0.99	0.85	0.98

Table 6. Release data fitting from voriconazole formulations to a zero-order kinetics model.

Formulation	Papp·10^{-6} (cm / s)	SE·10^{-7}	Flux (µg / min)	SE	R^2
VFEND®	4.31	4.88	2.58	0.29	0.96
VFEND®HAH	4.37	0.48	2.62	0.02	0.99
VZS	3.76	3.45	2.25	0.20	0.97
VZHAH	2.67	0.92	1.60	0.05	0.99
VZISH 0.65	3.21	1.05	1.92	0.06	0.99

4.5. pH AND ISOTONICITY MEASURES

Osmolality and pH values are shown in Table 7. The VFEND® formulations, both the solution and the mucoadhesive gel (VFEND®HAH), presented osmolality values of 817.33 mOsm/kg and 884.33 mOsm/kg respectively, unlike the VZS, VZHAH and VZISH 0.65 formulations, which showed osmolality values of 176.66 mOsm/kg, 203.33 mOsm/kg and 170.87 mOsm/kg, respectively. The difference in osmolality values may be due to the SBECD's monovalent sodium ions in the VFEND® formulation. This conclusion is supported by the resulting data obtained in the comparison of a 20% (w/v) SBECD solution and a 20% (w/v) HPβCD solution, where 578.5 ± 7.141 mOsm/kg and 185 ± 1.414 mOsm/kg osmolality results were obtained, respectively.

Likewise, osmolality was considered a secondary aspect in the development of topical ophthalmic formulations, but it should be taken into account as a key factor, where hyperosmolality was observed to produce an osmotic movement towards the conjunctival sac, leading to an increase in the dilution and removal processes (42).

The ophthalmic formulations should also be formulated to have a similar pH to that of the tear (7.4), but the presence of bicarbonate ions, proteins and mucins in the tear (16) may give it some buffering ability, so the eye may tolerate small pH deviations without producing ocular surface irritation and tearing (which could produce an increase in drug elimination due to the formulation dilution). Thus, formulations prepared with the voriconazole-HPβCD inclusion complex showed lower pH values (approx. 5.5) than those made with VFEND® (VFEND® pH 6.82 and VFEND®HAH pH 6.62), so the pH values of all the formulations tested would be within the buffer capacity of the tear (4 to 8 pH range) (43). According to this, all the formulations studied (VFEND®, VFEND®HAH, VZN, VZHAH, VZISH 0.65) would be suitable for topical ophthalmic administration.

Table 7. Osmolality and pH results.

Formulation	Osmolality (mOsm / kg)		pH	
	Mean	SD	Mean	SD
VFEND®	817.33	5.50	6.82	0.025
VFEND®HAH	884.33	16.25	6.62	0.037
VZS	176.66	3.78	5.54	0.141
VZHAH	203.33	15.63	5.52	0.023
VZISH 0.65	170.87	0.57	5.63	0.034

4.6. *EX VIVO* CORNEAL PERMEABILITY STUDIES

Corneal fungal infections frequently reach the aqueous humor and, subsequently, other ocular internal structures. Hence, an *ex vivo* transcorneal permeability test was performed to assess the ability of hydrogels to allow voriconazole to pass through the corneal structure into the aqueous humor.

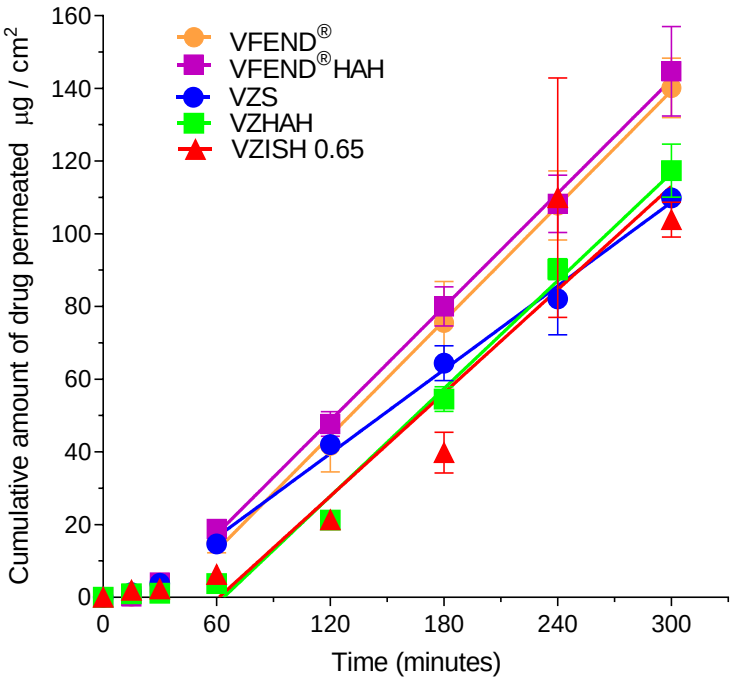

Figure 15. Corneal permeability profile of voriconazole formulations.

Corneal permeability profiles of different formulations were compared to each other, as presented in Figure 15. The non-parametric analysis (Kruskal-Wallis) performed for release profiles did not showed significant differences among formulations. It must be taken into account that the lag time values the flux and Papp values were obtained starting the fitting of permeability values to a linear model from 55 min. Slopes were used to calculate the flux and Papp values. Apparent permeability, flux and time lag data were calculated and are represented in Table 8. Voriconazole shows similar apparent permeability values for all formulations and,

formulations do not affect the corneal flux. Non-parametric Kruskal-Wallis test shows that no statistical differences (p > ns) were observed between formulation for flux and Papp, but one way-ANOVA and the Tukey test shows statistical differences ($p < 0.05$) for lag time between VZS and VZHAH, VZS and VZISH 0.65, VZSHAH and VFEND®HAH.

Previous studies made by Rodriguez et al. (2017) (59) revealed an apparent corneal permeability data for thymolol/HPβCD complex of $0.77x10^{-6}$ cm/s, lower than those obtained in the present study for the voriconazole/HPβCD (VZS) complexes (1.42×10^{-6} cm/s) despite similar molecular weights (thymolol: 316.421 g/mol; voriconazole: 349.317 g/mol). In addition, Rodriguez et al. also observed that the apparent permeability of the thymolol/HPβCD inclusion complexes considerably decreased when hyaluronic acid was added ($0.07x10^{-6}$ cm/s), while in the present study a slight increase in the apparent permeability of the voriconazole/HPβCD complexes with HA (VZHAH) ($1.65x10^{-6}$ cm/s) was observed, compared to that of the complex without HA ($1.42x10^{-6}$ cm/s).

Malhotra et al. (2014) (41) evaluated the effect of different polymers on the voriconazole/HPβCD complexes' corneal permeability. They observed that the addition of GG or other polymers significantly decrease the voriconazole permeability compared to voriconazole/HPβCD aqueous solution. However, in the present study, no significant differences in voriconazole permeability were found between non-polymer solutions (VZS and VFEND®) and polymer formulations (VFEND®HAH, VZISH 0.65, VZHAH).

All formulations showed good permeability through the bovine cornea, and none of the formulations affected the corneal flow of the drug.

Table 8. Corneal permeability values of voriconazole formulations.

Formulation	Papp·10^{-6} (cm / s)	SE · 10^{-7}	Flux (µg / min)	SE	T_{lag} (min)	SE
VFEND®	1.73	2.58	0.52	0.01	29.26	10.01
VFEND®HAH	1.73	2.73	0.52	0.01	24.18	3.09
VZS	1.29	0.74	0.38	0.01	20.59	4.18
VZHAH	1.64	1.50	0.49	0.02	48.91	0.09
VZISH 0.65	1.57	3.16	0.47	0.10	46.15	2.27

4.7. OCULAR IRRITATION TEST

BCOP and HET-CAM were used to assess the potential irritation on the ocular surface of the components of all formulations.

According to HET-CAM results, VFEND®, VFEND®HAH, VZS, VZHAH and VZISH 0.65, formulations have been classified as non-irritants since no hemorrhage, vascular lysis and/or coagulation phenomena were observed in the CAM vessels after a 5 min period of contact with all formulations.

The results obtained in the BCOP test also showed that none of the formulations tested (VZS, VZHAH, VZISH 0.65, VFEND® and VFEND®HAH) cause significant changes in transparency and opacity (Figure 16) or fluorescein permeability (Table 9). The initial opacity values

(corneas treated with PBS for 60 min) and the values obtained after treatment with the formulations for 10 min and 120 min with PBS are also shown in Table 9. No significant differences were observed between the control (PBS-treated cornea) and the tested formulations (VFEND®, VFEND®HAH, VZS, VZHAH and VZISH 0.65) in both transmittance) and opacity measurements, compared to the positive control (ethanol-treated cornea).
Both irritation studies conclude that developed formulations are not irritant and do not produce corneal structure alterations.

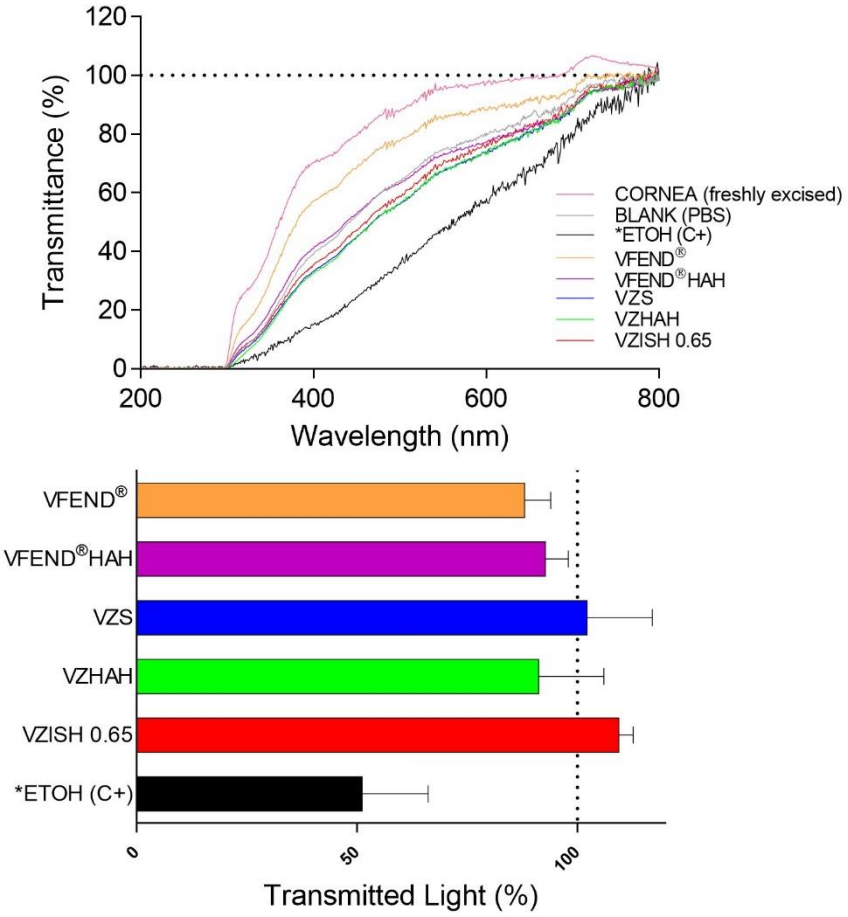

Figure 16. Top: Ultraviolet-visible (UV-Vis) scan (from 200 to 800 nm) of corneal transmittance (%) after 10 min drug treatment and 120 min PBS treatment. Bottom: Opacity (TL %) values of bovine corneas treated with VFEND®, VFEND®HAH, VZS, VZHAH, VZISH 0.65 and Ethanol after 10 min drug treatment and 120 min PBS treatment. 100% corresponds to the total light transmitted through bovine corneas incubated in PBS. Graph was obtained from Table 9 data. *ETOH (C+): Ethanol (positive control).

Table 9. Bovine Corneal Opacity and Fluorescein Permeability results for all formulations, negative control (PBS) and positive control (ethanol).

Formulation	%TL initial*		%TL 10**		Permeability µg/cm²	
	Mean	SD	Mean	SD		SD
PBS (negative control)	88.27	5.87	62.93	7.13	0.721	0.89
***ETOH (C+)**	63.89	9.75	39.86	11.64	15.64	9.75
VFEND®	71.21	6.55	68.54	4.64	0.00	0.00
VFEND®HAH	82.16	8.15	72.24	4.04	0.00	0.00
VZS	76.02	16.23	79.60	11.54	0.00	0.00
VZHAH	73.53	2.92	71.05	11.50	1.73	1.32
VZISH 0.65	86.05	2.60	85.22	2.54	0.00	0.00

*Opacity values after incubation of the corneas for 60 min in PBS

** Opacity values after incubation of the corneas for 60 min in PBS, 10 min in formulation and 120 min in PBS

*** Ethanol (positive control)

4.8. CORNEAL MUCOADHESIVENESS

The bioadhesion properties of the ophthalmic formulations allow to know their residence time in the ocular surface.

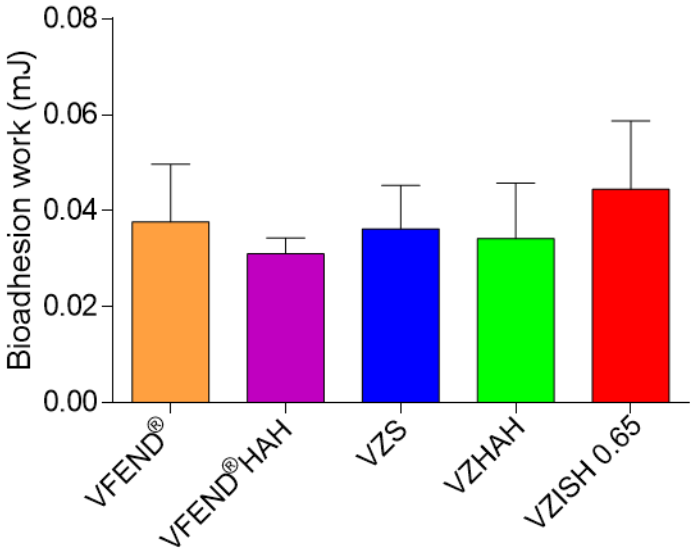

Figure 17. Maximum breaking strength and bioadhesion work obtained for each formulation using bovine cornea as a substrate.

The bioadhesion work (Figure 17) for VZISH 0.65 shows a value of 0.044 ± 0.014 mJ higher than the rest of the formulations (from 0.031 to 0.0377 mJ) due to the presence of the GG and CK polymers. It should be taken into account that the test was carried out without the presence of tears, so the viscosity of the gel would be mainly influenced by the amount of GG (even though no one-way ANOVA statistically differences were observed). In the presence of teardrops, the bioadhesivity values would probably increase due to the cross-linking process of

GG (due to the divalent calcium ions (Ca^{2+})) and CK (by the presence of monovalent potassium ions (K^{+})) and would decrease in the rest of the formulations due to their dilution phenomenon with the teardrops. The bioadhesion work would also be increased in the case of VZISH 0.65, increasing the permanence of VZISH 0.65 in the eye (25). In order to corroborate the conclusions obtained after this test, an *in vivo* permanence study was carried out using the PET/CT imaging technique.

4.9. PET/CT *IN VIVO* ASSAY: QUANTITATIVE OCULAR PERMANENCE STUDY

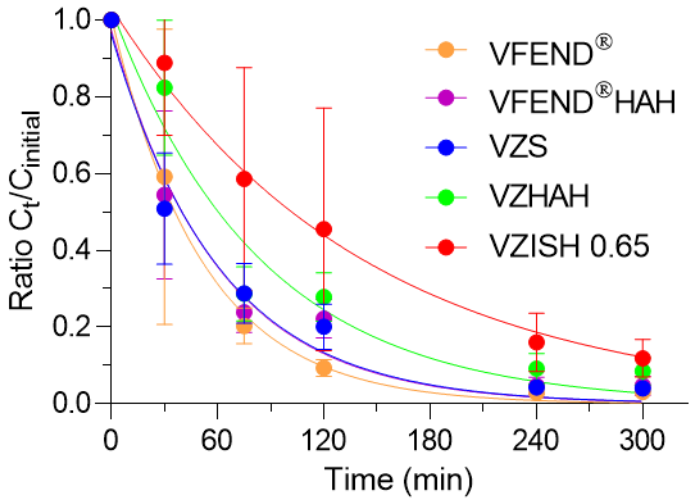

Figure 18. VFEND®, VFEND®HAH, VZN, VZHAH and VZISH 0.65, clearance ratio from the ocular surface determined by PET. $C_t/C_{initial}$ radioactivity ratio remaining on the ocular surface over time was calculated assuming $C_{inicial}$ value recorded in the ROI (ocular globe) equaled 1.

Table 10. Pharmacokinetic parameters ($t_{1/2}$ (min), AUC_0^{300} (mg/L·min) and MRT (min)) obtained by $C_t/C_{initial}$ ratio fitting to a monoexponential model on the ocular surface obtained by PET imaging.

Formulation	$t_{1/2}$ (min)		AUC_0^{300} (mg/L·min)		MRT (min)	
	Mean	SD	Mean	SD	Mean	SD
VFEND®	32.27	15.56	52.79	12.61	84.85	17.85
VFEND®HAH	40.78	7.64	67.28	8.03	98.42	17.99
VZS	42.19	12.61	67.28	14.28	92.16	8.46
VZHAH	58.91	13.4	89.86	15.01	118.40	21.69
VZISH 0.65	96.28	49.11	104.56	30.29	119.80	20.57

Figure 18 shows the clearance ratio ($C_t/C_{initial}$) of the formulations from the ocular surface. The percentage of formulation that remained on the eye surface after 60 minutes of administration was calculated from the graph. VZISH 0.65 and VZHAH showed values of 67.42% and 50.25%, compared to 35.9%, 31.31% and 35.75% for VZS, VFEND® and VFEND®HAH respectively.

The pharmacokinetic parameters obtained from the PET images are shown in Table 10. VZISH 0.65 and VZHAH show MRT values of 119.80 ± 20.57 and 118.40 ± 21.69 min respectively,

higher than those obtained for VZS or VFEND® solutions with values of 92.16 ± 8.46 and 84.85±17.85 min, and 98.42 ± 17.99 min for VFEND®HAH, respectively. The values of $t_{1/2}$ (Table 10) were 96.28 ± 49.11 min for VZISH 0.65 and 58.91 ± 13.4 min for VZHAH. Both values were significantly higher than those obtained for VZS, VFEND® and VFEND®HAH: 42.19 ± 12.61 min, 32.27 ± 15.56 min and 40.78 ± 7.64 min, respectively.

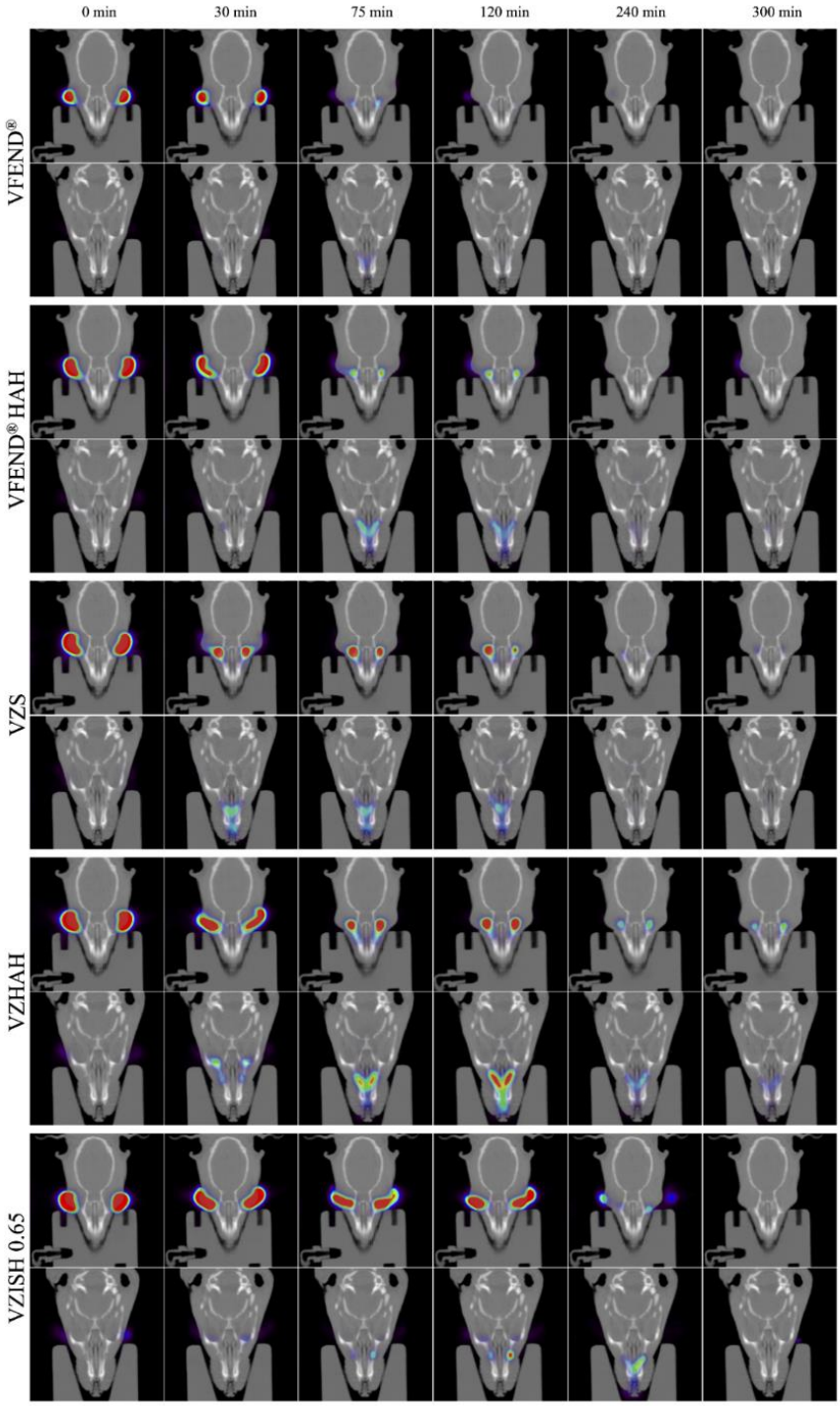

Figure 19. Coronal PET/CT images of rat's eyes treated with VFEND®, VFEND®HAH, VZN, VZHAH and VZISH 0.65, over time. The amount of formulation on the ocular surface is coded on a color scale: blue areas show a low radioactive activity; red areas show a high radioactive activity.

Figure 19 shows the coronal PET/CT images of rat's eyes after VFEND®, VFEND® HAH, VZS, VZHAH and VZISH 0.65, 0 and 30, 75, 120, 240 and 300 min post-administration. PET/CT images show ^{18}F-FDG-labelled formulation distributions on the rat eye and nasolacrimal duct. As can be appreciated in the Figure 19, VZHAH and VZISH 0.65 are retained in the ocular cavity longer than VZS, VFEND® and VFEND®HAH.

The GG and CK corneal retention profiles were previously studied by Rupenthal et al. (2011), whereas better ocular retention time for each one where observed, compared to other studied polymers (60). In addition, in this study, AUC_0^{15} value for GG (81.644% min) and CK (78.400% min) was about double that solution without polymers (45.605% min), used as control. These results support the obtained data in present study: AUC_0^{300} value for VZISH 0.65 was 104.56 mg/L·min and AUC_0^{300} value for VZS was 67.28 mg/L·min.

The ocular permanence differences between VZHAH and VFEND®HAH formulations, where VZHAH has shown a longer permanence time than VFEND®HAH, are probably related to the VFEND®HAH hyperosmolality, which leads to a higher hydrogel dilution and, consequently, a faster elimination.

VZISH 0.65 and VZHAH have shown a longer permanence on the ocular surface compared to the voriconazole formulation used in hospital pharmacy departments as pharmaceutical compounding (VFEND®) (61–63).

5. CONCLUSION

Voriconazole hydrogels were successfully developed as a new topical ophthalmic alternative intended for the treatment of fungal keratitis. *In vitro* characterization was carried out according to different parameters, including: (I) solubility studies, (II) NMR characterization, and (III) squeezing force, mainly.

Solubility and NMR results showed that the inclusion complex formation was similar for both types of cyclodextrin. The voriconazole/HPβCD inclusion complex formation was based on the internalization of the voriconazole's difluorophenyl ring into the cyclodextrin cavity. On the other hand, in the voriconazole/HPγCD inclusion complex, the entire voriconazole structure was included into the cyclodextrin cavity due to its bigger size. Even so, stability and solubility parameters showed similar values for both inclusion complexes.

Osmolality and pH values were in the appropriate range. *In vitro* release studies were successfully performed, and a zero-order kinetic profile was observed in all the voriconazole hydrogels. All formulations also showed good permeability through the *ex vivo* permeability assay. Moreover, ocular toxicity studies have proven the safety of these hydrogels on the ocular surface through the BCOP and HET-CAM tests. PET/CT studies confirm the mucoadhesive properties of all the voriconazole hydrogels, where VZHAH and VZISH 0.65 were selected as the best topical ophthalmic formulations for the controlled release of voriconazole. On the basis of these results, it can be concluded that voriconazole hydrogels (VZISH 0.65 and VZHAH) may significantly improve the fungal keratitis treatment, decreasing the number of applications and increasing the adherence to the patient's treatment.

Besides all of that, all the hydrogels show a high versatility in terms of controlled drug release and biopermanence intended for topical ophthalmic administration. Based on this, new drugs

could be included for the treatment of different ocular pathologies, not just aimed for anterior chamber diseases, but also for posterior chamber diseases.

BIBLIOGRAFY

1. Ahn M, Yoon KC, Ryu SK, Cho NC, You IC. Clinical aspects and prognosis of mixed microbial (bacterial and fungal) keratitis. Cornea. abril de 2011;30(4):409-13.
2. Shukla PK, Kumar M, Keshava GBS. Mycotic keratitis: an overview of diagnosis and therapy. Mycoses. mayo de 2008;51(3):183-99.
3. Bourcier T, Sauer A, Dory A, Denis J, Sabou M. Fungal keratitis. J Fr Ophtalmol. noviembre de 2017;40(9):e307-13.
4. Rai M, Occhiutto ML. Mycotic Keratitis. CRC Press; 2019. 367 p.
5. Samudio M, Laspina F, Fariña N, Franco A, Mino de Kaspar H, Giusiano G. [Keratitis by Lasiodiplodia theobromae: a case report and literature review]. Rev Chil Infectologia Organo Of Soc Chil Infectologia. diciembre de 2014;31(6):750-4.
6. Taechajongjintana M, Kasetsuwan N, Reinprayoon U, Sawanwattanakul S, Pisuchpen P. Effectiveness of voriconazole and corneal cross-linking on Phialophora verrucosa keratitis: a case report. J Med Case Reports. 19 de agosto de 2018;12(1):225.
7. Thamke DC, Mendiratta DK, Dhabarde A, Shukla AK. Mycotic keratitis due to Engyodontium album: first case report from India. Indian J Med Microbiol. junio de 2015;33(2):303-4.
8. Lund OE, Miño de Kaspar H, Klauss V. [Strategy for examination and therapy of mycotic keratitis]. Klin Monatsbl Augenheilkd. marzo de 1993;202(3):188-94.
9. Saha S, Banerjee D, Khetan A, Sengupta J. Epidemiological profile of fungal keratitis in urban population of West Bengal, India. Oman J Ophthalmol. 2009;2(3):114-8.
10. FlorCruz NV, Evans JR. Medical interventions for fungal keratitis. Cochrane Database Syst Rev. 9 de abril de 2015;(4):CD004241.
11. Hung N, Hsiao CH, Yang CS, Lin HC, Yeh LK, Fan YC, et al. Colletotrichum keratitis: A rare yet important fungal infection of human eyes. Mycoses. abril de 2020;63(4):407-15.
12. Vyawahare CR, Misra RN, Gandham NR, Angadi KM, Paul R. Pencillium keratitis in an Immunocompetent Patient from Pune, Maharashtra, India. J Clin Diagn Res JCDR. julio de 2014;8(7):DD01-02.
13. Anutarapongpan O, Thanathanee O, Suwan-Apichon O. Penicillium keratitis in a HIV-infected patient. BMJ Case Rep. 17 de agosto de 2016;2016.
14. Ogawa A, Matsumoto Y, Yaguchi T, Shimmura S, Tsubota K. Successful treatment of Beauveria bassiana fungal keratitis with topical voriconazole. J Infect Chemother. abril de 2016;22(4):257-60.
15. Mannis MJ, Holland EJ. Cornea E-Book. Elsevier Health Sciences; 2016. 2014 p.
16. Manzouri B, Vafidis GC, Wyse RKH. Pharmacotherapy of fungal eye infections. Expert Opin Pharmacother. 2001;2(11):1849-57.
17. Müller GG, Kara-José N, Castro RS de. Antifungals in eye infections: drugs and routes of administration. Rev Bras Oftalmol. abril de 2013;72(2):132-41.

18. Hariprasad SM, Mieler WF, Lin TK, Sponsel WE, Graybill JR. Voriconazole in the treatment of fungal eye infections: a review of current literature. Br J Ophthalmol. julio de 2008;92(7):871-8.
19. Ludwig A. The use of mucoadhesive polymers in ocular drug delivery. Adv Drug Deliv Rev. 3 de noviembre de 2005;57(11):1595-639.
20. Ghorbanzad'e M, Mohammad H. F, Masoumeh K, Patrik L. A. Quantitative and qualitative prediction of corneal permeability for drug like compounds. octubre de 2011;85(5):2686-94.
21. Shen J, Deng Y, Jin X, Ping Q, Su Z, Li L. Thiolated nanostructured lipid carriers as a potential ocular drug delivery system for cyclosporine A: Improving *in vivo* ocular distribution. Int J Pharm. 15 de diciembre de 2010;402(1-2):248-53.
22. Boddu SHS, Gunda S, Earla R, Mitra AK. Ocular microdialysis: a continuous sampling technique to study pharmacokinetics and pharmacodynamics in the eye. Bioanalysis. marzo de 2010;2(3):487-507.
23. Bravo-Osuna I, Andrés-Guerrero V, Pastoriza Abal P, Molina-Martínez IT, Herrero-Vanrell R. Pharmaceutical microscale and nanoscale approaches for efficient treatment of ocular diseases. Drug Deliv Transl Res. 2016;6(6):686-707.
24. Jitendra, Sharma B, Dixit S. A new trend: ocular drug delivery system. Pharma Sci Monit [Internet]. julio de 2011 [citado 20 de febrero de 2020];2(3). Disponible en: https://www.semanticscholar.org/paper/A-NEW-TREND-%3A-OCULAR-DRUG-DELIVERY-SYSTEM-Jitendra-Banik/b1fb13f814726a805e7ed2fcd2b8b15cd129832c
25. Fernández-Ferreiro A, González Barcia M, Gil-Martínez M, Vieites-Prado A, Lema I, Argibay B, et al. *In vitro* and *in vivo* ocular safety and eye surface permanence determination by direct and Magnetic Resonance Imaging of ion-sensitive hydrogels based on gellan gum and kappa-carrageenan. Eur J Pharm Biopharm. agosto de 2015;94:342-51.
26. Sun CQ, Prajna NV, Krishnan T, Rajaraman R, Srinivasan M, Raghavan A, et al. Effect of pretreatment with antifungal agents on clinical outcomes in fungal keratitis. Clin Experiment Ophthalmol. diciembre de 2016;44(9):763-7.
27. Sharma S, Das S, Virdi A, Fernandes M, Sahu SK, Kumar Koday N, et al. Re-appraisal of topical 1% voriconazole and 5% natamycin in the treatment of fungal keratitis in a randomised trial. Br J Ophthalmol. septiembre de 2015;99(9):1190-5.
28. Ferreiro AF, Barcia MG. Current use of Antifungal Eye Drops and How to Improve Therapeutic Aspects in Keratomycosis. Fungal Genomics Biol [Internet]. 2016 [citado 16 de abril de 2019];6(1). Disponible en: https://www.omicsgroup.org/journals/current-use-of-antifungal-eye-drops-and-how-to-improve-therapeuticaspects-in-keratomycosis-2165-8056-1000130.php?aid=69192
29. Connors KA HT. Advances in Analitycal Chemistry and Instrumentation. Vol. Phase-Solubility Techniques. New York: Interscience; 1965. 117-212 p.
30. Loftsson T, Brewster ME. Cyclodextrins as Functional Excipients: Methods to Enhance Complexation Efficiency. J Pharm Sci. 1 de septiembre de 2012;101(9):3019-32.

31. Mayer M, Meyer B. Mapping the Active Site of Angiotensin-Converting Enzyme by Transferred NOE Spectroscopy. J Med Chem. 1 de junio de 2000;43(11):2093-9.
32. Fernández-Ferreiro A, Fernández Bargiela N, Varela MS, Martínez MG, Pardo M, Piñeiro Ces A, et al. Cyclodextrin–polysaccharide-based, in situ-gelled system for ocular antifungal delivery. Beilstein J Org Chem. 8 de diciembre de 2014;10:2903-11.
33. Luaces-Rodríguez A, Díaz-Tomé V, González-Barcia M, Silva-Rodríguez J, Herranz M, Gil-Martínez M, et al. Cysteamine polysaccharide hydrogels: Study of extended ocular delivery and biopermanence time by PET imaging. Int J Pharm. 7 de agosto de 2017;528(1-2):714-22.
34. Cox CH. Squeeze force measuring system [Internet]. US7441468B2, 2008 [citado 11 de febrero de 2020]. Disponible en: https://patents.google.com/patent/US7441468B2/en
35. EUR-Lex - 02010L0063-20190626 - EN - EUR-Lex [Internet]. [citado 26 de abril de 2020]. Disponible en: https://eur-lex.europa.eu/legal-content/EN/TXT/?uri=CELEX%3A02010L0063-20190626
36. Wilhelmus KR. The Draize Eye Test. Surv Ophthalmol. 1 de mayo de 2001;45(6):493-515.
37. Test No. 437: Bovine Corneal Opacity and Permeability Test Method for Identifying i) Chemicals Inducing Serious Eye Damage and ii) Chemicals Not Requiring Classification for Eye Irritation or Serious Eye Damage [Internet]. [citado 13 de febrero de 2020]. Disponible en: https://www.oecd-ilibrary.org/environment/test-no-437-bovine-corneal-opacity-and-permeability-test-method-for-identifying-i-chemicals-inducing-serious-eye-damage-and-ii-chemicals-not-requiring-classification-for-eye-irritation-or-serious-eye-damage_9789264203846-en
38. Fernández-Ferreiro A, Santiago-Varela M, Gil-Martínez M, González-Barcia M, Luaces-Rodríguez A, Díaz-Tome V, et al. *In Vitro* Evaluation of the Ophthalmic Toxicity Profile of Chlorhexidine and Propamidine Isethionate Eye Drops. J Ocul Pharmacol Ther Off J Assoc Ocul Pharmacol Ther. 2017;33(3):202-9.
39. ICCVAM. (2010). Recommended Test Method Protocol: Hen's Egg Test Chorioallantoic Membrane (HET-CAM) Test Method. Obtained from https://ntp.niehs.nih.gov/iccvam/docs/protocols/ivocular-hetcam.pdf.
40. Díaz-Tomé V, Luaces-Rodríguez A, Silva-Rodríguez J, Blanco-Dorado S, García-Quintanilla L, Llovo-Taboada J, et al. Ophthalmic Econazole Hydrogels for the Treatment of Fungal Keratitis. J Pharm Sci. mayo de 2018;107(5):1342-51.
41. Malhotra S, Khare A, Grover K, Singh I, Pawar P. Design and Evaluation of Voriconazole Eye Drops for the Treatment of Fungal Keratitis. J Pharm [Internet]. 2014;2014. Disponible en: https://www.ncbi.nlm.nih.gov/pmc/articles/PMC4590801/
42. Moya-Ortega MD, Alves TFG, Alvarez-Lorenzo C, Concheiro A, Stefánsson E, Thorsteinsdóttir M, et al. Dexamethasone eye drops containing γ-cyclodextrin-based nanogels. Int J Pharm. 30 de enero de 2013;441(1):507-15.
43. Abdelkader H, Fathalla Z, Moharram H, Ali TFS, Pierscionek B. Cyclodextrin Enhances Corneal Tolerability and Reduces Ocular Toxicity Caused by Diclofenac. Oxid Med Cell Longev. 2018;2018:5260976.

44. Loftsson T, Stefánsson E. Cyclodextrins and topical drug delivery to the anterior and posterior segments of the eye. Int J Pharm. 15 de octubre de 2017;531(2):413-23.
45. K. A. Connors TH. Phase Solubility Techniques. Advanced Analytical Chemistry of Instrumentation. 1965;4:117-212.
46. Buchanan CM, Buchanan NL, Edgar KJ, Ramsey MG. Solubilty and dissolution studies of antifungal drug:hydroxybutenyl-β-cyclodextrin complexes. Cellulose. 1 de febrero de 2007;14(1):35-47.
47. Miletic T, Kyriakos K, Graovac A, Ibric S. Spray-dried voriconazole–cyclodextrin complexes: Solubility, dissolution rate and chemical stability. Carbohydr Polym. 15 de octubre de 2013;98(1):122-31.
48. Nogueiras-Nieto L, Sobarzo-Sánchez E, Gómez-Amoza JL, Otero-Espinar FJ. Competitive displacement of drugs from cyclodextrin inclusion complex by polypseudorotaxane formation with poloxamer: Implications in drug solubilization and delivery. Eur J Pharm Biopharm. 1 de abril de 2012;80(3):585-95.
49. Barbosa TM, Morris GA, Nilsson M, Rittner R, Tormena CF. 1 H and 19F NMR in drug stress testing: the case of voriconazole. RSC Adv. 4 de julio de 2017;7(54):34000-4.
50. Williamson MP. Using chemical shift perturbation to characterise ligand binding. Prog Nucl Magn Reson Spectrosc. agosto de 2013;73:1-16.
51. Zhao R, Sandström C, Zhang H, Tan T. NMR Study on the Inclusion Complexes of β-Cyclodextrin with Isoflavones. Molecules. abril de 2016;21(4):372.
52. Evans R, Deng Z, Rogerson AK, McLachlan AS, Richards JJ, Nilsson M, et al. Quantitative Interpretation of Diffusion-Ordered NMR Spectra: Can We Rationalize Small Molecule Diffusion Coefficients? Angew Chem Int Ed. 2013;52(11):3199-202.
53. Braga MA, Martini MF, Pickholz M, Yokaichiya F, Franco MKD, Cabeça LF, et al. Clonidine complexation with hydroxypropyl-beta-cyclodextrin: From physico-chemical characterization to *in vivo* adjuvant effect in local anesthesia. J Pharm Biomed Anal. 5 de febrero de 2016;119:27-36.
54. European Medicines Agency (EMA). Background review for cyclodextrins used as excipients. noviembre de 2014;17.
55. Kristinsson JK, Fridriksdóttir H, Thórisdóttir S, Sigurdardóttir AM, Stefánsson E, Loftsson T. Dexamethasone-cyclodextrin-polymer co-complexes in aqueous eye drops. Aqueous humor pharmacokinetics in humans. Invest Ophthalmol Vis Sci. mayo de 1996;37(6):1199-203.
56. Siefert B, Pleyer U, Müller M, Hartmann C, Keipert S. Influence of Cyclodextrins on the *In Vitro* Corneal Permeability and *In Vivo* Ocular Distribution of Thalidomide. J Ocul Pharmacol Ther. 1 de octubre de 1999;15(5):429-38.
57. Connor AJ, Severn PS. Force requirements in topical medicine use—the squeezability factor. Eye. abril de 2011;25(4):466-9.
58. Van Santvliet L, Ludwig A. Determinants of eye drop size. Surv Ophthalmol. abril de 2004;49(2):197-213.

59. Rodríguez I, Vázquez JA, Pastrana L, Khutoryanskiy VV. Enhancement and inhibition effects on the corneal permeability of timolol maleate: Polymers, cyclodextrins and chelating agents. Int J Pharm. 30 de agosto de 2017;529(1-2):168-77.
60. Rupenthal ID, Green CR, Alany RG. Comparison of ion-activated in situ gelling systems for ocular drug delivery. Part 1: Physicochemical characterisation and *in vitro* release. Int J Pharm. 15 de junio de 2011;411(1–2):69-77.
61. Dupuis A, Tournier N, Le Moal G, Venisse N. Preparation and Stability of Voriconazole Eye Drop Solution. Antimicrob Agents Chemother. febrero de 2009;53(2):798-9.
62. Al-Badriyeh D, Neoh CF, Stewart K, Kong DCM. Clinical utility of voriconazole eye drops in ophthalmic fungal keratitis. Clin Ophthalmol Auckl NZ. 6 de mayo de 2010;4:391-405.
63. Lau D, Fedinands M, Leung L, Fullinfaw R, Kong D, Davies G, et al. Penetration of voriconazole, 1%, eyedrops into human aqueous humor: a prospective open-label study. Arch Ophthalmol Chic Ill 1960. marzo de 2008;126(3):343-6.

Chapter 3

ANTIFUNGAL COMBINATION EYE DROPS FOR FUNGAL KERATITIS TREATMENT

1. INTRODUCTION

Fungal keratitis (FK) is a corneal mycotic infection mainly caused by corneal trauma with contaminated plants or objects (1,2), the misuse of contact lenses (3,4), prolonged use of topical antibiotics or corticosteroids (5), eye surgeries (6), or the immunocompromised state of the patient (7,8) among others. FK is a severe disease that can lead to vision loss or even complete loss of the eye. FK is usually caused by yeasts like *Candida albicans* or filamentous fungi such as *Aspergillus* spp. *or Fusarium* spp., but it can be caused by more than 100 different species (3,8,9).

The prognosis of FK lies in early diagnosis and correct treatment. One of the biggest problems of FK diagnosis is that the patient may be asymptomatic after the trauma, so the diagnosis might be delayed for days or even weeks until the patient suffers some symptom (ocular pain or sensitivity to light, among others) (10). Furthermore, the non-specific symptoms of FK can lead to erroneous diagnosis and treatment; for this reason, the microbiological diagnosis must be mandatory to choose a suitable treatment.

There is currently only one formulation approved by the Food and Drug Administration (FDA) for the treatment of FK, Natacyn®, which is a conventional natamycin suspension. Natamycin penetration through the cornea to the deeper structures of the eye is hindered by its low aqueous solubility and high molecular weight. Therefore, to achieve therapeutic concentrations, Natacyn® is administered every hour, leading to poor adherence of patients to the treatment.

Natamycin is a polyene drug of amphipathic nature, and it is practically insoluble in water (30–50 mg/l). Natamycin has a broad spectrum of action against filamentous fungi (e.g. *Aspergillus* spp., *Fusarium* spp.) (11) and yeasts (e.g. *Candida Albicans*) (12). However, although *in vitro* studies showed natamycin to be effective against *Fusarium* spp., this did not translate into favorable clinical outcomes, probably due to its poor penetration into the deeper corneal layers (13).

On the other hand, voriconazole (a fluconazole derivative) is a triazole with a broad spectrum against *Aspergillus* spp., *Candida* spp., *Fusarium* spp., *Scedosporium sp*p. and *Paecilomyces* spp., among other fungal species (14). Voriconazole is widely used for the treatment of FK (6,15,16), but there is still no commercial ophthalmic formulation approved by the FDA or the European Medicines Agency (EMA). Only formulations marketed and approved for oral and intravenous routes are available (17,18). For this reason, hospital pharmacy departments must reformulate voriconazole formulations intended for other administration routes, usually intravenous. These formulations are reconstituted with ophthalmic buffers, but their toxicity, bioavailability, and stability remain unknown in most cases. Moreover, the high nasolacrimal drainage leads to short ocular permanence and to systemic absorption of the formulation that may trigger side effects.

The severity of FK is aggravated by the emergence of resistant fungal species. Antifungal combination therapy is more useful than monotherapy in antifungal-resistant fungi infections (19). For this reason, several studies have been conducted to evaluate different antifungals combinations (20) or combinations between antifungals and other drugs (21). Previous studies have shown that the combination of natamycin and voriconazole may be more effective, showing synergism or an additive effect in certain species like *Fusarium* spp. (20,22,23).

Ocular formulations must also be designed considering excipients that are safe for ophthalmic administration and that enhance the formulation properties. The use of cyclodextrins might be considered a suitable approach to improve drug solubility (24). Moreover, according to EMA, some cyclodextrins, such as 2-hydroxypropyl-β-cyclodextrin (HPβCD), have demonstrated ophthalmic safety, as well as improved drug permanence on the ocular surface and transcorneal permeability (25).

The main goal of this work was to develop a new ophthalmic formulation for the combination of natamycin and voriconazole based on the need to find an effective and non-invasive treatment for FK. Natamycin and voriconazole formulations were characterized by means of solubility, Nuclear Magnetic Resonance (NMR), pH, osmolality, and viscosity studies. The *in vitro* release was evaluated to assess the release kinetics. Ocular safety was evaluated by two different organotypic cytotoxicity models, Bovine Corneal Opacity and Permeability (BCOP) assay and Hen´s Egg Test - Chorioallantoic Membrane (HET-CAM). Bioavailability properties were evaluated using freshly excised bovine corneas. Ocular permanence was assessed by a corneal mucoadhesiveness test and confirmed by an *in vivo* ophthalmic permanence assay using Positron Emission Tomography/Computed Tomography imaging (PET/CT imaging). In addition, the antifungal susceptibility was studied by a disc diffusion method.

2. MATERIALS AND METHODS

2.1. MATERIALS

Natamycin was purchased from LabNetwork® (Saint Paul MN, US); Voriconazole was procured by Normon® (Madrid, Spain); Hyaluronic Acid (HA) (MW 1.4 x 106 Da) was obtained from Acofarma® (Barcelona, Spain); 2-hydroxypropyl-β-cyclodextrin (HPβCD) (Kleptose®, 0.65 molar substitution ratio, MW 1399 Da) was obtained from Roquette® Laisa S.A. (Valencia, Spain); 2-hydroxypropyl-γ-cyclodextrin (HPγCD) (0.6 molar substitution ratio, MW 1580 Da) was purchased from Sigma Aldrich® (Darmstadt, Germany); Liquifilm® was obtained from Allergan® Pharmaceuticals Ireland (Mayo, Ireland); Poloxamer (P407) and Polyvinyl alcohol (PVA) (Mw 30.000-70.000 Da) were procured by Sigma Aldrich, Methyl Cellulose (MC) (1500 cP) was procured by Shin-Etsu (Japan).

2.2. PHASE SOLUBILITY DIAGRAMS

Solubility diagrams of natamycin were obtained according to the Higuchi and Connors methodology (26). Natamycin complex stability constants were determined using the solubility diagrams.

The solubility assay was based on the addition of an excess of the drug to different solutions with increasing concentrations of two different cyclodextrins, 2-hydroxypropyl-β-cyclodextrin (HPβCD) or 2-hydroxypropyl-ɣ-cyclodextrin (HPγCD). Cyclodextrin solutions were maintained for 7 days in an orbital shaker (VWR®) (25±0.5°C, 200 rpm) to achieve the maximum solubility of natamycin. Afterwards, the resultant solutions were centrifugated (Eppendorf® Centrifuge 5804R) at 12,000 rpm for 30 min and 25°C. Natamycin concentration

was determined by UV-vis spectrophotometry (Agilent® Cary UV 60, λ = 310 nm) after dilution of an aliquot in 0.1 M acetic acid. Each measurement was performed in triplicate.
Solubility diagrams were obtained by representing the concentration of natamycin (mM) against the concentration of cyclodextrins (mM). The slope obtained from the solubility diagrams, the natamycin water solubility (S_0), and the natamycin solubility in the intercept ($S_{0\ extrap}$) were used to calculate the apparent stability constant ($K_{1:1}$ or K_d) assuming the obtention of 1:1 ratio inclusion complexes. The equations described by Loftsson et al. (27) were used to calculate the complexation efficiency (CE) and the natamycin:cyclodextrin molar ratio (D:CD) values.

2.3. MORPHOLOGICAL ANALYSIS BY TRANSMISSION ELECTRON MICROSCOPY (TEM)

The morphological analysis of the particles of the saturated solution of natamycin in 40% (w/v) HPβCD solution and the saturated solution of natamycin in 40% (w/v) HPβCD solution and 1% (w/v) voriconazole solution were evaluated using a JEOL JEM-F200CF-HR microscope (JEOL®. Peabody, USA). Samples were placed on copper grids and stained with 2% (w/v) phosphotungstic acid. Samples were dried and evaluated by TEM observation using an accelerating voltage of 200 kV.
Particle size was measured using Image-Pro Plus Image Analysis Software (Media Cybernetics, Inc. USA).

2.4. NATAMYCIN SOLUBILITY WITH HPβCD AND DIFFERENT HYDROPHILIC POLYMERS

The solubility of natamycin was studied with 20% (w/v) HPβCD and different ratios of hydrophilic polymers, these being: polyvinyl alcohol (PVA), hyaluronic acid (HA) and poloxamer 407 (P407). This study was carried out to assess the differences of natamycin in terms of solubilization efficiency.
Solubility was determined by adding an excess of natamycin to solutions made up of 20% (w/v) of HPβCD and different concentrations of hydrophilic polymers (see Table 1).

The hydrophilic polymer concentrations were chosen based on previous studies (28,29).

Table 1. Composition of polymeric solutions to assess the potential increase in water solubilization efficiency of natamycin.

Solution	HPβCD % (w/v)	Polymer % (w/v)
I	20	-
II	20	0.5% PVA
III	20	1% PVA
IV	20	0.4% HA
V	20	0.1% P407
VI	20	0.5% MC

2.5. NATAMYCIN AND VORICONAZOLE SOLUBILITY WITH HPβCD

The solubility of natamycin was studied at different concentrations of HPβCD and a fixed concentration of voriconazole. Three solutions were made at increasing concentrations of HPβCD (20%, 30% and 40% (w/v)) and 1% (w/v) voriconazole. An excess of natamycin was subsequently added to each solution. Similarly, voriconazole solubility was also studied at different concentrations of HPβCD and a fixed concentration of 0.4% (w/v) natamycin.
The resultant solutions were incubated for 7 days. Afterwards, the solutions were centrifugated (Eppendorf® Centrifuge 5804R) at 12,000 rpm for 30 min and 25°C. Natamycin concentration was determined by UV-Vis spectrophotometry (Agilent® Cary UV 60 λ = 310 nm) by previously diluting an aliquot in acetic acid 0.1 M. Each measurement was made in triplicate.

2.6. NUCLEAR MAGNETIC RESONANCE (NMR) STUDIES

Liquid-state NMR spectra were conducted at 25˚C on a Bruker NEO 17.6 T spectrometer (proton resonance 750 MHz), equipped with a $^{1}H/^{13}C/^{15}N$ triple resonance PA-TXI probe and PFG shielded z-gradient that uses 5 mm standard OD tubes. The spectrometer control software was TopSpin® 4.0. The chemical shifts are referenced to the lock deuterium solvent. Spectra were processed and analyzed with Mestrenova® software v14.0 (Mestrelab® Inc.).
Samples containing natamycin, voriconazole and/or HPβCD were prepared in 5 mm standard tubes. The exact concentration of the compounds is indicated in each case.
A two-dimensional 2D HSQC multiplicity edited ^{1}H-^{13}C spectrum was measured (pulse sequence "hsqcedetgpsisp2.4" of the Bruker library) for a sample prepared with 10 mM of natamycin in 0.6 mL of CD_3OD. The INEPTs transfers were optimized for a nominal value of the scalar coupling 1JCH of 145 Hz. The delay for multiplicity selection was set to 1/ (2·1JCH) to detect with the same sign signals of CH_3 and CH groups and with opposite phase CH_2 groups. The relaxation delay (d^1) and the FID acquisition time (at) were 1.6 and 0.112 s, respectively. The spectrum was acquired with 2048 and 160 complex points in the t_2 and t_1 dimensions, respectively. The number of scans per t_1 increment was 16 and the total measurement time was ~1 h.
One dimensional Saturation Transferred Difference ^{1}H spectra (STD) (30,31) were measured for a sample prepared with 10 mM of natamycin and 10 mM of HPβCD in 0.6 mL of D_2O. The selective saturation consisted of a train of soft gaussian-shaped pulses of 50 ms duration with a 1 ms interpulse delay. This saturation was applied during 2 s at a specific frequency of the ^{1}H spectrum and covers a region of the spectrum of ± 125 Hz around the chosen frequency (i.e. ± 0.17 ppm in a 750 spectrometer). The STD^{off} saturation was applied at 20 ppm. The STD^{on} saturation was applied at the frequency of one specific aromatic proton signal of natamycin and does not affect any of the signals of the cyclodextrin receptor. The STD^{on} and STD^{off} scans were measured in alternate scans and subtracted by the phase cycling providing the subtracted STD^{off-on} spectrum. Two STD spectra were measured by placing the STD^{on} saturation over a specific signal of natamycin at 6.79, 6.05 and 5.91 ppm corresponding respectively to protons H^3, H^{17}-H^{22} and H^2. Each spectrum was acquired in 15 min with 128 scans and a 6.75 s per scan distributed as 2 s of pre-scan delay d_1, 2 s of STD saturation-time and 2.75 s of FID acquisition time.

A ^{1}H-NMR titration assay was carried out with the one-dimensional ^{1}H spectrum (pulse sequence "zg" of the Bruker library) with 32 scans, a relaxation delay (d_1) of 2 s and a fid (free induction decay) acquisition time (aq) of 2.75 s was measured. The titration study was carried out at a constant concentration of voriconazole and HPβCD of 5.62 and 5.56 mM. The concentrations of natamycin explored during the titration were 0, 1.05, 2.10, 3.15, 4.21, 5.26, 6.31, 7.36, 8.41, 9.46 and 10.51 mM.

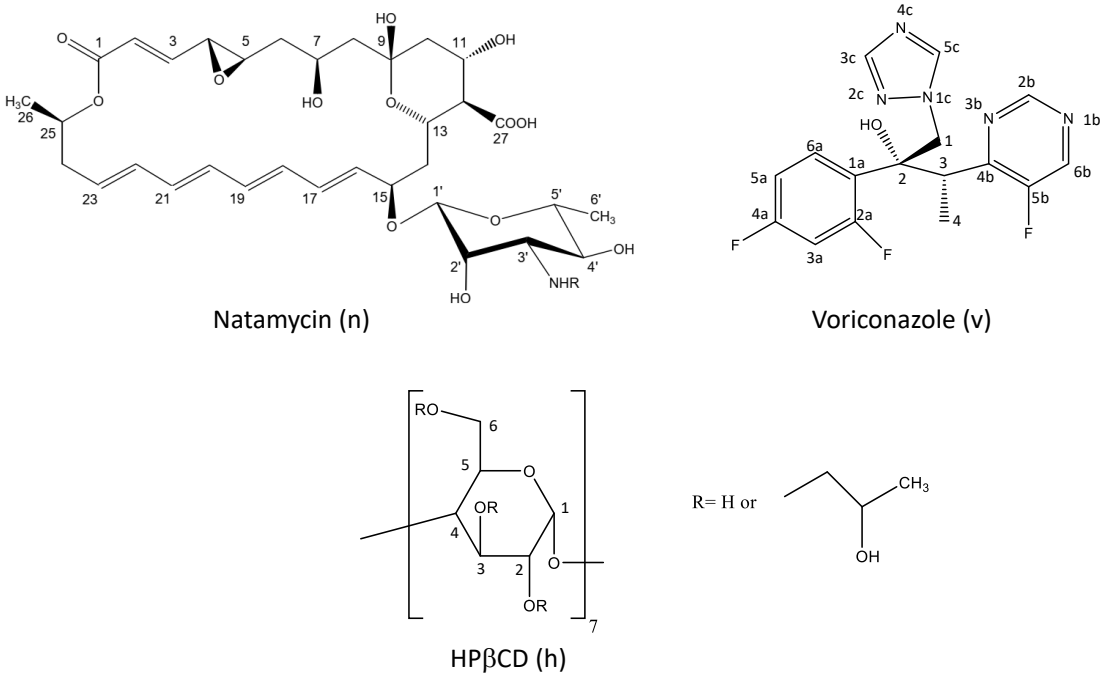

Figure 1. Natamycin (n), voriconazole (v) and HPβCD (h) structures showing the numbering scheme referred in the NMR study.

2.7. PREPARATION OF FORMULATIONS

Based on the results of the previous sections, formulations with 40% (w/v) HPβCD, 1% (w/v) voriconazole and 0.7% (w/v) natamycin were prepared.

The concentration of cyclodextrin (HPβCD) required to solubilize 1% (w/v) of voriconazole was established at 20% (w/v) in previous studies by using voriconazole solubility diagrams (32).

An aqueous solution (SLV) was prepared by adding 40% (w/v) HPβCD to MilliQ® water until completely solubilization Then, 1% (w/v) voriconazole and 0.7% (w/v) natamycin were added to the cyclodextrin solutions and subsequently dispersed by magnetic stirring (200 rpm) at room temperature until complete solubilization.

Two types of hydrogels were prepared with the purpose of increasing the permanence of the formulations on the ocular surface, these being: hyaluronic acid hydrogel (AHNV), and polyvinyl alcohol-based hydrogel (Liquifilm®) (LNV).

Preparation of the hyaluronic acid hydrogel (AHNV)
The AHNV was prepared based on previous studies (33,34). 0.4% (w/v) HA was added to the aqueous solution (SNV) and dispersed by magnetic stirring (200 rpm) at room temperature until complete solubilization.

Preparation of the polyvinyl alcohol-based (Liquifilm®) hydrogel (LNV)
The LNV was prepared based on previous studies where Liquifilm® was chosen as a vehicle for the preparation of a topical ophthalmic formulation of tacrolimus (35). In addition, Liquifilm® is used in ophthalmic pharmaceutical compounding for the preparation of antibacterial eye drops in the hospital pharmacy department (36). 40% (w/v) HPβCD was added to 50% of the final volume of Liquifilm® and dispersed under low-intensity magnetic stirring (50 rpm) until its complete solubilization for 12 h at room temperature to avoid bubble formation. Afterwards, the formulation was made up to the final volume, and 1% (w/v) voriconazole and 0.7% (w/v) natamycin were added under magnetic stirring (200 rpm) until complete dissolution.

2.8. TRANSPARENCY

The transparency of the formulations was measured by recording the transmittance in a wavelength range from 800 to 200 nm, using a spectrophotometer (Agilent® Cary UV 60). The wavelength range includes the infrared light band (780 nm onwards), the visible light (380 to 780 nm) and the ultraviolet light band (100 to 380 nm) (37). Maximum transparency is considered when the transmittance values are 100% in the visible light range. Each formulation was measured in triplicate.

2.9. OSMOLALITY, pH AND VISCOSITY MEASUREMENTS.

Osmolality measurements were taken with a Micro-Osmometer (Fiske® Model 210). The pH was measured using a pH meter (HI5221 HANNA®) at 25±0.5°C. Viscosity was tested with a rotational viscosimeter (Visco QC 300 Anton Paar®) at 25ºC and 20 rpm. Each determination was carried out in triplicate.

2.10. QUANTITATIVE ANALYSIS: ULTRA-HIGH PERFORMANCE LIQUID CHROMATOGRAPHY (UHPLC)

The concentrations of natamycin and voriconazole were determined using a UPLC Waters HClass Plus (Waters, France) with an FTN injector and PDA detector. The column used was a Waters Acquity BEH C18 (2.1 x 50 mm, 1.7µm) thermostated at 25ºC. The mobile phase was acetonitrile:ammonium acetate buffer (30:70 v/v) using a 0.5 mL/min flow rate. The concentration determination was performed at a wavelength of 310 nm for natamycin and a wavelength of 256 nm for voriconazole. The chromatographs were analyzed using the software Empower 3 (Waters®). 10 µl of sample were injected and the retention time was 0.58 s for natamycin and 1.47 s for voriconazole. Calibration curves were constructed and the R^2 values obtained were 0.99 for both drugs.

2.11. *IN VITRO* RELEASE STUDIES

The *in vitro* release study of natamycin and voriconazole from the developed formulations is useful for predicting their *in vivo* performance. Franz diffusion cells were used to determine the release profile. Visking® dialysis membranes (Medicel® membranes Ltd) with a 12-14 KDa cut-off (0.784 cm^2 available surface area) were placed between donor and receptor compartments. 0.5 mL of formulation was added into the donor compartment, while the receptor compartment was filled in with 6 mL of simulated lacrimal fluid (SLF). The composition of SLF was described in a previous publication by Ceulemans et al. (38). The Franz cells were kept thermostated at 37ºC and homogenized by magnetic stirring (200 rpm) in a bath during the assay.

The concentration of both drugs was determined by the UPHLC method previously described (see Ultra-High Performance Liquid Chromatography section). Apparent permeability (Papp) and flux across the membrane were calculated as described in previous studies (32).

2.12. *EX VIVO* CORNEAL PERMEABILITY STUDIES

The *ex vivo* corneal permeability was carried out using fresh bovine eyes obtained from the local slaughterhouse (Compostelana de Carnes S.L., Santiago de Compostela, Spain). The corneas were excised with a scalpel and immediately placed between the Franz cell donor and the receptor compartment with the outer side towards the donor so that the outer part of the cornea was in contact with the formulation. The receptor compartment was filled in with 6 mL of PBS, while 0.5 mL of formulation was placed in the donor chamber. The Franz cells were kept thermostated at 37ºC and homogenized by magnetic stirring (200 rpm) in a bath during the assay. The concentrations of both drugs were determined by the UHPLC method previously described (see Ultra-High Performance Liquid Chromatography section). Apparent permeability (Papp) and flux across the membrane were calculated as described in previous studies (32).

2.13. OCULAR IRRITATION TEST

BCOP and HET-CAM assays were chosen to evaluate the potential irritation produced on the ocular surface. These methods comply with the 3Rs principles (replacement, reduction, and refinement) as described in Directive 2010/63/EU of the European Parliament and of the Council of 22 September 2010 on the protection of animals used for scientific purposes (39).

Bovine Corneal Opacity and Permeability Assay (BCOP)

Corneal Opacity

A variation of the method previously described in the Invittox Protocol nº 437 (40) was carried out to detect potential ocular corrosives and severe irritants using fresh bovine corneas. The assessment of ocular irritation was extensively described in previous studies (32). Opacity (transmitted light (TL)) and corneal transparency (transmittance values) were measured with a luxmeter (Gossen Mavolux 5032C USB) and a spectrophotometer (Agilent® Cari 60 UV) respectively.

First, the two parameters (opacity and transparency) were measured with fresh corneas. Immediately, the corneas were placed in Franz cells as described in the "*Ex vivo* corneal permeability studies" section. Then, the corneas were treated for 60 min by introducing 1 mL of PBS into the donor chamber and both parameters were subsequently measured. Following this period, 1 mL of the formulation was added to the corneas and maintained for 10 min, then the formulation was withdrawn, and 1 mL of PBS was added to the corneas and maintained for 120 min. The previous parameters were measured again. Each formulation was tested in triplicate.

Corneal permeability

The corneas used in the "Corneal Opacity" section were placed back into the Franz cells. The receptor chamber was filled in with 6 mL of PBS, while 1 mL of 0.4% (w/v) fluorescein was placed into the donor chamber. A sample of each Franz cell was collected from the receptor chamber to determine the amount of fluorescein that crossed the treated corneas at 90 min. Fluorescein concentration was measured by a spectrophotometer (Agilent® Cary 60 UV) at a wavelength of 490 nm.

Hen´s Egg Test - Chorioallantoic Membrane (HET-CAM)

HET-CAM is described in The Interagency Coordinating Committee on the Validation of Alternative Methods (ICCVAM) (41). Fertilized broiler chicken eggs were placed in an automatic rotation incubator and kept for 8 days at 38 ± 0.5°C and 65% relative humidity (RH). 24 h before the test, the automatic rotation was stopped and on the 9th day of incubation the test was conducted. Each egg was opened, and the inner membrane was removed. 0.3 mL of formulation, positive control (0.1% (w/v) NaOH solution), or negative control (0.9% (w/v) NaCl solution) were administered onto the surface of the chorioallantoic membrane (CAM). Hemorrhage, vascular lysis, or coagulation reactions were assessed (if applicable) by direct observation of the CAM for 300 s.

2.14. CORNEAL MUCOADHESIVENESS

The corneal mucoadhesiveness method was designed and described in previous studies (32). Fresh bovine corneas were excised and fixed to the upper probe of a Universal Testing Machine (Shimadzu® AGS-X Precision Universal Tester). The formulations were introduced into the weighing bottles. The corneas were immersed 2 mm into the formulations for 30 s and then retired to register the force-displacement curve. The bioadhesion work (J) was calculated from the area under de curve (AUC).

2.15. PET *IN VIVO* ASSAY: QUANTITATIVE OCULAR PERMANENCE STUDY

The ocular permanence of natamycin/voriconazole on the ocular surface was evaluated in Sprague-Dawley rats by a Positron Emission Tomography (PET) and Computed Tomography (CT) combined system (PET/CT Albira® microPET/CT Bruker Biospin, Woodbridge, Connecticut, United States). The procedure was described in previous studies (32,34,35,42). All the animal studies and their protocols were approved by the Galician Network Committee

for Ethics Research in accordance with the Spanish and EU applicable legislation (86/609/CEE, 2003/65/CE, 2010/63/EU, RD 1201/2005 and RD 53/2013). SNV, AHNV, and LNV were radiolabeled with 2-[^{18}F]-fluoro-2-deoxy-D-glucose (^{18}F-FDG). 7.5 µL of formulation containing 0.25 MBq of radioactivity was administrated into each eye of the rat. Immediately, a static PET frame was acquired at 0, 30, 75, 120, 240, and 300 min. Animals were only anesthetized during the image acquisition. Rats were fitted with an Elizabethan collar to prevent them from touching their eyes and removing part of the formulation. ROIs (Regions of interest) were manually obtained from the PET images to obtain the ocular remaining formulation (%) curve. Then, data were corrected considering the radioisotope decay (^{18}F half-life: 109.7 min). Each formulation was evaluated in quadruplicate. The results were analyzed using a non-compartmental model. The area under the curve (AUC $_0^\infty$), terminal half-life ($t_{1/2}$) and mean residence time (MRT) were calculated.

2.16. DISC DIFFUSION METHOD BY THE KIRBY-BAUER METHOD

Candida albicans ATCC 90231 (C.A 90231), *Candida albicans* ATCC 90028 (C.A 90028), *Paelomyces lilacinus* ATCC 90028 (PL), *Aspergillus fumigatus* (AF), *Paelomyces lilacinus* (PL) and *Fusarium solanii* (FS) were used to perform the diffusion disc method. *Aspergillus fumigatus, Paelomyces lilacinus*, and *Fusarium solanii* isolates were obtained at the bank of the University Clinical Hospital of Santiago de Compostela from FK infections. The isolates were morphologically, biochemically, and molecularly characterized prior to testing. Modified Mueller-Hinton plates were inoculated with suspensions of fungal stock (1 x 10^6 – 5 x 10^6 UFC/mL). The inoculated plates were incubated at 35ºC for 24 h. Then, antifungals discs (containing 20 µL of different formulations (Table 2)) were placed on the inoculated plates. The inhibition zone diameters were measured after incubating the plates containing antifungal discs at 35ºC for 24 h for *Candida Albicans* species and 48 h for *Paelomyces* and *Aspergillus* species.

Table 2. Composition of tested formulations in Kirby-Bauer Disc Diffusion Method.

Formulation	Composition
SV	40% (w/v) HPβCD + 1% (w/v) voriconazole
SN	40% HPβCD + 0.7 % (w/v) natamycin
SNV	40% HPβCD+ 0.7 % (w/v) natamycin + 1% (w/v) voriconazole
VFEND	Vfend® (1% (w/v) voriconazole+ 16% (w/v) SBEβCD*)
NTC	Natacyn® (5% (w/v) natamycin)

*Sulfobutyl-ether-β-cyclodextrin

3. RESULTS AND DISCUSSION

3.1. PHASE SOLUBILITY DIAGRAMS

Due to the low water solubility of natamycin (30-50 mg/L (43)), improving its aqueous solubility was essential for the development of new ophthalmic formulations.

Solubility diagrams were created with HPβCD and HPγCD (Figure 2). The cyclodextrins were chosen based on their large size (1135 and 1761 g/mol respectively) and the volume of their cavities. In addition, both have been previously studied for the development of ophthalmic formulations, demonstrating their compatibility with this route (44,45). In addition, the literature prior to these studies has demonstrated the ability of cyclodextrins to reduce ocular irritation, improve corneal permeability, and increase the bioavailability of drugs with very low water solubility (46,47).

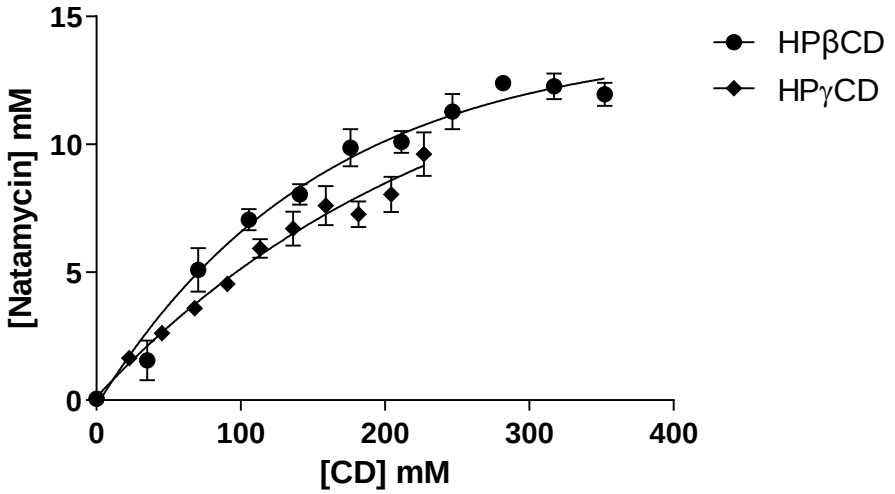

Figure 2. Phase solubility diagrams for natamycin, obtained with 2 different types of cyclodextrin (HPβCD and HPγCD) at 25°C in water (mean ± SD, n=6).

The phase solubility diagrams for natamycin/cyclodextrin inclusion complexes (Figure 2) were A_N type. These data agree with the study of Koontz and Marcy (43). They evaluated the solubility of natamycin with three natural cyclodextrins (αCD, βCD, and γCD) and with HPβCD, a βCD derivative. However, A_N-type phase solubility diagrams occurred only with γCD and HPβCD. In the solubility studies, an initial solubility of 0.0353 ± 0.014 mg/mL was obtained for natamycin without cyclodextrin. Similar values were obtained in Koontz and Marcy's study (0.034 mg/mL) (43).

The A_N-type phase solubility diagram shows the self-association of cyclodextrin aggregates or their complexes, which can decrease the drug solubility (48).

The possible existence of cyclodextrin aggregates or their complexes was evaluated for saturated solutions of natamycin in 40% (w/v) HPβCD solution (Figure 3) and saturated solution of natamycin in 40% (w/v) HPβCD solution and 1% (w/v) voriconazole solution (Figure 3A). The resulting Transmission Electron Microscopy (TEM) images (Figure 3)

showed the formation of nanometric spheric aggregates. The saturated solution of natamycin in 40% (w/v) HPβCD solution showed an average particle size of 80.25 ± 35.81 nm. However, the saturated solution of natamycin in 40% (w/v) HPβCD solution in presence of 1% (w/v) voriconazole showed larger particles with an average particle size of 148.96 ± 32.89 nm.

The cyclodextrin aggregation occurs because of intermolecular hydrogen bonds among cyclodextrin hydroxyl groups (OH). These hydrogen bonds lead to the assembly of the dissolved CD molecules into CD aggregates (49). The resultant nanoparticles, formed by drug/CD complexes, have demonstrated the ability to improve drug permeation across corneal membranes better than the individual inclusion complexes. The CD aggregates can behave in the same way as nanosystems, controlling drug release and increasing residence time at the site of administration. Loftsson and Stefansson (2007) described a system based on dexamethasone/γCD complex aggregates intended for topical ocular administration with sustained delivery and enhanced bioavailability of dexamethasone (50). Other authors have described similar results for drugs like dorzolamide (51), irbesartan (52), or cyclosporin A (53), among others.

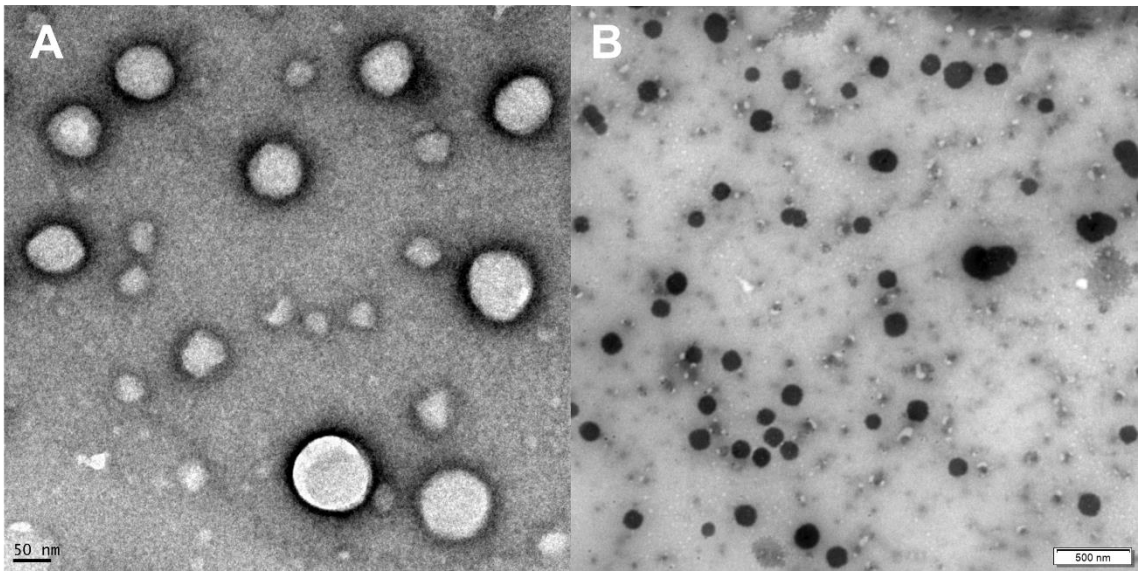

Figure 3. Transmission Electron Microscopy (TEM) images of saturated solution of A) natamycin in 40% (w/v) HPβCD solution and 1% (w/v) voriconazole solution and B) saturated solution of natamycin in 40% (w/v) HPβCD solution.

Table 3 shows the apparent stability constant ($K_{1:1}$), complexation efficiency (CE), natamycin:cyclodextrin complex molar ratio (D:CD), coefficient of determination (R^2), and water natamycin solubility S_0.

$K_{1:1}$ was calculated on the linear portion of the phase diagram due to the negative deviation previously shown (54). The HPβCD showed a higher $K_{1:1}$ than HPγCD, suggesting that the natamycin/HPβCD interactions were stronger than those of natamycin/HPγCD. Furthermore, HPβCD obtained the best solubilization properties for the natamycin and showed higher CE values than HPγCD (0.061 and 0.049, respectively). D:CD values were high for both

cyclodextrins (1:17.50 and 1:21.41, respectively), but HPβCD showed the lowest value, so its bioavailability would be better than that of HPγCD (55).

Table 3. Values for $K_{1:1}$, CE, and the D:CD ratio, obtained from the natamicyn/cyclodextrin complex in water at 25°C.

Inclusion Complex	R^2	$K_{1:1}$ (M^{-1})*	CE (M)	S_0 (M)	D:CD (mol:mol)
Natamycin/HPβCD	0.9717	1102.32 ± 89.09	0.061	$5.50 \cdot 10\text{-}5 \pm 2.06 \cdot 10^{-5}$	1:17.50
Natamycin/HPγCD	0.9943	891.08 ± 26.39	0.049	$5.50 \cdot 10\text{-}5 \pm 2.06 \cdot 10^{-5}$	1:21.41

*$K_{1:1}$ calculated using S_0 (free drug solubility)

3.2. NATAMYCIN SOLUBILITY WITH HPβCD AND DIFFERENT HYDROPHILIC POLYMERS

The drug solubility in presence of hydrophilic polymers can be enhanced by ternary complexation (56). Natamycin solubility with 20% (w/v) HPβCD and different hydrophilic polymers is shown in Table 4. Data were compared with natamycin solubility in absence of polymers. These data do not show significant differences in natamycin solubility when the hydrophilic polymers were added to the system.

Table 4. Natamycin concentration in presence of 20% (w/v) HPβCD and different hydrophilic polymers.

HPβCD and Polymers solutions	Natamycin concentration (mg/mL)
20% HPβCD	5.151 ± 0.206
20% HPβCD + 0.5% PVA	5.740 ± 0.867
20% HPβCD + 1% PVA	5.117 ± 0.484
20% HPβCD + 0.4% AH	4.625 ± 0.464
20% HPβCD + 0.1% P407	4.222 ± 0.574
20% HPβCD + 0.5% MC	4.181± 0.309

3.3. NATAMYCIN AND VORICONAZOLE SOLUBILITY WITH HPβCD AND VORICONAZOLE

Figure 4a shows the natamycin concentration reached with 20%, 30%, and 40% (w/v) of HPβCD and 1% (w/v) of voriconazole. The voriconazole concentration remained stable in all HPβCD solutions. Natamycin concentration increased from 6.175 ± 0.658 to 7.951 ± 0.389 mg/mL with increasing HPβCD concentration. These data agree with the data obtained by interpolation in the phase diagram (Table 5). Figure 3B shows the voriconazole concentration reached with 20%, 30%, and 40% (w/v) of HPβCD and 0.4% (w/v) of natamycin. Voriconazole concentrations obtained in presence of 0.4% (w/v) natamycin and 20%, 30%, and 40% (w/v) of HPβCD were 12.43 ± 4.71, 15.937 ± 5.05 and 25.04 ± 1.44 mg/mL respectively. The concentrations of voriconazole obtained in the presence of natamycin are similar to those obtained without natamycin in previous studies (32) (see Table 5).

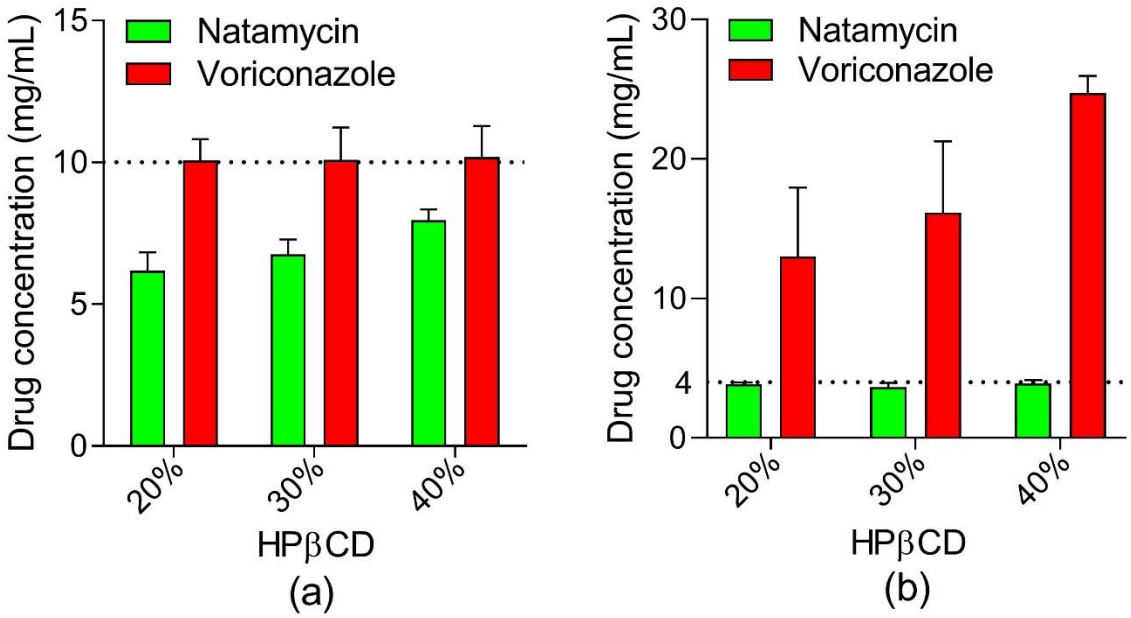

Figure 4. a) Voriconazole concentration obtained in presence of 4 mg/mL of natamycin and different concentrations of HPβCD. b) Natamycin concentration obtained in presence of 10 mg/mL of voriconazole and different concentrations of HPβCD.

Table 5. Concentration of natamycin and voriconazole in HPβCD solutions obtained from interpolation in the phase diagrams (Figure 2). The HPβCD phase diagram of voriconazole was published in previous studies (32).

	Natamycin (mg/mL)	**Voriconazole (mg/mL)**
20% HPβCD (w/v)	6.351	15.203
30% HPβCD (w/v)	7.639	22.252
40% HPβCD (w/v)	8.372	29.301

These results suggest that the incorporation of natamycin into the voriconazole/HPβCD complexes solution does not affect the solubility of voriconazole in presence of cyclodextrin. To clarify this statement, a competition study of the two drugs for cyclodextrin was performed using Nuclear Magnetic Resonance (NMR).

3.4. NUCLEAR MAGNETIC RESONANCE (NMR) STUDIES

Molecular interactions are essential for many biological processes. The binding process is promoted by the establishment of a number of favorable non-covalent forces between the molecule that interact and there is a dynamic equilibrium between association and dissociation events. NMR is one of the methods for screening of ligands that bind to a receptor and detect the ligand binding epitope and/or receptor binding site with quantitative results (57,58).

3.4.1. DETECTION OF BINDING INTERACTION BETWEEN NATAMYCIN AND HPβCD

The ^{1}H-NMR signal assignment of natamycin in CD_3OD was obtained from the ^{1}H and ^{13}C predicted spectrum at 800 MHz in the Human Metabolomic Database (59,60) in concordance with the experimental 2D edited-HSQC spectrum obtained by us in Figure 5.

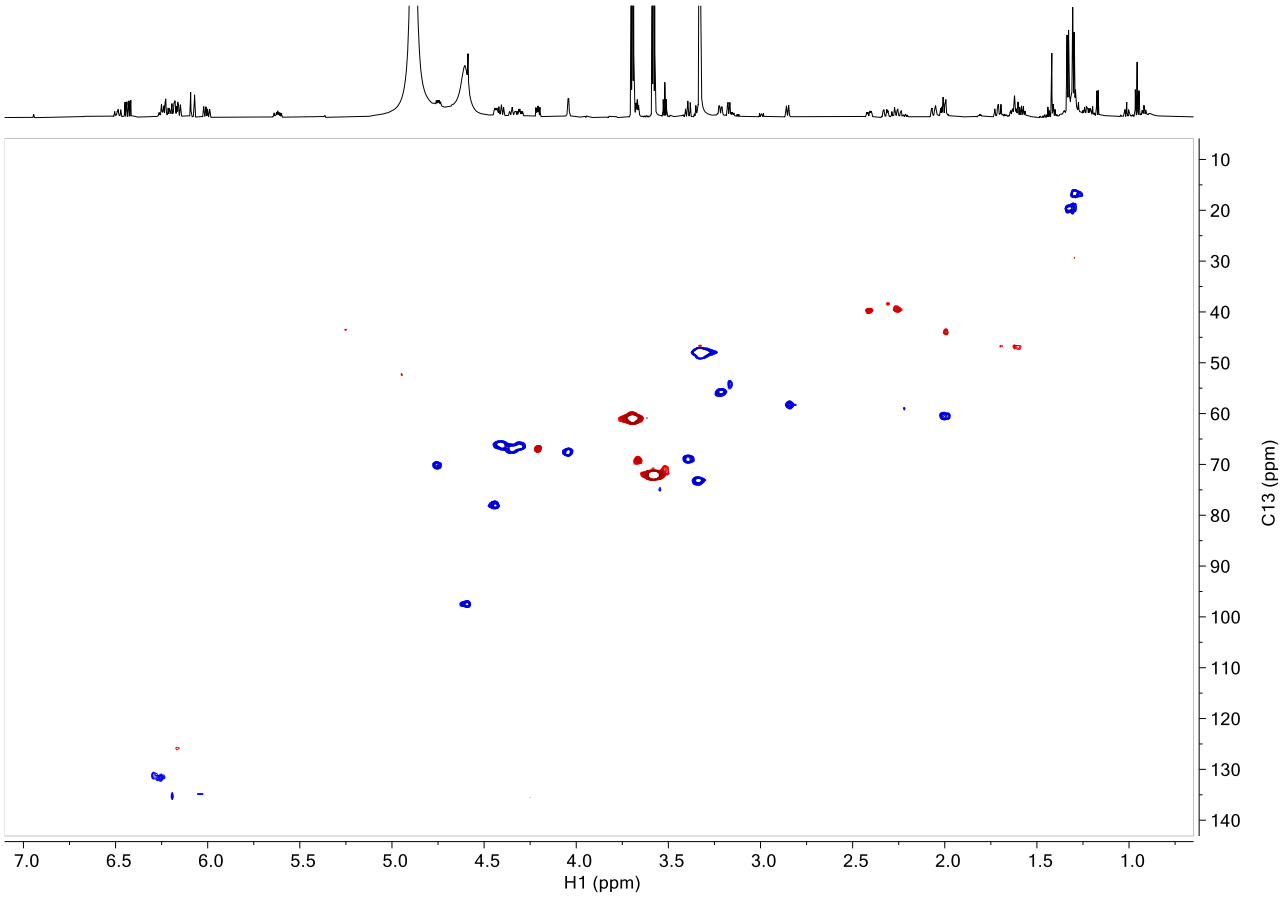

Figure 5. 2D edited-HSQC spectrum of pure natamycin in CD_3OD. Peaks in blue color correspond to CH and CH_3 groups. Peaks in red color correspond to CH_2 groups. The ^{1}H spectrum is shown in the horizontal trace.

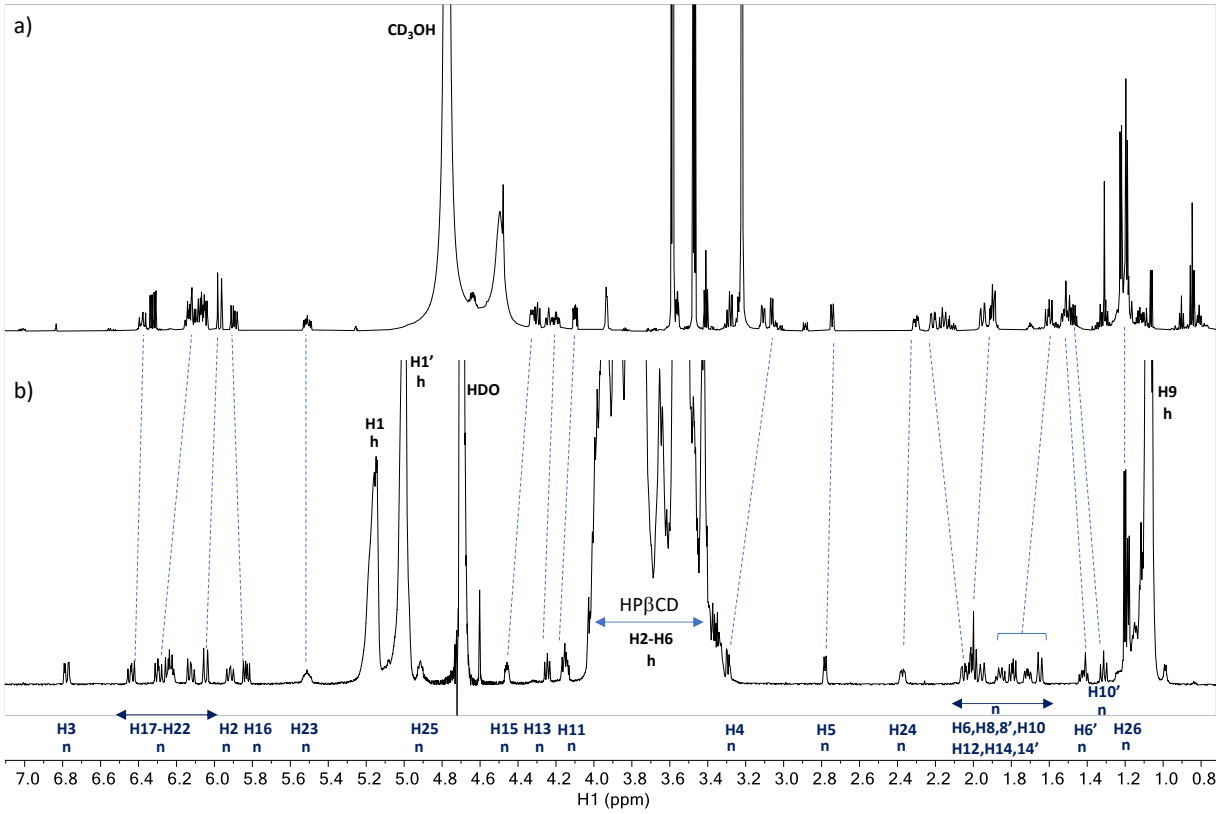

Figure 6. ^{1}H-NMR spectra of a) pure natamycin in MeOD. b) the mixture natamycin:HPβCD 10mM:10mM in D_2O. The atom numbering used to identify natamycin (n) and HPβCD (h) follows Figure 1. Stripped lines were drawn to guide the eye to the changes in chemical shift (i.e. CSPs) of the signals of n. Signal H23 n was chosen as a reference for the CSPs.

The comparison of the ^{1}H spectrum of pure natamycin in CD_3OD and the mixture natamycin:HPβCD 1:1 in D_2O denotes relevant changes in the chemical shifts (i.e. CSPs) that could be due to either a change in the conformation due to the solvent and/or its binding to HPβCD. To further investigate the possibility of binding interaction between ligand natamycin and receptor HPβCD *in water solution* was tested by STD experiments (30,31). The STD^{off} reference ^{1}H spectrum of the mixture natamycin:HPβCD 1:1 is shown in Figure 7a. STD$^{on\text{-}off}$ spectra were measured to determine possible intermolecular contacts between the ligand and receptor in the mixture. A requisite for the STD$^{off\text{-}on}$ experiment is that the on-saturation should only affect the signal/s of one of the two components in the mixture. In this case, placing the on-saturation in the region where the ^{1}H spectrum the majority of the protons of HPβCD appear in the ^{1}H spectrum between 3.2 and 4.6 ppm should be avoided because in this region there a few signals of natamycin are also present (Figure 5). For this reason, the on-saturation was placed over specific aromatic signal/s of the ligand natamycin that are well isolated in the ^{1}H spectrum. The STD$^{on\text{-}off}$ spectra (Figure 7a to Figure 7d) show the STD responses; some of them are intramolecular NOE contacts in natamycin while those that appear well extended and with broad features in the region between 3.2 and 4.6 ppm were assigned to HPβCD. This result confirms that there is binding affinity between natamycin and HPβCD.

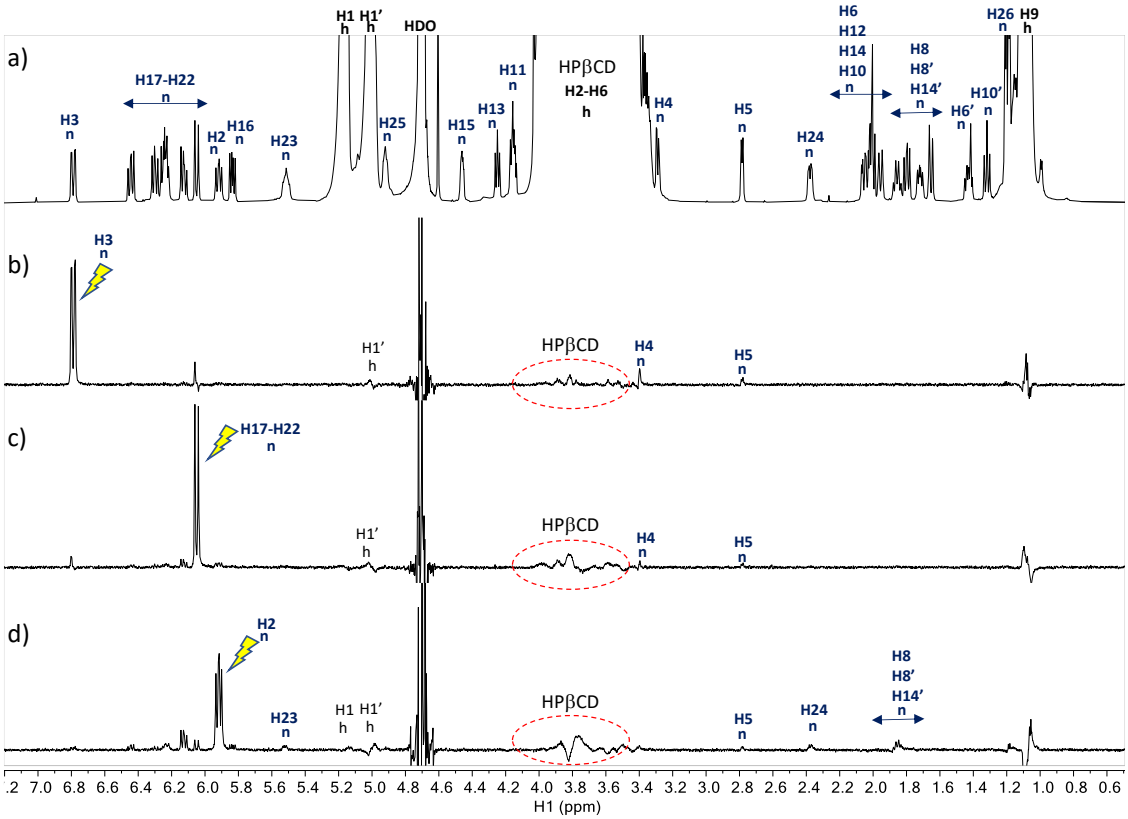

Figure 7. NMR spectra of natamycin:HPβCD 1:1 in D_2O showing the assignment of signals of natamycin (n) and HPβCD (h). a) ^1H reference spectrum. b) $STD^{off\text{-}on}$ spectrum with on-saturation at 6.79 ppm (H-3 signal of n). c) $STD^{off\text{-}on}$ with on-saturation at 6.05 ppm (H-17 to H-22 signal of n). d) $STD^{off\text{-}on}$ with on-saturation at 5.91 ppm (H-2 signal of n). The atom numbering used to identify the signals of voriconazole follows Figure 1.

3.4.2. NMR TITRATION COMPETITION STUDY OF NATAMYCIN AND VORICONAZOLE FOR BINDING TO HPβCD

Having established the affinity between natamycin and HPβCD, the binding affinity of natamycin was tested in a competition experiment with the ligand voriconazole in water. The affinity of this later ligand for HPβCD was tested in our laboratory and showed the formation of an inclusion complex of stoichiometry 1:1 with a dissociation constant K_D of 250 mM (32). Under conditions of weak binding equilibrium of a ligand to a receptor (typically for K_D in the 1 to 1000 mM range), a chemical shift titration is a feasible method to map a ligand-binding site on a target receptor such as a protein (58) or a cyclodextrin (61) and may serve to estimate the K_D of the equilibrium. The basis of this method under weak binding there is a fast exchange equilibrium between the free and bound species in the NMR time scale, and the observed chemical shift d^{obs} is a weighted average given by Eq. 1 (57):

$$d^{obs} = c^{free} \cdot d^{free} + c^{bound} \cdot d^{bound} \quad \text{(Eq. 1)}$$

where d^{free} and d^{bound} are the chemical shifts in the free and bound state, respectively, and c^{free} and c^{bound} are the molar fraction of the species in the free and bound state respectively with c^{free}

+ c^{bound} = 1. Chemical Shift Perturbations (CSPs) can be quantified as d^{obs} - d^{free} (in units of Hz) for any signal in the spectrum at any point in the titration to map the ligand-binding site.

The ^{1}H-NMR spectra of the titration competition assay for the mixtures prepared of natamycin, voriconazole, and HPβCD are shown in Figure 8. The experiment was carried out by the addition of natamycin to a sample containing equimolar concentrations of voriconazole and HPβCD. It can be seen in Figure 8 that in the course of the titration certain signals of voriconazole have CSPs, while all the signals of natamycin remain at the same chemical shift and only increase their intensity. Qualitatively, this observation strongly suggests that natamycin competes for the same binding site of HPβCD and has a stronger affinity than voriconazole because as the concentration of natamycin is raised in the titration the signals of voriconazole move towards their characteristic values in the free state d^{free} which can be explained by a higher molar fraction c^{free} in Eq. 1. In Table 6 are given the CSPs of several signals of voriconazole in this competition assay. The data was fit to a competitive binding model (described in supplementary calculations) and provided a K_I=0.334 mM which is a value that represents ca. 700 times higher affinity of natamycin than voriconazole for binding to HPβCD. In our previous work, the molecular model of the complex HPβCD:voriconazole (32) showed that voriconazole can be inserted almost completely in the cavity of HPβCD. Natamycin is a larger molecule than voriconazole and can only be incorporated partially inside the cavity of HPβCD as can be seen in the optimized molecular mechanics optimized model of Figure 9. In this model, the double bonds of natamycin are disposed towards the most hydrophobic side of HPβCD in proximity to the hydroxypropyl pendant chains and the two polar six-member rings of natamycin disposed towards the most hydrophilic side of HPβCD.

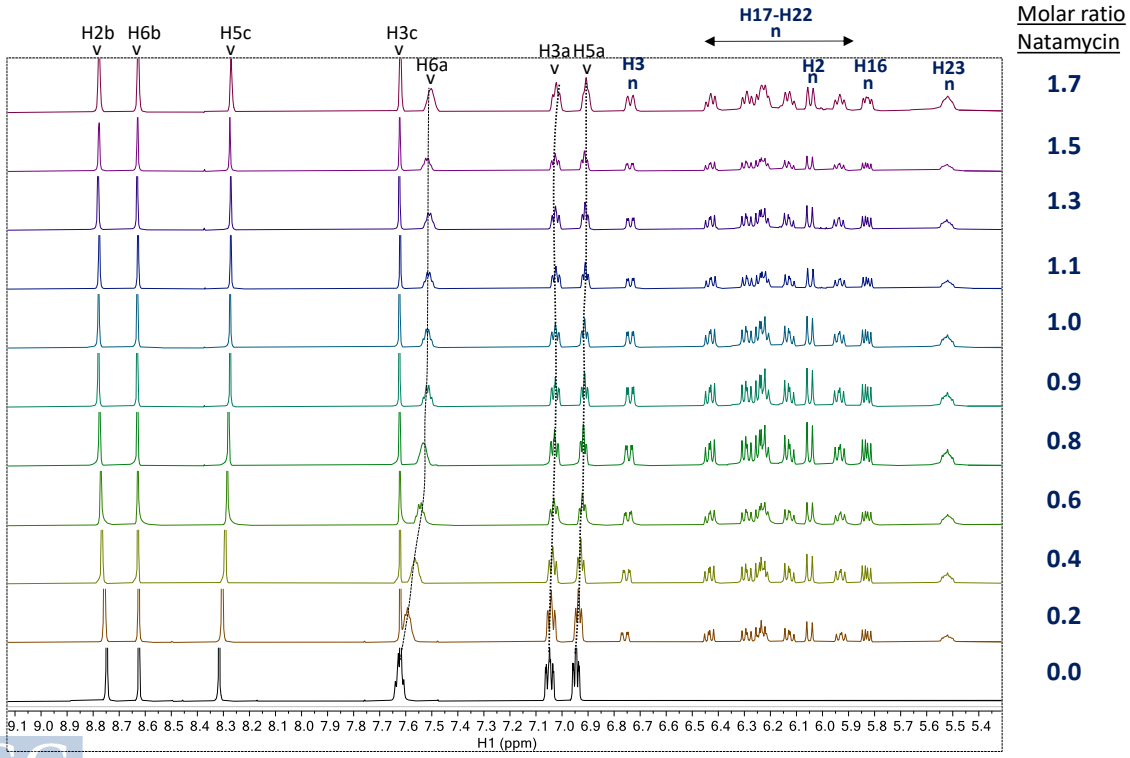

Figure 8. NMR titration competition assay with natamycin at a constant molar ratio voriconazole:HPβCD 1:1. Stack of spectra showing the aromatic region of the ^{1}H-NMR spectrum during

the titration. The atom numbering used to identify voriconazole (v) and natamycin (n) follows Figure 1. Stripped lines were drawn to guide the eye for the changes in chemical shift (i.e. CSPs) of certain signals of v.

Table 6. Signals of voriconazole with relevant CSPs measured by ^{1}H-NMR during the titration competition assay with natamycin at constant molar ratio voriconazole:HPβCD 1:1.

Equivalents Natamycin	H6a CSP (Hz)	H3a CSP (Hz)	H5a CSP (Hz)	H1 CSP (Hz)
0.0	89	32	30	51
0.2	61	26	23	39
0.4	40	22	15	25
0.6	29	19	11	16
0.8	22	17	8	11
0.9	8	15	5	5
1.1	8	14	4	4
1.3	5	14	2	4
1.5	3	14	2	4
1.7	0	12	3	2
1.9	0	0	0	0

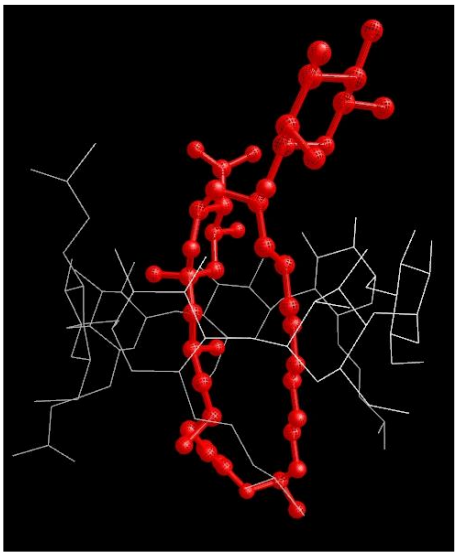

Figure 9. Molecular Mechanics optimized model of the complex natamycin with HPβCD (red balls and sticks indicate natamycin; white lines indicate HPβCD).

3.5. TRANSPARENCY

One of the problems that usually leads to a discontinuation of the FK treatment is the number of required instillations (1 drop every 1-2 h). In addition, some eye drops may cause blurred vision due to their organoleptic or physicochemical characteristics (e.g., color, high viscosity, among other factors), increasing the treatment dropout. Natacyn® is a cloudy white to yellow aqueous suspension containing natamycin particles that can cause blurred vision after administration. For this reason, transparency measurements were carried out.

Natacyn® showed transmittance values close to 0 in all light ranges. The results obtained from transparency measurements are shown in Figure 10. All formulations (SLV, AHNL, and LNV) were practically transparent (transmittance ≃ 100%) in the infrared (780 nm onwards) and visible light range (from 380 to 780 nm). The decrease in transmittance values in the UV range for all the formulations was possibly associated with the presence of molecules that absorb in the UV range, such as natamycin 310 nm or voriconazole 256 nm.

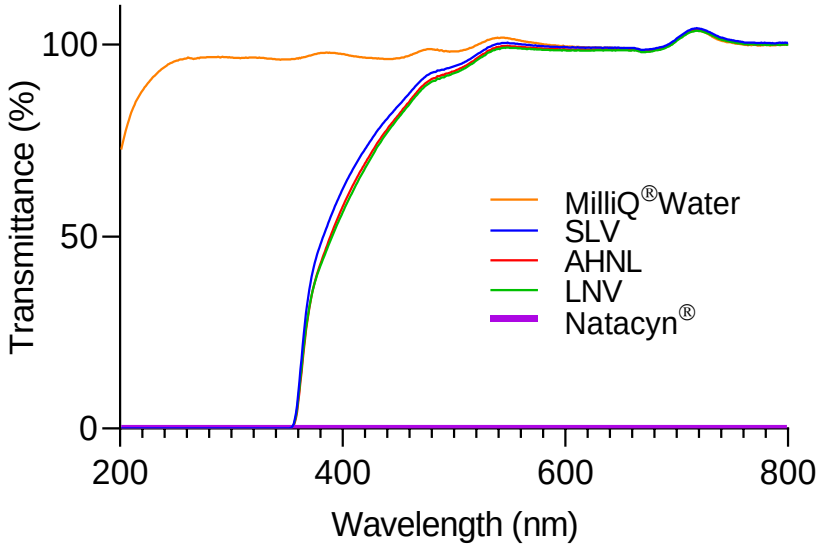

Figure 10. Scan light transmittance from 200 to 800 nm for the formulations including natamycin. MilliQ® water was used as a transparent formulation in all light ranges.

3.6. OSMOLALITY AND PH MEASUREMENTS

Table 7 shows the pH, osmolality, and viscosity data of the ocular formulations. The viscosity of AHNV (265.5±37.56 mPa·s) is higher than the viscosity obtained for LNV (54.292±2.88). The viscosity data for Liquifilm® were 5.827±0.284 mPa·s.

The osmolality data obtained for SNV and AHNV were lower than the osmolality data for Liquifilm® formulation (LNV). The high osmolality value of LNV (500 ± 3.46 mOsm/kg) is due to the osmolality values of the Liquifilm® vehicle (256.5 ± 8 mOsm/kg (62)) used to formulate the LNV formulation. The osmolality values of all formulations are higher than the physiological value (290 mOsm/kg), however, in an *in vivo* system, the high precorneal clearance would protect the ocular surface from hyperosmolality by removing the formulation from the corneal surface (63,64).

The new formulations (SNV, AHNV, and LNV) showed pH values within the tolerable range of the eye (pH range 4 to 8) (46).

Table 7. pH, osmolality, and viscosity results.

Formulation	pH	Osmolality (mOsm / kg)	Viscosity (mPa·s)
SNV	6.10±0.16	304 ± 3.46	9.853±0.326
AHNV	6.34±0.08	344 ± 3.46	265.5±37.56
LNV	7.09±0.02	500 ± 3.46	54.29±2.880

3.7. *IN VITRO* RELEASE STUDIES

The *in vitro* release profile of the resulting formulations is shown in Figure 11. Papp (cm/s), flux (µg/min), and R^2 are shown in Table 8. All profiles were fitted to a Korsmeyer-Peppas model, and the R^2 values were > 0.96 for all tested formulations. The resulting n values show that both drugs are released by a Fickian diffusion process ($n \leq 0.45$) from all the formulations (SNV, AHNV, and LNV), while natamycin in the Natacyn® formulation presents an anomalous diffusion mechanism ($0.45 < n > 0.89$) (65). However, this value of n for Natacyn® (0.629) is due to the compensation of the amount of natamycin that diffuses with the amount of natamycin that dissolves from the solid particles of the suspension in the diffusion process.

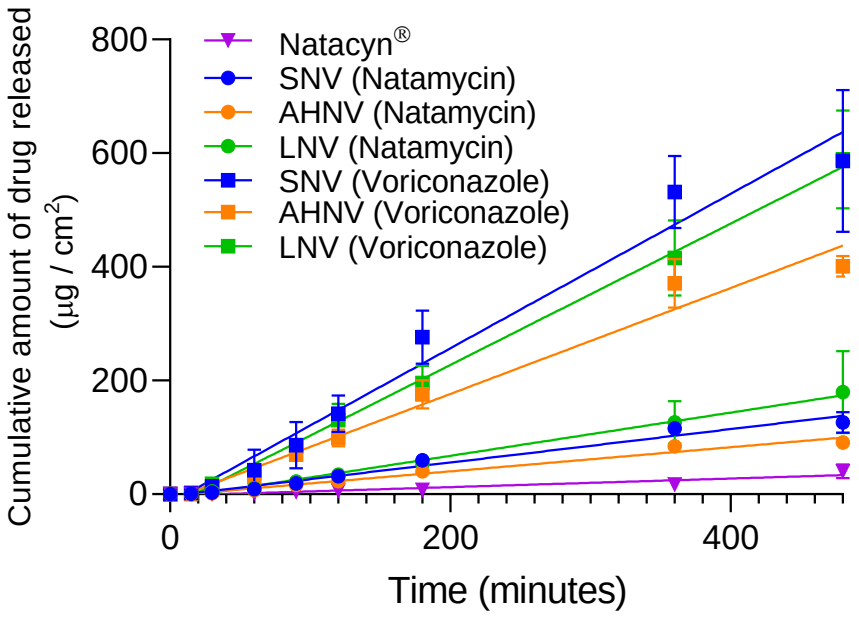

Figure 11. *In vitro* release profiles of natamycin/voriconazole formulations. All data were fitted to Korsmeyer-Peppas model.

With respect to Natacyn®, the natamycin particles must be dissolved in the medium to diffuse through the dialysis membrane, unlike the newly developed formulations in which the natamycin was already dissolved. For this reason, Natacyn® Papp values ($0.05 \cdot 10^{-06}$ cm/s) were lower than SNV, HAV, and LNV release values ($1.398 \cdot 10^{-06}$, $1.010 \cdot 10^{-06}$, and $1.810 \cdot 10^{-06}$ cm/s respectively).

Table 8. *In vitro* release data from natamycin/voriconazole formulations.

Formulation	P_{app} (cm/s)	SE · 10^{-7}	Flux (µg/min)	SE	R^2	n
SNV Natamycin	$1.398 \cdot 10^{-6}$	$0.8663 \cdot 10^{-7}$	0.293	0.018	0.981	0.163
HAV Natamycin	$1.010 \cdot 10^{-6}$	$0.5985 \cdot 10^{-7}$	0.212	0.012	0.965	0.194
LNV Natamycin	$1.810 \cdot 10^{-6}$	$0.8780 \cdot 10^{-7}$	0.380	0.018	0.998	0.053
Natacyn®	$0.050 \cdot 10^{-6}$	$0.0612 \cdot 10^{-7}$	0.075	0.009	0.971	0.629
SNV Voriconazole	$4.52 \cdot 10^{-6}$	$2.722 \cdot 10^{-7}$	1.358	0.081	0.981	0.163
HANV Voriconazole	$3.110 \cdot 10^{-6}$	$1.800 \cdot 10^{-7}$	0.931	0.053	0.982	0.160
LNV Voriconazole	$4.145 \cdot 10^{-6}$	$1.606 \cdot 10^{-07}$	1.243	0.048	0.998	0.064

3.8. *EX VIVO* CORNEAL PERMEABILITY STUDIES

The fungal infection, which usually occurs on the corneal surface, reaches the internal ocular structures such as the aqueous or vitreous humor, causing endophthalmitis. The corneal epithelium consists of a cell layer bound by tight junctions that resist the permeability of large drug molecules like natamycin (molecular weight of 665.75 g/mol), preventing them from reaching the internal structures of the eye. For this reason, it is common in clinical practice to carry out corneal scrapings to remove the epithelium and, thus, favor the penetration of drugs. Overall, the infections usually lead to the epithelium breakdown (66). The corneal permeability of the developed formulations (SNV, HAV, and LNV) and Natacyn® was studied to know the natamycin and voriconazole capacity to go through the corneal structure with and without corneal epithelium.

The corneal permeation data for the epithelized and de-epithelized bovine corneas are presented in Figure 12. Apparent permeability (Papp), flux, and lag time data were calculated for both studies and are represented in Figure 13.

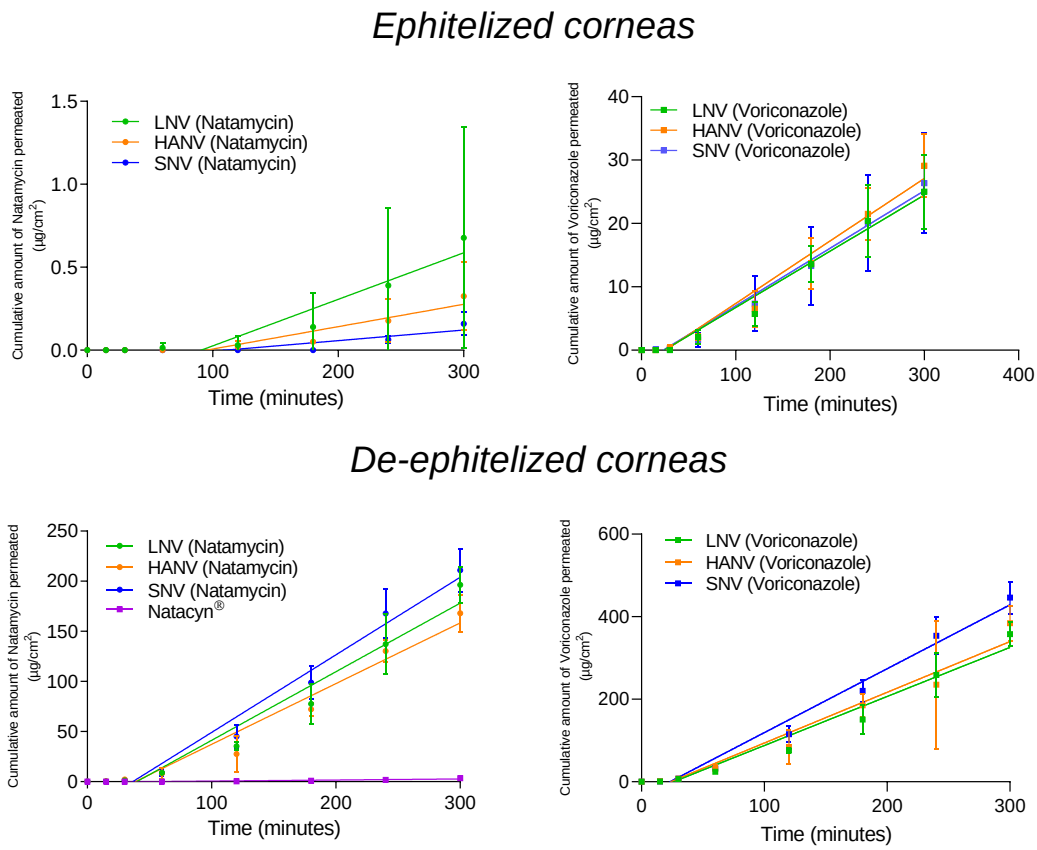

Figure 12. Cumulative amount of drug permeated (µg/cm^2) through epithelized bovine and de-epithelized corneas for natamycin (left) and voriconazole (right).

Natamycin and voriconazole Papp values were higher in absence of corneal epithelium than in presence of corneal epithelium (see data details in Figure 13 (a)(b)). Natacyn® did not show natamycin permeability in presence of corneal epithelium but it was improved in de-epithelized corneas ($7.17 \cdot 10^{-9} \pm 8.90 \cdot 10^{-9}$ cm^2/s). Other authors, such as O'Day et al. (67), also described an improvement in the passage of natamycin when the corneal epithelium was removed.

The administration of natamycin solubilized with HPβCD (In SNV; AHNV and LNV formulations) improved the passage of natamycin in presence of corneal epithelium. This may be because cyclodextrins decrease the resistance of the aqueous layer exerted by the tear and the ocular mucosa. Also, cyclodextrins enhance the passage across the cornea by the extraction of cholesterol from the corneal epithelium (68). Lorenzo Veiga et al. (69) developed a natamycin micelle formulation in which the values of the cumulative amount of permeated natamycin were below 0.01 µg/cm^2 at 5 h of permeation in epithelized corneas. The quantities of natamycin permeated with SNV, AHNV, and LNV were 0.15 ± 0.06, 0.37 ± 0.20, and 0.67 ± 0.66 µg/cm^2 respectively at 5 h of permeation in epithelized corneas.

The values obtained for voriconazole showed, both in the presence and absence of epithelium, better Papp and flux values than natamycin in the presence of corneal epithelium (Figure 13(a)(b)(c)(d)).

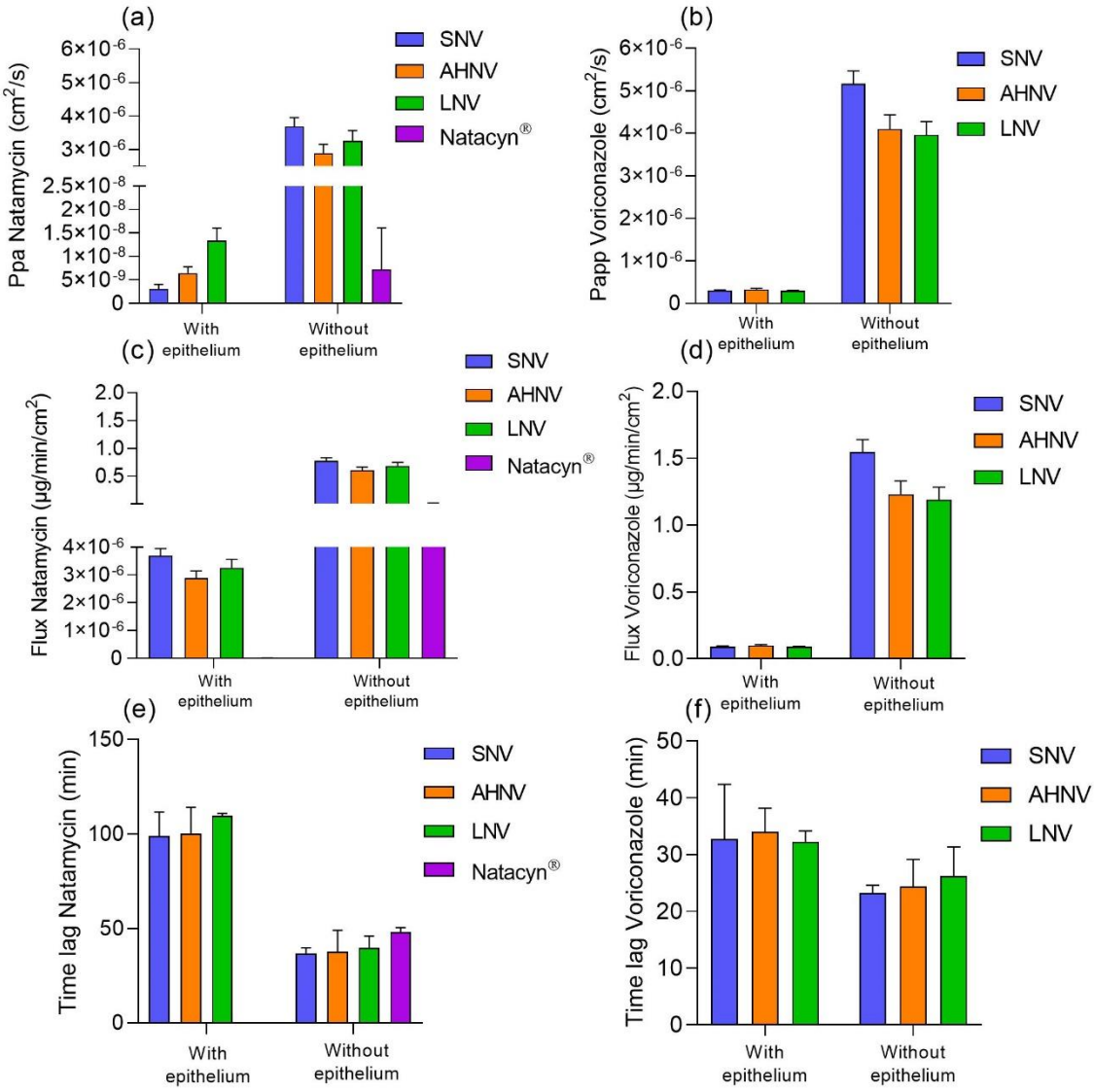

Figure 13. (a) Apparent permeability (Papp) of natamycin, (b) apparent permeability (Papp) of voriconazole, (c) flux of natamycin, (d) flux of voriconazole, (e) lag time of natamycin and (f) lag time of voriconazole of natamycin and voriconazole formulations across epithelized and de-epithelized bovine corneas. *Natacyn® permeability values are not shown because there was no permeability of natamycin from this formulation.

In addition, in the presence of epithelium, the lag time values show that voriconazole takes less time to cross the cornea than natamycin (see data details in Figure 13 (e)(f)). However, in absence of epithelium the time lag data (see data details in Figure 13 (e)), decreased considerably for natamycin (SNV 36.77 ± 3.028, AHNV 37.85 ± 11.22, and LNV 39.87 ± 6.144 min) with an average of 38.49 ± 1.19 min instead of 102.98±5.81 min with corneal epithelium. Permeability, flux, and lag time data show that the limiting step in the penetration of natamycin through the cornea is mainly the passage through the corneal epithelium.

3.9. OCULAR IRRITATION TEST

Bovine Corneal Opacity and Permeability Assay (BCOP)

BCOP data (Figure 14) showed that there were no significant modifications in transparency and opacity after treating the bovine corneas with SNV, AHNV, and LNV for 10 min. ANOVA test showed no significant differences between C- (PBS) and all formulations tested.

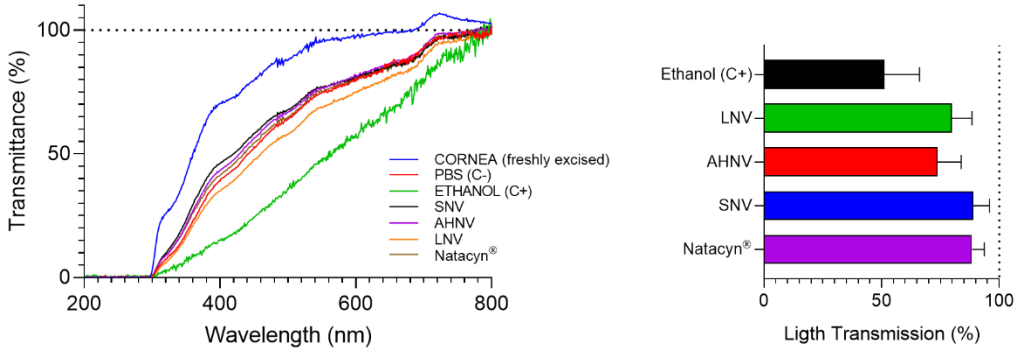

Figure 14. Left: Transmittance values in the ultra-visible light spectrum (200-800 nm) of bovine corneas treated 10 min with SNV, AHNV, and LNV. Values are compared with ethanol (C+: positive control), PBS (C-: negative control), and untreated corneas. Right: Transmitted light (%) (opacity) values of bovine corneas treated with SNV, AHNV, and LNV. Data were compared with ethanol (C+: positive control).

The data obtained in the corneal permeability test showed no passage of fluorescein and therefore the tested formulations did not modify corneal permeability, maintaining the integrity of the cornea.

Hen´s Egg Test - Chorioallantoic Membrane (HET-CAM)

Natamycin-voriconazole formulations (SNV, AHNV, and LNV) were tested on the egg's chorioallantoic membrane (Figure 15). None of the formulations showed vessel modifications (hemorrhage, lysis, or coagulation at 5 min) compared to a NaOH solution (positive control). Consequently, all formulations can be considered non-ocular irritants.

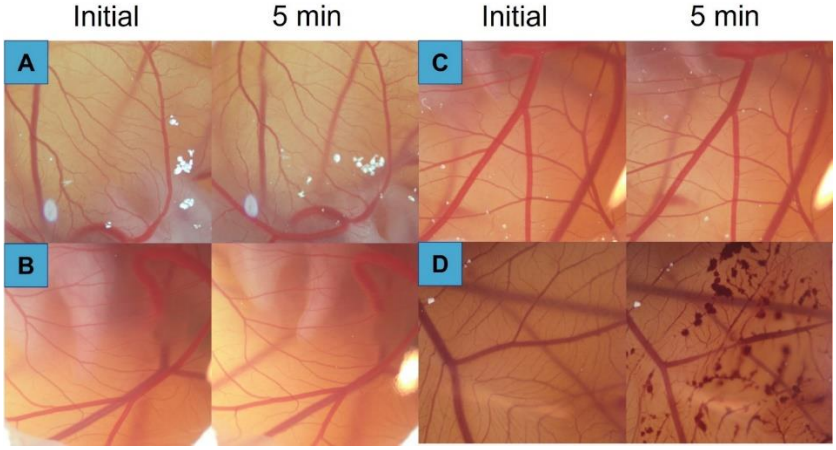

Figure 15. 5 min post-instillation images of Hen´s egg test on the chorioallantoic membrane (HET-CAM) for different natamycin-voriconazole formulations. A) SNV B) AHNV C) LNV D) NaOH 0.1M.

The data obtained in the two irritation tests concluded that none of the tested formulations were irritating and that they did not produce changes in corneal structure or transparency.

3.10. CORNEAL MUCOADHESIVENESS

The study of the mucoadhesive properties of the topical ophthalmic formulations can predict the prolonged permanence on the ocular surface improving the effectiveness of the treatment. The bioadhesion work for all formulations is represented in Figure 16.

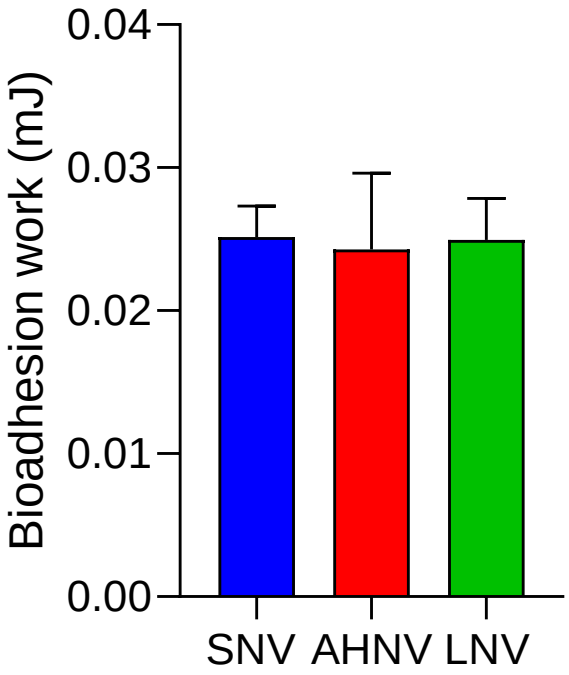

Figure 16. Bioadhesive work obtained for SNV, AHNV, and LNV in bovine corneas.

All formulations showed similar values of bioadhesion work (mJ) (SNV: 0.0251 ± 0.002 mJ, AHNV: 0.0242 ± 0.005 mJ, LNV: 0.0249 ± 0.002 mJ). These results can be explained because, during the traction stage of the assay, the bond between the cornea and the formulation is broken within the formulation itself, not at the corneal surface. As all the formulations are low-viscosity systems, the interaction between the vehicle molecules is low, and therefore lower than the bioadhesive forces between the cornea and the formulation itself. A one-way ANOVA test was performed, and no significant differences were found in the bioadhesion work data for SNV, AHNV, and LNV. For this reason, an *in vivo* permanence study was carried out by PET to quantify the amount of formulation that remains on the ocular surface over time.

3.11. PET *IN VIVO* ASSAY: QUANTITATIVE OCULAR PERMANENCE STUDY

An eye drop formulation with low ocular permanence cannot ensure the necessary time for the drug to diffuse through the corneal tissue. A PET *in vivo* assay was carried out to quantify the amount of formulation remaining on the ocular surface over time.

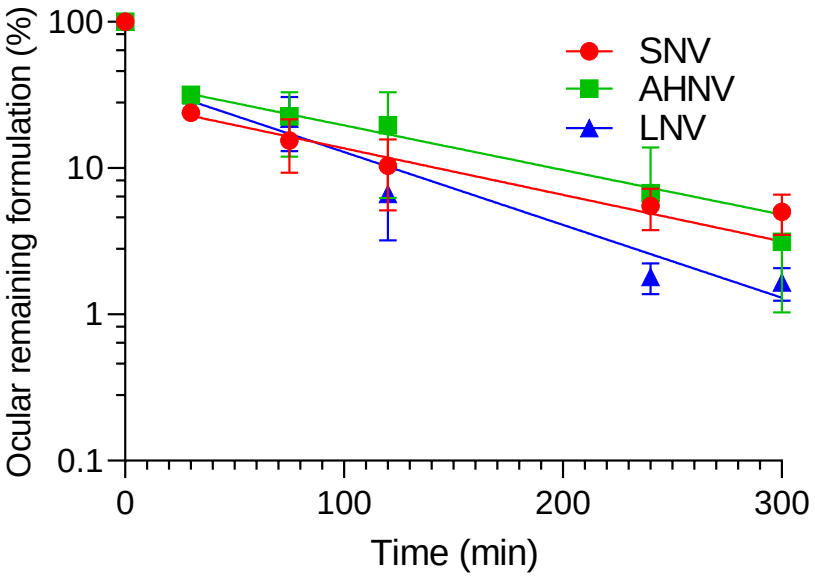

Figure 17. SNV, AHNV and LNV clearance ratio from the ocular surface determination by PET. Ratio $CT/C_{initial}$ was calculated assuming $C_{initial}$ value obtained in the Regions of Interest (ROI).

The semi-logarithmic plot (Figure 17) shows the data of the clearance rate of the formulations as a function of the remaining radioactivity in the eye. Table 10 shows the pharmacokinetic parameters (elimination constant *K*, $t_{1/2}$, AUC_{0}^{∞}, and MRT) obtained by fitting the formulation percentage remaining in the eye over time.

Table 10. Pharmacokinetic parameters (*K*, $t_{1/2}$, AUC_{0}^{∞}, and MRT) obtained by fitting the formulation percentage remaining in the eye over time by PET imaging.

Formulations	***K*** **(min^{-1})**		**$t_{1/2}$** **(min)**		**AUC_{0}^{∞}** **(%*min)**		**MRT** **(min)**		**R^2**	**Remaining Formulation at 75 min (%)**	
	Mean	SD	Mean	SD	Mean	SD	Mean	SD		Mean	SD
SNV	0.010	0.007	12.02	2.23	46.77	8.19	68.47	4.45	0.96	15.42	6.107
AHNV	0.009	0.005	15.74	1.62	60.93	23.72	70.26	20.99	0.98	22.53	11.27
LNV	0.011	0.001	16.94	3.80	43.13	4.22	53.41	4.67	0.93	21.85	8.77

One-way ANOVA and Kruskal-Wallis tests were performed, and no significant differences were found for any formulation pharmacokinetic parameters. This suggests that HPβCD is responsible for ocular permanence independently of the added polymer. Previous studies obtained similar results, proving the mucoadhesive capacity of HPβCD at high concentrations (40 % (p/v)) (35).

The results show that there is a high clearance in the first few minutes due to the loss of the formulation by blinking (Figure 18). This is consistent with the mucoadhesion values indicating that the breakage of the bioadhesive bond occurs at the level of the vehicle itself. After those

first few minutes, the layer of formulation that remains bioadhered to the cornea is slowly removed.

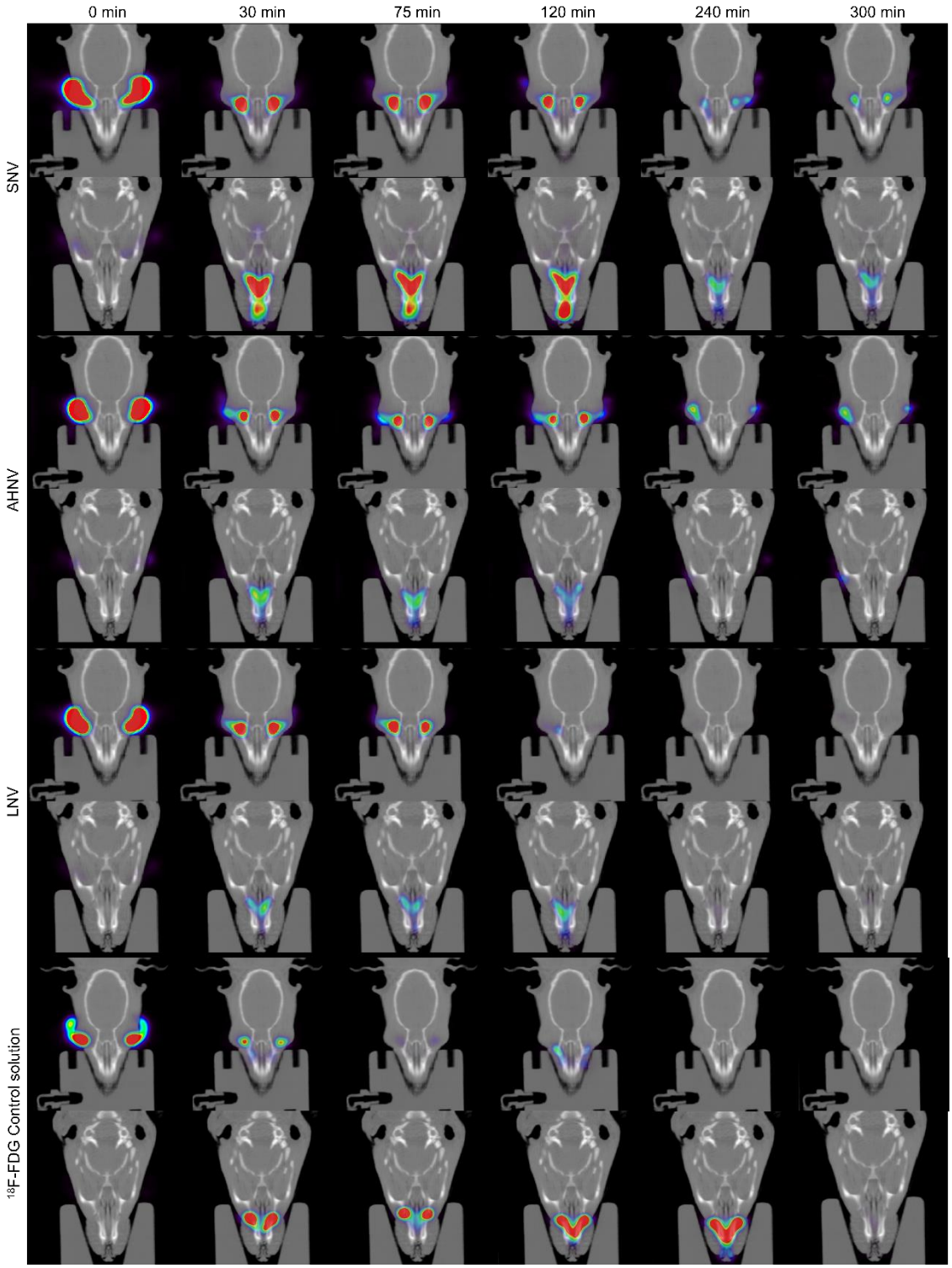

Figure 18. Coronal PET/CT images of rat eyes treated with SNV, AHNV and LNV over time. Data were compared with a ^{18}F-FDG control solution. The amount of formulation on the ocular surface is coded on a color scale: blue areas show a low radioactive activity; red areas show high radioactive activity.

Although the addition of polymers like HA in AHNV and PVA in LNV has not increased the ocular permanence compared with the solution without polymers (SNV), the advantages of the presence of polymers must be considered. The addition of high molecular weight HA (>1000 KDa) (70) to eye drops can promote faster corneal wound healing. This is due to the binding of the HA to the CD44 protein (CD44 receptor is expressed when there is damage in the corneal epithelium), which enhances the migration and regeneration of epithelial cells (71). Furthermore, the expression of inflammatory cytokines (e.g. IL-1beta and MMP-9) is decreased following the HA administration, suppressing inflammatory responses (72,73). In addition, high molecular weight HA retains water, increasing tear film stability and decreasing the friction during the blink. Also, HA increase eye hydration (74). On the other hand, PVA is used in ophthalmic formulations as a lubricant and to improve ocular surface hydration, which can increase the sense of well-being during the treatment of FK.

3.12. DISC DIFFUSION METHOD BY THE KIRBY-BAUER METHOD

Inhibition zone diameters (Figure 19) obtained in Kirby-Bauer Disc Diffusion Method are shown in Table 11. The inhibitory zone is influenced by several parameters, including the culture medium, the drug diffusion capacity, the amount of inoculum, the time of microorganism generation, the sensitivity to the antifungal, or the incubation period (75). SN shows larger inhibitory zone diameters for all fungal species than NTC. These results are due to enhanced diffusion of natamycin from the disc into the inoculum when natamycin is complexed with HPβCD. SN and NTC show no inhibitory activity for PL. PL resistance to natamycin has been previously reported in cases of FK (76,77).

Table 11. Inhibition zone diameters (mm) obtained in Kirby-Bauer Disc Diffusion Method.

Fungal specie / Formulation	C.A 90231	C.A 90028	AF	PL	FS
SV	72	58	81	68	85
SN	33-35	32	28	0	47
SNV	74-76	62	72	80	77
VFEND®	61	61	87	84	103
NTC®	10	14	12	0	26

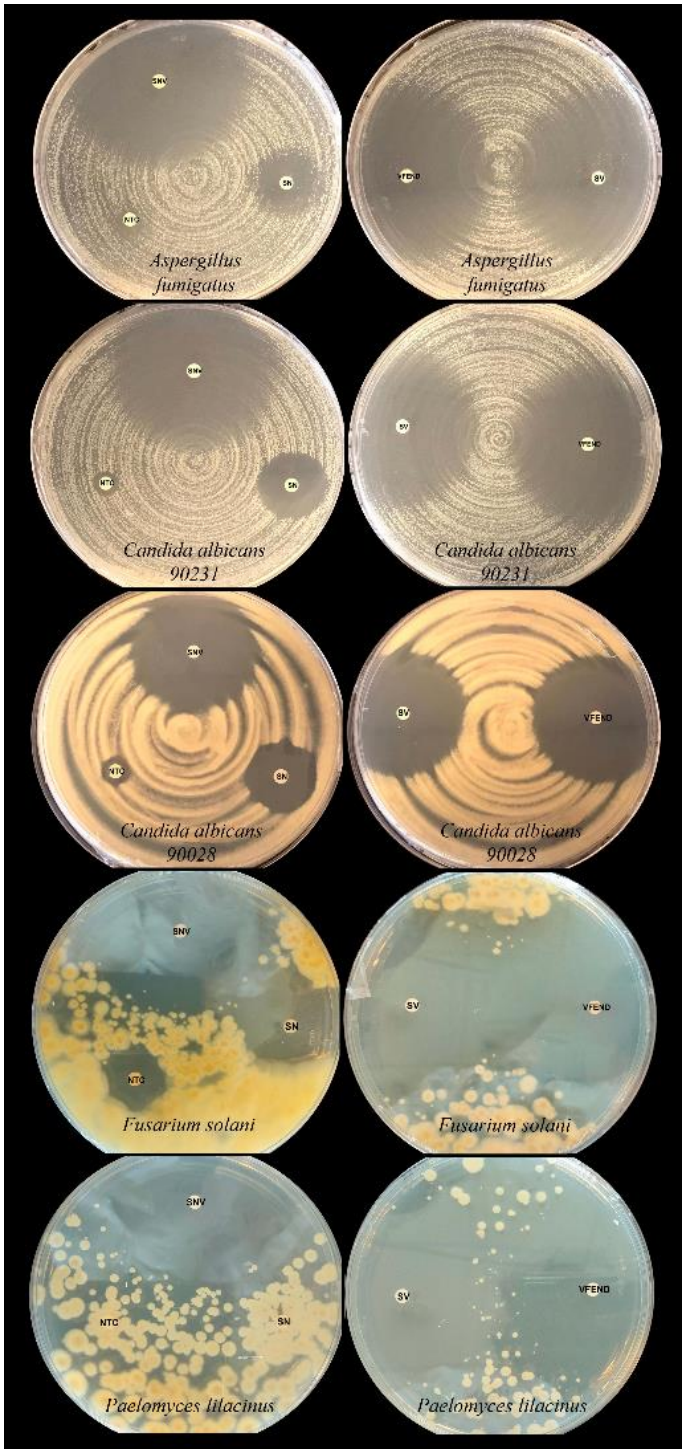

Figure 19. Inhibition zone images of SV, SN, SNV, NTC and VFEND against *Aspergillus fumigatus*, *Candida albicans* ATCC 90231, *Candida albicans* ATCC 90028, *Fusarium solani and Paelomyces lilacinus.*

The inhibition zone diameters obtained for the formulation with both drugs solubilized with HPβCD (SNV) show slightly higher values than those obtained with the single drug formulations (SN and SV) for all species except for AF and FS.

The combined formulation of natamycin and voriconazole was effective for the species tested. However, to confirm an additive or synergistic effect produced by the combination of natamycin and voriconazole, further studies using other more representative techniques such as the checkerboard method (78) or ETEST® strips (79) would be necessary. Also, additional *in vivo*, *ex vivo* would be required to asses the antifungal efficacy.

4. CONCLUSION

Natamycin and voriconazole formulations were developed as a new alternative for the treatment of FK. The formulations were developed to have characteristics suitable for topical ophthalmic administration.

Solubility and NMR studies demonstrated the formation of stable complexes between natamycin and HPβCD where the double bonds of natamycin are arranged towards the more hydrophobic side of HPβCD and the polar rings of natamycin are arranged on the more hydrophilic side of HPβCD. Furthermore, NMR results showed that natamycin competes with voriconazole for the same binding site of HPβCD although this did not affect the solubility of voriconazole in the formulations due to the presence of free cyclodextrin molecules.

In addition, the formation of aggregates of HPβCD molecules and their complexes with natamycin and voriconazole was observed by TEM. These can control drug release, improve residence time and enhance their permeability across the cornea.

The pH, osmolality, viscosity, and transparency values were found to be within the accepted range for ophthalmic topical formulations. *In vitro* release studies were successfully carried out and Kickian-type diffusions were obtained for all formulations developed. All formulations showed an improvement in transcorneal permeability in the presence or absence of corneal epithelium compared to Natacyn®. In addition, the ocular toxicity studies performed (BCOP and HET-CAM) showed that the formulations are safe. *Ex vivo* and *in vivo* mucoadhesion studies suggested that the mucoadhesive capacity of the formulations is due to the presence of HPβCD and is not increased by the addition of HA or PVA. Antifungal activity studies demonstrated the ability to inhibit the growth of several fungal species. All these results concluded that the formulations developed in the present study could significantly improve the treatment of FK. Additionally, formulations can also be prepared using only one of the drugs, making it a versatile pharmaceutical system that can be tailored to meet the different needs of patients. Therefore, they could be used as a first-choice treatment in cases of FK where the causative agent is unknown, species resistant to one of the antifungal agents are suspected, or where no commercial drug is available.

Appendix 1. Details of the calculation of the inhibition equilibrium constant K_I for natamycin for the titration competition assay with natamycin at constant molar ratio voriconazole:HPβCD 1:1. The following forked two-site binding model was used:

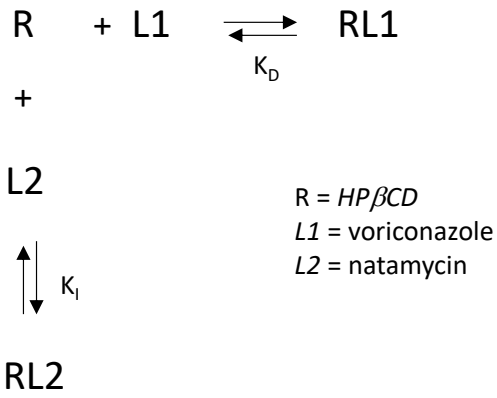

The equilibrium can be described by Eq. 2 (57):

$$K_D = \frac{([L1]_0\, K_I)}{IC_{50(L2)} - K_I} \qquad \text{Eq. 2}$$

The dissociation constant of the voriconazole-HPβCD complex was previously determined to be K_D=250 mM (32) and $[L1]_0$ was 5.62 mM. The ^{1}H NMR signal of voriconazole with the maximum CSP during the titration is H6a. This signal was chosen to determine IC_{50} by representing d^{obs} normalized by the maximum variation in this property with respect to the molar ratio natamycin:voriconazole. The curve was fitted to an exponential equation and the IC_{50} obtained was 0.34, which introduced in Eq. 2 provides K_I = 0.334 mM.

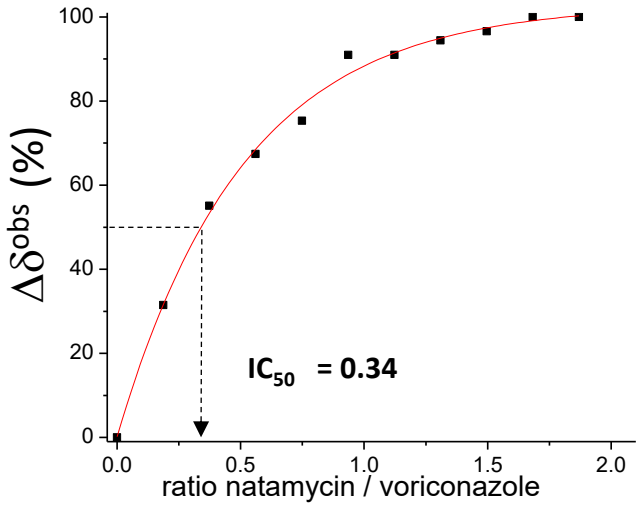

BIBLIOGRAPHY

1. Rai M, Occhiutto ML. Mycotic Keratitis. CRC Press; 2019. 367 p.
2. Taechajongjintana M, Kasetsuwan N, Reinprayoon U, Sawanwattanakul S, Pisuchpen P. Effectiveness of voriconazole and corneal cross-linking on Phialophora verrucosa keratitis: a case report. J Med Case Rep. 2018 Aug 19;12(1):225.
3. Bourcier T, Sauer A, Dory A, Denis J, Sabou M. Fungal keratitis. J Fr Ophtalmol. 2017 Nov;40(9):e307–13.
4. Lund OE, Miño de Kaspar H, Klauss V. [Strategy for examination and therapy of mycotic keratitis]. Klin Monbl Augenheilkd. 1993 Mar;202(3):188–94.
5. Saha S, Banerjee D, Khetan A, Sengupta J. Epidemiological profile of fungal keratitis in urban population of West Bengal, India. Oman J Ophthalmol. 2009;2(3):114–8.
6. Ogawa A, Matsumoto Y, Yaguchi T, Shimmura S, Tsubota K. Successful treatment of Beauveria bassiana fungal keratitis with topical voriconazole. Journal of Infection and Chemotherapy. 2016 Apr;22(4):257–60.
7. Anutarapongpan O, Thanathanee O, Suwan-Apichon O. Penicillium keratitis in a HIV-infected patient. BMJ Case Rep. 2016 Aug 17;2016.
8. Shukla PK, Kumar M, Keshava GBS. Mycotic keratitis: an overview of diagnosis and therapy. Mycoses. 2008 May;51(3):183–99.
9. Brown L, Leck AK, Gichangi M, Burton MJ, Denning DW. The global incidence and diagnosis of fungal keratitis. Lancet Infect Dis. 2021 Mar;21(3):e49–57.
10. Mannis MJ, Holland EJ. Cornea E-Book. Elsevier Health Sciences; 2016. 2014 p.
11. Lalitha P, Vijaykumar R, Prajna NV, Fothergill AW. *In Vitro* Natamycin Susceptibility of Ocular Isolates of Fusarium and Aspergillus Species: Comparison of Commercially Formulated Natamycin Eye Drops to Pharmaceutical-Grade Powder. J Clin Microbiol. 2008 Jan 10;46(10):3477–8.
12. Aparicio JF, Barreales EG, Payero TD, Vicente CM, de Pedro A, Santos-Aberturas J. Biotechnological production and application of the antibiotic pimaricin: biosynthesis and its regulation. Appl Microbiol Biotechnol. 2016;100:61–78.
13. Pradhan L, Sharma S, Nalamada S, Sahu SK, Das S, Garg P. Natamycin in the treatment of keratomycosis: correlation of treatment outcome and *in vitro* susceptibility of fungal isolates. Indian J Ophthalmol. 2011 Dec;59(6):512–4.
14. Maschmeyer G, Haas A. Voriconazole: a broad spectrum triazole for the treatment of serious and invasive fungal infections. Future Microbiol. 2006 Dec;1(4):365–85.
15. Bunya VY, Hammersmith KM, Rapuano CJ, Ayres BD, Cohen EJ. Topical and oral voriconazole in the treatment of fungal keratitis. Am J Ophthalmol. 2007 Jan;143(1):151–3.
16. Al-Badriyeh D, Neoh CF, Stewart K, Kong DCM. Clinical utility of voriconazole eye drops in ophthalmic fungal keratitis. Clin Ophthalmol. 2010 May 6;4:391–405.
17. Voriconazole Teva 200 mg polvo para solución para perfusión (EFG) [Internet]. https://cima.aemps.es/. [cited 2020 Feb 24]. Available from: https://cima.aemps.es/cima/publico/detalle.html?nregistro=80047

18. EMA. Vfend [Internet]. European Medicines Agency. 2018 [cited 2022 Aug 29]. Available from: https://www.ema.europa.eu/en/medicines/human/EPAR/vfend
19. Johnson MD, MacDougall C, Ostrosky-Zeichner L, Perfect JR, Rex JH. Combination Antifungal Therapy. Antimicrobial Agents and Chemotherapy. 2004 Mar;48(3):693–715.
20. Al-Hatmi AMS, Meletiadis J, Curfs-Breuker I, Bonifaz A, Meis JF, De Hoog GS. *In vitro* combinations of natamycin with voriconazole, itraconazole and micafungin against clinical Fusarium strains causing keratitis. J Antimicrob Chemother. 2016 Apr;71(4):953–5.
21. Jiang T, Tang J, Wu Z, Sun Y, Tan J, Yang L. The combined utilization of Chlorhexidine and Voriconazole or Natamycin to combat Fusarium infections. BMC Microbiology. 2020 Sep 5;20(1):275.
22. Sradhanjali S, Yein B, Sharma S, Das S. *In vitro* synergy of natamycin and voriconazole against clinical isolates of Fusarium, Candida, Aspergillus and Curvularia spp. Br J Ophthalmol. 2018;102(1):142–5.
23. Shapiro BL, Lalitha P, Fothergill AW, Apakupakul K, Srinivasan M, Prajna NV, et al. Synergy, Indifference, or Antagonism? *In Vitro* Susceptibility of Fusarium and Aspergillus spp Isolated From Keratitis in South India Against Combinations of Natamycin, Voriconazole, and Anidulafungin. Investigative Ophthalmology & Visual Science. 2011 Apr 22;52(14):5854.
24. Brewster ME, Loftsson T. Cyclodextrins as pharmaceutical solubilizers. Advanced Drug Delivery Reviews. 2007 Jul 30;59(7):645–66.
25. European Medicines Agency (EMA). Background review for cyclodextrins used as excipients. 2014 Nov;17.
26. Connors KA HT. Advances in Analitycal Chemistry and Instrumentation. Vol. Phase-Solubility Techniques. New York: Interscience; 1965. 117–212 p.
27. Loftsson T, Brewster ME. Cyclodextrins as Functional Excipients: Methods to Enhance Complexation Efficiency. Journal of Pharmaceutical Sciences. 2012 Sep 1;101(9):3019–32.
28. Loftsson T, Masson M. The effects of water-soluble polymers on cyclodextrins and cyclodextrin solubilization of drugs. Journal of Drug Delivery Science and Technology. 2004 Jan 1;14(1):35–43.
29. Selvam AP, Geetha D. Ultrasonic studies on lamivudine: beta-cyclodextrin and polymer inclusion complexes. Pak J Biol Sci. 2008 Feb 15;11(4):656–9.
30. Mayer M, Meyer B. Mapping the active site of angiotensin-converting enzyme by transferred NOE spectroscopy. J Med Chem. 2000 Jun 1;43(11):2093–9.
31. Unravelling the Time Scale of Conformational Plasticity and Allostery in Glycan Recognition by Human Galectin-1 - Bertuzzi - 2020 - Chemistry – A European Journal - Wiley Online Library [Internet]. [cited 2022 May 5]. Available from: https://chemistry-europe.onlinelibrary.wiley.com/doi/full/10.1002/chem.202003212
32. Díaz-Tomé V, García-Otero X, Varela-Fernández R, Martín-Pastor M, Conde-Penedo A, Aguiar P, et al. In situ forming and mucoadhesive ophthalmic voriconazole/HPβCD hydrogels for the treatment of fungal keratitis. Int J Pharm. 2021 Mar 15;597:120318.

33. Luaces-Rodríguez A, Díaz-Tomé V, González-Barcia M, Silva-Rodríguez J, Herranz M, Gil-Martínez M, et al. Cysteamine polysaccharide hydrogels: Study of extended ocular delivery and biopermanence time by PET imaging. Int J Pharm. 2017 Aug 7;528(1–2):714–22.
34. Díaz-Tomé V, Luaces-Rodríguez A, Silva-Rodríguez J, Blanco-Dorado S, García-Quintanilla L, Llovo-Taboada J, et al. Ophthalmic Econazole Hydrogels for the Treatment of Fungal Keratitis. J Pharm Sci. 2018 May;107(5):1342–51.
35. García-Otero X, Díaz-Tomé V, Varela-Fernández R, Martín-Pastor M, González-Barcia M, Blanco-Méndez J, et al. Development and Characterization of a Tacrolimus/Hydroxypropyl-β-Cyclodextrin Eye Drop. Pharmaceutics. 2021 Jan 23;13(2):149.
36. Fernández Ferreiro A. Formulación magistral oftálmica antiinfecciosa. 2019.
37. Sliney DH. What is light? The visible spectrum and beyond. Eye (Lond). 2016 Feb;30(2):222–9.
38. Ceulemans J, Ludwig A. Optimisation of carbomer viscous eye drops: an *in vitro* experimental design approach using rheological techniques. European Journal of Pharmaceutics and Biopharmaceutics. 2002 Jul;54(1):41–50.
39. EUR-Lex - 02010L0063-20190626 - EN - EUR-Lex [Internet]. [cited 2020 Apr 26]. Available from: https://eur-lex.europa.eu/legal-content/EN/TXT/?uri=CELEX%3A02010L0063-20190626
40. OECD. Test No. 437: Bovine Corneal Opacity and Permeability Test Method for Identifying i) Chemicals Inducing Serious Eye Damage and ii) Chemicals Not Requiring Classification for Eye Irritation or Serious Eye Damage [Internet]. Paris: Organisation for Economic Co-operation and Development; 2013 [cited 2016 Jan 18]. Available from: http://www.oecd-ilibrary.org/content/book/9789264203846-en
41. ICCVAM. Recommended Test Method Protocol: Hen's Egg Test – Chorioallantoic Membrane (HET-CAM) Test Method. Obtained from [Internet]. 2010. Available from: https://ntp.niehs.nih.gov/iccvam/docs/protocols/ivocular-hetcam.pdf.
42. Fernández-Ferreiro A, Silva-Rodríguez J, Otero-Espinar FJ, González-Barcia M, Lamas MJ, Ruibal A, et al. Positron Emission Tomography for the Development and Characterization of Corneal Permanence of Ophthalmic Pharmaceutical Formulations. Invest Ophthalmol Vis Sci. 2017 Feb 1;58(2):772–80.
43. Koontz JL, Marcy JE. Formation of Natamycin:Cyclodextrin Inclusion Complexes and Their Characterization. J Agric Food Chem. 2003 Nov 1;51(24):7106–10.
44. Malhotra S, Khare A, Grover K, Singh I, Pawar P. Design and Evaluation of Voriconazole Eye Drops for the Treatment of Fungal Keratitis. J Pharm (Cairo) [Internet]. 2014;2014. Available from: https://www.ncbi.nlm.nih.gov/pmc/articles/PMC4590801/
45. CIMA: VOLTAREN 1 mg/ml COLIRIO EN SOLUCION [Internet]. [cited 2021 Oct 7]. Available from: https://cima.aemps.es/cima/publico/detalle.html?nregistro=58308
46. Abdelkader H, Fathalla Z, Moharram H, Ali TFS, Pierscionek B. Cyclodextrin Enhances Corneal Tolerability and Reduces Ocular Toxicity Caused by Diclofenac. Oxid Med Cell Longev. 2018;2018:5260976.

47. Loftsson T, Stefánsson E. Cyclodextrins and topical drug delivery to the anterior and posterior segments of the eye. Int J Pharm. 2017 Oct 15;531(2):413–23.
48. Haimhoffer Á, Rusznyák Á, Réti-Nagy K, Vasvári G, Váradi J, Vecsernyés M, et al. Cyclodextrins in Drug Delivery Systems and Their Effects on Biological Barriers. Scientia Pharmaceutica. 2019 Dec;87(4):33.
49. Muankaew C, Saokham P, Jansook P, Loftsson T. Self-assembly of cyclodextrin complexes: detection, obstacles and benefits. Die Pharmazie - An International Journal of Pharmaceutical Sciences. 2020 Jul 1;75(7):307–12.
50. Loftsson T, Hreinsdóttir D, Stefánsson E. Cyclodextrin microparticles for drug delivery to the posterior segment of the eye: aqueous dexamethasone eye drops. J Pharm Pharmacol. 2007 May;59(5):629–35.
51. Jansook P, Stefánsson E, Thorsteinsdóttir M, Sigurdsson BB, Kristjánsdóttir SS, Bas JF, et al. Cyclodextrin solubilization of carbonic anhydrase inhibitor drugs: formulation of dorzolamide eye drop microparticle suspension. Eur J Pharm Biopharm. 2010 Oct;76(2):208–14.
52. Muankaew C, Jansook P, Stefánsson E, Loftsson T. Effect of γ-cyclodextrin on solubilization and complexation of irbesartan: influence of pH and excipients. Int J Pharm. 2014 Oct 20;474(1–2):80–90.
53. Jóhannsdóttir S, Jansook P, Stefánsson E, Loftsson T. Development of a cyclodextrin-based aqueous cyclosporin A eye drop formulations. International Journal of Pharmaceutics. 2015 Sep 30;493(1):86–95.
54. Phillip Lee YH, Sathigari S, Jean Lin YJ, Ravis WR, Chadha G, Parsons DL, et al. Gefitinib–cyclodextrin inclusion complexes: physico-chemical characterization and dissolution studies. Drug Development and Industrial Pharmacy. 2009 Sep 1;35(9):1113–20.
55. Jambhekar SS, Breen P. Cyclodextrins in pharmaceutical formulations II: solubilization, binding constant, and complexation efficiency. Drug Discovery Today. 2016 Feb 1;21(2):363–8.
56. Jansook P, Praphanwittaya P, Sripetch S, Loftsson T. Solubilization and *in vitro* permeation of dovitinib/cyclodextrin complexes and their aggregates. J Incl Phenom Macrocycl Chem. 2020 Aug 1;97(3):195–203.
57. Fielding L. NMR methods for the determination of protein-ligand dissociation constants. Prog Nucl Magn Reson Spectrosc. 2007;3(1):219–42.
58. Furukawa A, Konuma T, Yanaka S, Sugase K. Quantitative analysis of protein-ligand interactions by NMR. Prog Nucl Magn Reson Spectrosc. 2016 Aug;96:47–57.
59. Human Metabolome Database: 1H NMR Spectrum (1D, 800 MHz, D2O, predicted) (HMDB0014964) [Internet]. [cited 2022 May 5]. Available from: https://hmdb.ca/spectra/nmr_one_d/153327
60. Human Metabolome Database: 13C NMR Spectrum (1D, 800 MHz, D2O, predicted) (HMDB0014964) [Internet]. [cited 2022 May 5]. Available from: https://hmdb.ca/spectra/nmr_one_d/153326

61. Cruz JR, Becker BA, Morris KF, Larive CK. NMR characterization of the host-guest inclusion complex between beta-cyclodextrin and doxepin. Magn Reson Chem. 2008 Sep;46(9):838–45.
62. Dutescu RM, Panfil C, Schrage N. Osmolarity of prevalent eye drops, side effects, and therapeutic approaches. Cornea. 2015 May;34(5):560–6.
63. Boddu SHS, Gunda S, Earla R, Mitra AK. Ocular microdialysis: a continuous sampling technique to study pharmacokinetics and pharmacodynamics in the eye. Bioanalysis. 2010 Mar;2(3):487–507.
64. Bravo-Osuna I, Andrés-Guerrero V, Pastoriza Abal P, Molina-Martínez IT, Herrero-Vanrell R. Pharmaceutical microscale and nanoscale approaches for efficient treatment of ocular diseases. Drug Deliv Transl Res. 2016;6(6):686–707.
65. Ahmed L, Atif R, Eldeen T, Yahya I, Omara A, Eltayeb M. Study the Using of Nanoparticles as Drug Delivery System Based on Mathematical Models for Controlled Release. 2019 May 1;8:52–6.
66. FlorCruz NV, Evans JR. Medical interventions for fungal keratitis. Cochrane Database Syst Rev. 2015 Apr 9;(4):CD004241.
67. O'Day DM, Head WS, Robinson RD, Clanton JA. Corneal penetration of topical amphotericin B and natamycin. Curr Eye Res. 1986 Nov;5(11):877–82.
68. Moiseev RV, Morrison PWJ, Steele F, Khutoryanskiy VV. Penetration Enhancers in Ocular Drug Delivery. Pharmaceutics. 2019 Jul;11(7):321.
69. Lorenzo-Veiga B, Sigurdsson HH, Loftsson T, Alvarez-Lorenzo C. Cyclodextrin–Amphiphilic Copolymer Supramolecular Assemblies for the Ocular Delivery of Natamycin. Nanomaterials (Basel). 2019 May 15;9(5):E745.
70. Snetkov P, Zakharova K, Morozkina S, Olekhnovich R, Uspenskaya M. Hyaluronic Acid: The Influence of Molecular Weight on Structural, Physical, Physico-Chemical, and Degradable Properties of Biopolymer. Polymers (Basel). 2020 Aug 11;12(8):1800.
71. Chen TY, Tseng CL, Lin CA, Lin HY, Venkatesan P, Lai PS. Effects of Eye Drops Containing Hyaluronic Acid-Nimesulide Conjugates in a Benzalkonium Chloride-Induced Experimental Dry Eye Rabbit Model. Pharmaceutics. 2021 Aug 30;13(9):1366.
72. Hyaluronate Acid-Dependent Protection and Enhanced Corneal Wound Healing against Oxidative Damage in Corneal Epithelial Cells - PubMed [Internet]. [cited 2022 May 3]. Available from: https://pubmed.ncbi.nlm.nih.gov/27190638/
73. Marinho A, Nunes C, Reis S. Hyaluronic Acid: A Key Ingredient in the Therapy of Inflammation. Biomolecules. 2021 Oct 15;11(10):1518.
74. Chang WH, Liu PY, Lin MH, Lu CJ, Chou HY, Nian CY, et al. Applications of Hyaluronic Acid in Ophthalmology and Contact Lenses. Molecules. 2021 Apr 24;26(9):2485.
75. Aristizabal LSR, Castaño DM. Metodologias para evaluar *in vitro* la actividad antibacteriana de compuestos de origen vegetal. Scientia et Technica. 2009;2(42):263–8.
76. Yuan X, Wilhelmus KR, Matoba AY, Alexandrakis G, Miller D, Huang AJW. Pathogenesis and Outcome of Paecilomyces Keratitis. American Journal of Ophthalmology. 2009 Apr 1;147(4):691-696.e3.

77. Wu PC, Lai CH, Tan HY, Ma DH, Hsiao CH. The Successful Medical Treatment of a Case of Paecilomyces lilacinus Keratitis. Cornea. 2010 Mar;29(3):357–8.
78. Hlebová M, Hleba L, Medo J, Kováčik A, Čuboň J, Ivana C, et al. Antifungal and synergistic activities of some selected essential oils on the growth of significant indoor fungi of the genus Aspergillus. Journal of Environmental Science and Health, Part A. 2021 Oct 15;56(12):1335–46.
79. Kiraz N, Dag I, Yamac M, Kiremitci A, Kasifoglu N, Oz Y. Synergistic activities of three triazoles with caspofungin against Candida glabrata isolates determined by time-kill, Etest, and disk diffusion methods. Antimicrob Agents Chemother. 2010 May;54(5):2244–7.

Chapter 4

OPHTHALMIC SAFETY AND OCULAR PERMANENCE OF CYCLODEXTRINS AT HIGH CONCENTRATIONS

1. INTRODUCTION

Cyclodextrins (CDs) are cyclic oligosaccharides formed by α-D-glucopyranose units linked by α-D-(1,4) bonds obtained during the enzymatic degradation of starch. Depending on the number of α-D-glucopyranose units forming them, natural CDs are classified as α-cyclodextrin (αCD) (6 units), β-cyclodextrin (βCD) (7 units) and ɣ-cyclodextrin (ɣCD) (8 units).

In addition to natural CDs, there are different types of synthetic CDs such as hydroxypropyl-α-cyclodextrin (HPαCD), hydroxypropyl-β-cyclodextrin (HPβCD), hydroxypropyl-ɣ-cyclodextrin (HPɣCD), sulfobutylether-β-cyclodextrin (SBEβCD) or methyl-β-cyclodextrin (RMβCD) among others. They are obtained mainly by the substitution of the hydroxyl groups present on the external surface of natural CDs. These substitutions improve certain characteristics of natural CDs, such as the low water solubility exhibited by βCD (1).

CDs have cone- or toroid-shaped structures with a hydrophobic interior cavity (lined by the carbons of the molecular backbone and the oxygens of the glucose residues) and a hydrophilic outer surface (with numerous hydroxyl groups, primary in C6 position and secondary in C2 and C3 position) (2).

CDs can internalize hydrophobic drug molecules or part of them in their cavity, forming inclusion complexes that can enhance drug aqueous solubility, reduce toxicity and improve drug stability (3–5). They are widely used as excipients in topical ophthalmic formulations as they have been shown to increase the bioavailability of poorly soluble drugs, enhance drug stability, reduce ocular irritation and improve corneal permeability (3,6–8). There are several approved topical ophthalmic drugs using CDs as an excipient in their composition (Table 1)

Table 1. Approved topical ophthalmic drugs using CDs as an excipient in their composition.

Cyclodextrin	Drug	Comercial Name
βCD	Naphasoline hydrochloride	Clear eyes®
	Dexamethasone	Glymesason®
	Thiromersal	Vitaseptol®
HPβCD	Indomethacin	Indocid® / Indocollyre®
	Bilastine	Bilaxten®/ Ibis®
	Ciprofloxacin+Desamethasone	Kominil-Duo®
	Azelastine	Antalerg®
	Diclofenac	Dyloject®
	Lanosterol	Lanomax®(veterinary)
	Levocabastine	Allergiflash®
	Methylethylpyridinol	Vixipin®
	Olopatadine	Opatanol®/Olantin®
HPɣCD	Diclofenac	Voltaren®/Voltadol®
RAMEB	Chloramphenicol	Clorocil®
HPβCD+ RAMEB	Lanosterol+n-acetylcarnosine	LumenPro®(veterinaty)

There are numerous studies on the use of CDs in the development of topical ophthalmic formulations such as aqueous solutions (9), nanoparticles (10,11), or hydrogels (8,12). However, there is a gap in the study of both, the mucoadhesive capacity and the ocular safety

of CDs as a function of their concentration in ophthalmic formulations. Some studies with CDs have demonstrated their mucoadhesive capacity by modifying CD radicals, such as the thiolated CD MβCD-SH (13,14), or by adding mucoadhesive polymers to the formulation (15).
In 2017, the European Medicines Agency (EMA) published a report on the safety of CDs according to routes of administration. Regarding the ophthalmic safety, EMA concluded that concentrations of 4% αCD and 5% RMβCD could be toxic to the corneal epithelium, while concentrations up to 10% SBEβCD and 12.5% HPβCD were non-toxic and non-irritating in rabbit trials (3). Since this report, some studies have shown that HPβCD concentrations of up to 40% were safe (8,16). In addition, the formation of diclofenac complexes with αCD, βCD and ɣCD, was found to reduce the corneal irritation of diclofenac topical ophthalmic formulations (6).
In this work the ocular safety of various CDs at high concentrations was determined *in vitro* by the Hen´s Egg Test on Chorioallantoic Membrane (HET-CAM) and *ex vivo* by the Bovine Corneal Opacity and Permeability Assay (BCOP). In addition, the potential use of CDs as ocular surface permanence promoters was determined *in vitro* with porcine mucin, *ex vivo* with bovine corneas and mucoadhesion studies, and *in vivo* with PET/CT.

2. MATERIALS AND METHODS

2.1. MATERIALS

α-cyclodextrin (αCD) (Cavamax® W8), β-cyclodextrin (βCD) (Cavamax® W7) and γ-cyclodextrin (γCD) (Cavamax® W8) were obtained from Wacker Chemie AG (Munich, Germany), 2-hydroxypropyl-α-cyclodextrin (HPαCD) (0.5-0.9 molar substitution ratio) and Sulfobutylether- β-cyclodextrin (SBEβCD) (3.00−6.50 molar substitution ratio) were provided by Cyclolab Ltd (Budapest, Hungary), 2-hydroxypropyl-β-cyclodextrin (HPβCD) (Kleptose®, 0.65 molar substitution ratio) and partially methylated β-cyclodextrin (RMβCD) (Crysmeb® was obtained from Roquette® Laisa S.A. (Valencia, Spain), 2-hydroxypropyl-γ-cyclodextrin HPγCD (0.6 molar substitution ratio, MW 1580 Da) and mucin from porcine stomach were purchased from Sigma Aldrich® (Darmstadt, Germany).

3. METHODS

3.1. CYCLODEXTRIN SOLUTIONS ELABORATION

The CD solutions were prepared at a concentration of 20% (w/v), except for αCD (15% w/v) and βCD (1.8% w/v), which were formulated according to their maximum solubility (17). An aqueous solution was prepared for each CD by adding the CD powder into MilliQ® water until its complete solubilization. The experiments were carried out with solutions at their original pH and with solutions that were adjusted to pH 7.4 by adding 0.1 M NaOH or 0.1 M HCl.

3.2. OSMOLALITY, PH AND VISCOSITY MEASUREMENTS.

Osmolality measurements were taken with a Micro-Osmometer (Fiske® Model 210). The pH was measured using a pH meter (HI5221 HANNA®) at 25±0.5°C. Viscosity was tested with a

rotational viscosimeter (Visco QC 300 Anton Paar®) at 25ºC and 20 rpm. Each determination was carried out in triplicate.

3.3. OCULAR IRRITATION TEST

BCOP and HET-CAM assays were chosen to evaluate the potential irritation produced on the ocular surface. These methods comply with the 3Rs principles (replacement, reduction, and refinement) as described in Directive 2010/63/EU of the European Parliament and of the Council of 22 September 2010 on the protection of animals used for scientific purposes (18).

3.4. BOVINE CORNEAL OPACITY AND PERMEABILITY ASSAY (BCOP)

Corneal Opacity

A variation of the method previously described in the Invittox Protocol nº 437 (19) was carried out to detect potential ocular corrosives and severe irritants using fresh bovine corneas. The assessment of ocular irritation was extensively described in previous studies (12). Opacity (transmitted light (TL)) and corneal transparency (transmittance values) were measured with a luxmeter (Gossen Mavolux 5032C USB) and a spectrophotometer (Agilent® Cari 60 UV) respectively.

Opacity and transparency were measured in fresh corneas. The corneas were then placed in Franz cells and treated for 60 min by introducing 1 mL of PBS into the donor chamber, after which both parameters were measured. Following this period, 1 mL of the CD solution was added to the corneas and maintained for 10 min, then the CD solution was withdrawn, and 1 mL of PBS was added to the corneas and maintained for 120 min. Finally, the aforementioned parameters were measured again. Each CD solution was tested in triplicate.

Corneal permeability

The corneas used in the "Corneal Opacity" section were placed back into Franz cells. The receptor chamber was filled in with 6 mL of PBS, while 1 mL of 0.4% (w/v) fluorescein was placed into the donor chamber. At 90 min, samples were collected and analyzed to determine the amount of fluorescein that crossed the treated corneas. Fluorescein concentration was measured by a spectrophotometer (Agilent® Cary 60 UV) at a wavelength of 490 nm.

3.5. HEN´S EGG TEST - CHORIOALLANTOIC MEMBRANE (HET-CAM)

HET-CAM is described in The Interagency Coordinating Committee on the Validation of Alternative Methods (ICCVAM) (20). Fertilized broiler chicken eggs were placed in an automatic rotation incubator and kept for 8 days at 38 ± 0.5°C and 65% relative humidity. 24 hours before the test, the automatic rotation was stopped and on the 9th day of incubation the test was conducted. Each egg was opened, and the inner membrane was removed. 0.3 mL of CD solution, positive control (0.1% (w/v) NaOH solution), or negative control (0.9% (w/v) NaCl solution) were administered onto the surface of the chorioallantoic membrane (CAM). Hemorrhage, vascular lysis, or coagulation reactions were assessed, if applicable, by direct observation of the CAM for 300 sec.

3.6. MUCOADHESION AND OCULAR PERMANENCE STUDIES

3.6.1. CORNEAL MUCOADHESIVENESS

The corneal mucoadhesiveness method was designed and described in previous studies (12). Fresh bovine corneas were excised and fixed to the upper probe of a Universal Testing Machine (Shimadzu® AGS-X Precision Universal Tester). The CD solutions were introduced into the weighing bottles. The corneas were immersed 2 mm into the formulations for 30 sec and then retired to register the force-displacement curve. The bioadhesion work (J) was determined from the area under de curve (AUC).

3.6.2. *IN VITRO* MUCOADHESIVE TEST

In vitro mucoadhesive test was carried out with minor modifications of the method described by Haimhoffer et al. (21). Interactions between mucin and the different CDs were studied using dynamic light scattering (DLS) and zeta potential (ζ) measurements. A 1 mg/mL (w/v) mucin dispersion was formulated by adding mucin to water. The dispersion was maintained under magnetic stirring for 12 h. Then, the dispersion was centrifugated for 5 min at 5000 rpm and the supernatant was collected to use in the experiment. 1:1 mixtures of CD solutions and the mucin dispersion were prepared. CD solutions, mucin dispersions and mixtures of CD solutions with mucin dispersion were measured by DLS (ZEN3600, Malvern Instruments Ltd., UK).

3.6.3. PET *IN VIVO* ASSAY: QUANTITATIVE OCULAR PERMANENCE STUDY

The ocular surface permanence of initial pH and pH 7.4 CD solutions was assessed in Sprague-Dawley rats by a Positron Emission Tomography (PET) and Computed Tomography (CT) combined system (PET/CT Albira® microPET/CT Bruker Biospin, Woodbridge, Connecticut, United States). The procedure was described in previous studies (8,12,22,23). All the animal studies and their protocols were approved by the Galician Network Committee for Ethics Research in accordance with the Spanish and EU applicable legislation (86/609/CEE, 2003/65/CE, 2010/63/EU, RD 1201/2005, and RD 53/2013). CD solutions were radiolabeled with 2-[^{18}F]-fluoro-2-deoxy-D-glucose (^{18}F-FDG). 7.5 µL of formulation containing 0.25 MBq of radioactivity was administrated into each eye of the rat. Immediately, a static PET frame was acquired at 0, 30, 75, 120, 240, and 300 min. Animals were only anesthetized during the image acquisition. Rats were fitted with an Elizabethan collar to prevent them from touching their eyes and removing part of the formulation. ROIs (Regions of interest) were manually obtained from the PET images to obtain the ocular remaining formulation (%) curve. Then, data were corrected considering the radioisotope decay (18F half-life: 109.7 min). Each formulation was evaluated in quadruplicate. The results were analyzed using a non-compartmental model. The area under the curve (AUC_{0-300}), terminal half-life ($t_{1/2}$) and mean residence time (MRT) were calculated.

4. RESULTS

4.1. OSMOLALITY, PH, AND VISCOSITY MEASUREMENTS

Table 2 shows the pH, osmolality, and viscosity data of the CD solutions. The viscosity of the derivatives CD solutions (HPαCD, HPβCD, HPγCD, SBEβCD and RMβCD: 4.548±0.00, 4.358±0.32, 4.548±0.00, 4.358±0.32 and 3.79±0.328 respectively) showed higher values than the solutions of the natural CDs solutions (αCD, βCD and γCD: 2.274±0.00, 2.843±0.00 and 2.843±0.00 respectively). The viscosity data of all the CD solutions are in the range of the viscosity reported for tear (1.5 mPa.s – 10 mPa.s) (24,25).

For Newtonian fluids and shear thinning fluids, viscosity does not affect the ocular drainage rate when values are below 4.4 mPa.s (25). Therefore, the viscosity of CD solutions at the tested concentrations is not a critical parameter regarding their ocular clearance. Only hydroxypropyl and sulfobutyl derivatives approached these limit values.

Table 2. pH, osmolality, and viscosity results.

Cyclodextrin	Osmolality (mOsm/kg)	pH	Viscosity (mPa·s)
αCD	135.50±0.707	4.577±0.070	2.274±0.00
βCD	18.50±0.707	5.457±0.067	2.843±0.00
γCD	155.667±3.78	6.297±0.115	2.843±0.00
HPαCD	235.667±3.055	6.647±0.131	4.548±0.00
HPβCD	185.00±1.414	5.023±0.130	4.358±0.32
HPγCD	200.50±0.707	6.037±0.050	4.548±0.00
SBEβCD	578.50±7.141	5.060±0.098	4.358±0.32
RMβCD	213.00±1.732	2.447±0.025	3.79±0.328

Regarding osmolality, all the CD solutions showed significant differences ($\alpha<0.05$). SBEβCD solution (578.50±7.141 mOsm/kg) showed the highest osmolality value obtaining a hyperosmolar solution. SBEβCD sodium salt is a polyanionic chemically modified βCD which is substituted with a sodium sulfonate salt with a butyl ether spacer group. In this study a SBEβCD with a 3.00-6.50 molar substitution ratio was used. The presence of the sulfonate sodium salt residues provided a high concentration of sodium ions responsible for the high osmolality value of the SBEβCD solution. SBEβCD osmolality value almost doubled the value of the physiological tear osmolality (285-295 mOsm/kg) (26). Hyperosmolar solutions cause discomfort and increase lacrimation, which may result in a decrease of the residence time on the ocular surface due to an increasement of the clearance (27,28).

In contrast, βCD showed the lowest osmolality (18.50±0.707 mOsm/kg) due to its low concentration in the solution caused by its limited solubility (1.8% (w/v)). HPαCD and RMβCD (235.667±3.055 and 213.00±1.732 mOsm/kg) showed the closest osmolality to the physiological values.

In addition, the effect of other ophthalmic excipients in the osmolality of ophthalmic formulations containing CDs must be considered. In the case of ophthalmic formulations with

low osmolality values, different osmotic agents (e.g. glycerol) approved for ophthalmic use could be added.
Finally, pH values of all the CD solutions were around 5-6 except for RMβCD, which had a pH value of 2.447±0.025. This value is outside the range of tear buffering capacity (4 to 8) (6) which may cause discomfort, irritation and tearing (increasing precorneal clearance and decreasing permanence on the ocular surface).

4.2. BCOP

4.2.1. CORNEAL OPACITY

Figures 1 and 2 show the changes in light transmission and the UV-Vis spectrum transmittance obtained for corneas in contact with the CD solutions. The comparison of the effect of the different CD solutions in the corneal transparency was assessed using a one-way ANOVA and Dunnett's multiple comparison test. The corneas incubated with the pH 7.4 αCD solution and both RMβCD pH solutions (unadjusted and pH 7.4 solution) showed significant alterations ($\alpha<0.05$) compared with the negative control (PBS), producing similar alterations as the positive control (ethanolic solution). The rest of the CD solutions did not produce alterations in corneal transparency, showing similar values to the negative control (α n.s.).
The unadjusted RMβCD aqueous solution showed acidic pH with values of 2.447±0.025, far out of the tear's supported pH range (6.5-8.5) increasing the likelihood of structural or functional damage (29). Solutions outside this pH range can produce direct cellular damage, disrupting junctional complexes and damaging the barrier function of the corneal endothelium (29). Additionally, acidic solutions can cause denaturation and precipitation of the proteins in the corneal epithelium and anterior stroma (30). These alterations can lead to changes in corneal transparency.
The fact that the neutralization of the RMβCD solution resulted in a minor change in transparency compared to the acidic pH RMβCD solution confirmed the role of the acidic pH in modifying corneal opacity.
The unadjusted αCD solution showed the lowest pH after the RMβCD solution (pH 4.577±0.070), however, it was found to be better supported by the cornea without altering transparency. Contrary to the case of the RMβCD solution, the adjustment of the αCD solution to pH 7.4 compromised the transparency of the cornea. This loss of transparency may be due to the interactions between the αCD with different membrane phospholipids and lipid components of the tear as explained below.

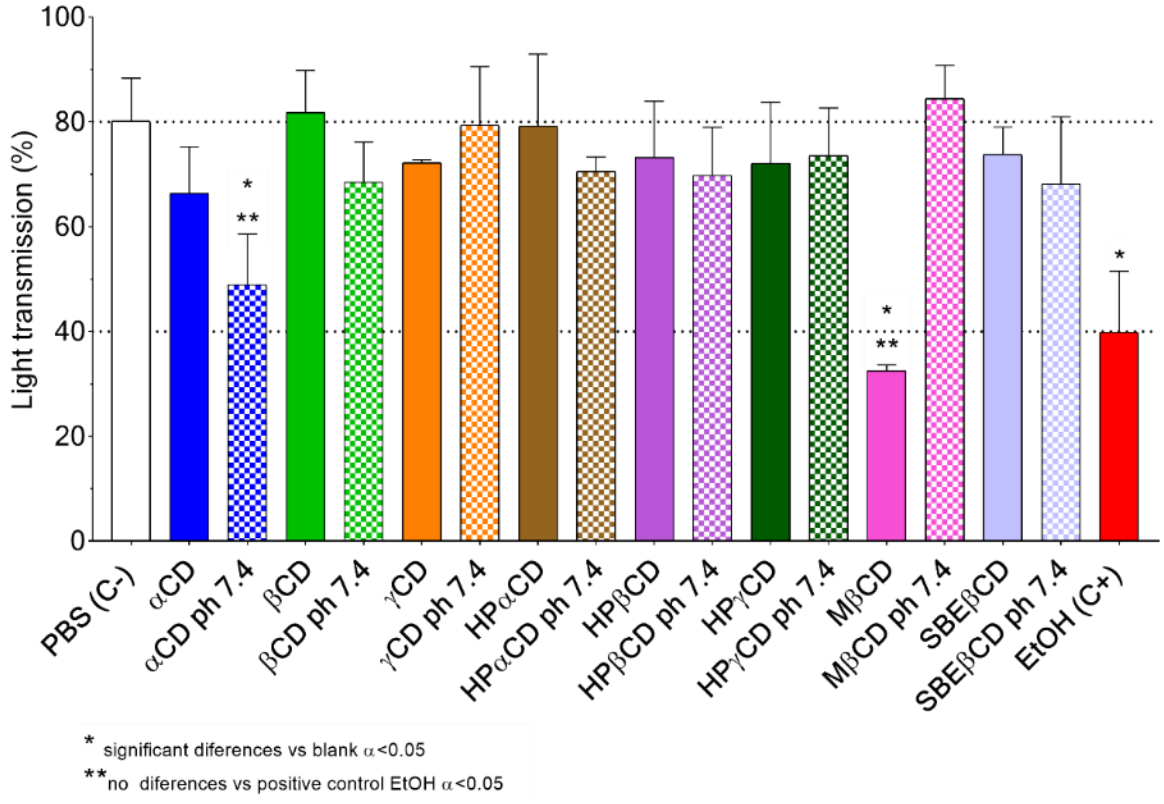

Figure 1. Opacity (Light transmission %) values of bovine corneas treated with CD solutions, PBS (negative control (C-)), EtOH (Positive control (C+)) after 10 min solutions treatment and 120 min PBS (C-). 100% of light transmission corresponds to total light transmitted through bovine cornea incubated in PBS.

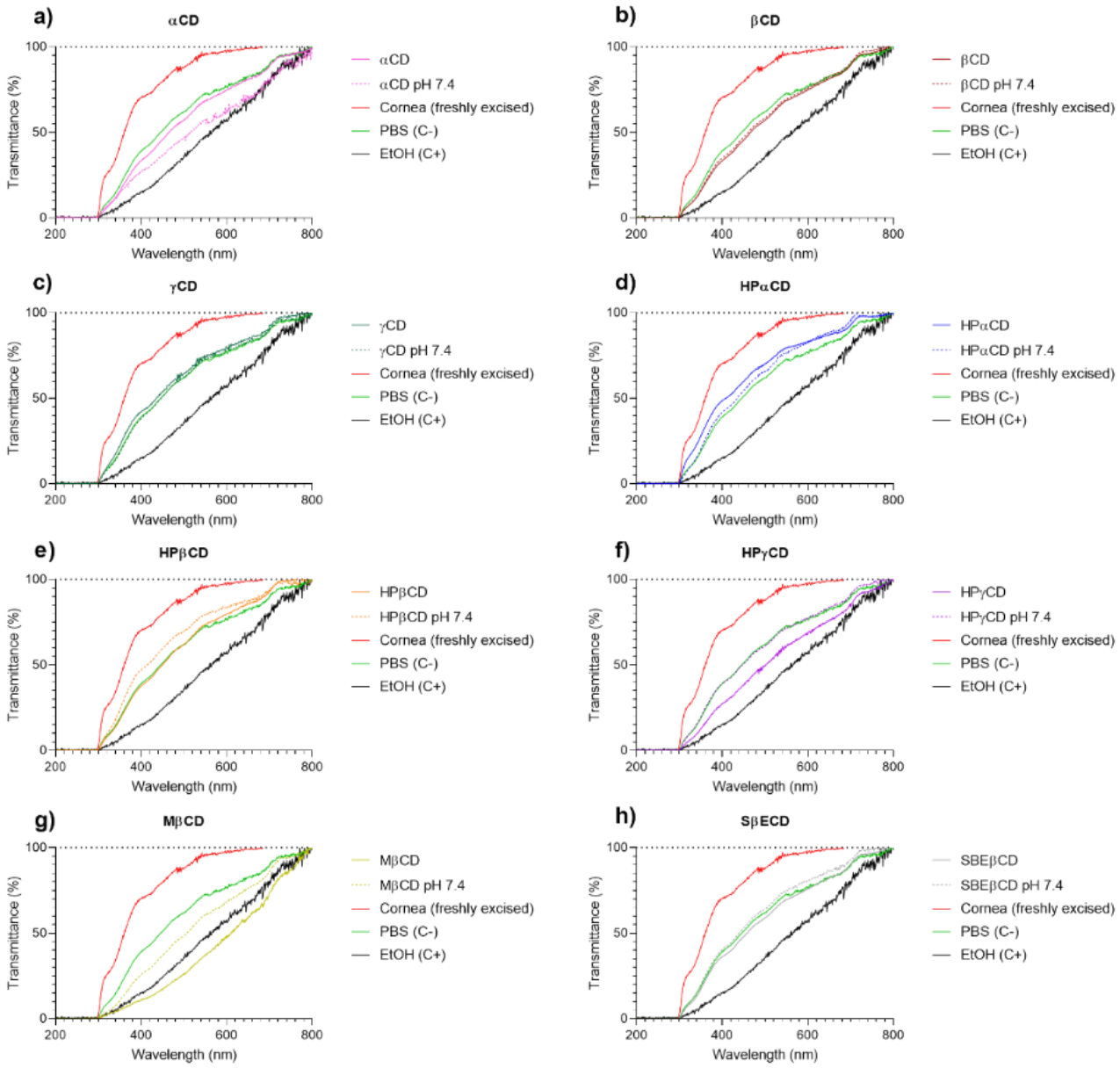

Figure 2. Transmittance values in the UV light spectrum (200 - 800 nm) obtained by treating the corneas for 10 min with the CD solutions: a) αCD, b) βCD, c) γCD, d) HPαCD, e) HPβCD, f) HPγCD, g) RMβCD and h) SBEβCD. Data were compared with positive control (EtOH C+), negative control (PBS C-) and freshly excised cornea.

4.2.2. CORNEAL PERMEABILITY

As can be observed in Figure 3, except for γCD at initial pH, all the CDs led to the passage of fluorescein through the cornea. There are numerous examples in the literature where cyclodextrins are able to increase the permeability of different drugs across the cornea and conjunctiva (6,31,32). Although cyclodextrins are large and hydrophilic molecules, unable to pass through the corneal epithelium, these cyclic oligosaccharides can interact with the epithelial cells, removing cholesterol and other lipid membrane components and promoting the

diffusion of smaller molecules (33). This reversible modification of the corneal permeability produced by CDs should be taken into account as an effective tool to improve the delivery of molecules with low transcorneal bioavailability.

High permeability values were observed for αCD and RMβCD, which were the CDs that also showed the greatest alterations in corneal transparency. Therefore, before their usage in ophthalmic formulations, their safety must be thoroughly studied by assessing their limiting concentrations.

A one-way ANOVA was performed, and no significant differences were found between the fluorescein permeability values of the CD solutions at initial pH and at pH 7.4. Furthermore, the ANOVA test showed that there were no significant differences between the solutions of the different CDs.

Finally, the BCOP studies confirmed that the rest of the CDs tested are safe for ocular administration up to the studied concentrations.

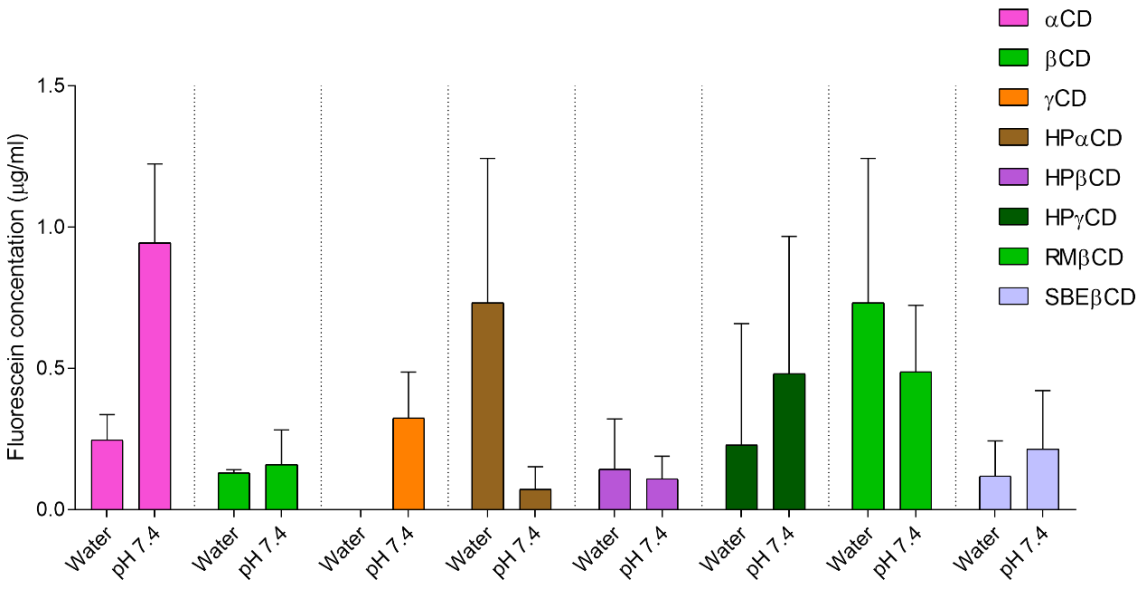

Figure 3. Fluorescein concentration in receptor medium after 90 of contact with corneas pretreated with cyclodextrin solutions.

4.3. HET-CAM

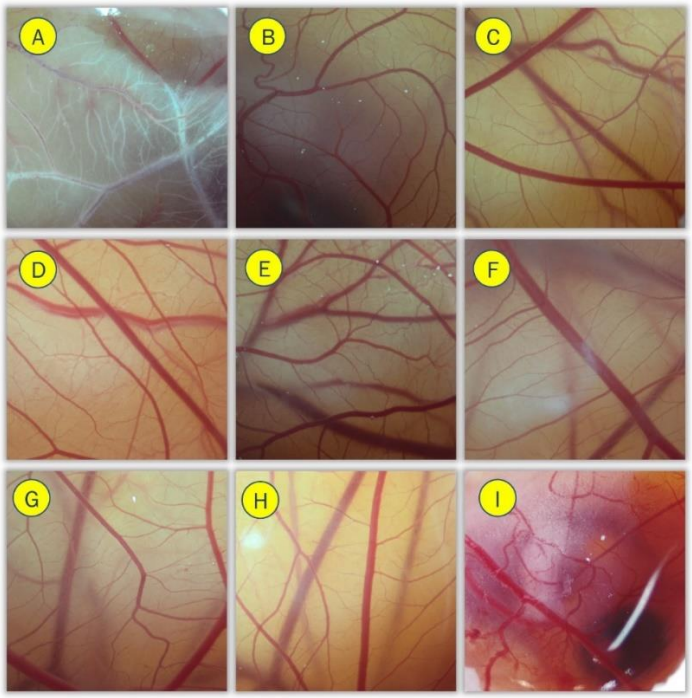

Figure 4. HET-CAM images 5 minutes post-instillation for the different CD solutions: A) 15% (w/v) αCD initial pH, B) 2% (w/v) βCD initial pH, C) 20% (w/v) ɣCD initial pH, D) 20% (w/v) HPαCD initial pH, E) 20% (w/v) HPβCD initial pH, F) 20% (w/v) HPɣCD initial pH, G) 20% (w/v) SBEβCD initial pH, H) 20% (w/v) MβCD initial pH and I) 15% (w/v) αCD pH 7.4.

Figure 4 shows the images of the chorioallantoic membrane (CAM) of the eggs instilled with CD solutions. According to the results obtained in the HET-CAM test, all aqueous solutions of CDs at the chosen concentrations were classified as non-irritant, as no hemorrhage, vascular lysis or coagulation processes were observed in the CAM after the solutions were in contact for 5 min.

However, upon contact of the unadjusted αCD solution and αCD pH 7.4 solution, a precipitation process was observed (Figure 4A and Figure 4I). This event was probably due to the precipitation of the insoluble inclusion complex formed between αCD and phospholipids present in the membrane of the endothelial cells from the blood vessels. The complexes between αCD and phospholipids present limited aqueous solubility and therefore tend to aggregate. Kluzec et al. demonstrated that αCD could interact with lipids, leading to their aggregation through a nucleation process followed by the growth of ordered, dense and insoluble stacks on the membrane (34). The intensity and reversibility of the process did not depend linearly on the concentration level of CD in solution. Takhiro Furune et al. demonstrated the appearance of a precipitate upon addition of a 5% (w/v) αCD solution in lecithin medium, suggesting the formation of a complex between αCD and lecithin (35). Wensheng Cai studied the complex formation with αCD and phosphatidylinositol, phosphatidylserine and phosphatidylethanolamine by molecular modelling and flexible docking showing the ability of

αCD to form complexes with lipids (36). In addition, another study showed that αCD has a greater ability to remove phospholipids from the cell membrane than any other CD (37).
The formation of these whitish aggregates could also be related to the change in transparency that occurred in the BCOP test upon contact with the αCD unadjusted and pH 7.4 solutions and to the change in corneal permeability.
However, the presence of other molecules that may also interact with αCD could modify this behavior. Previous works studied the ability of αCD to solubilize econazole in water and its ability to produce a mucoadhesive eye drop for the treatment of fungal keratitis (22). This study revealed strong interactions between the drug and αCD, especially in water, with high stability constant values ($K_{1:1}$~1000M-1). Under these conditions, the formation of the whitish precipitate was hardly observed in the HET-CAM studies, probably because econazole competed for the formation of a soluble complex with αCD, preventing the formation of phospholipids/αCD aggregates.

4.4. CORNEAL MUCOADHESIVENESS

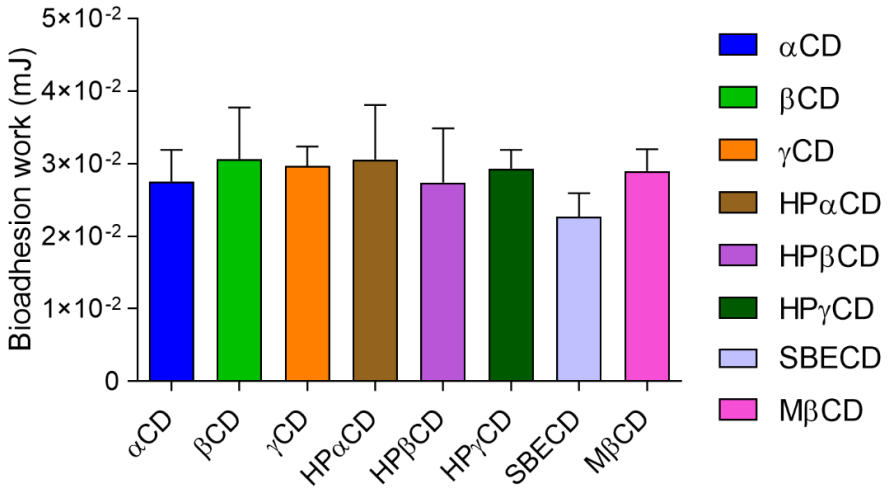

Figure 5. Bioadhesion work obtained for in bovine corneas.

The bioadhesion work data for all CD solutions are represented in Figure 5. All CD solutions showed similar bioadhesion work. A one-way ANOVA test was carried out, and no significant differences were identified.
The bioadhesion results were similar to those found for bioadhesive ophthalmic solutions using a similar method to determine bioadhesive capacity. Diaz Tomé et al (12) found values in the same range for bioadhesive ophthalmic solutions of voriconazole/HPβCD complex in hyaluronic acid or in ion sensitive hydrogels with gellan gum and kappa-carrageenan. Garcia Otero et al (8) obtained similar values in tacrolimus/HPβCD solutions containing polyvinyl alcohol as bioadhesive agent. At first glance these results suggested that at the concentrations studied the CD solutions had a high bioadhesive capacity almost similar to that obtained using mixtures of CD and mucoadhesive polymers.

To confirm the interaction capacity between CDs and the ophthalmic mucosa, additional *in vitro* mucoadhesion studies were performed.

4.5. *IN VITRO* MUCOADHESIVE TEST

The results of the *in vitro* mucoadhesive test are shown in Figure 6. The mucin dispersion (1 mg/mL) presented aggregates with a mean size of 564.2±28.87 nm and ζ-potential (ζ) values very close to electroneutrality (-3.215±0.19 mV) indicating that they hardly have surface charge in water. The different CDs also showed the formation of some aggregates, but the dynamic light scattering (DLS) signal indicated that they were formed in very low proportions. In all cases, the mixture of aqueous CD solutions with mucin dispersions resulted in an increase in the aggregate size, which is indicative of the interaction between the molecules of the aqueous dispersion.

Neutralization of the mucin to pH 7.4 resulted in an increase in aggregate size (2026±288 nm), probably due to the ionization of the sialic acid residues and amino acids that produces swelling of the mucin because of the repulsion between the negative electric charges.

However, the mixture of HPβCD with mucin at pH 7.4 resulted in a reduction in the aggregate size, suggesting that the ionization of the mucin reduced the intensity of the interactions with the CD. It is likely that the CDs interacted with the mucin chains by establishing hydrogen bonds with the different residues that were prevented by their ionization at pH 7.4.

In all cases, an increase in particle size was observed, which shows that the ζ values changed considerably in the case of αCD (-6.642 to -15.07) and HPγCD (-4.693 to -9.778). In the rest of the solutions the PZ did not change or became less negative, as in the case of HPαCD (PZ -7.8 to 0.47) or γCD (-7.56 to -4.42) among others.

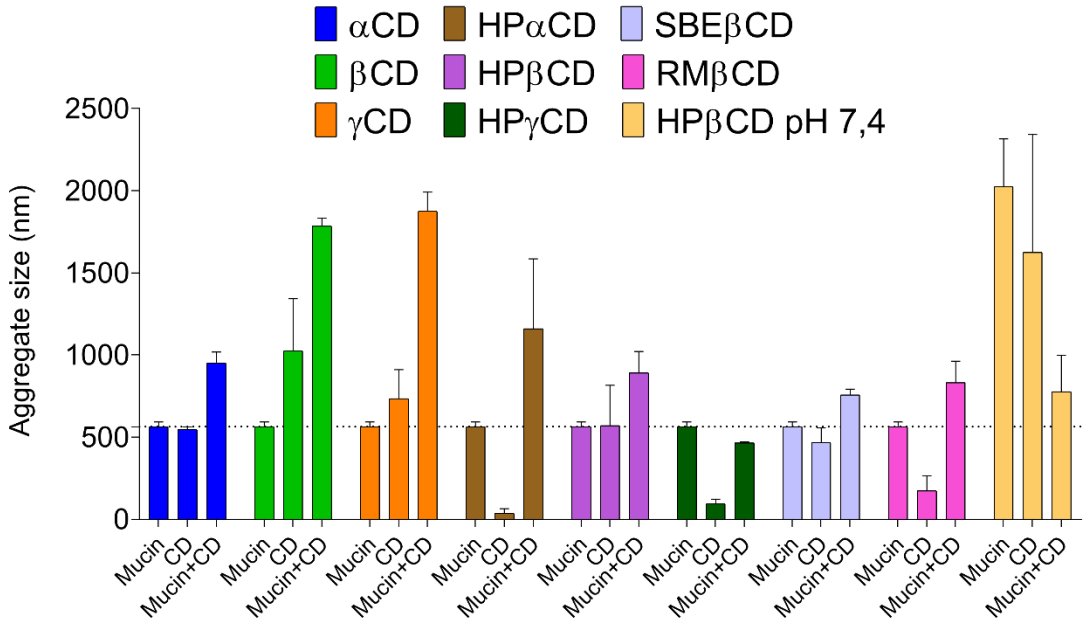

Figure 6. Interaction of mucin with different CD measured by DLS (data are presented as means ± SD).

4.6. *IN VIVO* PET/CT

The clearance ratio (Ct/Cinitial) results of the CD solutions from the ocular surface are shown in Figure 7. The pharmacokinetic parameters (AUC, MRT, $t_{1/2}$) obtained from the PET images are shown in Figure 7.

Figure 7 shows some of the images obtained by PET/CT at different times after administering the CD solutions to the animals. The profiles were fitted to a mono exponential equation to estimate the first order elimination constant kinetics and the non-compartmental pharmacokinetic parameters AUC, MRT and $t_{1/2}$ were calculated (Figure 8).

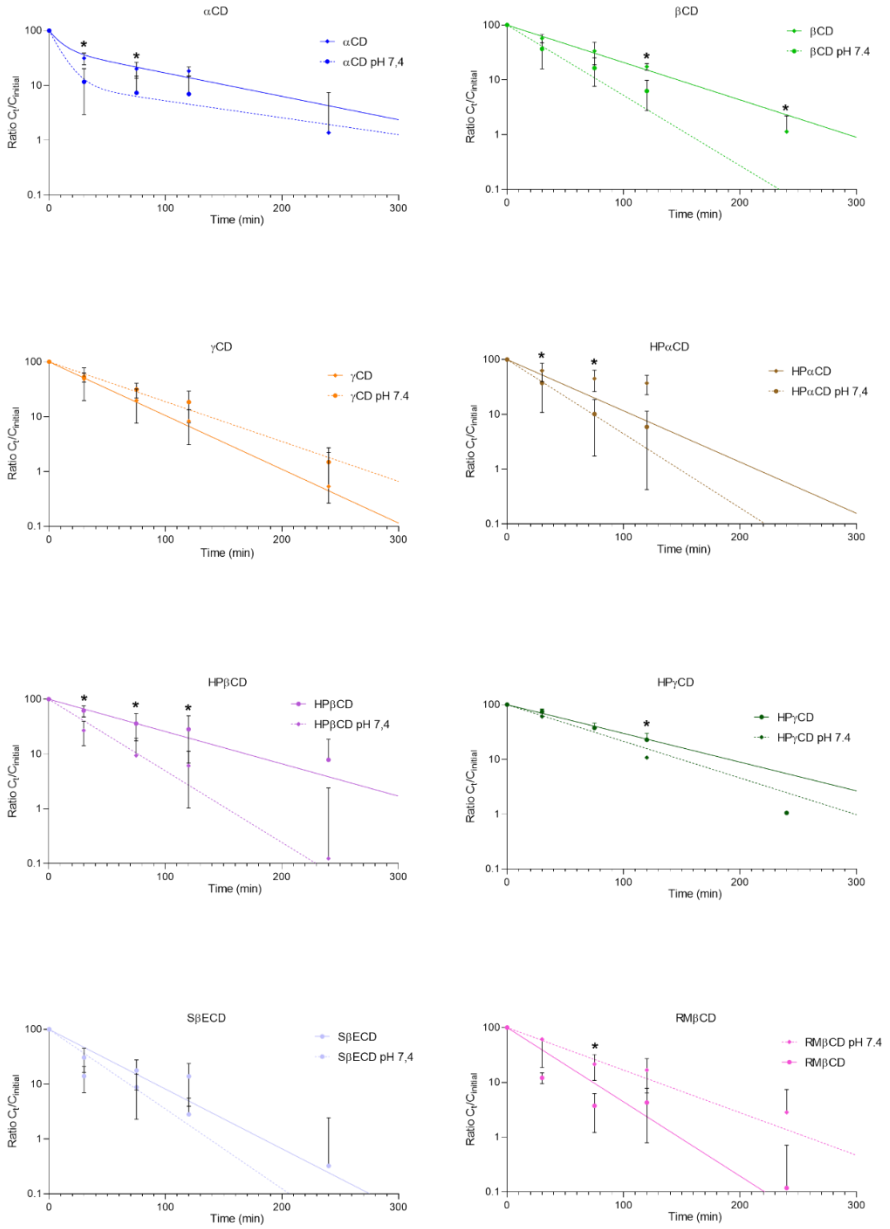

Figure 7. A) αCD, B) 2% (w/v) βCD, C) 20% (w/v) ɣCD, D) 20% (w/v) HPαCD, E) 20% (w/v) HPβCD, F) 20% (w/v) HPɣCD, G) 20% (w/v) SBβECD, H) 20% (w/v) MβCD clearance ratio at initial pH values and pH 7.4 from the ocular surface determination by PET Ratio CT/Cinitial was calculated assuming Cinitial value obtained in the Regions of Interest (ROI).

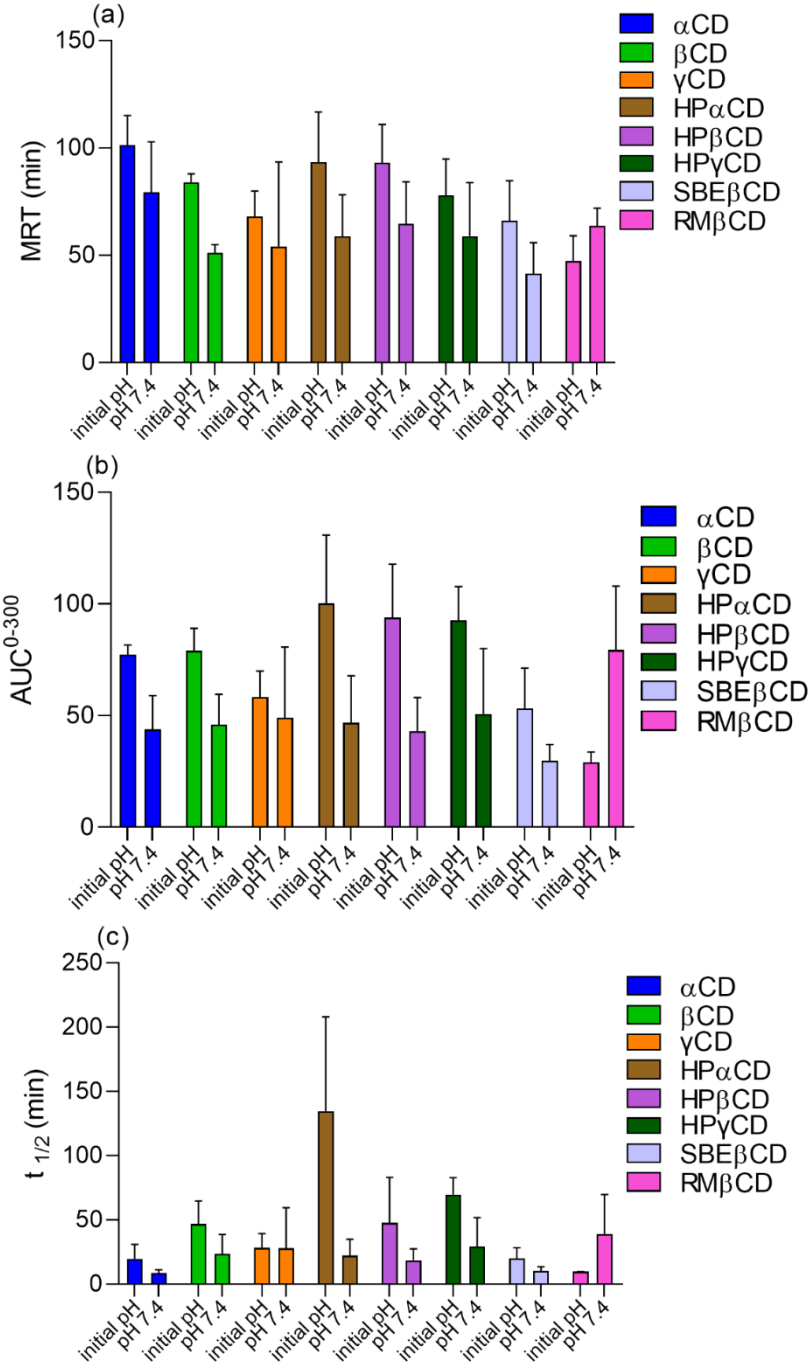

Figure 8. Pharmacokinetic parameters ((a)MRT, (b) $AUC_{0\text{-}300}$, (c) $t_{1/2}$) obtained by fitting the formulation percentage remaining in the eye over time by PET imaging.

A two-way ANOVA was performed with CD type and solution pH as factors to compare each of the pharmacokinetic parameters obtained in the PET study.

The highest MRT values were obtained for the αCD (101.270±13.770 min), HPαCD (93.303±23.426 min) and HPβCD (93.069±17.919 min) unadjusted solutions, although

significant differences ($\alpha<0.05$) in MRT values were only observed between HPβCD and RMβCD unadjusted solutions.

The high MRT value of the unadjusted αCD solution was probably due to the retention of the insoluble complexes between αCD and phospholipids of the corneal epithelium on the ocular surface which reduced the clearance of the radiolabeled probe.

The MRT decreased for all CD solutions when their pH was adjusted to 7.4, with the exception of RMβCD, whose MRT values went from 47.172±11.936 min to 63.635±8.278 min. The unadjusted RMβCD solution caused an increase in the tear flow and blink frequency of the animal due to the discomfort caused by its low pH (2.447±0.025). However, no signs of toxicity such as reddening, clouding or increased blinking were observed on the eye surface of rats after a single administration. This resulted in an increase in the clearance rate of the solution and as a consequence the MRT value for the RMβCD unadjusted solution was the lowest of all the CD solutions. When adjusting the RMβCD solution to pH 7.4, no significant difference in MRT values were observed with respect to other CD solutions.

The highest $t_{1/2}$ value was 134.759±73.313 min for HPαCD, followed by HPγCD (69.733±13.064 min) and HPβCD (47.502±35.449 min). This suggests that the hydroxylated CD solutions remained longer on the ocular surface. Significant differences were observed between the HPαCD unadjusted solution and the αCD, βCD, γCD, HPβCD, SBEβCD and RMβCD unadjusted solutions. At pH 7.4, no CD solution showed significant differences from the others in terms of $t_{1/2}$ values.

Comparing the MRT and $t_{1/2}$ values of the CD solutions with those previously published for formulations with bioadhesive capacity, the CDs showed excellent mucoadhesive capacity and equivalent residence times at the tested concentrations. Mucoadhesive solutions of voriconazole (12), voriconazole/natamycin (16) or tacrolimus (8) made with mixtures of HPβCD (20% (w/v)) and mucoadhesive polymers such as polyvinyl alcohol, hyaluronic acid, gellan gum or kappa-carrageenan showed MTR and $t_{1/2}$ values in the range of 50-120 min and 30-97 min respectively. Similarly, equivalent values for these two parameters were found in ocular permanence studies of polymeric nanoparticles (38), nanostructured lipid systems (39) and chitosan nanoparticles (10).

The mucoadhesion of CD solutions may be due to various processes that may occur when CD solutions come in contact with the ocular mucosa. Mucins are large, highly glycosylated glycoproteins. They have tandem repeats of amino acids such as serine, threonine and proline (40,41). These amino acids are linked via ester bonds to oligosaccharides such as sialic acid, the main oligosaccharide in ocular human mucin (42), N-acetylgalactosamine and N-acetylglucosamine (43). It is possible that sialic acid and amino acids form hydrogen bonds with the OH_2 and OH_3 protons of the broad side (secondary hydroxyl group) of CDs. Zoppi et al. in 2019 characterized a ternary inclusion complex between βCD, proline and ketoconazole by nuclear magnetic resonance spectroscopy. They concluded that ketoconazole bound to the βCD by inclusion in the CD cavity, while proline interacted with the OH_2 and OH_3 protons of the wide part of the CD (44).

The decrease in the permanence observed on the ocular surface of the CD solutions when adjusted to pH 7.4 may be due to a decrease in hydrogen bond formation generated by the

ionization of sialic acid (pKa 2.2). In addition, previous studies on gastric mucosa (41) have shown that mucins change conformation to form a highly viscous gel in acidic media. Thus, when administering CD solutions at pH 7.4, the mucin may lose viscosity due to swelling and expansion of the mucin. This swelling is due to the ionization of the acid groups with the consequent binding of water molecules, causing the mucin to expand and reducing its viscosity.

5. CONCLUSION

In this study was evaluated the potential of various CDs as vehicles to prepare safer and more effective ophthalmic topical forms. The biopharmaceutical characterization of the CD solutions showed that most of them met the necessary requirements for ophthalmic use. However, the unadjusted aqueous solutions of RMβCD had pH values outside the acceptable range for ocular solutions and were unsuitable. Similarly, SBEβCD resulted in hyper-osmolar solutions at the studied concentration, while the rest of CDs showed hypo-osmolar solutions close to the tear osmolarity.

Safety evaluations using BCOP and HET-CAM tests showed that except for unadjusted solutions of RMβCD and αCD, all the prepared vehicles were safe and non-irritating. CDs, except for unadjusted γCD solution, modified the corneal permeability of fluorescein but this effect was reversible and posed no risk to corneal integrity, as shown by several safe formulations containing CDs authorized for clinical use. However, more detailed studies are required to evaluate the toxicity of RMβCD and αCD and determine their usability for this route of administration.

In vitro and *in vivo* mucoadhesion studies demonstrated excellent ocular mucoadhesive capacity of CDs, which depended on the pH of the solution. CDs showed high mucoadhesive capacity resulting in high permanence times on the ocular surface, similar to highly mucoadhesive polymers. Thus, CDs can act as penetration promoters, improve ocular bioavailability of drugs, especially with low aqueous water solubility.

Furthermore, BCOP showed that none of the CDs modified corneal transparency at the stated concentration, except for RMβCD at the initial pH and αCD at pH 7.4, which was resolved by adjusting the pH of the solution. The HET-CAM study showed no hemorrhage, lysis, or coagulation for any CD, except for αCD (initial pH and pH 7.4) that showed a white precipitate, probably due to the formation of insoluble complexes with phospholipids present in the CAM.

In vitro and *in vivo* mucoadhesion studies suggested the capacity of the CDs to interact with the mucin present on the ocular surface. However, adjusting the pH of the solution to 7.4 may decrease the binding between the CDs and the ocular mucins, leading to a decrease in mucoadhesion. Overall, hydroxypropyl derivatives and gamma cyclodextrins showed the best characteristics among all the varieties studied to be used as vehicles in ophthalmic solutions.

BIBLIOGRAPHY

1. Brewster ME, Loftsson T. Cyclodextrins as pharmaceutical solubilizers. Adv Drug Deliv Rev. 30 de julio de 2007;59(7):645-66.
2. Loftsson T, Jarho P, Másson M, Järvinen T. Cyclodextrins in drug delivery. Expert Opin Drug Deliv. marzo de 2005;2(2):335-51.
3. European Medicines Agency (EMA). Background review for cyclodextrins used as excipients. noviembre de 2014;17.
4. Santana ACSGV, Nadvorny D, da Rocha Passos TD, de La Roca Soares MF, Soares-Sobrinho JL. Influence of cyclodextrin on posaconazole stability, release and activity: Improve the utility of the drug. J Drug Deliv Sci Technol. 1 de octubre de 2019;53:101153.
5. Loftsson T, Brewster ME. Pharmaceutical applications of cyclodextrins. 1. Drug solubilization and stabilization. J Pharm Sci. octubre de 1996;85(10):1017-25.
6. Abdelkader H, Fathalla Z, Moharram H, Ali TFS, Pierscionek B. Cyclodextrin Enhances Corneal Tolerability and Reduces Ocular Toxicity Caused by Diclofenac. Oxid Med Cell Longev. 2018;2018:5260976.
7. Loftsson T, Stefánsson E. Cyclodextrins and topical drug delivery to the anterior and posterior segments of the eye. Int J Pharm. 15 de octubre de 2017;531(2):413-23.
8. García-Otero X, Díaz-Tomé V, Varela-Fernández R, Martín-Pastor M, González-Barcia M, Blanco-Méndez J, et al. Development and Characterization of a Tacrolimus/Hydroxypropyl-β-Cyclodextrin Eye Drop. Pharmaceutics. 23 de enero de 2021;13(2):149.
9. Jóhannsdóttir S, Jansook P, Stefánsson E, Loftsson T. Development of a cyclodextrin-based aqueous cyclosporin A eye drop formulations. Int J Pharm. 30 de septiembre de 2015;493(1):86-95.
10. Varela-Fernández R, García-Otero X, Díaz-Tomé V, Regueiro U, López-López M, González-Barcia M, et al. Design, Optimization, and Characterization of Lactoferrin-Loaded Chitosan/TPP and Chitosan/Sulfobutylether-β-cyclodextrin Nanoparticles as a Pharmacological Alternative for Keratoconus Treatment. ACS Appl Mater Interfaces. 27 de enero de 2021;13(3):3559-75.
11. Jansook P, Loftsson T. Self-assembled γ-cyclodextrin as nanocarriers for enhanced ocular drug bioavailability. Int J Pharm. 25 de abril de 2022;618:121654.
12. Díaz-Tomé V, García-Otero X, Varela-Fernández R, Martín-Pastor M, Conde-Penedo A, Aguiar P, et al. In situ forming and mucoadhesive ophthalmic voriconazole/HPβCD hydrogels for the treatment of fungal keratitis. Int J Pharm. 15 de marzo de 2021;597:120318.
13. Grassiri B, Cesari A, Balzano F, Migone C, Kali G, Bernkop-Schnürch A, et al. Thiolated 2-Methyl-β-Cyclodextrin as a Mucoadhesive Excipient for Poorly Soluble Drugs: Synthesis and Characterization. Polymers. 3 de agosto de 2022;14(15):3170.
14. Budai-Szűcs M, Kiss EL, Szilágyi BÁ, Szilágyi A, Gyarmati B, Berkó S, et al. Mucoadhesive Cyclodextrin-Modified Thiolated Poly(aspartic acid) as a Potential Ophthalmic Drug Delivery System. Polymers. febrero de 2018;10(2):199.
15. Bíró T, Aigner Z. Current Approaches to Use Cyclodextrins and Mucoadhesive Polymers in Ocular Drug Delivery—A Mini-Review. Sci Pharm. septiembre de 2019;87(3):15.

16. Díaz-Tomé V, Bendicho-Lavilla C, García-Otero X, Varela-Fernández R, Martín-Pastor M, Llovo-Taboada J, et al. Antifungal Combination Eye Drops for Fungal Keratitis Treatment. Pharmaceutics. enero de 2023;15(1):35.
17. Saokham P, Muankaew C, Jansook P, Loftsson T. Solubility of Cyclodextrins and Drug/Cyclodextrin Complexes. Mol J Synth Chem Nat Prod Chem [Internet]. 11 de mayo de 2018 [citado 8 de septiembre de 2020];23(5). Disponible en: https://www.ncbi.nlm.nih.gov/pmc/articles/PMC6099580/
18. EUR-Lex - 02010L0063-20190626 - EN - EUR-Lex [Internet]. [citado 26 de abril de 2020]. Disponible en: https://eur-lex.europa.eu/legal-content/EN/TXT/?uri=CELEX%3A02010L0063-20190626
19. OECD. Test No. 437: Bovine Corneal Opacity and Permeability Test Method for Identifying i) Chemicals Inducing Serious Eye Damage and ii) Chemicals Not Requiring Classification for Eye Irritation or Serious Eye Damage [Internet]. Paris: Organisation for Economic Co-operation and Development; 2013 [citado 18 de enero de 2016]. Disponible en: http://www.oecd-ilibrary.org/content/book/9789264203846-en
20. ICCVAM. Recommended Test Method Protocol: Hen's Egg Test – Chorioallantoic Membrane (HET-CAM) Test Method. Obtained from [Internet]. 2010. Disponible en: https://ntp.niehs.nih.gov/iccvam/docs/protocols/ivocular-hetcam.pdf.
21. Haimhoffer Á, Dossi E, Béresová M, Bácskay I, Váradi J, Afsar A, et al. Preformulation Studies and Bioavailability Enhancement of Curcumin with a 'Two in One' PEG-β-Cyclodextrin Polymer. Pharmaceutics. octubre de 2021;13(10):1710.
22. Díaz-Tomé V, Luaces-Rodríguez A, Silva-Rodríguez J, Blanco-Dorado S, García-Quintanilla L, Llovo-Taboada J, et al. Ophthalmic Econazole Hydrogels for the Treatment of Fungal Keratitis. J Pharm Sci. mayo de 2018;107(5):1342-51.
23. Fernández-Ferreiro A, Silva-Rodríguez J, Otero-Espinar FJ, González-Barcia M, Lamas MJ, Ruibal A, et al. Positron Emission Tomography for the Development and Characterization of Corneal Permanence of Ophthalmic Pharmaceutical Formulations. Invest Ophthalmol Vis Sci. 1 de febrero de 2017;58(2):772-80.
24. Tiffany JM. The viscosity of human tears. Int Ophthalmol. noviembre de 1991;15(6):371-6.
25. Zhu H, Chauhan A. Effect of viscosity on tear drainage and ocular residence time. Optom Vis Sci Off Publ Am Acad Optom. agosto de 2008;85(8):715-25.
26. Willshire C, Buckley RJ, Bron AJ. Estimating basal tear osmolarity in normal and dry eye subjects. Contact Lens Anterior Eye J Br Contact Lens Assoc. febrero de 2018;41(1):34-46.
27. Boddu SHS, Gunda S, Earla R, Mitra AK. Ocular microdialysis: a continuous sampling technique to study pharmacokinetics and pharmacodynamics in the eye. Bioanalysis. marzo de 2010;2(3):487-507.
28. Bravo-Osuna I, Andrés-Guerrero V, Pastoriza Abal P, Molina-Martínez IT, Herrero-Vanrell R. Pharmaceutical microscale and nanoscale approaches for efficient treatment of ocular diseases. Drug Deliv Transl Res. 2016;6(6):686-707.

29. Gonnering R, Edelhauser HF, Van Horn DL, Durant W. The pH tolerance of rabbit and human corneal endothelium. Invest Ophthalmol Vis Sci. abril de 1979;18(4):373-90.
30. Kuckelkorn R, Schrage N, Keller G, Redbrake C. Emergency treatment of chemical and thermal eye burns. Acta Ophthalmol Scand. febrero de 2002;80(1):4-10.
31. Morrison PWJ, Connon CJ, Khutoryanskiy VV. Cyclodextrin-Mediated Enhancement of Riboflavin Solubility and Corneal Permeability. Mol Pharm. 4 de febrero de 2013;10(2):756-62.
32. Conde Penedo A, Díaz Tomé V, Fernández Ferreiro A, González Barcia M, Otero Espinar FJ. Enhancement in corneal permeability of riboflavin using cyclodextrin derivates complexes as a previous step to transepithelial cross-linking. Eur J Pharm Biopharm. 1 de mayo de 2021;162:12-22.
33. Moiseev RV, Morrison PWJ, Steele F, Khutoryanskiy VV. Penetration Enhancers in Ocular Drug Delivery. Pharmaceutics. julio de 2019;11(7):321.
34. Kluzek M, Schmutz M, Marques CM, Thalmann F. Kinetic evolution of DOPC lipid bilayers exposed to α-cyclodextrins. Soft Matter. 18 de julio de 2018;14(28):5800-10.
35. Furune T, Ikuta N, Ishida Y, Okamoto H, Nakata D, Terao K, et al. A study on the inhibitory mechanism for cholesterol absorption by α-cyclodextrin administration. Beilstein J Org Chem. 2014;10:2827-35.
36. Studies on the interaction of α-cyclodextrin with phospholipid by a flexible docking algorithm | Request PDF [Internet]. [citado 17 de noviembre de 2022]. Disponible en: https://www.researchgate.net/publication/238171403_Studies_on_the_interaction_of_a-cyclodextrin_with_phospholipid_by_a_flexible_docking_algorithm
37. Leclercq L. Interactions between cyclodextrins and cellular components: Towards greener medical applications? Beilstein J Org Chem. 7 de diciembre de 2016;12:2644-62.
38. Varela-Fernández R, García-Otero X, Díaz-Tomé V, Regueiro U, López-López M, González-Barcia M, et al. Mucoadhesive PLGA Nanospheres and Nanocapsules for Lactoferrin Controlled Ocular Delivery. Pharmaceutics. abril de 2022;14(4):799.
39. Varela-Fernández R, García-Otero X, Díaz-Tomé V, Regueiro U, López-López M, González-Barcia M, et al. Lactoferrin-loaded nanostructured lipid carriers (NLCs) as a new formulation for optimized ocular drug delivery. Eur J Pharm Biopharm. 1 de marzo de 2022;172:144-56.
40. Mantelli F, Argüeso P. Functions of ocular surface mucins in health and disease. Curr Opin Allergy Clin Immunol. octubre de 2008;8(5):477-83.
41. Boegh M, Nielsen HM. Mucus as a Barrier to Drug Delivery – Understanding and Mimicking the Barrier Properties. Basic Clin Pharmacol Toxicol. 2015;116(3):179-86.
42. Royle L, Matthews E, Corfield A, Berry M, Rudd PM, Dwek RA, et al. Glycan structures of ocular surface mucins in man, rabbit and dog display species differences. Glycoconj J. noviembre de 2008;25(8):763-73.
43. Henrich PB, Monnier CA, Halfter W, Haritoglou C, Strauss RW, Lim RYH, et al. Nanoscale topographic and biomechanical studies of the human internal limiting membrane. Invest Ophthalmol Vis Sci. 29 de junio de 2012;53(6):2561-70.

44. Zoppi A, Buhlman N, Cerutti JP, Longhi MR, Aiassa V. Influence of proline and β-Cyclodextrin in ketoconazole physicochemical and microbiological performance. J Mol Struct. 15 de enero de 2019;1176:470-7.

CONCLUSIONS

In this doctoral thesis we have carried out the design and development of different topical-ophthalmic formulations containing econazole, voriconazole or a combination of natamycin and voriconazole to improve the treatment of fungal keratitis:

Initially, two types of hydrogels containing econazole as an antifungal have been developed, which meet the requirements of the ophthalmic topical route in terms of pH and osmolality. Due to the low aqueous solubility of econazole, it was necessary to resort to its complexation with cyclodextrins to reach the required dose of antifungal in the eye drops. Of the DCs tested, αCD has shown the highest efficacy for drug hydrosolubilization. Nuclear magnetic resonance studies demonstrate the inclusion of the imidazole ring of econazole within the cavity of the αCD, forming stable inclusion complexes in solution. The solutions containing the econazole and αCD complexes showed inhibition values similar to those obtained with Vfend® (voriconazole solubilized with SBEβCD) and much higher than those observed with first choice drugs such as amphotericin or natamycin.

Ion-sensitive hydrogels and hyaluronic acid mucoadhesive hydrogels demonstrated good ability to prolong econazole release *in vitro* and to increase its corneal permeability *ex vivo*, allowing the drug to reach deeper tissues. *In vivo* permanence studies performed by PET/CT molecular imaging showed the high retention time of the hydrogels on the ocular surface compared to aqueous econazole solution.

During ophthalmic irritation studies using HET-CAM, no changes were observed in the blood vessels of the egg chorioallantoic membrane. However, a significant change in corneal transparency was observed by BCOP assay. Therefore, until more information is available on the origin and causes of these changes in transparency, these formulations should be used only in cases where other effective antifungals with similar activity (such as voriconazole) are not available or where treatment outweighs the risks associated with their use.

Secondly, two types of hydrogels of voriconazole have been successfully developed as a new alternative to the eye drops reformulated from injectables, which are used in hospital pharmacy services (Vfend®). Solubility and NMR results show that HPβCD is an excellent alternative for the hydrosolubilization of voriconazole that occurs due to the formation of a stable inclusion complex based on the internalization of the difluorophenyl ring of voriconazole in the cavity of HPβCD.

Ocular compatibility and toxicity studies of voriconazole hydrogels have demonstrated safety for administration on the ocular surface. The pH values, osmolarity or evaluation by BCOP and HET-CAM show their adaptation to the conditions of this route of administration.

In vitro release and *ex vivo* penetration studies show a zero-order kinetic profile for all voriconazole hydrogels and excellent transcorneal permeability respectively. In addition, *ex vivo* bioadhesion and *in vivo* ocular permanence studies by PET/CT molecular imaging confirm the excellent mucoadhesive properties of both ion-sensitive hydrogels made from 1:1 mixtures of gellan gum and 0.65% (w/v) kappa carrageenan and hyaluronic acid hydrogel. Based on these results, it can be concluded that the two types of ophthalmic voriconazole hydrogels developed have great potential to improve the treatment of fungal keratitis based on their good capacity for controlled drug release and their high ocular permanence, which should allow a decrease in the number of applications and favor adherence to the patient's treatment.

Third, hydrogels combining natamycin and voriconazole have been developed as a new alternative to improve the efficacy of topical treatment of fungal keratitis. Solubility and NMR studies demonstrated the formation of stable complexes between natamycin and HPβCD in which the double bonds of natamycin are arranged toward the more hydrophobic side of the cyclodextrin and the polar rings on the more hydrophilic side. Furthermore, NMR results confirmed that natamycin competes with voriconazole for the same binding site in the HPβCD cavity. Characterization of this competition allowed us to optimize the concentration of cyclodextrin in the hydrogels to avoid precipitation problems.

Transmission electron microscopy confirmed the formation of spherical nano-aggregates of natamycin and voriconazole inclusion complexes. Published studies suggest that these aggregates can control drug release, improve ocular residence time and increase its permeability across the cornea.

The pH, osmolality, viscosity and transparency values of the combined hydrogels within the accepted range for topical ophthalmic formulations and the ocular irritation studies performed (BCOP and HET-CAM) confirmed that the formulations are safe for ophthalmic administration. In addition, they demonstrated a significant improvement in the permeability of natamycin in the presence or absence of corneal epithelium compared to Natacyn®.

Ex vivo and *in vivo* mucoadhesion studies show excellent bioadhesive capabilities of the hydrogles and suggest that the mucoadhesive ability of the formulations is largely due to the presence of HPβCD at high concentration and is not increased by the addition of HA or PVA. Furthermore, *in vitro* antifungal effectiveness studies confirmed the ability of the inclusion complexes to effectively inhibit the growth of several fungal species.

Therefore, the obtained results allow us to conclude that the developed formulations of natamycin and voriconazole could significantly improve the treatment of fungal keratitis. Furthermore, the developed hydrogels have the ability to be formulated using only one of the antifungals or combining both, which makes them a very versatile pharmaceutical system that can be adapted to meet different patient needs. Due to the broad spectrum covered by the combination of both antifungals they could be used as first choice treatment in cases of fungal keratitis where the causative agent is unknown, species resistant to one of the antifungal agents are suspected or no commercial drug is available.

Finally, in the last section of this doctoral thesis we have addressed the characterization of the bioadhesive and ophthalmic safety properties of solutions of different cyclodextrin types at high concentrations. The results have shown that most of them meet the requirements for ophthalmic use. However, some cyclodextrin types fall outside the desirable parameters for ophthalmic formulations. Aqueous solutions of RMβCD at 20% (w/v) presented acidic pH values, outside the accepted range for ophthalmic formulations. Similarly, 20% (w/v) SBEβCD dilutions in water and in PBS produced hyperosmolar dilutions. Safety evaluations using the BCOP and HET-CAM tests showed that, except for the unadjusted 20% (w/v) RMβCD and 15% (w/v) αCD dilutions, the rest of the vehicles studied were safe and non-irritating. The 15% (w/v) dilutions of αCD in water or neutralized at pH 7.4 formed an off-white precipitate on CAM, probably due to the formation of insoluble complexes with the phospholipids present in CAM. This phenomenon is also what probably caused the observed change in corneal transparency in

the BCOP assay. The modification in corneal transparency caused by econazole eye drops described in the first chapter, is probably due to this same phenomenon. In the case of RMβCD 20% (w/v) in water, the modification of corneal transparency was resolved by adjusting the pH to 7.4. *In vitro* and *in vivo* mucoadhesion studies demonstrated excellent mucoadhesive capacity for all DCs. However, this capacity is dependent on the final pH of the solution, and a decrease in the permanence of the solutions adjusted to pH 7.4 was observed, probably due to a lower interaction through hydrogen bonds between the mucin and the DCs. In short, hydroxypropyl derivatives and γCD showed the best characteristics among all the varieties studied for use as vehicles in ophthalmic solutions.

En esta tesis doctoral se ha llevado a cabo el diseño y desarrollo de diferentes formulaciones tópico-oftálmicas que contienen econazol, voriconazol o una combinación de natamicina y voriconazol para mejorar el tratamiento de queratitis fúngicas:

Inicialmente se han desarrollado dos tipos de hidrogeles conteniendo econazol como antifúngico, que cumplen las exigencias de la vía tópica oftálmica en cuanto a pH y osmolaridad. Debido a la baja solubilidad acuosa del econazol fue necesario acudir a su complejación con ciclodextrinas para alcanzar la dosis necesaria de antifúngico en los colirios. De las CD ensayadas, la αCD ha sido la que ha mostrado la mayor eficacia para la hidrosolubilización del fármaco. Los estudios de resonancia magnética nuclear demuestran la inclusión del anillo imidazol del econazol dentro de la cavidad de la αCD, formando complejos de inclusión estables en disolución. Las disoluciones conteniendo los complejos de econazol y αCD mostraron valores de inhibición similares a los obtenidos con Vfend® (voriconazol solubilizado con SBEβCD) y muy superiores a los observados en los fármacos de primera elección como anfotericina o natamicina.
Los hidrogeles ión-sensible y los mucoadhesivos de ácido hialurónico demostraron buena capacidad para prolongar la liberación del econazol *in vitro* y para aumentar su permeabilidad corneal *ex vivo*, permitiéndole al fármaco alcanzar tejidos más profundos. Los estudios de permanencia *in vivo* realizados mediante imagen molecular PET/CT mostraron el elevado tiempo de retención de los hidrogeles en la superficie ocular en comparación con la disolución acuosa de econazol.
Durante los estudios de irritación oftálmica mediante HET-CAM no se observaron modificaciones en los vasos sanguíneos de la membrana corioalantoidea del huevo. Sin embargo, se ha observado un cambio importante en la transparencia corneal mediante el ensayo BCOP. Por lo tanto y mientras que no se dispongan de más información del origen y causas de estos cambios en la transparencia, estas formulaciones deben utilizarse exclusivamente en casos en que no se dispongan de otros antifúngicos efectivos con actividad similar (como el voriconazol) o en el caso de que el tratamiento supere los riesgos asociados a su utilización.

En segundo lugar, se han desarrollaron con éxito dos tipos de hidrogeles mucoadhesivos de voriconazol como una nueva alternativa al colirio reformulado a partir de los inyectables, que se emplea en los servicios de farmacia hospitalaria (Vfend®). Los resultados de solubilidad y RMN muestran que la HPβCD es una excelente alternativa para la hidrosolubilización del voriconazol que se produce gracias a la formación de un complejo de inclusión estable basado en la internalización del anillo difluorofenilo del voriconazol en la cavidad de la HPβCD.
Los estudios de compatibilidad y toxicidad ocular de los hidrogeles de voriconazol han demostrado seguridad para ser administrados en la superficie ocular. Los valores de pH, osmolaridad o la evaluación mediante BCOP y HET-CAM muestran su adaptación a las condiciones de esta vía de administración.
Los estudios de liberación *in vitro* y de penetración *ex vivo* muestran un perfil cinético de orden cero para todos los hidrogeles de voriconazol y una excelente permeabilidad transcorneal respectivamente. Además, los estudios de bioadhesión *ex vivo* y de permanencia ocular *in vivo*

mediante imagen molecular PET/CT confirman las excelentes propiedades mucoadhesivas, tanto de los hidrogeles ión-sensible elaborados a partir de mezclas 1:1 de goma gellan y carragenato kapa al 0,65% (p/v) como del hidrogel de ácido hialurónico. En base a estos resultados, se puede concluir que los dos tipos de hidrogeles oftálmicos de voriconazol desarrollados poseen un gran potencial para mejorar el tratamiento de la queratitis fúngica basada en su buena capacidad de liberación controlada del fármaco y su elevada permanencia ocular, que debería permitir una disminución del número de aplicaciones y favorecer la adherencia al tratamiento del paciente

En tercer lugar, se han desarrollado hidrogeles combinando natamicina y voriconazol como una nueva alternativa para mejorar la eficacia del tratamiento tópico de la queratitis fúngica. Los estudios de solubilidad y RMN demostraron la formación de complejos estables entre la natamicina y la HPβCD en los que los dobles enlaces de la natamicina se disponen hacia el lado más hidrófobo de la ciclodextrina y los anillos polares en el lado más hidrófilo. Además, los resultados de RMN confirmaron que la natamicina compite con el voriconazol por el mismo sitio de unión en la cavidad de la HPβCD. La caracterización de esta competición nos ha permitido optimizar la concentración de la ciclodextrina en los hidrogeles para evitar problemas de precipitación.

Mediante microscopía electrónica de transmisión se pudo confirmar la formación de nanoagregados esféricos de los complejos de inclusión de natamicina y voriconazol. Estudios publicados sugieren que estos agregados pueden controlar la liberación del fármaco, mejorar el tiempo de residencia ocular y aumentar su permeabilidad a través de la córnea.

Los valores de pH, osmolalidad, viscosidad y transparencia de los hidrogeles combinados dentro del intervalo aceptado para formulaciones tópicas oftálmicas y los estudios de irritación ocular realizados (BCOP y HET-CAM) confirmaron que las formulaciones son seguras para su administración oftálmica. Además, demostraron una mejora significativa en la permeabilidad de la natamicina en presencia o ausencia de epitelio corneal en comparación con el Natacyn®.

Los estudios de mucoadhesión *ex vivo* e *in vivo* muestran unas excelentes capacidades bioadhesivas de los hidrogles y sugirieren que la capacidad mucoadhesiva de las formulaciones se debe en gran medida a la presencia de HPβCD en alta concentración y no aumenta por la adición de HA o PVA. Además, los estudios de efectividad antifúngica *in vitro* confirmaron la capacidad de los complejos de inclusión para inhibir de forma efectiva el crecimiento de varias especies fúngicas.

Por lo tanto, los resultados obtenidos nos permiten concluir que las formulaciones de natamicina y voriconazol desarrolladas podrían mejorar significativamente el tratamiento de la queratitis fúngica. Además, los hidrogeles desarrollados tienen la capacidad de formularse empleando uno solo de los antifúngicos o combinando ambos, lo que los convierte en un sistema farmacéutico muy versátil que puede adaptarse para satisfacer las diferentes necesidades de los pacientes. Debido al amplio espectro que cubre la combinación de ambos antifúngicos podrían ser utilizadas como tratamiento de primera elección en casos de queratitis fúngica en los que se desconozca el agente causal, se sospeche de especies resistentes a uno de los agentes antifúngicos o no se disponga de ningún fármaco comercial.

Finalmente, en la última sección de esta tesis doctoral hemos abordado la caracterización de las propiedades bioadhesivas y de seguridad oftálmica de disoluciones de diferentes variedades de ciclodextrina en concentraciones elevadas. Los resultados han demostrado que la mayoría de ellas cumplen los requisitos requeridos para su uso oftálmico. Sin embargo, algunas variedades se sitúan fuera de los parámetros deseables para formulaciones oftálmicas. Las disoluciones acuosas de RMβCD al 20% (p/v) presentaron valores ácidos de pH, fuera del rango aceptado para las formulaciones oftálmicas. Del mismo modo, las disoluciones de SBEβCD al 20% (p/v) en agua y en PBS producen disoluciones hiperosmolares. Las evaluaciones de seguridad mediante las pruebas de BCOP y HET-CAM, mostraron que, excepto las disoluciones no ajustadas de RMβCD al 20% (p/v) y de αCD al 15% (p/v), el resto de los vehículos estudiados eran seguros y no irritantes. Las disoluciones al 15% (p/v) de αCD en agua o neutralizadas a pH 7,4, formaron un precipitado blanquecino sobre la CAM, probablemente debido a la formación de complejos insolubles con los fosfolípidos presentes en la CAM. Este fenómeno es también el que causó probablemente la modificación observada en la trasparencia corneal en el ensayo de BCOP. La modificación en la transparencia corneal ocasionada por los colirios de econazol descrita en el primer cápitulo, se debe probablemente a este mismo fenómeno. En el caso de la RMβCD al 20% (p/v) en agua, la modificación de la transparencia corneal se resolvió al ajustar el pH a 7,4. Los estudios de mucoadhesión *in vitro* e *in vivo*, demostraron una excelente capacidad mucoadhesiva para todas las CD. Sin embargo, esta capacidad es dependiente del pH final de la solución, observándose una disminución en la permanencia de las soluciones ajustadas a pH 7,4, probablemente debida a una menor interacción mediante puentes de hidrógeno entre la mucina y las CD. En definitiva, los derivados hidroxipropílicos y la γCD mostraron las mejores características entre todas las variedades estudiadas para ser utilizadas como vehículos en soluciones oftálmicas.

APPENDIX

CONFLICT OF INTEREST

The doctoral student declares that there is no conflict of interest regarding the doctoral thesis.

ANIMAL EXPERIMENTS

In the present thesis, male adult Sprague-Dawley rats with a 200-300 g average weight were used, supplied by the animal facility of the University of Santiago de Compostela (Santiago de Compostela, Spain). During the experiments, the animals were kept in individual cages with free access to food and water in a room under controlled temperature (22 ± 1°C) and humidity (60 ± 5%) and with day–night cycles regulated by artificial light (12/12 hours). The animals were reated according to the guidelines for the care and use of laboratory animals. Animal experiments complied with the ARRIVE guidelines (Kilkenny C, Browne WJ, Cuthill IC, Emerson M, Altman DG. Improving bioscience research reporting: the ARRIVE guidelines for reporting animal research. PLoS Biol. 2010 Jun 29;8(6):e1000412.). Experiments were performed at the Preclinical Imaging Service of the Experimental Biomedicine Center (CEBEGA) (REGA number: ES150780292901). Experiments were approved by the Conselleria de Medio Rural da Xunta de Galicia (15012/2021/001 and 15010/2019/006) and were authorized by the Animal Research Committee of the Health Research Institute of Santiago de Compostela (IDIS). They followed the Spanish and European Union (EU) regulations for animal experimentation (86/609/CEE, 2003/ 65/CE, 2010/63/EU, and RD53/2013).

FUNGDING AND ACKNOWLEDGEMENTS

This thesis has been partially funded by RETICS Oftared, RD16/0008/0003 and RD12/0034/0017 and co-funded by the European Union, Axencia Galega Innovación (Grupos de Potencial Crecimiento IN607B2020/11, Grupo de Referencia Competitiva ED431C2021/26 and Proyectos de Excelencia IN607D 2021/001) and Spanish Ministry of Science, Innovation and Universities (RTI2018-099597-B-100). In addition, the PhD student is grateful for the funding of the contract obtained with Faes Farma through IDIS.

ARTICLES DERIVED FROM THIS THESIS

In compliance with the rules of doctoral studies at Universidade de Santiago de Compostela in Regulamento dos estudos de doutoramento na USC, DOG de 16 de Setembro de 2020, it was provided some information regarding the articles on which this work is based and the journals that published those articles. In particular it was given the names of the authors, the title of the journals, the year each article was published, the publisher, the DOI-type link, the Journal Impact Factor and the quartile from the Journal Citation Reports, some relevant information regarding copyright and use of the articles and the author contribution.

- **INTRODUCTION**

  BOOK TITLE: Mycotic Keratitis© 2019
  EDITORS: Mahendra Rai, Marcelo Luis Occhiutto
  AUTHORS: Victoria Díaz Tomé, María Teresa Rodríguez Ares, Rubén Varela Fernández, Rosario Touriño Peralba, Miguel González Barcia, Laura Martínez Pérez, María Jesús Lamas, Francisco J. Otero Espinar, Anxo Fernández Ferreiro.
  CHAPTER TITLE: Therapeutic Approach in Fungal Keratitis © 2019
  YEAR: 2019

PUBLISHER: Taylor & Francis Group
LINK: https://doi.org/10.1201/9780429021473
INFORMATION REGARDING COPYRIGHT AND USE:
Title: 9780367075934 | Mycotic Keratitis | Edn. 1 | Hardback
Material requested: Chapter 13 pg.189-216
Territory: World
Rights: A&Q
Language: English
Format: Print and online
Academic Institution: University of Santiago de Compostela
Name of Course of Study: Research Pharmacist
Title of Dissertation or Thesis: Unknown
Terms & Conditions:
1. Permission is non-transferable and granted on a one-time, non-exclusive basis.
2. Permission is for non-exclusive, INSERT language rights, and covers academic, non-commercial use in printed or electronic format only. Any further use (including, but not limited to any publication, storage, distribution, transmission or reproduction) that is not directly related to the fulfilment of the specific academic requirements that are the subject of this request shall require a separate application for permission.
3. Permission extends only to material owned or controlled by Taylor & Francis. Please check the credits in our title for material in which the copyright is not owned or controlled by us. If another source is acknowledged then you must apply to the owner of the copyright for permission to use this material.
4. Each copy containing our material must bear the following credit line, including full details of the figure/page numbers where relevant, the title, edition, author(s) or editor(s), year of publication and imprint (e.g. Routledge, Psychology Press or CRC Press): From: Title, Edition by Author(s)/Editor(s), Copyright (insert © Year) by Imprint. Reproduced by permission of Taylor & Francis Group.
5. Except as permitted in law, Taylor & Francis Group reserves all rights not specifically granted under this permission
AUTHOR CONTRIBUTION: The contributions of the Ph.D. candidate were essential in all the included articles. The candidate contributed to the design of the research and proofs, to the analysis of the results and to the writing of the manuscripts.

- **CHAPTER 1**

TITLE: Ophtalmic Econazole Hydrogels for the treatment of Fungal Keratitis
AUTHORS: Victoria Díaz Tomé, Andrea Luaces Rodríguez, Jesús Silva Rodríguez, Sara Blanco Dorado, Laura García Quintanilla, José Llovo Taboada, José Blanco Méndez, Xurxo García Otero, Rubén Varela Fernández, Michel Herranz, María Gil Martínez, María Jesús Lamas, Miguel González Barcia, Francisco J. Otero Espinar, Anxo Fernández Ferreiro.
JOURNAL: Journal Of Pharmaceutical Sciences
YEAR: 2018
PUBLISHER: ELSEVIER
LINK: https://doi.org/10.1016/j.xphs.2017.12.028
JOURNAL IMPACT FACTOR: 3.197 (Q2)

INFORMATION REGARDING COPYRIGHT AND USE:
AUTHOR CONTRIBUTION: The contributions of the Ph.D. candidate were essential in all the included articles. The candidate contributed to the design of the research and proofs, to the analysis of the results and to the writing of the manuscripts.

- **CHAPTER 2**

TITLE: *In situ* Forming and Mucoadhesive Ophthalmic Voriconazole/HPβCD Hydrogels for the treatment of Fungal Keratitis
AUTHORS: Victoria Díaz Tomé, Xurxo García Otero, Rubén Varela-Fernández, Manuel Martín Pastor, Andrea Conde Penedo, Pablo Aguiar, Miguel González Barcia, Anxo Fernández Ferreiro, Francisco J. Otero Espinar.
JOURNAL: International Journal of Pharmaceutics
YEAR: 2021
PUBLISHER: ELSEVIER
LINK: https://doi.org/10.1016/j.ijpharm.2021.120318
JOURNAL IMPACT FACTOR: 6.510 (Q1)
INFORMATION REGARDING COPYRIGHT AND USE: Please note that, as the author of this Elsevier article, you retain the right to include it in a thesis or dissertation, provided it is not published commercially. Permission is not required, but please ensure that you reference the journal as the original source.
AUTHOR CONTRIBUTION: The contributions of the Ph.D. candidate were essential in all the included articles. The candidate contributed to the design of the research and proofs, to the analysis of the results and to the writing of the manuscripts.

- **CHAPTER 3**

TITLE: Antifungal Combination Eye Drops for Fungal Keratitis Treatment
AUTHORS: Victoria Díaz Tomé, Carlos Bendicho Lavilla, Xurxo García Otero, Rubén Varela Fernández, Manuel Martín Pastor, José Llovo Taboada, Pilar Alonso Alonso, Pablo Aguiar, Miguel González Barcia, Anxo Fernández Ferreiro, Francisco J. Otero Espinar.
JOURNAL: Pharmaceutics
YEAR: 2022
PUBLISHER: MDPI
LINK: https://doi.org/10.3390/pharmaceutics15010035
JOURNAL IMPACT FACTOR:6.525 (Q1)
INFORMATION REGARDING COPYRIGHT AND USE: Information about permissions can be found on the website: https://www.mdpi.com/authors/rights where the following statement is placed:
"For all articles published in MDPI journals, copyright is retained by the authors. Articles are licensed under an open access Creative Commons CC BY 4.0 license, meaning that anyone may download and read the paper for free. The article may be reused and quoted provided that the original published version is cited."

AUTHOR CONTRIBUTION: The contributions of the Ph.D. candidate were essential in all the included articles. The candidate contributed to the design of the research and proofs, to the analysis of the results and to the writing of the manuscripts.

FIGURES AUTHORSHIP

The author declares that all unreferenced figures of this thesis are of his authorship.

Dr. José Castillo Sánchez, acting as Scientific Director of the Health Research Institute of Santiago de Compostela (IDIS),

To whom it may concern,

The research project entitled "*Técnicas de Imagen Molecular farmacocinéticas para la determinación de posologías oftálmicas de diferentes vehículos oculares en ratas Sprawey-Dawley*", presented by the researcher Dr. Anxo Fernández Ferreiro has been evaluated positively and, acting as Institutional Committee for the revision animal experimentation ethical issues, CERTIFIES:

1. That the project is feasible in all its aspects, and appropriate for the scientific development of the center.
2. That those aspects of the research involving the use of research animals are in agreement with the current legislation according to the European Union (EU) and Spanish rules (86/609/CEE, 2003/65/CE, 2010/63/EU, RD 1201/2005 and RD53/2013), about protection of animals used for research and other scientific means.

Signed:

Dr. José Castillo Sánchez.
Scientific Director of IDIS
12/07/2017

USC
UNIVERSIDADE DE SANTIAGO DE COMPOSTELA

XUNTA DE GALICIA
CONSELLERÍA DO MEDIO RURAL

Xefatura Territorial
Sº de Gandaría
Edificio administrativo Monelos, 4º andar
Rúa Vicente Ferrer, Nº 2
15008 A Coruña
Tfno.: 981 184 565
Correo electrónico: servizo.gandaria.a.coruna@xunta.gal

galicia

RESOLUCIÓN DE AUTORIZACIÓN DE PROXECTO DE EXPERIMENTACIÓN ANIMAL

Expediente núm.: 15012/2021/001
Persoa solicitante: Anxo Vidal Figueroa
Forma de inicio: solicitude da persoa interesada

Data de inicio do expediente: 28.2.2021
Procedemento: resolución de autorización

ANTECEDENTES

A persoa solicitante presentou con data 28.2.2021 unha solicitude para a realización do proxecto de experimentación animal (entrada no Rexistro Electrónico da Xunta de Galicia 2021/430700), cuxos datos se detallan a continuación:

Denominación do proxecto: *Estudo da farmacocinética intravítrea de anticorpos marcados con circonio-89 mediante inxección intravítrea en ratas*

Nome do centro usuario: Centro de Biomedicina Experimental (CEBEGA) da Universidade de Santiago de Compostela
Persoa responsable do proxecto: Anxo Fernández Ferreiro

Establecemento onde se realizarán os procedementos do proxecto (ou lugar xeográfico no caso de traballos de campo): Centro de Biomedicina Experimental (CEBEGA)

Clasificación do proxecto : Tipo I [ ] Tipo II [X] Tipo III [ ]

CONSIDERACIÓNS LEGAIS E TÉCNICAS

1 O Real decreto 53/2013, de 1 de febreiro (BOE 34, do 8 de febreiro), polo que se establecen as normas básicas aplicables para a protección dos animais utilizados en experimentación e outros fins científicos, incluíndo a docencia, establece no seu artigo 33 as condicións de autorizacións dos proxectos con animais de experimentación.

2 O artigo 88 da Lei 39/2015, de 1 de outubro, do procedemento administrativo común das administracións públicas (BOE 236, do 2 de outubro de 2015) establece que a resolución que poña fin o procedemento decidirá todas as cuestións expostas polos interesados e aquelas outras derivadas deste.

XUNTA DE GALICIA
CONSELLERÍA DO MEDIO RURAL

Xefatura Territorial
Sº de Gandaría
Edificio administrativo Monelos, 4º andar
Rúa Vicente Ferrer, Nº 2
15008 A Coruña
Tfno.: 981 184 565
Correo electrónico: servizo.gandaria.a.coruna@xunta.gal

galicia

3 O Servizo de Gandaría da Coruña revisou a documentación achegada na solicitude e o resultado favorable da avaliación do proxecto realizada polo órgano habilitado, a Sección de Experimentación Animal do Comité de Bioética da Universidade de Santiago de Compostela.

Esta xefatura territorial é competente para ditar unha resolución, de conformidade co Decreto 149/2018, do 5 de decembro, polo que se establece a estrutura orgánica da Consellería do Medio Rural e se modifica parcialmente o Decreto 177/2016, do 15 de decembro, polo que se fixa a estrutura orgánica da Vicepresidencia e das consellerías da Xunta de Galicia (DOG 235, do 11 de novembro).

De acordo con todo o indicado, RESOLVO:

1 Autorizar o proxecto solicitado.

2 O proxecto non precisa someterse a unha avaliación retrospectiva.

3 A autorización deste proxecto terá unha duración de tres anos e unha vez transcorrido este tempo deberá ser renovada.

A citada autorización é unicamente válida nas condicións que figuran no expediente. Ante calquera cambio significativo no proxecto que poida ter efectos negativos sobre o benestar dos animais, deberá solicitar a confirmación da autorización ao Servizo Provincial de Gandaría.

Esta autorización poderá ser suspendida no caso de que o proxecto non se leve a cabo de acordo coas condicións de autorización e retirala, previo expediente tramitado ao que se lle dará audiencia.

Contra a presente resolución, que non pon fin á vía administrativa, poderá interpoñer un recurso de alzada ante o conselleiro de Medio Rural. O prazo comezará a contar dende o día seguinte ao da recepción desta resolución. Todo isto, segundo o disposto nos artigos 121 e 122 da citada Lei 39/2015.

Mediante este escrito notifícaselle a Anxo Vidal Figueroa esta resolución segundo o esixido no artigo 40.1 da antedita Lei 39/2015.

USC UNIVERSIDADE DE SANTIAGO DE COMPOSTELA

Xacobeo 2021

In the present thesis, different topical-ophthalmic formulations of antifungals and cyclodextrins were developed for the treatment of fungal keratitis. In addition, the safety and permanence on the ocular surface of different cyclodextrins were evaluated in order to know their behavior in the eye and to optimize their use in the development of new ophthalmic formulations.